

CDM

Camp Dresser & McKee

Report

Indiana Department of Environmental Management

Continental Steel Superfund Site
Remedial Investigation

Volume VII

-Appendix H

Groundwater Modeling

-Appendix I

ABB-ES Data

October 15, 1996

EPA Region 5 Records Ctr.



381441

Draft Final

Project Number: 2673

APPENDIX H

Groundwater Modeling

Appendix H

Groundwater Modeling

Table of Contents

<i>Section 1</i>	Introduction	1
<i>Section 2</i>	Numerical Groundwater Model	3
2.1	DYNFLOW Model	3
2.2	Model Geometry	3
2.2.1	Finite Element Mesh	4
2.2.2	Stratigraphy	4
2.2.3	Bedrock Fracture Systems	9
2.3	Hydraulic Parameters	16
2.4	Boundary Conditions	17
2.5	Pumping	23
2.6	Recharge	25
2.7	Model Calibration	25
2.7.1	Method	25
2.7.2	Calibration Targets	26
2.7.3	Calibration Procedure	26
2.7.4	Calibration Results	27
<i>Section 3</i>	Contaminant Transport Model	39
3.1	Purpose	39
3.1a	DYNTRACK Model	39
3.2	Conceptual Model and Source Characterization	39
3.3	Fate and Transport Parameter Estimation	40
3.4	Contaminant Transport Simulations	41
3.4.1	Particle Tracking Simulations	42
3.4.2	Contaminant Transport Simulations	45
3.5	Summary of Contaminant Transport Modeling	46

Section 4	References	63
-----------	------------------	----

Appendix H Groundwater Modeling

1 Introduction

Numerical groundwater flow and solute transport modeling in the vicinity of the Continental Steel Superfund Site (CSSS) in Kokomo, Indiana has been conducted according to the objectives listed in the RI Work Plan document for the CSSS (CDM 1995). Objectives for construction, calibration and use of the model during the RI and FS include:

- Determination of both present day and future flow pathways from the site (including consideration of potential remediation activities);
- Estimation of potential exposure point concentrations for discharge to Kokomo and Wildcat Creeks, residential wells and the Martin Marietta Quarry;
- Estimation of contaminant front arrival times at various exposure points;
- Evaluation of containment and cleanup scenarios on potential exposure pathways; and
- Assistance in evaluation of technical practicability of groundwater cleanup.

Groundwater flow modeling was conducted using CDM's DYNFLOW™ model, a fully three-dimensional finite element groundwater flow model, and DYNTRACK™, a companion computer program for simulation of three-dimensional solute transport using the random walk method. The model was developed using hydrogeologic data collected on and near the facility, and compiled from other available records during the Remedial Investigation (RI). The site was modeled as porous media equivalent to approximate the fractured dolomitic limestone sequence underlying the glacial drift deposits. Use of this simplified approach allows consideration of areal flow rather than flow along individual fracture swarms.

This modeling effort is at a reconnaissance level of detail and is not intended to mathematically represent all processes active at the site, nor exactly duplicate all features of the groundwater flow system. This level of detail is adequate for the intended use of the model for estimation of potential concentrations at receptors under various flow regimes and the comparative analysis of potential remedial alternatives.

The groundwater model was developed using the following steps:

1. Regional and site specific hydrogeologic data were reviewed and compiled for use in the model.
2. A hydrogeologic Site Conceptual Model was developed using results of previous regional investigations and site-specific investigations including geologic logs and cross-sections, well construction records, groundwater elevation data, surface recharge estimates, contaminant distributions and aquifer tests.
3. A numerical groundwater flow model was developed including mesh generation, specification of boundary conditions, and incorporation of the site conceptual model into the finite element mesh.
4. A steady-state groundwater flow model calibration was performed using pumping records and water level data for the year 1995, supplemented by use of historic regional water level data distant from the site.
5. Two constituents, tetrachloroethene (PCE) and trichloroethene (TCE), were selected for use in the groundwater transport model, based on evaluation of groundwater quality information collected during the remedial investigation and provided by the Haynes International, Inc.

The groundwater model as calibrated succeeds in simulating the regional groundwater flow system in the vicinity of the CSSS. The model was used to simulate interactions between groundwater and surface water and to simulate influences from pumping wells (i.e., residential wells, industrial wells, groundwater supply wells, and dewatering wells at the Martin Marietta quarry). The groundwater model was used to reach the primary conclusions presented below.

- Contaminant transport in the vicinity of the CSSS is controlled by two major hydraulic influences: (1) Martin Marietta quarry pumping and (2) Wildcat and Kokomo Creeks.
- Simulated groundwater flow path tracks and dissolved contaminants TCE and PCE are generally confined to a central contaminant transport pathway following the course of Wildcat and Kokomo Creeks in the westerly direction. Transport pathways do not diverge significantly from site source areas to the north or south of this main transport pathway.
- Capture of contaminated groundwater originating on the CSSS by domestic wells in a subdivision located southwest of the site is unlikely under either of the quarry operational scenarios.

Additional fate and transport analyses will be performed using the model to evaluate various remedial scenarios during the FS. A quantitative risk assessment will also be performed using the model during the time frame of the FS. The model will prove a valuable tool in addressing these key elements of the FS.

2 Numerical Groundwater Model

2.1 DYNFLOW Model

DYNFLOW is a versatile computer program written in the FORTRAN computer language, which simulates three-dimensional groundwater flow using the finite element technique. DYNFLOW was developed by CDM and is based on an earlier model, AQUIFEM (Wilson, *et al.* 1979), developed at the Massachusetts Institute of Technology. The DYNFLOW model has been reviewed by the International Ground Water Modeling Center. A copy of this peer review is included in **Appendix A**.

DYNFLOW incorporates the conventional equations of saturated flow in porous media and can be used to simulate the response of groundwater flow systems to several types of natural and artificial stress. These include: induced infiltration from streams; artificial and natural recharge or discharge (e.g., precipitation, infiltration, groundwater discharge to local streams, well withdrawals); and nonhomogeneous and anisotropic aquifer hydraulic properties. It solves both confined and nonlinear unconfined aquifer flow equations and includes special routines to simulate a change in status from a confined to an unconfined situation, such as might occur due to heavy pumping from limestone quarries operated by the Martin Marietta Corporation to the west of the CSSS during transient simulations. The program has a scheme to allow drainage to local streams if the piezometric head in an unconfined aquifer rises above the elevation of the streambed. DYNFLOW also has special algorithms for simulating multi-aquifer pumping, similar to the existing regional water supply and quarry dewatering pumping in the vicinity of the CSSS. **Appendix B** provides more detail on the capabilities and mathematical basis for this model.

2.2 Model Geometry

The extent of the model was selected to extend to physical boundaries, where possible, or at a sufficient distance from the area of interest to minimize the impact of selected boundary conditions on flow fields in the area of interest. Model geometry was configured to include the major hydrogeologic influences on the aquifer in the vicinity of the CSSS. These include:

- Subsurface hydrostratigraphy near the site;
- Surface water bodies Kokomo Creek and Wildcat Creek; and
- Municipal, domestic, agricultural, and industrial groundwater pumping.

Horizontal model boundaries were selected based on evaluation of the regional groundwater potentiometric surface, as presented in Smith, *et al.* (1985). These model boundaries were selected to

represent either a no flow boundary, that is, the mesh boundary lies along a flow line, or a constant head boundary, where the mesh limit follows a potentiometric surface contour.

The location of the CSSS and the regional model study area are illustrated in **Figure 1**.

2.2.1 Finite Element Mesh

A finite element mesh comprised of 1,268 nodes and 2,468 elements in plan view was prepared within the regional model study area. Maximum nodal spacing ranged from approximately 4,721 feet toward the outside of the mesh to a minimum of 300 feet in the vicinity of the CSSS site (**Figure 2**). Finest nodal spacing was used in the vicinity of the confluence of Wildcat and Kokomo Creeks, and in the area of the Martin Marietta quarry, where the maximum pumping stress occurs in the model. This spacing allowed simulations to be conducted without use of a two stage modeling approach with local and regional meshes. Based on previous modeling experience, the 300 foot spacing near the area of interest is appropriate for treating the fractured aquifers as porous media equivalent for purposes of the modeling analysis. **Figure 2a** presents the mesh at a more detailed scale near the CSSS.

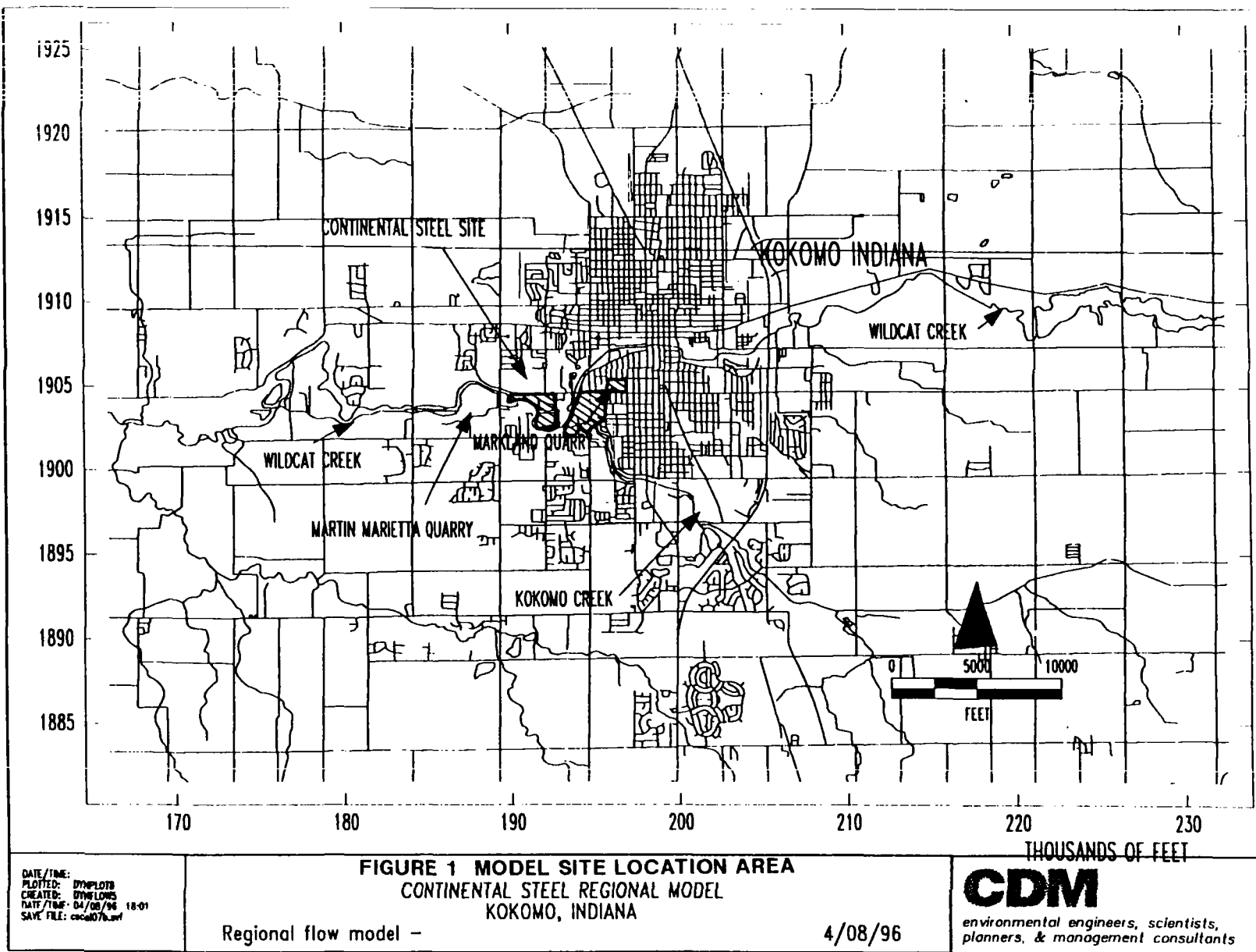
2.2.2 Stratigraphy

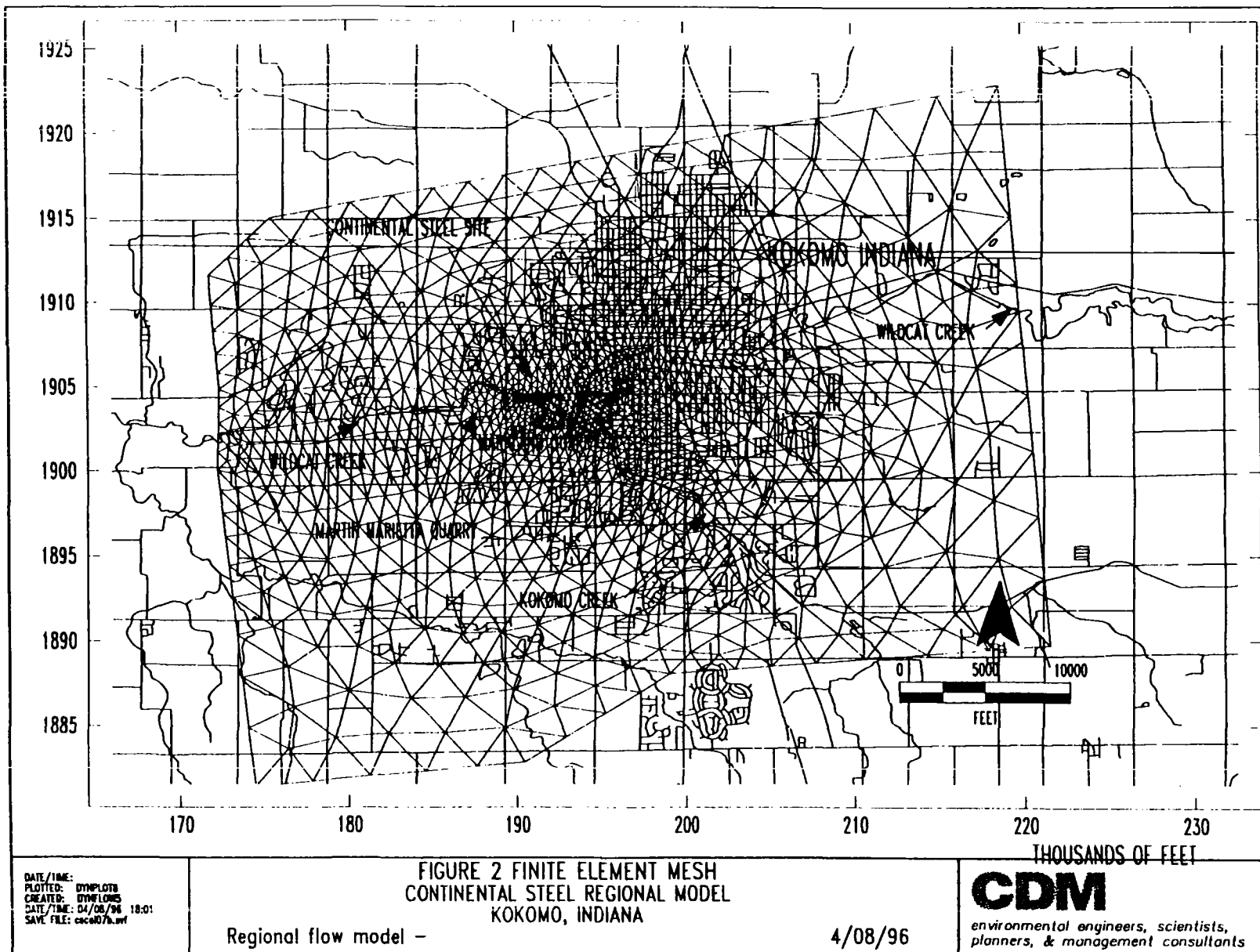
Originally a single layer application of the DYNFLOW model was planned for purposes of simplification (CDM 1995). Following more detailed analysis of the regional and site lithology, hydraulic gradients, and contaminant distribution, a multi-layer model approach was adopted to provide more detailed and accurate results with respect to the stated objectives. The occurrence of vertical hydraulic gradients and vertical stratification of groundwater contaminants were the primary reasons for using a multi-layered model.

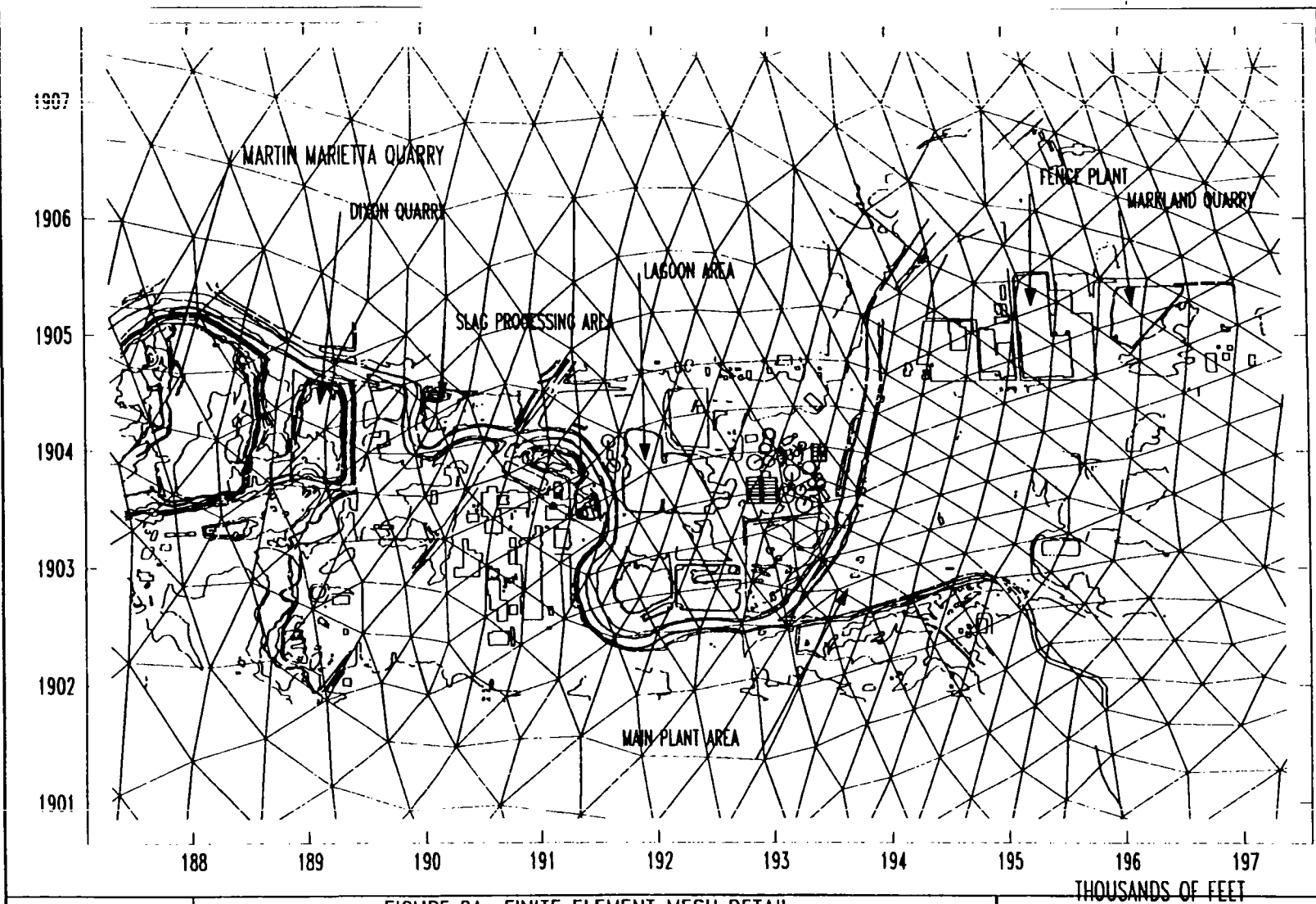
The lower fractured zone of the Liston Creek A Limestone and the upper fractured zone of the Kokomo Limestone/Liston Creek A Limestone are in close hydraulic communication at the site. As significant pumping stress is not applied to either of these layers, the vertical hydraulic gradient between these two layers tends to be minimal. The steady-state flow calibration simulation additionally tends to lead to greater equilibration between adjacent layers in the absence of pumping stresses. The majority of discharge withdrawn at the quarry is acknowledged to originate primarily in the highly fractured rock zone immediately above the contact with the Mississinewa shale. As expected, a significant vertical hydraulic gradient develops between this relatively thin highly fractured zone and the overlying layers with the quarry pumping.

Vertical stratification of contamination is another important reason to include multiple layers in the model simulation. The monitoring data indicates that significant variations in the distribution of TCE and PCE occur with depth at the site. This stratification yields important information regarding potential source areas, and may lead to significantly different projections of concentrations at receptor locations than if contaminant levels were averaged in the vertical direction.

In consideration of these factors, the numerical groundwater flow model was constructed to include six model layers. The model layer boundaries do not necessarily follow boundaries of







DATE/TIME: DYNPLOT8
 PLOTTED: DYNPLOT8
 CREATED: DYNPLOT8
 DATE/TIME: 04/08/96 18:01
 SAVE FILE: C:\CAL07B.SVF

FIGURE 2A FINITE ELEMENT MESH DETAIL
 CONTINENTAL STEEL REGIONAL MODEL
 KOKOMO, INDIANA

Regional flow model -

4/08/96

CDM

environmental engineers, scientists,
 planners, & management consultants

named stratigraphic units, but are defined over depth intervals where aquifer materials on the aquifer hydraulic properties of these intervals. Figure 2-2 in Volume II of the RI illustrates the correlation between stratigraphic units and model layers. Definition of the model hydrostratigraphic framework was based on information collected during the remedial investigation, review of regional geologic literature, and lithologic logs from on-site monitoring and area water supply wells. The simplified single-layer groundwater model proposed in the "Focused RI/FS Work Plan" (CDM 1995) was expanded to account for this information and to simulate groundwater flow in the vicinity of the Martin Marietta quarry and in residential area located southwest of the site more accurately. This current model with six model layers will be more helpful for evaluating corrective action scenarios during the FS. A comprehensive description of the site hydrogeology is presented in Section 4.4.6 (Groundwater). These six layers, described in descending order from the surface, include the following stratigraphic intervals.

The Kokomo Limestone is part of the Salina Group, Cayugan Series, and the Liston Creek Limestone and Mississinewa Shale are part of the Lockport Group, Niagaran Series. The Liston Creek Limestone is a cherty, fine - to medium-grained dolomitic limestone with irregular argillaceous (clayey) partings. The upper Mississinewa Shale is a dolomitic siltstone and the lower Mississinewa Shale is composed of interbedded limestone and argillaceous dolomite. The Mississinewa Shale is not a shale in the vicinity of the site.

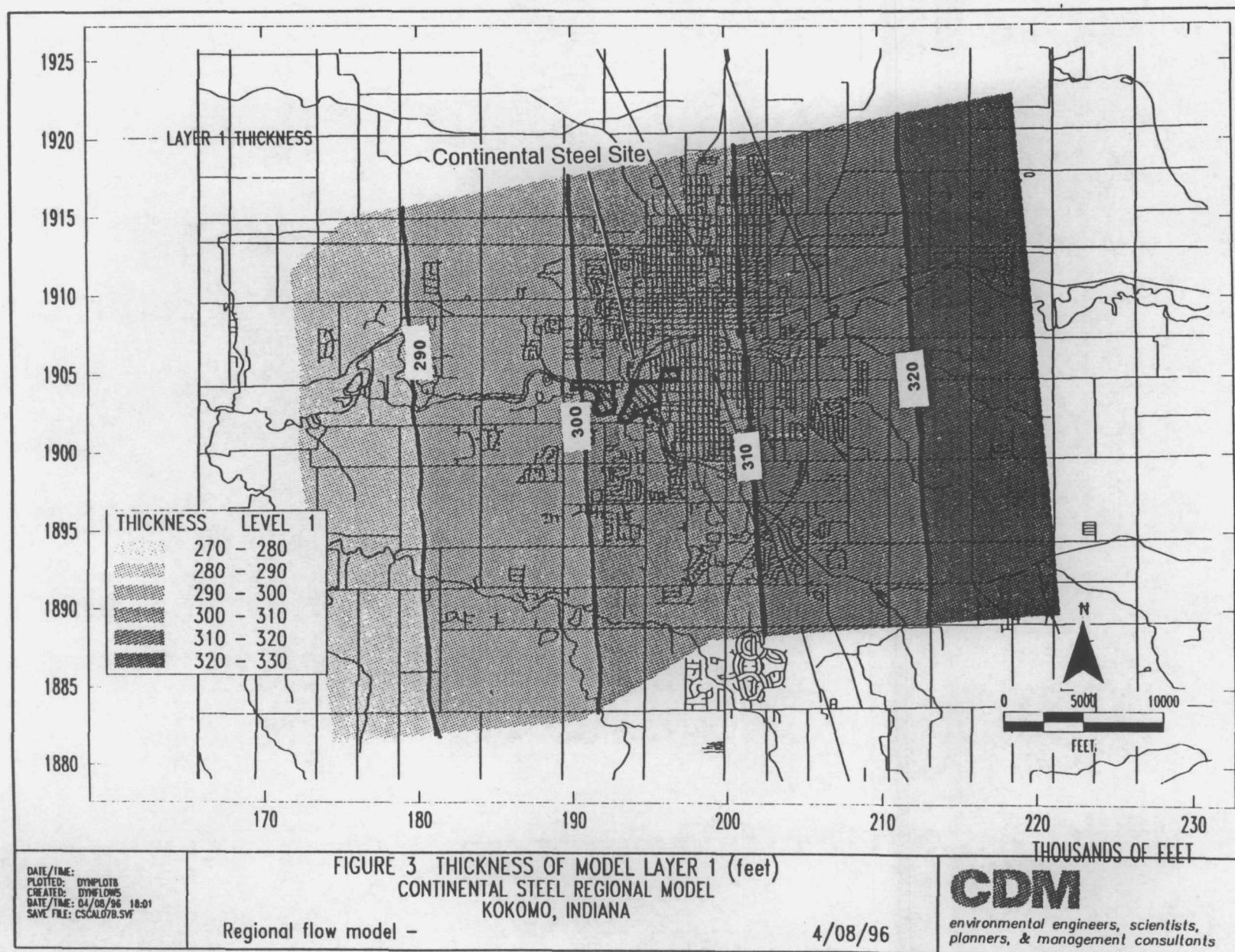
- Model Layer 6 - Overburden layer (approximately 2 - 140 feet thick). Lithologic logs from domestic wells located southwest of CSSS indicate the potential presence of an ancient river channel in this area. These lithologic logs show that the overburden thickness is significantly greater southwest of CSSS (50 to 100 feet) than beneath CSSS (5 to 20 feet). This layer was included in the model because of concern about potential impacts from the site on these domestic wells.
- Model Layer 5 - Upper fractured interval of Kokomo limestone/dolostone and Liston Creek A (approximately 10 to 30 feet thick). The Kokomo Limestone is a thinly bedded dolomitic limestone. The Liston Creek Limestone is a cherty, fine - to medium-grained dolomitic limestone with irregular argillaceous (clayey) partings. This layer is the most prolific water producer of the layers in the model; however, the ability to produce water at a specific well location depends upon whether the well intersects a water-bearing fracture or bedding plane and how well-developed the intersected fracture system is at that location.
- Model Layer 4 - Lower fractured interval of the Liston Creek A (approximately 5 to 45 feet thick). This layer produces less groundwater than the overlying layer, but more groundwater than the underlying layer. As stated above, however, the ability to produce water at a specific well location depends upon whether the well intersects a water-bearing fracture or bedding plane and how well-developed the intersected fracture system is at that location.
- Model Layer 3 - Massive limestone interval of Liston Creek B (approximately 25 to 45 feet thick). Wells completed within this layer tend to produce less water than those completed in the overlying and underlying layer. Groundwater flow at a specific location depends upon the intersection of water-bearing fractures and bedding planes at that location.

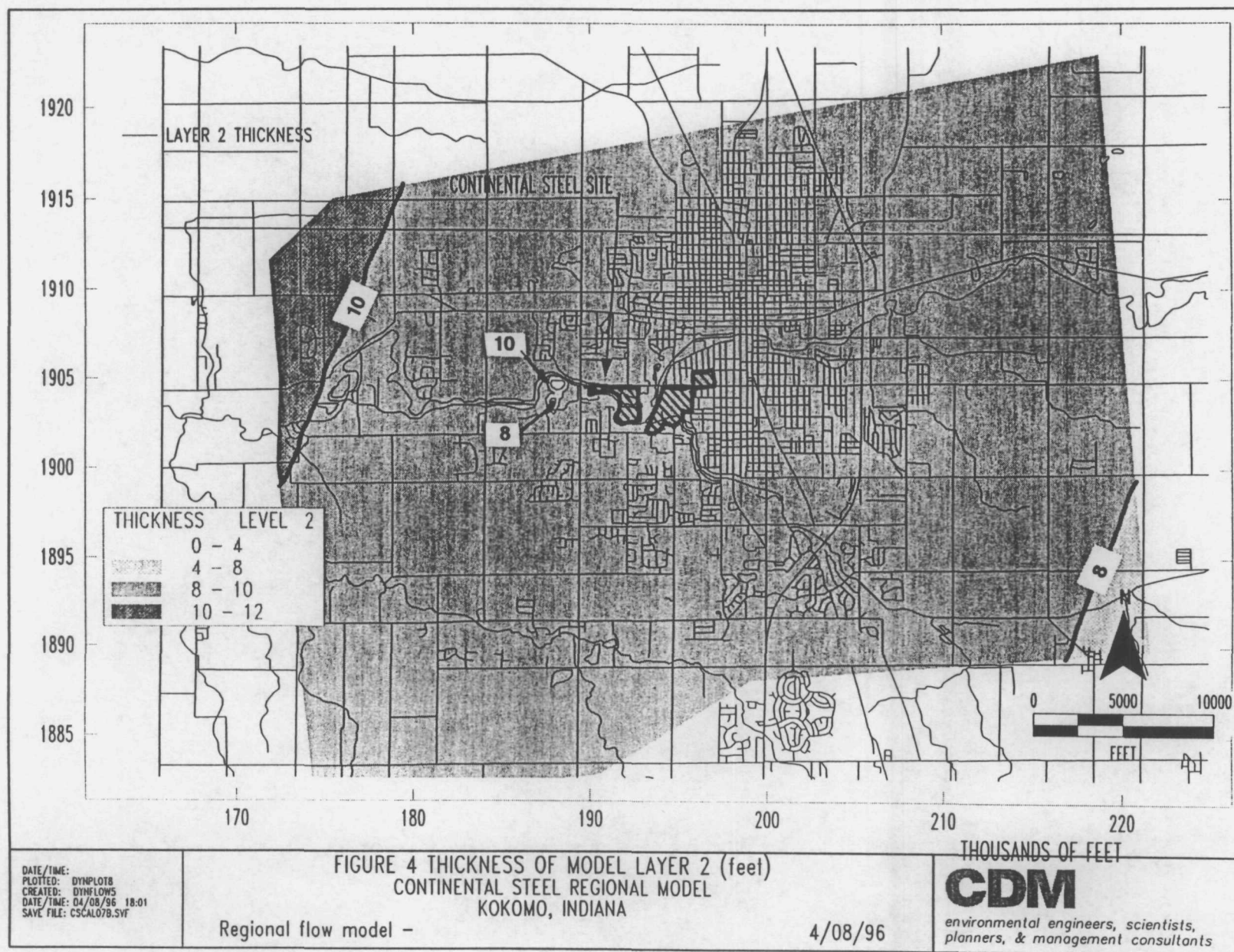
- Model Layer 2 - High permeability fractured basal zone of the Liston Creek B (approximately 2 to 11 feet thick). The existence of this zone became apparent during the field investigation conducted during 1995 and 1996. During an interview with staff at the Martin Marietta quarry, Mr. John Wakefield concluded that groundwater enters the quarry primarily through this zone, located immediately above the Mississinewa Shale (Personal communication, John Wakefield-Martin Marietta quarry plant manager, February 6, 1996). This layer developed along bedding plane fractures that were weathered by groundwater flow along the top of the Mississinewa Shale. Wells completed in this layer generally produce more water than the layer 3 and less water than layer 5.
- Model Layer 1 - Low permeability base layer comprised of Mississinewa Shale and underlying Silurian age dolomite (assumed thickness of 270 - 330 feet), based on using a uniform base elevation of 377 feet Mean Sea Level (MSL), and a westerly slope of the elevation of the contact with the overlying fractured zone. The upper Mississinewa Shale is a dolomitic siltstone and the lower Mississinewa Shale is composed of interbedded limestone and argillaceous dolomite. The Mississinewa Shale is not a shale in the vicinity of the CSSS. Most of the domestic wells located southwest of the site are completed in this layer. The average depth of the domestic wells located southwest of the site is greater than 200 feet.

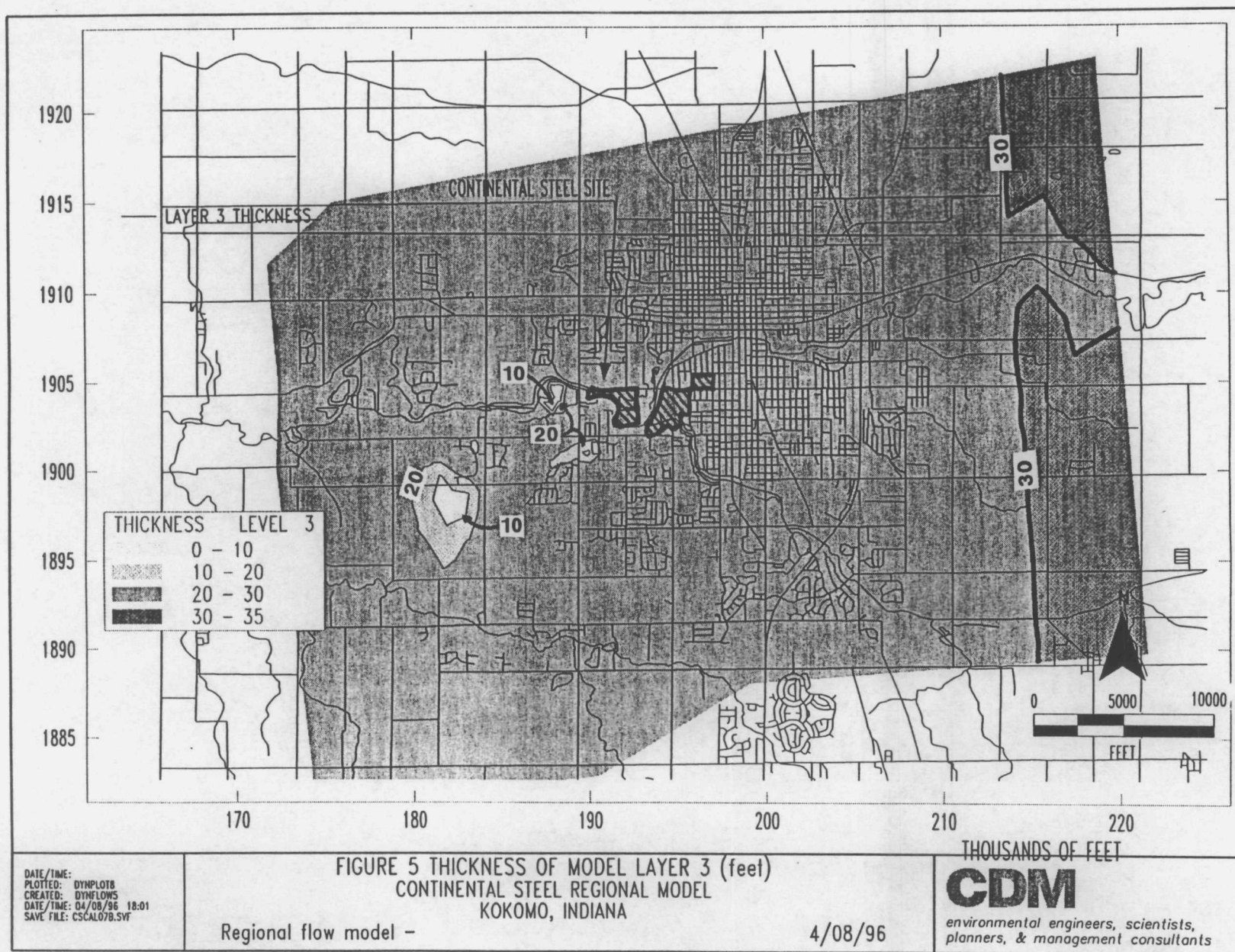
Lithologic logs from monitoring wells were used to interpret layer elevations in the vicinity of the CSSS site. Regional geologic literature was used to interpret thickness of the overburden (Model Layer 6) and the depth of the Mississinewa Shale contact (top of Model Layer 1) in outlying areas of the mesh (U.S.G.S. 1994 and Smith *et al.* 1985). Lithologic logs from domestic wells located southwest of the site indicate the potential presence of an ancient river channel, contributing to overburden thicknesses up to 140 feet. Layer contact elevations for model layers 2 through 5 were estimated based on analysis of site well logs and projected off-site using the regional dip of the bedrock units as reported in Smith *et al.* (1985). Contours of Model Layer thicknesses based on estimated layer contact elevations are illustrated in Figures 3 through 8. It should be noted that a detailed representation of stratigraphy was not attempted in this evaluation and the model stratigraphy is a highly idealized representation of the field. The contact between layer 4 and 5 is highly variable, since it is defined based on a subjective evaluation of intensity of fracturing observed at wells. The thicknesses of various units are representative of those that occur near the site and these characteristics were assumed to extend through the domain of the model. Lithologic layers were assumed to be continuous beneath the Martin Marietta quarry, and as such model layers 3 through 6 were artificially reduced to approximately 1 foot thickness within the quarry. Thus, the inherent accuracy of the modeling will degrade outside of the area of the CSSS.

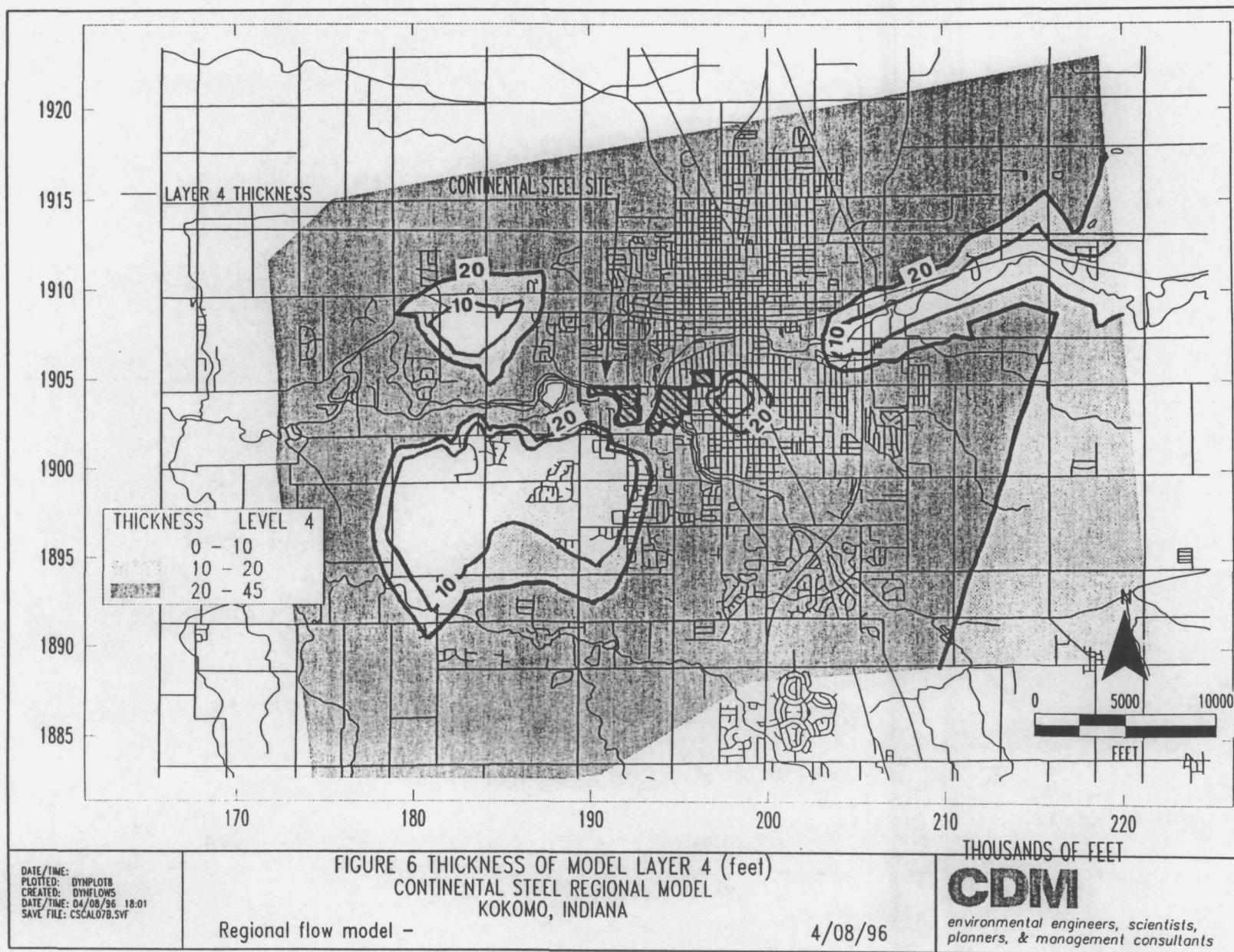
2.2.3 Bedrock Fracture Systems

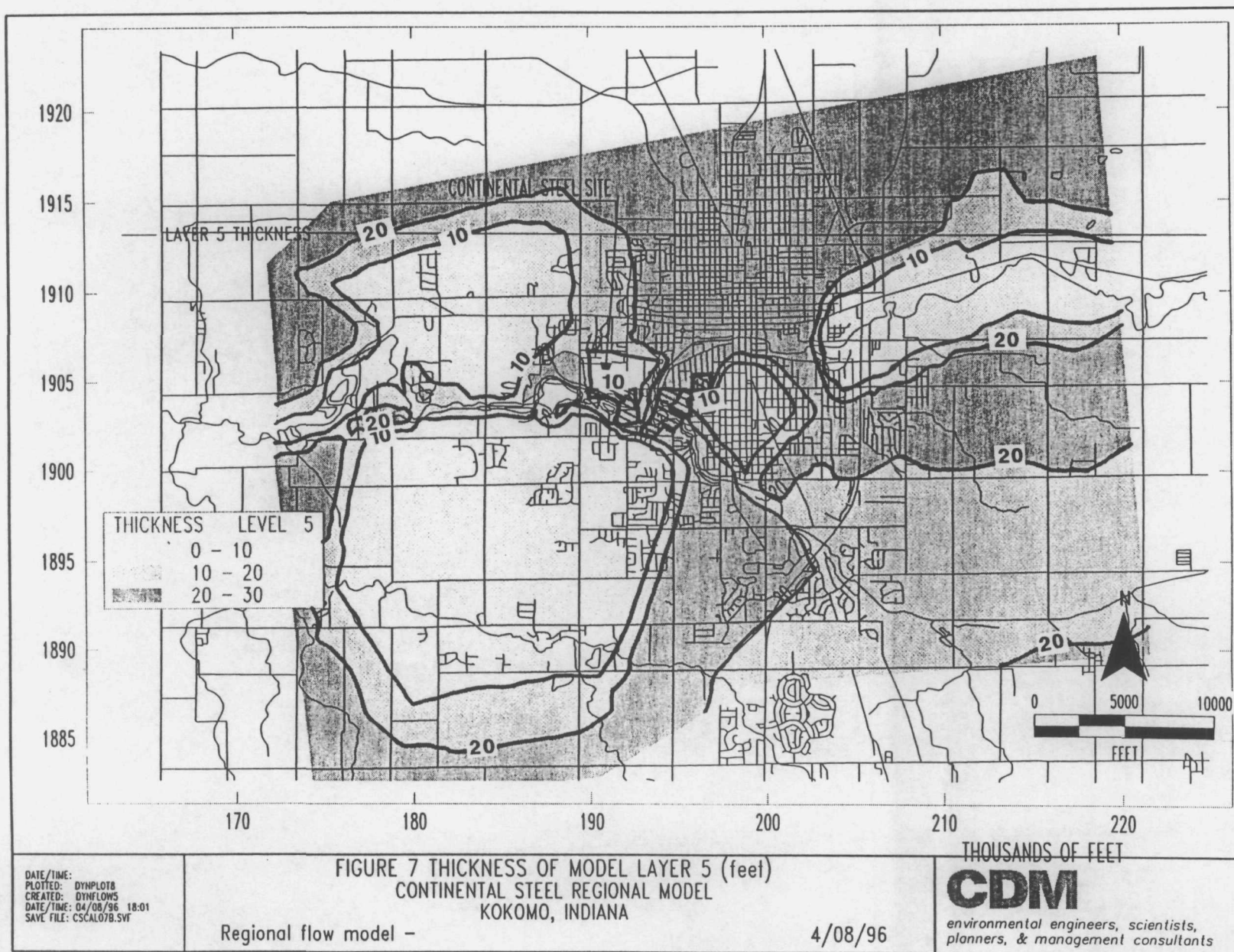
A detailed discussion of the bedrock stratigraphy and fracture systems at the CSSS has been presented in the RI/FS Work Plan presented to IDEM (CDM 1995) and is presented in the main RI report text (CDM 1996). During the RI, CDM and/or ABB-ES conducted a literature review, and

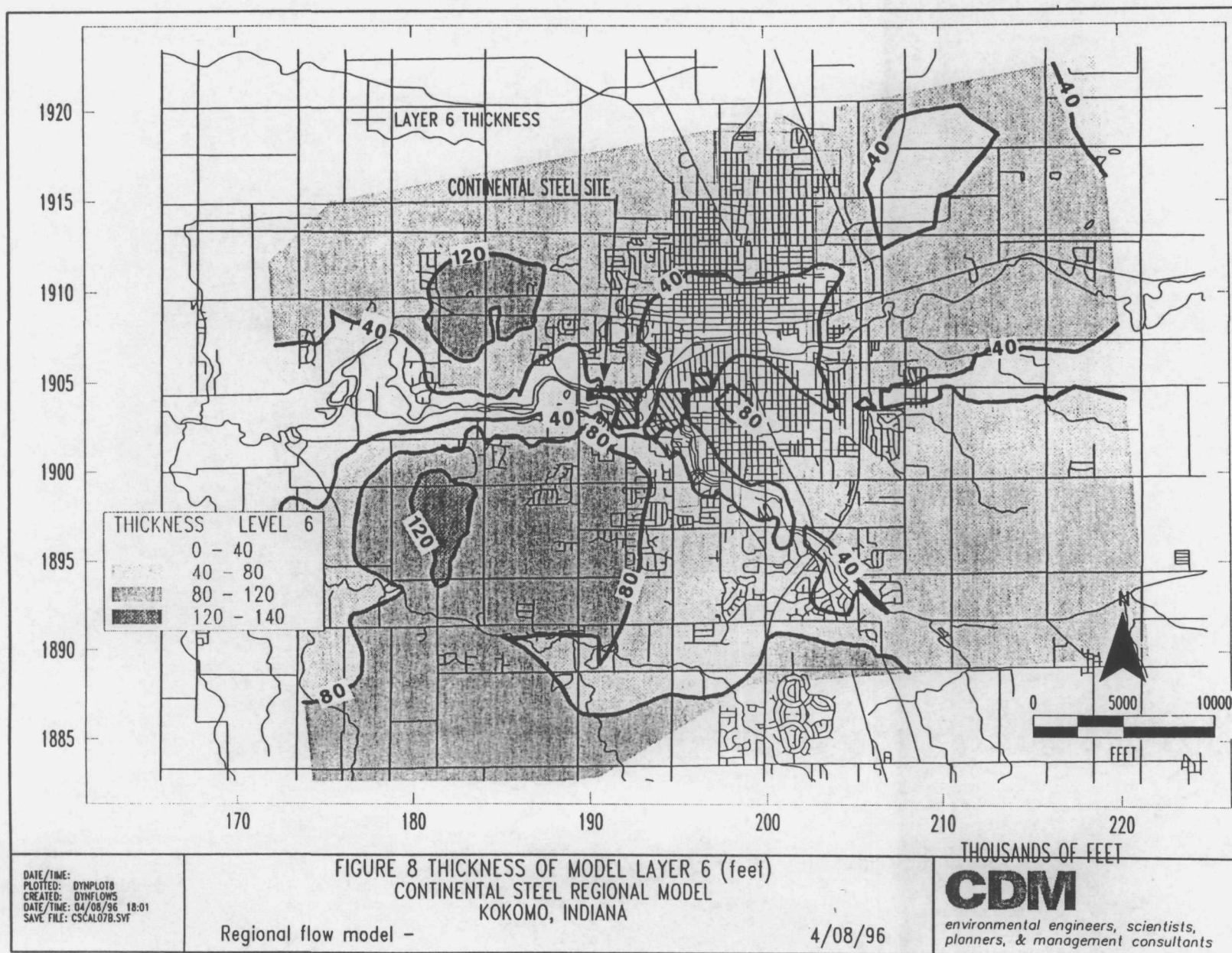












analysis of rock cores, borehole geophysical logs, and rock outcrops, in addition to a fracture trace analysis. Evaluation of monitor well water levels indicated regional hydraulic communication among wells in the study area. Water levels presented in Smith, *et al.* (1985) indicated regional continuity in bedrock hydraulic gradients, also indicative of widespread hydraulic communication. Such continuity of hydraulic gradients and widespread hydraulic communication serves as the justification for the equivalent porous media assumption.

The orientation of the principal axis of flow for the model was set at North 80 degrees East, which represents the average of the principal fracture orientations for the Kokomo Limestone and the Liston Creek Limestone (CDM 1995). As observed in the rose histogram of fracture orientations (Appendix I), the principal fracture orientation of these lithologic units range from North 70 degrees East to North 90 degrees East. The average orientation of North 80 degrees East provided the best match of computed water levels to measured water levels during the flow model calibration.

For further substantiation of these assumptions, the reader is referred to the reference by Ault (1988) on bedrock jointing in central and northern Indiana.

2.3 Hydraulic Parameters

Initial estimates of hydraulic parameters were prepared based on ranges provided in Smith *et al.* (1985) for regional aquifer materials. Initial estimates for hydraulic conductivity, storage coefficient, and specific yield are summarized in Table 1. Though initial estimates were established for storage coefficient and specific yield for use in transient simulations, model calibration and flow simulations were all conducted in the steady-state mode. Effective porosities, which are related to specific yields are utilized in the solute transport evaluation. No information was available on the primary porosity or permeability of the unfractured matrix material. The noted hydraulic conductivities represent the bulk properties of large blocks of the aquifer that can be treated as the equivalent of porous media at the scale of interest. The fractured nature of the bedrock aquifer system also leads to the presence of directional anisotropy. Based on fracture orientations present in the area, the hydraulic conductivity is higher along the direction of the principal fracture set in the east-west direction. This anisotropy was assumed to be 2:1 between the maximum conductivity direction and the minimum conductivity direction. Similarly, due to the interbedded nature of the deposits and the presence of bedding plane partings, a ratio of horizontal to vertical conductivity of from 10:1 to 100:1 was used in the modeling, based on previous experience in modeling fractured limestone systems.

<p>Table 1 Initial Hydraulic Parameter Estimates</p>				
Model Layer	Horizontal Hydraulic Conductivity (ft/day)	Vertical Hydraulic Conductivity (ft/day)	Storage Coefficient (dimensionless)	Specific Yield (dimensionless)
1	10.	1.	1.0E-05	0.20
2	100.	10.	1.0E-05	0.20
3	2.8E-05	2.8E-06	1.0E-05	0.10
4	10.	1.	1.0E-05	0.20
5	100.	10.	1.0E-05	0.20
6	100.	10.	1.0E-05	0.20

2.4 Boundary Conditions

Model boundary locations were established based on regional bedrock aquifer water levels in the model area, as reported by Smith *et al.* (1985). As noted above, model boundaries were selected to coincide with lines of approximate equivalent potentiometric head or along flow lines based on the regional potentiometric surface. Regional water levels used in setting boundary conditions were based on measurements made in 1980 to 1982. Surface water elevations from USGS topographic maps were also used to select boundary elevations. Long-term water levels recorded beginning in 1966 indicated water level fluctuations of less than 2 feet, as a result of changes in local pumpage. Long-term regional water levels are not expected to substantially differ from those measured in 1980 since pumping rates in the area are relatively stable (Smith *et al.* 1985).

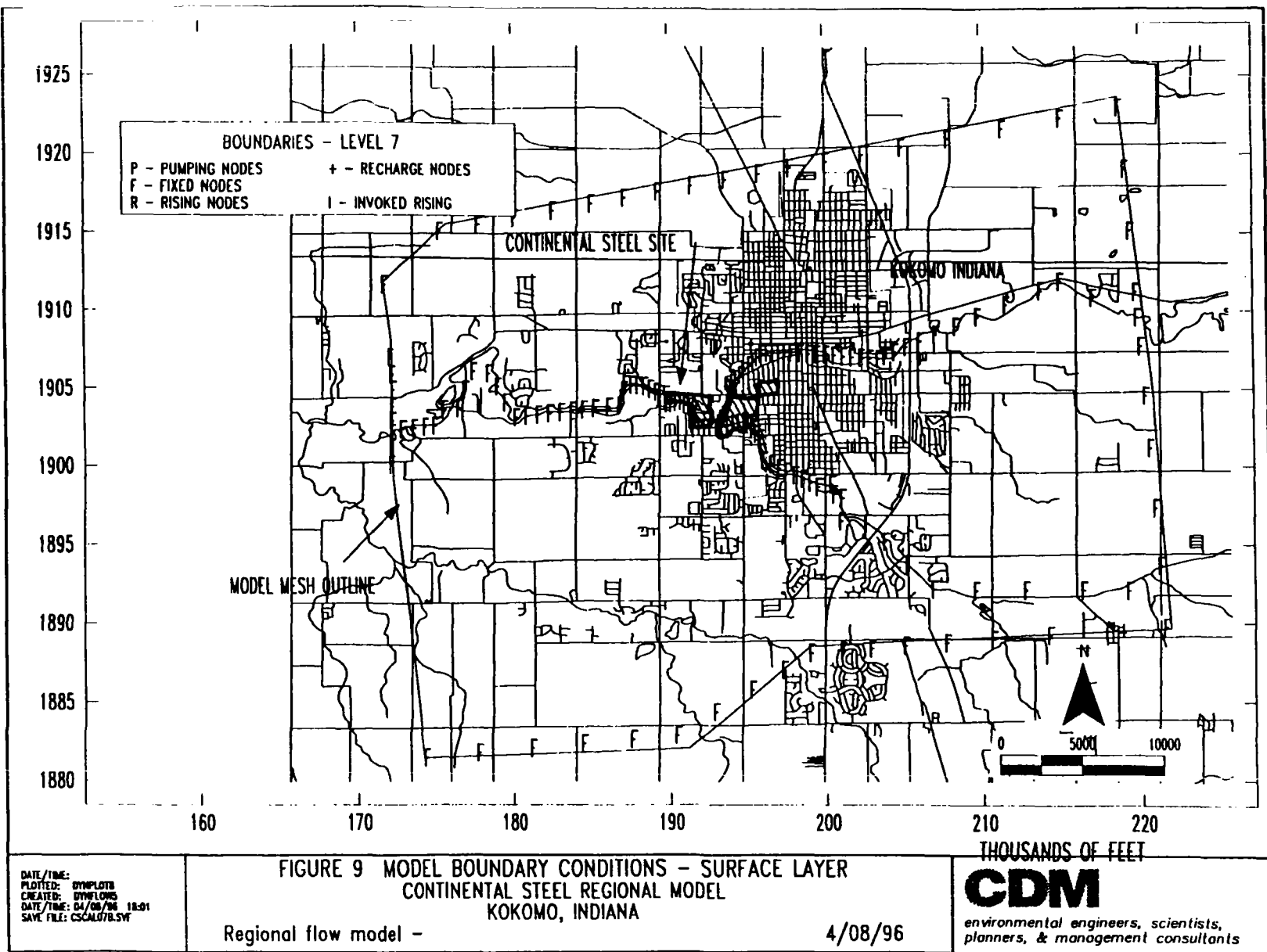
Regional water levels in the model were established using water level data reported in Smith, *et al.* (1985) based on the assumption that over the regional model study area, water levels in the bedrock had not substantially changed from the time of 1980 (as reported by Smith *et al.*) and 1994 (the period simulated by the model). As stated by Smith *et al.* on page 24 "Seasonal and periodic fluctuations of less than 2 feet superimposed on a long-term trend are shown in hydrographs of the continuous-record wells. Minor gains and losses in aquifer storage are indicated by seasonal and periodic fluctuation; however, the long-term trend is approximately steady state." These minor fluctuations are produced primarily by seasonal variations in recharge from precipitation, water use by pumping from wells and streamflow recharge to the aquifers. A direct comparison of reported pumpage by Smith *et al.* in 1980 with that used in the RI model cannot be performed as the Smith document uses a much larger area than the model. Smith *et al.* reports an approximate pumping rate of 2.0 cubic feet per second for the Martin Marietta quarry in 1980 (which translates to approximately 900 gallons per minute), compared to a record of 3290 gallons per minute (gpm) in 1994. This difference in quarry pumping level is acknowledged to be significant, just as short-term

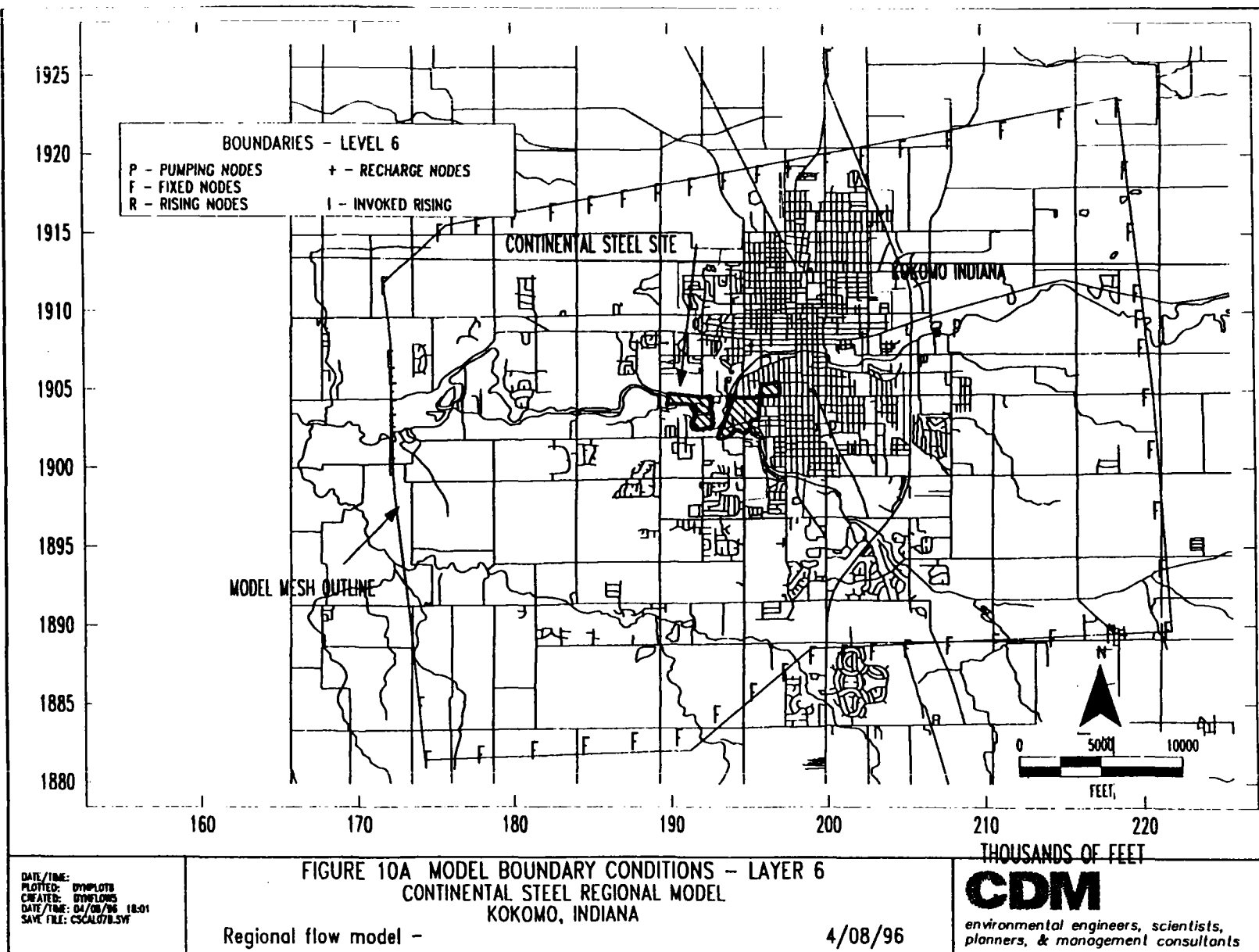
local contrasts in seasonal pumpage within the model domain are also relatively significant. However, due to the location of this pumpage near the center of the model, and the location of the model boundaries several miles from the CSSS site, this discrepancy is unlikely to have a significant impact on water levels in the bedrock aquifer at the model boundaries at such a distance. The model boundaries are intended to reflect a long-term stable, regional potentiometric surface upon which to impose the more localized constraints in hydraulic parameters and pumping stress at the CSSS site scale.

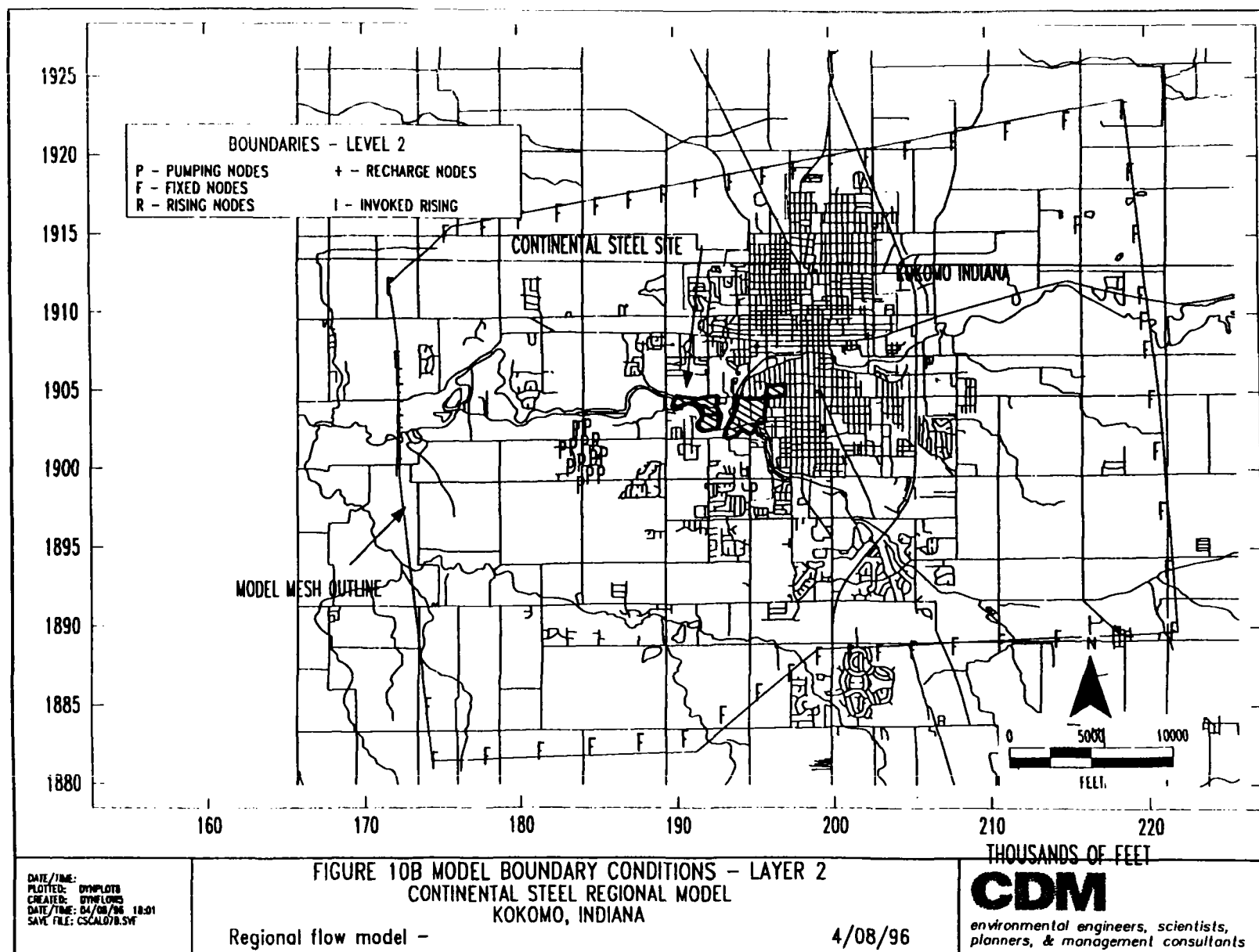
Further, although a direct comparison of water levels cannot be made between those reported by Smith *et al.* for bedrock wells in 1980, and those reported from CSSS monitor wells in 1994, Smith *et al.* illustrates bedrock water levels in the vicinity of the CSSS site that are consistent with regional bedrock water levels presented in the RI Work plan in the vicinity of the site (CDM 1995, Figure 2-10). This consistency in reported bedrock water levels in the vicinity of the CSSS supports the overall consistency of regional water levels between 1980 and the recent time frame of 1994-1995.

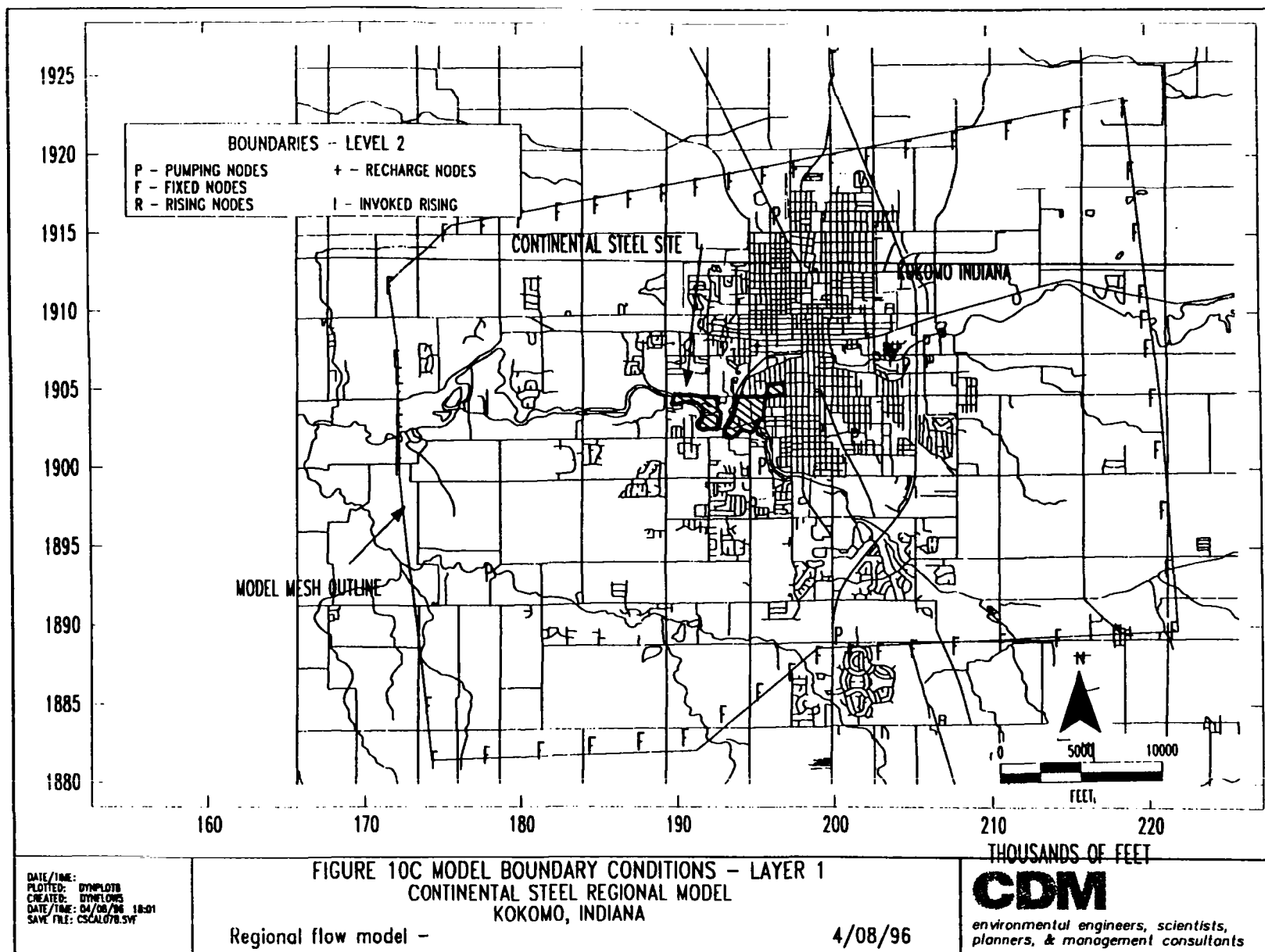
Fixed head boundary conditions were established at model mesh boundaries where regional water levels were stable. A fixed head boundary in the model will allow inflow or outflow of water sufficient to maintain the specified water level. No flow boundary conditions were established along model mesh boundaries that occurred along regional aquifer flow lines. A fixed head boundary condition was imposed at surface finite element mesh nodes that occurred along Wildcat and Kokomo Creeks in the model area. Fixed heads were imposed at a level equivalent to the topographic surface elevation at these nodes. Rising head boundary conditions, which invoke a fixed head condition if the upper level water level rises above land surface and flow is inward, were specified at all land surface nodes. Fixed head boundary conditions specified for the top model layer (Level 7, top of model layer 6) are illustrated in Figure 9. The "F" symbol in these illustrations indicates the location of a node at which the initially specified head at that node was held constant for model simulations.

Boundary conditions specified for model layers 6, 2, and 1 are illustrated in Figures 10a through 10c, respectively. The fixed head boundary conditions illustrated in these figures are common to model layers 1 - 6. This specification of boundary head values common to all layers was made as the most reasonable assumption for boundary conditions given the alternatives. Layer specific water level data in the outlying areas of the model grid were not available, leaving the alternative of inferring a vertical hydraulic gradient at the model boundaries based on those observed in the vicinity of the site. As the vertical hydraulic gradients at the site develop mainly due to recharge from surface water in the shallow layers and pumping stress in the deeper layers, extrapolation of known vertical gradients to the model boundaries would be a less valid assumption than the one of uniformity of hydraulic head at the model boundaries. Due to the distance of the model boundaries from the site, the imposition of surface recharge and local pumping stress would still result in model-computed vertical hydraulic gradients at the site that reasonably approximated those observed in the site monitoring data. As indicated in the Section 2.6 discussion on model calibration, the calibrated model does produce reasonable approximations of measured vertical hydraulic gradients in the vicinity of the site.









The pumping nodes differ among the layers as shown. Appropriate intervals for pumping wells was determined from well construction data. These pumping wells are discussed below in Section 2.5 of this memorandum.

2.5 Pumping

Model pumping was specified using rates in the Indiana state records obtained for 1994 for the area of the model mesh (Table 2). Construction records for water supply wells indicated that wells are typically constructed using casing from ground surface to the depth at which bedrock is encountered, and finished as open-hole borings for the remainder of the depth.

As such, pumping flow was attributed to model layers according to the hydraulic conductivity of the layers across which the well was completed. This manner of allocating pumpage across the entire completion interval is accomplished using a 1-dimensional element to connect all layers that contribute to production at the well. The properties of the 1-dimensional element are set such that no significant resistance to flow between the layers is present at the well location. One-dimensional elements were specified at all locations of pumping wells completed as open holes within bedrock. The wells illustrated as pumping nodes in Figures 10b and 10c (model layers 2 and 1, respectively) draw water from overlying bedrock zones, in addition to the specified layers, to simulate the open borehole effect.

A large subdivision located to the southwest of the site uses individual household domestic wells for its water supply. A cumulative frequency analysis of well casing depth and total depth for these wells indicates that the average depth of these wells exceeds 200 feet. Most of the wells are completed within the deepest bedrock model layer, Layer 1. Pumpage from this area was estimated based on an average household water use rate of 250 gallons per day, based on information obtained from the National Groundwater Association (NGWA 1996). The total number of wells was multiplied by the estimated average of 250 gpd, and this pumpage was distributed among 13 nodes in the vicinity of the subdivision. Pumpage was distributed among model layers at these nodes according to hydraulic conductivity using the One Dimensional element feature of DYNFLOW.

Domestic well, DW-282, located north of the Slag Processing Area, was not included in the construction of this model. CDM contacted the Indiana Department of Natural Resources to obtain the well construction log for this well; however, no well construction log is available. Analytical information for samples collected from the three new monitoring wells (UA-105, LA-105C and LA-105E) installed during the remedial investigation will be used during the FS to characterize groundwater quality in the area of DW-282. None of these monitoring wells is a pumping well.

Discharge at the Martin Marietta quarry was of interest as a potential calibration target. To estimate the flows that would result under dewatering conditions, the quarry was simulated as a large excavation with layers connected using 1-dimensional elements, with a fixed head set at the elevation of the seepage face for the quarry. The relationship of flux through a porous medium with hydraulic gradients is fundamental to groundwater flow.

Section 2
Numerical Groundwater Model

Table 2
Model Pumpage

ID	Owner	X (Easting) meters	Y Northing (meters)	Comp. Depth (ft)	Capac. (gpm)	Total '94 Use (cu.ft.)
63-IR	CHIPPENDALE GOLF COURSE	572150.00	4473075.00	297 feet.	500 GPM	240625
83-PS	FLOWING WELLS INC	574100.00	4474900.00	468 feet.	320 GPM	6418003
83-PS	FLOWING WELLS INC	574150.00	4475900.00	465 feet.	250 GPM	5618593.4
83-PS	FLOWING WELLS INC	574175.00	4474825.00	312 feet.	400 GPM	2177856.1
83-PS	FLOWING WELLS INC	574175.00	4475650.00	400 feet.	200 GPM	1542673.5
52-IR	RICES GOLF CENTER	573950.00	4475775.00	175 feet.	80 GPM	84218.74
82-IR	KOKOMO COUNTRY CLUB	572650.00	4479350.00	188 feet.	300 GPM	1685711.7
82-IR	KOKOMO COUNTRY CLUB	572500.00	4478800.00	140 feet.	600 GPM	2803281.05
82-IR	KOKOMO COUNTRY CLUB	572475.00	4478725.00	245 feet.	50 GPM	307465.25
33-IN	DELCO ELECTRONICS	574445.00	4480010.00	182 feet.	180 GPM	8977985.5
33-IN	DELCO ELECTRONICS	574238.00	4480105.00	45 feet.	100 GPM	3739044.88
33-IN	DELCO ELECTRONICS	574239.00	4480105.00	45 feet.	100 GPM	506849.27
33-IN	DELCO ELECTRONICS	574232.00	4480109.00	26 feet.	100 GPM	37430.55
33-IN	DELCO ELECTRONICS	574232.00	4480110.00	26 feet.	100 GPM	40104.16
33-IN	DELCO ELECTRONICS	574233.00	4480105.00	30 feet.	1250 GPM	1859496.4
33-IN	DELCO ELECTRONICS	574234.00	4480105.00	30 feet.	1250 GPM	10694.44
33-IN	DELCO ELECTRONICS	574236.00	4480105.00	40 feet.	100 GPM	4922117.7
33-IN	DELCO ELECTRONICS	574237.00	4480105.00	40 feet.	100 GPM	1189756.86
63-PS	IN AMERICAN WATER CO	578875.00	4484175.00	140 feet.	500 GPM	20386283.31
63-PS	IN AMERICAN WATER CO	579100.00	4484175.00	120 feet.	500 GPM	3292551.85
63-PS	IN AMERICAN WATER CO	579250.00	4484175.00	78 feet.	500 GPM	12671578.98
63-PS	IN AMERICAN WATER CO	575075.00	4481825.00	295 feet.	500 GPM	2092100.55
63-PS	IN AMERICAN WATER CO	575125.00	4481800.00	300 feet.	500 GPM	1469149.2
63-PS	IN AMERICAN WATER CO	576050.00	4481725.00	325 feet.	500 GPM	37292862
63-PS	IN AMERICAN WATER CO	576050.00	4482025.00	265 feet.	500 GPM	26849737.72
63-PS	IN AMERICAN WATER CO	574825.00	4481800.00	383 feet.	300 GPM	8904461.19
63-PS	IN AMERICAN WATER CO	575700.00	4481950.00	202 feet.	500 GPM	8030190.4
63-PS	IN AMERICAN WATER CO	575500.00	4481500.00	347 feet.	300 GPM	113628.46
63-PS	IN AMERICAN WATER CO	576350.00	4481975.00	50 feet.	300 GPM	9606284.057
63-PS	IN AMERICAN WATER CO	576400.00	4481975.00	49 feet.	300 GPM	2081406.106
63-PS	IN AMERICAN WATER CO	576475.00	4481975.00	49 feet.	300 GPM	5352569.074
63-PS	IN AMERICAN WATER CO	576850.00	4482400.00	72 feet.	300 GPM	15510953.79
63-PS	IN AMERICAN WATER CO	576925.00	4482400.00	62 feet.	500 GPM	16306353.04
22-PS	SOUTHWEST CIVIC ASSOC	567150.00	4477150.00	180 feet.	75 GPM	372968.724
12-IN	MOON FABRICATING CORPORATIO	572950.00	4484100.00	234 feet.	100 GPM	192499.98
50-IR	HENNINGER, TIM	570600.00	4484825.00	108 feet.	550 GPM	282065.9527
63-IR	CHIPPENDALE GOLF COURSE	572000.00	4473150.00	PD	500GPM	606909.68
63-IR	CHIPPENDALE GOLF COURSE	572050.00	4473175.00	PD	500GPM	1138958.254
63-IR	CHIPPENDALE GOLF COURSE	572025.00	4473125.00	PD	500GPM	2160277.628
63-IR	CHIPPENDALE GOLF COURSE	572050.00	4473175.00	PD	100GPM	240624.9833
11-IN	MARTIN MARIETTA MATERIALS, INC	570275.00	4480550.00	OT	3800GPM	134776728.8
11-IN	MARTIN MARIETTA MATERIALS, INC	570325.00	4480550.00	OT	3500GPM	96584194.7
63-PS	IN AMERICAN WATER CO	575700.00	4481950.00	RS	16688GPM	374514071.3

Darcy's law states that:

$$Q = KIA$$

where

Q=volumetric flow rate (volume per time)

K=hydraulic conductivity (length per time)

I = hydraulic gradient (change in head (length) per change in distance (length))

A= cross sectional area of porous medium.

As such, a specific flux for a given area of aquifer (such as the Martin Marietta pit wall) may be realized by either fixing the flux, or fixing the hydraulic gradient in the surrounding formation. As hydraulic conductivity was a variable and calibration target in the flow model calibration process, the authors chose to fix the head within the quarry (having verified that heads in the quarry pumping condition were held near the base of the quarry at the contact with the Mississinewa Shale), and vary hydraulic conductivity in model layer 2 (the highly fractured zone above the base of the Mississinewa which contributes the majority of flow from the quarry) until the appropriate measured quarry pumping rate was realized by the model. In this manner, the authors used the known factors in the equation (head at the quarry base and measured total flow rate out of the quarry) to aid in determining the unknown factor of the layer 2 hydraulic conductivity. This approach was selected because it was more efficient in terms of model operation than specifying pumping at the quarry.

2.6 Recharge

Areal surface recharge to the uppermost aquifer from precipitation was estimated as 2.6 inches per year, based on Smith *et al.* (1985). This recharge was assumed to be uniformly distributed across the model mesh. The recharge is applied to the uppermost saturated zone in the model. Recharge to the model from surface impoundments in the vicinity of the CSSS occurs and is apparent in contours of water levels measured in monitor wells. Due to the large scale of the model, water levels in the vicinity of the lagoons were controlled by the larger hydraulic influence of Wildcat Creek. Recharge flux introduced into the lagoon nodes during modeling became assimilated into the predominant groundwater flow toward the Creek in this area. As such, it was determined that meaningful simulation of recharge from these sources was probably not appropriate with the relatively coarse finite element mesh used in this analysis.

2.7 Model Calibration

2.7.1 Method

Calibration of the groundwater flow model was performed under steady-state conditions, using 1995 water levels measured in on-site monitoring wells as the measured data set. Model hydraulic parameters were varied from initial estimates within reasonable ranges during successive model calibration simulations in order to obtain a reasonable concordance between model-computed and measured water levels, and calculated vs. measured discharge at the Martin Marietta quarry.

2.7.2 Calibration Targets

Due to local variability in measured groundwater elevations, likely as a result of fracture flow patterns, the mean difference in model-computed versus measured water levels was used as a preliminary measure of water level fit in the individual model layers. In using the mean difference of computed and measured water levels, negative differences can cancel out positive differences, resulting in an apparent low average difference. To account for this effect, the standard deviation of the computed differences was also considered as a measure of the absolute difference of measured and computed heads. Groundwater flow rates and velocities are directly influenced by hydraulic gradients. As such, the similarity of measured and computed horizontal and vertical hydraulic gradients in the various model layers was also established as a secondary calibration target. Additionally, the rate of dewatering pumpage from the Martin Marietta quarry was also used as a primary calibration target. Flow from the Martin Marietta quarry was not explicitly simulated as pumping, but by setting fixed heads near the base of the quarry. The flow computed by the model at nodes coinciding with the quarry was then compared with measured flow rates. Calibration fit parameters were not computed for model Layer 1 due to the absence of water level data specific to that zone. Likewise, no calibration was attempted for the drift zone (Layer 6) again due to sparse water level data for this zone. The extreme variability of water levels on a local scale, due mainly to local variations in fractured rock hydraulic properties, limits the ability to obtain very close agreement between the model calculated water levels and observed water levels without a great deal more field data and variation in hydraulic properties.

2.7.3 Calibration Procedure

Model calibration began using the original assumed estimates for vertical and horizontal hydraulic conductivity, anisotropy (as applied to horizontal hydraulic conductivity), surface recharge, and fracture orientation. Calibration proceeded by introducing an offset of the primary axes of horizontal hydraulic conductivity to correspond to the primary fracture system orientation at N80E. An anisotropy ratio of 2:1 for the X:Y horizontal directions was also introduced to account for directional variations in hydraulic conductivity resulting from major and minor directions of fracture orientation as documented in the RI. Subsequent changes were made in an effort to improve the model fit as gauged by the calibration targets presented in Section 2.7.2. Subsequent calibration simulations focused on the hydraulic conductivity of model layer 2 and the manner in which node and element properties were configured in the vicinity of the Martin Marietta quarry pit in order to best simulate the pumping open pit configuration and to approximate the measured dewatering flow from the pit as closely as possible. Hydraulic conductivity of the massive layer 3 limestone and the layer 6 overburden were also adjusted to be more consistent with available data and to improve the overall model fit to the calibration target parameters. The ranges of values used for horizontal and vertical hydraulic conductivity during calibration are summarized in Table 3.

Table 3 Model Calibration - Range of Hydraulic Conductivities (ft/day)				
Model Layer	Description	K_x	K_y	K_z
1	Mississinewa/Silurian	10.0	5.0 - 10.0	0.1
2	Frac. Limestone above Mississinewa	100 - 210.0	62.5 - 105.0	1.0 - 2.10
3	Massive Limestone	2.8×10^{-5} - 0.003	2.8×10^{-5} - 0.0015	2.8×10^{-7} - 0.00003
4	Lower Fractured zone	10.0	5.0 - 10.0	0.1
5	Upper Fractured zone	100.0	50.0 - 100.0	1.0
6	Overburden	10.0 - 100.0	10.0 - 100.0	0.1 - 1.0

Although a rigorous sensitivity analysis was not included within the scope of this modeling task, the ranges of these parameters used in the model calibration provides a general indication of which parameters had the largest influence on water levels during calibration. As indicated in Table 3, the hydraulic conductivity of model layer 2, which controls the rate of flow to the Martin Marietta quarry, had the largest range of variability during calibration, had the largest influence on the overall fit of the model-computed water levels to measured water levels, and was the most sensitive model parameter during calibration.

2.7.4 Calibration Results

Beginning with initial estimates of hydraulic parameters, successive steady-state flow simulations were performed, varying selected model parameters within reasonable ranges to improve the model fit to calibration targets. Model fit improved significantly, and mass balance error was reduced, when the horizontal to vertical anisotropy ratio was increased to 100 from the original assumed value of 10. This ratio was preserved in subsequent simulations. This horizontal to vertical anisotropy ratio is necessary due to the simulation of contrasting permeability layers as single layers, rather than increasing the amount of vertical discretization. To simplify the calibration discussion, only the final simulation has been selected for discussion in detail. Numerous iterations on the calibration process were required to select the final calibrated model.

Hydraulic conductivity was varied to achieve satisfactory agreement between calculated and measured values for head and quarry discharge. The range of this variation was selected based on a review of hydraulic conductivity reported in Smith *et al.* (1985), results of on-site tests and the

scientific literature for aquifer materials of similar lithologic composition, in those cases where no other data was available. During calibration, directional anisotropy was introduced, based on analysis of regional fracture orientation reported in previous studies at the site (CDM 1995). Hydraulic conductivity transverse to the primary direction of flow was reduced by a factor of 2 relative to the hydraulic conductivity along the principal axis of flow in fractured rock layers (model layers 1 - 5). In addition, the principal axis of flow was rotated to coincide with the orientation (strike) of the predominant fracture orientation at the CSSS site, at ten degrees north of east (E10N) (CDM 1995).

Table 4 summarizes the simulation mass balance error, the model-computed flow from the Martin Marietta quarry, the arithmetic mean difference between model-computed and measured heads at observations wells, and the standard deviation of the differences for each model layer.

<p>Table 4 Model Calibration - Head Comparisons</p>					
Calibration Simulation ID	Discharge at Quarry (gpm)	Mass Balance Error (%)	Model Layer	Mean Head Difference (feet)	Standard Deviation (feet)
CSCAL07B	3265	-0.25	2	5.37	17.86
			3	-8.532	14.1
			4	0.738	18.277
			5	-0.524	5.89
			6	-2.1	4.89
Measured Flow from Quarry: 3290 gpm					

The average difference between modeled and measured heads generally improved progressing toward the shallower model layers. A relatively high standard deviation resulted for all model layers due to the high local variability in measured water levels. Such variability is typical of water levels in fractured rock aquifer materials. Vertical gradients computed between the deeper bedrock (model Layer 2) and the upper fractured zone (model Layer 5) at selected monitoring well locations compared well with those computed based on 1993 water levels (CDM 1995) (Table 5). The exception to this fit was most pronounced at the UA-20/LA-08 nest, which is very near the Martin Marietta quarry. The proximity of this nest to the large stress imposed by the quarry on the aquifer system and local variability due to fracture flow limits the ability to fit the observed data at this location.

Table 5 Final Model Calibration - Vertical Hydraulic Gradients			
Monitoring Well Location	Vertical Gradient(Measured, 1993)^a	Vertical Gradient(Measured, 1995)^b	Vertical Gradient(Modeled)^c
UA-01/LA-01	0.03	-0.01	0.11
UA-17/LA-06	0.38	0.39	0.52
UA-20/LA-08	0.86	0.88	-0.03

^a Based on values reported in CDM (1995). Positive gradient indicates downward flow

^b Based on November 1995 water level measurements

^c Based on model simulation CSCALO7B results.

Final calibrated hydraulic parameters are summarized in Table 6. Model boundary conditions, regional pumping levels, and surface recharge were not changed from the original estimates.

Table 6 Final Calibrated Hydraulic Conductivities (ft/day)				
Model Layer	Description	K_x	K_y	K_z
1	Mississinewa/Silurian	10.0	5.0	0.1
2	Frac. Shale above Mississinewa	210.0	105.0	2.10
3	Massive Limestone	0.003	0.0015	0.00003
4	Lower Fractured zone	10.0	5.0	0.1
5	Upper Fractured zone	100.0	50.0	1.0
6	Overburden	10.0	10.0	0.1

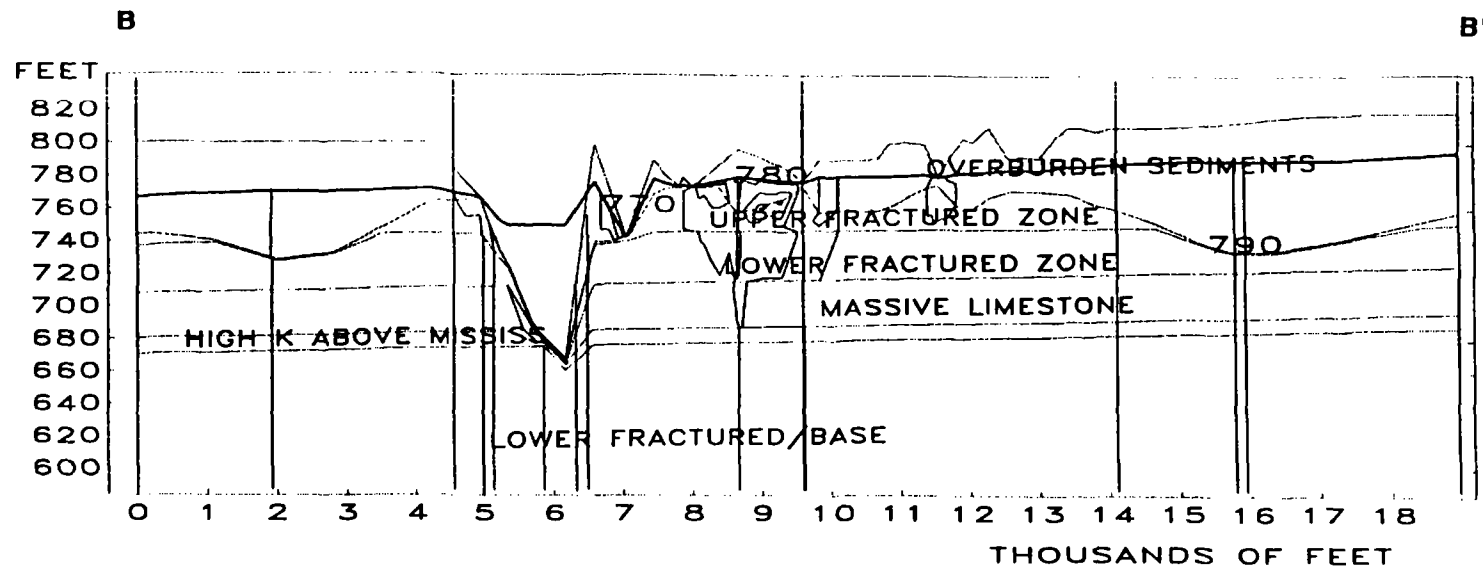
The configuration of the calibrated potentiometric surface in the area of the site is shown on Figures 11 to 13 for layers 5, 4 and 2 respectively. As can be seen by these figures, the flow regime in the vicinity of the site is dominated by the discharge to Kokomo and Wildcat creeks and the pumping at the Martin Marietta quarry. Figure 14 shows a cross-section with potentiometric contours and flow vectors plotted running through the site and the quarry.

An additional steady state flow field was developed to assess what the affects on groundwater flow directions might be if dewatering at the quarry were shut down in the future and the pit was allowed to fill. This simulation used all of the previous parameters, with the exception that the fixed heads to represent quarry pumping were disabled and the resulting steady state flow field calculated. Figures 15 to 17 show resulting potentiometric surfaces for layers 5, 4 and 2 respectively.

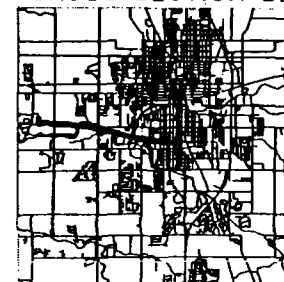
Figure 18 shows the same cross-section presented previously for the new conditions. This case indicates that the discharge to streams will control the flow direction.

Results of the flow modeling were used to develop velocity fields to simulate contaminant transport at the site as described in the next section. The results of the flow modeling show that the site conceptual model, as implemented in the numerical model is capable of approximately reflecting the flow field observed at the site using hydraulic parameters that are within an acceptable range of those measured. The use of porous media equivalent to describe the flow system adequately reproduces the principal features observed at the site, including very close approximation of discharge to the Martin Marietta quarry.

The model calibration adequately meets the stated goals of reconnaissance level modeling for estimation of potential concentrations at receptor locations under alternative flow regimes and for comparison of potential remedial alternatives in the FS.



CROSS SECTION BB'



DATE/TIME: DYNPLOTB
PLOTTED: DYNPLOTB
CREATED: DYNPLOTB
DATE/TIME: 4/15/96 13:39
SAVE FILE: CSCAL08C.SVT

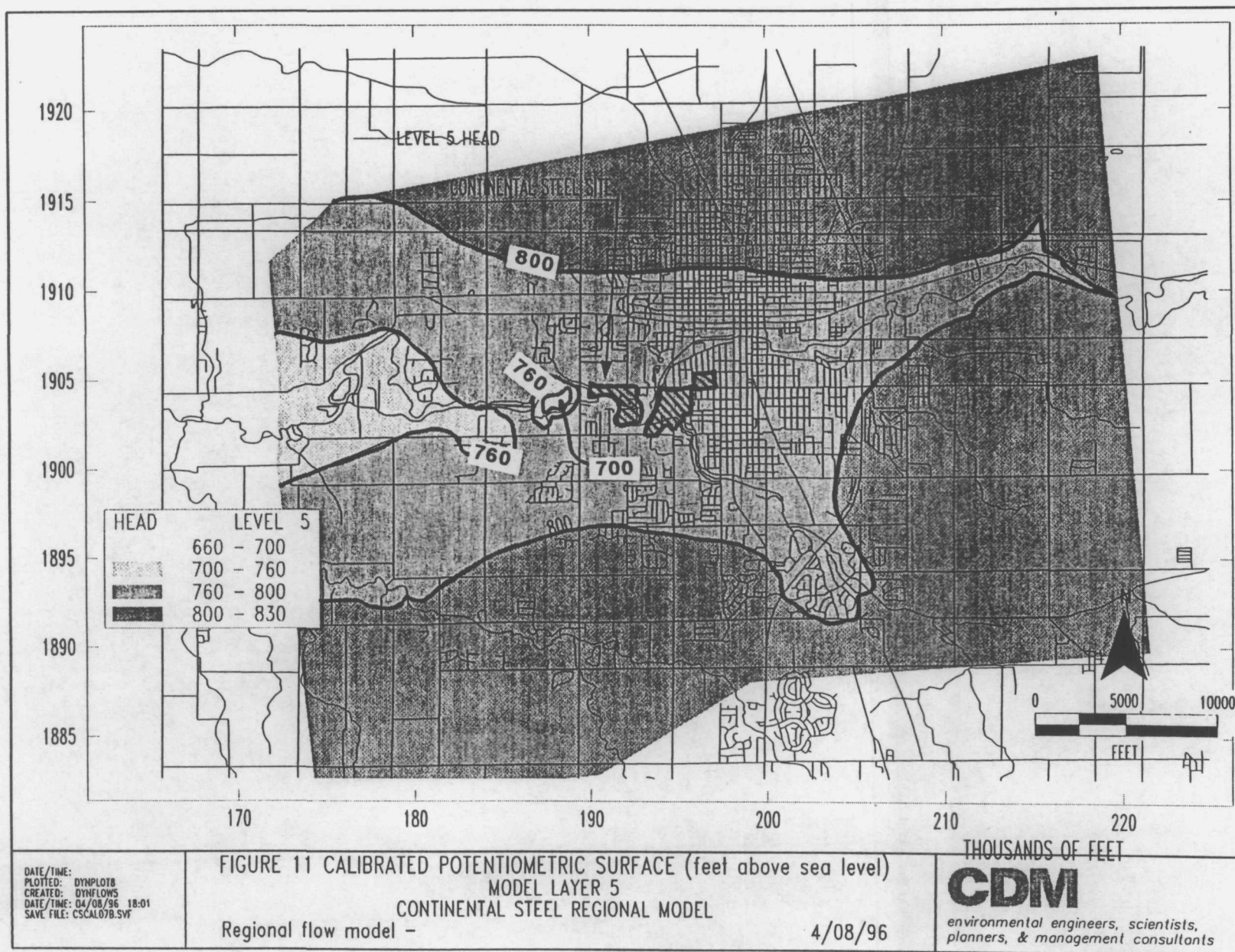
FIGURE 18 CROSS SECTION BB - NO QUARRY PUMPING
CONTINENTAL STEEL REGIONAL MODEL
KOKOMO, INDIANA

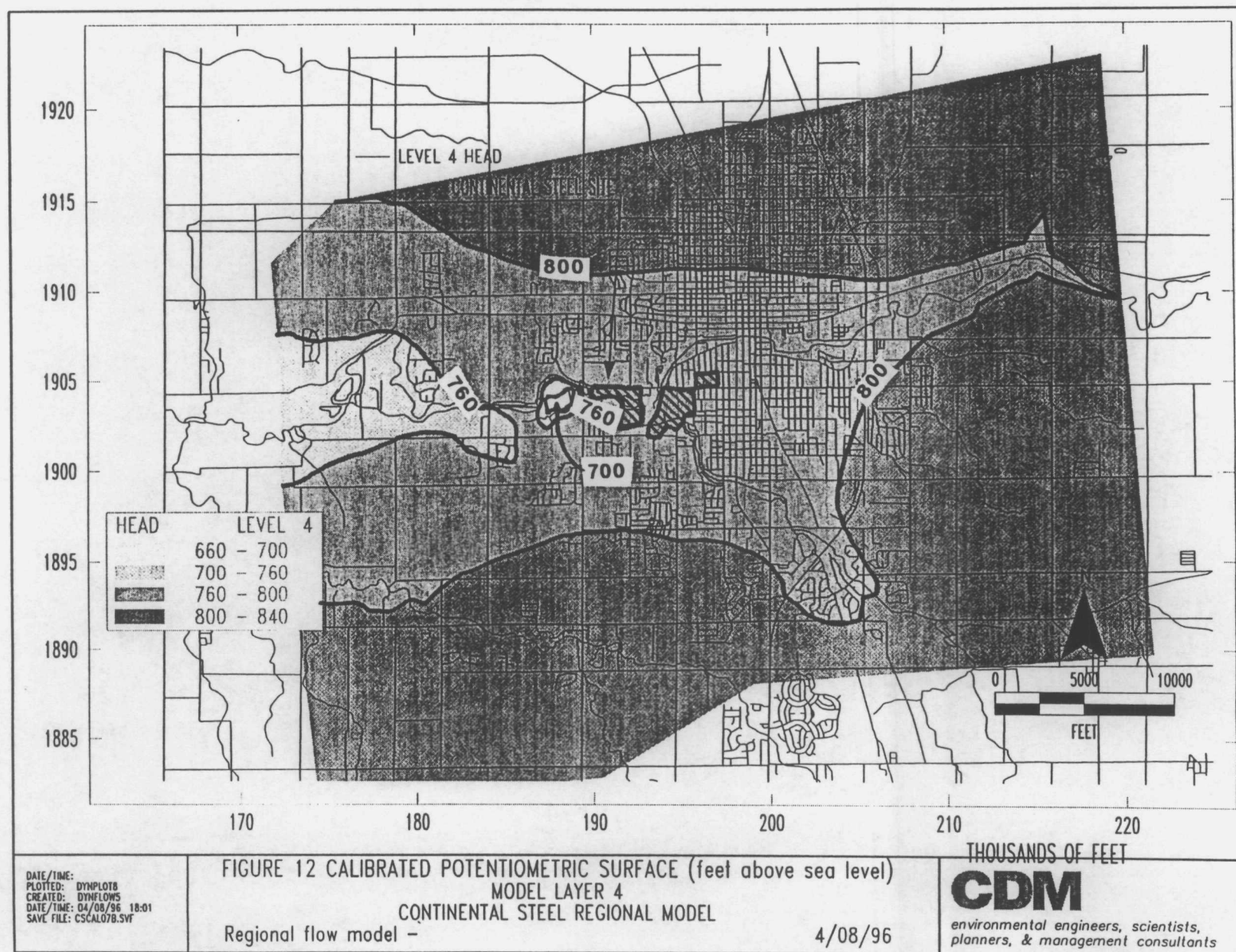
Regional flow model -

4/09/96

CIDMI

environmental engineers, scientists,
planners, & management consultants





3 Contaminant Transport Model

3.1 Purpose

Contaminant transport modeling was performed to achieve the following objectives:

- Characterize groundwater flow pathways between suspected source areas and potential receptors.
- Estimate potential concentrations of the selected target chemicals TCE and PCE at specific receptor points.
- Evaluate the effect of the Martin Marietta quarry pumping on groundwater flow pathways and receptor point contaminant concentrations.

This contaminant transport modeling is done at a reconnaissance level of detail sufficient to meet the objectives of the modeling. The solute transport model incorporated advection and dispersion, but not degradation or sorption.

3.1a DYNTRACK Model

The computer code DYNTRACK was used for analysis of solute transport. DYNTRACK is a computer program for the simulation of three-dimensional contaminant transport, and is the companion code for DYNFLOW. DYNTRACK uses the same three-dimensional finite element grid representation of aquifer geometry, flow field, and stratigraphy developed for a particular application of the DYNFLOW model.

DYNTRACK simulates the movement of dissolved contaminants in the saturated zone using the calibrated flow fields generated by DYNFLOW. DYNTRACK can perform either simple, single particle tracking of advective flow, or can model three-dimensional contaminant transport with advection, dispersion, adsorption, desorption and first-order decay of constituents. Solute transport simulation uses the random walk method with large numbers of particles to represent advection and dispersion processes. Advective flow particle tracking was simulated to evaluate groundwater flow pathlines to potential receptors. Solute transport was simulated to estimate potential concentrations of the selected constituents PCE and TCE at receptor points. **Appendix C** provides more detail on the capabilities and mathematical basis for this model.

3.2 Conceptual Model and Source Characterization

Suspected source areas include the Markland Quarry, the Main Plant area, the vicinity of the Fence Plant, the Lagoon Area and the vicinity of Haynes International Inc. Defenbaugh Street Operations

As solute transport model calibration was not within the scope of the RI modeling, sensitivity simulations of solute transport varying the dispersivity over a range of values was not performed.

Transverse dispersivity was also estimated from typical ranges of the transverse to longitudinal dispersivity ratio reported in the literature. A study performed by Bredehoeft (1976) for a variety of hydrogeologic settings, including fractured limestone, reported a range of 0.2 to 1.0 for this ratio. A ratio of approximately 0.3 was the most prevalent in this report (including the fractured limestone evaluation), and was adopted for use in this analysis. As such, transverse dispersivity was approximated as one-third that of the longitudinal dispersivity at 10 feet.

Effective porosity and anisotropy properties of the aquifer materials were similarly estimated from the scientific literature for materials of similar properties (Mercer *et al.*, 1982). The effective porosity of the fractured material was assumed to be 10 percent. Effective porosity of the overburden material was assumed to be 20 percent. Vertical to horizontal anisotropy for dispersivity was assumed to be 0.01.

These assumptions lead to development of a very conservative estimate of potential concentrations at downgradient receptors. Several processes operating at the site will attenuate concentrations of these constituents by the time they reach receptors or points of discharge. Anaerobic degradation of chlorinated solvents is taking place at the site, as evidenced by the presence of cis-1,2-dichloroethylene and vinyl chloride. Sorption of the contaminants of concern will also take place on organic carbon likely to be present in the fractures through which transport takes place. Clay minerals and other large surface area contributors such as complex iron hydroxides are also likely present and will serve as sorption sites that will attenuate the movement of contaminants in the subsurface. Matrix diffusion processes where concentration gradients in the active flow pathways drive contamination into pore space in the unfractured rock will also be a significant source of attenuation that will delay movement of contaminants to potential receptors.

3.4 Contaminant Transport Simulations

Contaminant transport was simulated initially by tracking single particles from identified source areas to characterize groundwater flow paths and velocities. This was followed by explicit solute transport simulation of dissolved TCE and PCE in groundwater. Both of these methods of contaminant transport simulation used the computed steady-state groundwater flow fields both for the Martin Marietta quarry pumping and for the flow field with the quarry not pumping. In total, six simulations were performed, summarized as follows:

1. Case A: Particle tracking from selected source areas - Martin Marietta quarry pumping.
2. Case B: Particle tracking from selected source areas - Martin Marietta quarry not pumping.
3. Case C: Solute transport of TCE - Martin Marietta quarry pumping.
4. Case D: Solute transport of PCE - Martin Marietta quarry pumping.

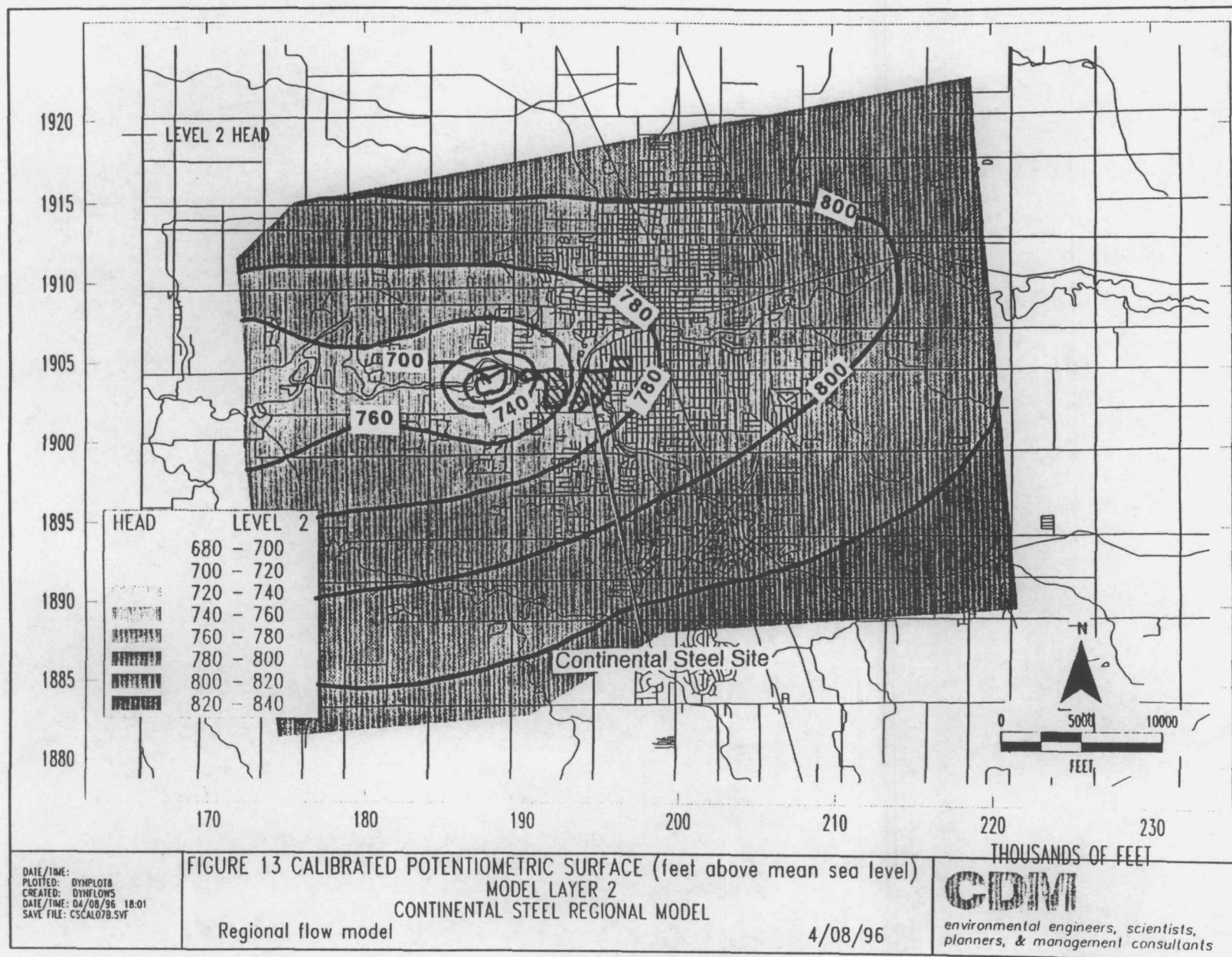
5. Case E: Solute transport of TCE - Martin Marietta quarry not pumping.
6. Case F: Solute transport of PCE - Martin Marietta quarry not pumping.

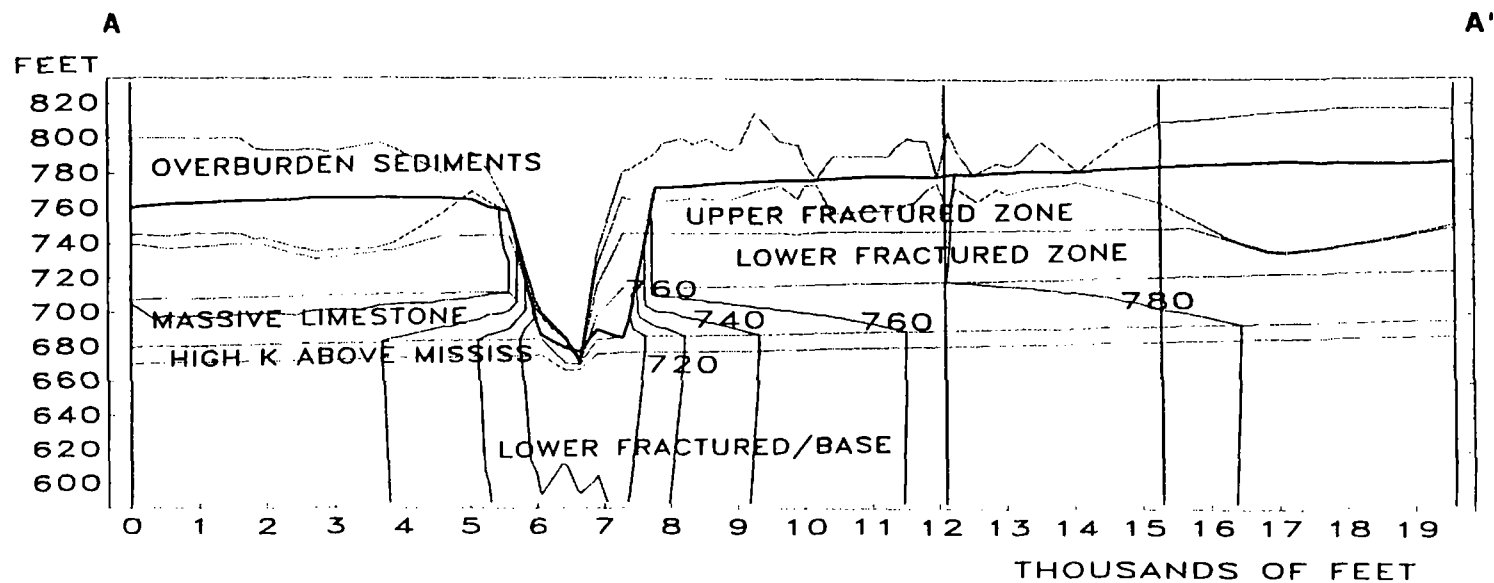
3.4.1 Particle Tracking Simulations

Particle tracking simulations were performed by introducing groundwater particles within model layers in which contamination was recorded based on monitoring well data at the following locations:

- Markland Quarry (suspected TCE source) - Layer 5
- Fence Plant near Well UA-06 (suspected PCE source) - Layer 5
- Vicinity of Wells LA-04 and UA-11 (suspected TCE source) - Layers 2, 4 and 5
- Vicinity of Well LA-07 (suspected TCE source) - Layer 5
- Vicinity of Well EW-08 (suspected source, compound uncertain) - Layer 6
- Slag Processing Area Landfill near Well EW-23 (suspected source, compound uncertain) - Layers 4 and 5
- Haynes International, Inc. vicinity near Well SP-07A (suspected PCE source) - Layer 5

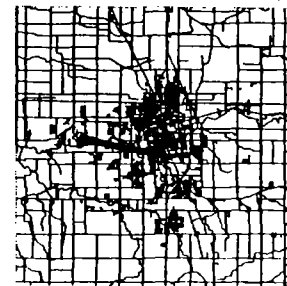
Particle tracking simulations were performed in order to gain a conceptual view of where particles introduced at the locations of the suspected source areas migrated horizontally. Particles were introduced at the seven locations within layers where they were believed to enter the groundwater system, based on available data. These source introduction layers included all but model layers 1 and 3, representing the low permeability units of the Mississinewa Shale/Silurian dolomite and the massive Liston Creek B Limestone interval, respectively. The low hydraulic conductivity of these zones and their locations within the stratigraphic section make them unlikely candidates for points of source introduction. Once introduced, the vertical migration of the particles within the tracking algorithm was not restricted to specific layers. Particles were introduced at these locations and tracked through the flow field for a period of 50 years. Plots of the particle flow paths emanating from these sources for the two flow field scenarios are presented in Figures 19 and 20. Figure 19 illustrates particle flow paths for Case A, Martin Marietta quarry pumping. Figure 20 illustrates particle flow paths for Case B, Martin Marietta quarry not pumping. Though these plots represent primarily horizontal flow, particles are also free to move in the vertical plane along these paths in response to vertical hydraulic gradients. In these plots, square symbols represent particle starting positions. Cross symbols represent intermediate particle locations during the simulation. Asterisk symbols represent positions where particles exit the subsurface flow system. Particles exit the system at both the quarry and at Wildcat Creek in Case A (Figure 19). Particles exit the system at nodes coinciding with Wildcat Creek (Figure 20) in Case B.





— HEAD

CROSS SECTION AA'



DATE/TIME:
PLOTED: DYNPLOT8
CREATED: DYNFLOW5
DATE/TIME: 04/08/96 18:01
SAVE FILE: CSCAL07B.SVF

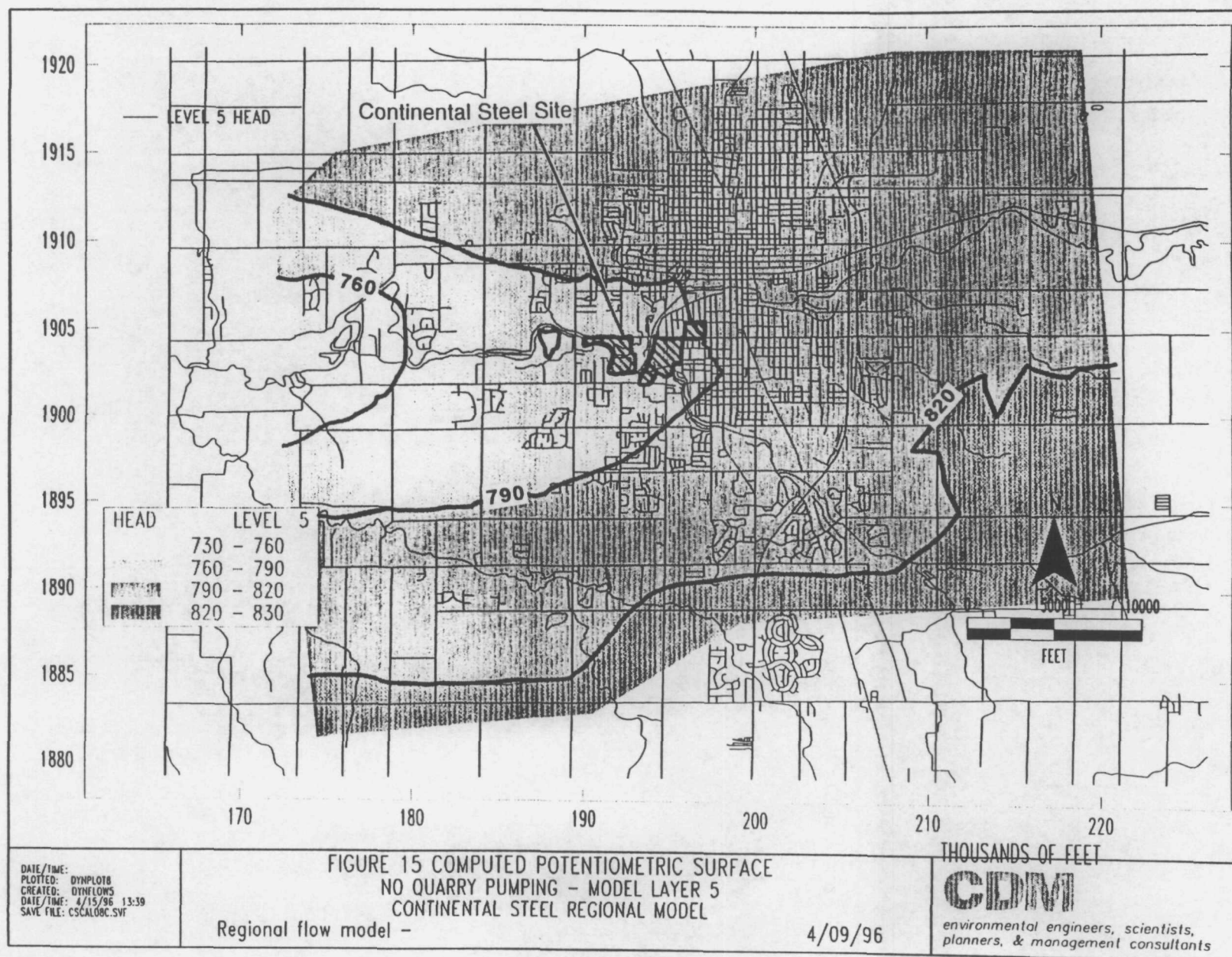
FIGURE 14 CROSS SECTION AA'
CONTINENTAL STEEL REGIONAL MODEL
KOKOMO, INDIANA

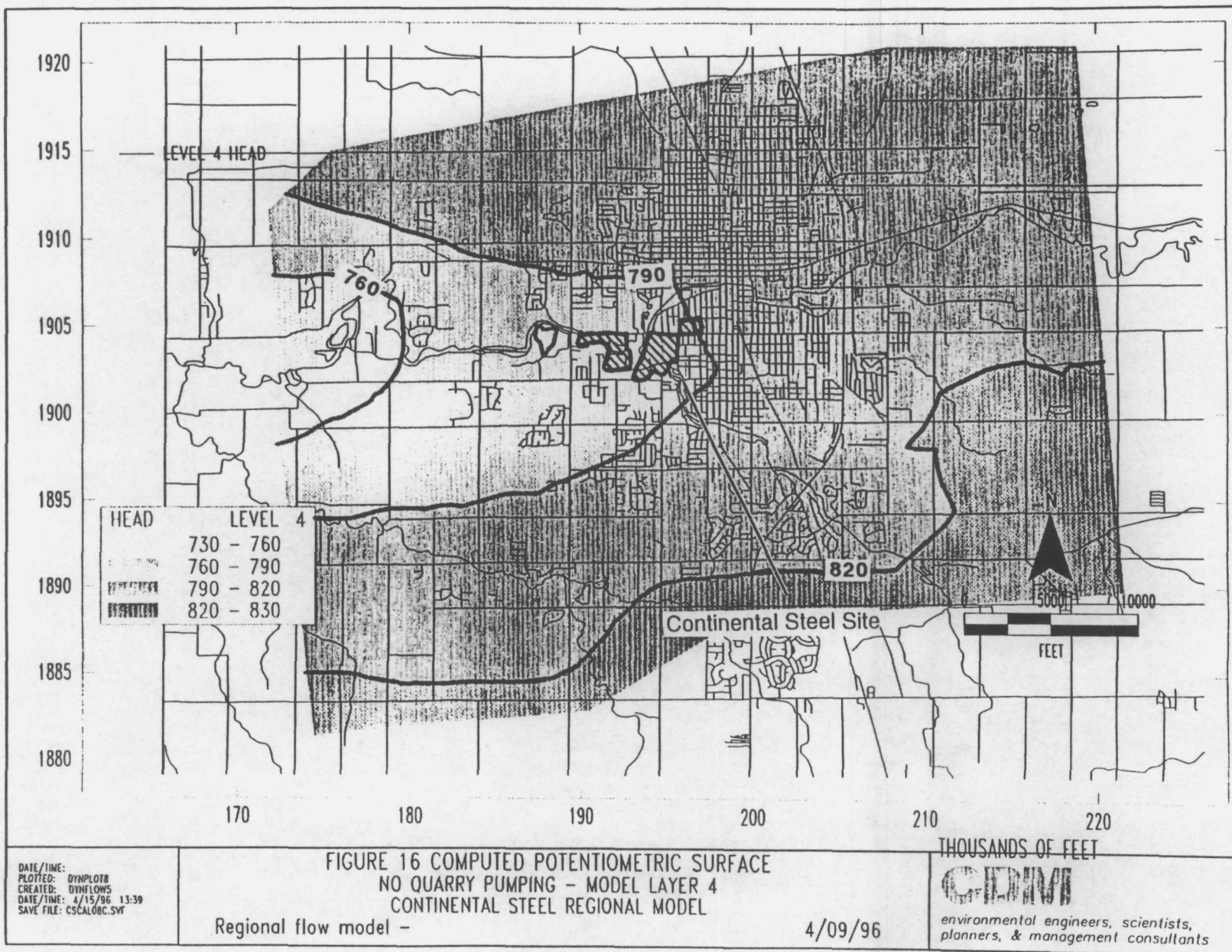
Regional flow model -

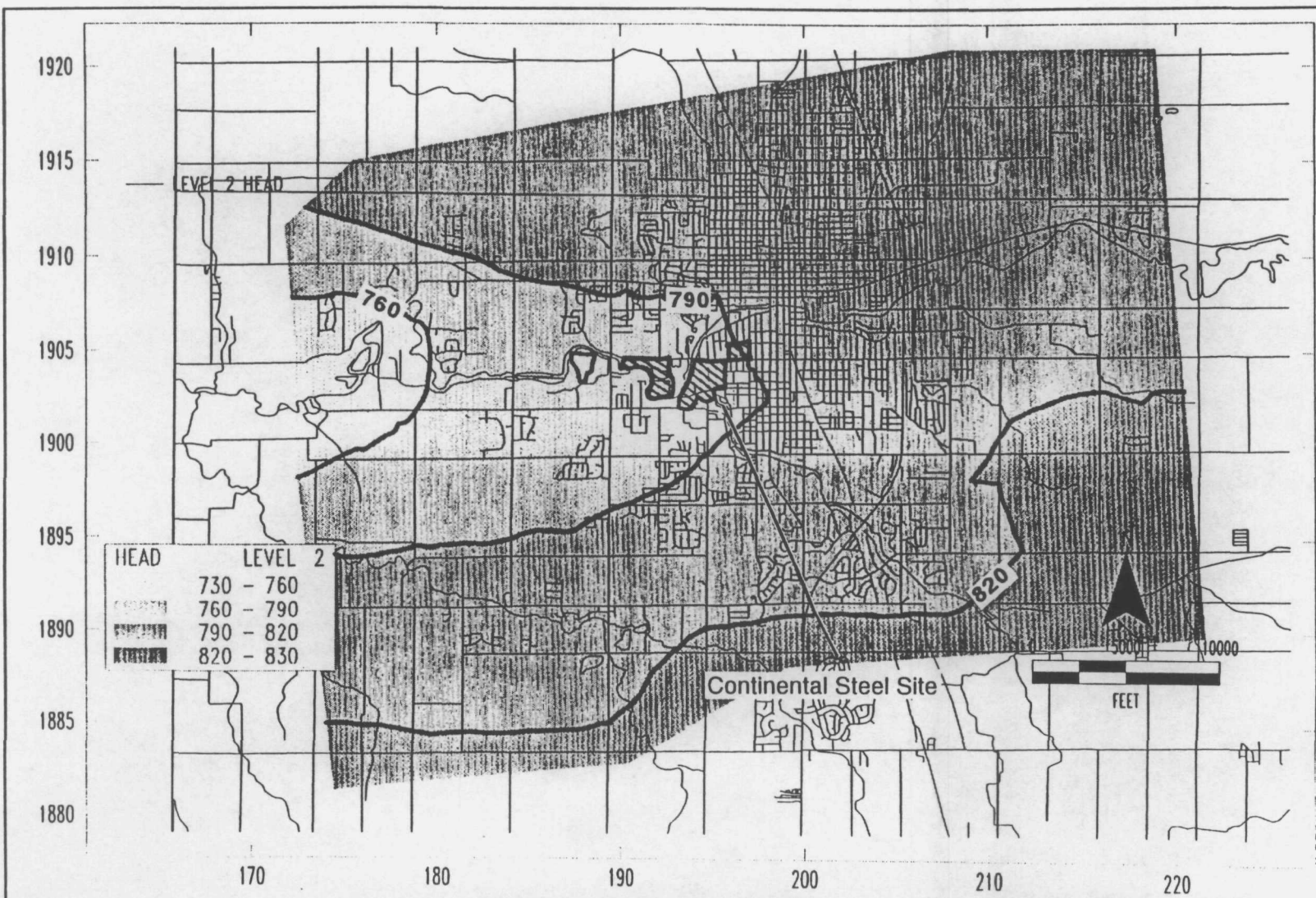
4/08/96

CIDM

environmental engineers, scientists,
planners, & management consultants







DATE/TIME:
 PLOTTED: DYNPLOT8
 CREATED: DYNFLOWS
 DATE/TIME: 4/15/96 13:39
 SAVE FILE: CSCAL08C.SVF

FIGURE 17 COMPUTED POTENTIOMETRIC SURFACE
 NO QUARRY PUMPING - MODEL LAYER 2
 CONTINENTAL STEEL REGIONAL MODEL

Regional flow model -

4/09/96

THOUSANDS OF FEET



environmental engineers, scientists,
 planners, & management consultants

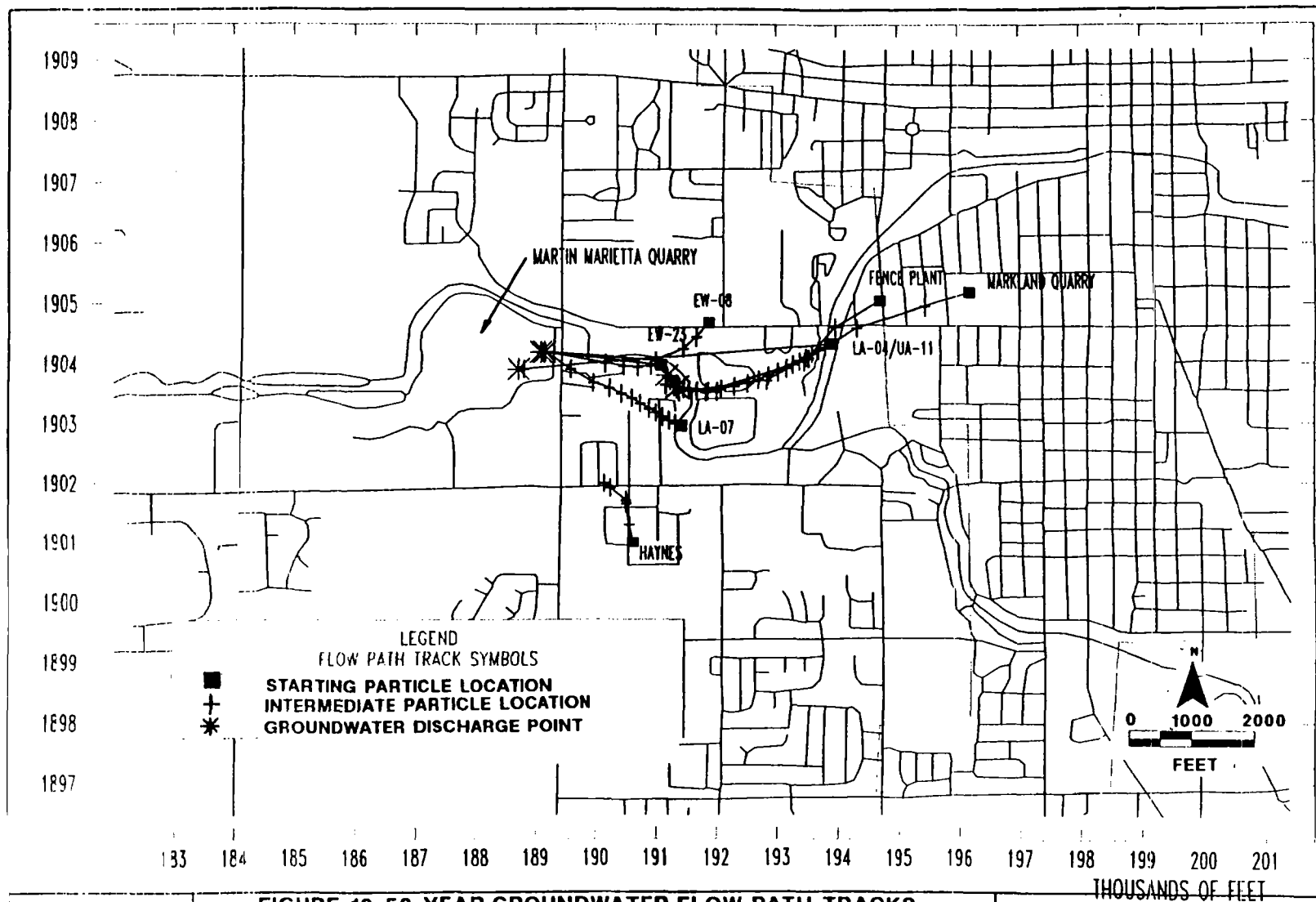


FIGURE 19 50 YEAR GROUNDWATER FLOW PATH TRACKS
(CASE A QUARRY PUMPING
CONTINENTAL STEEL REGIONAL MODEL

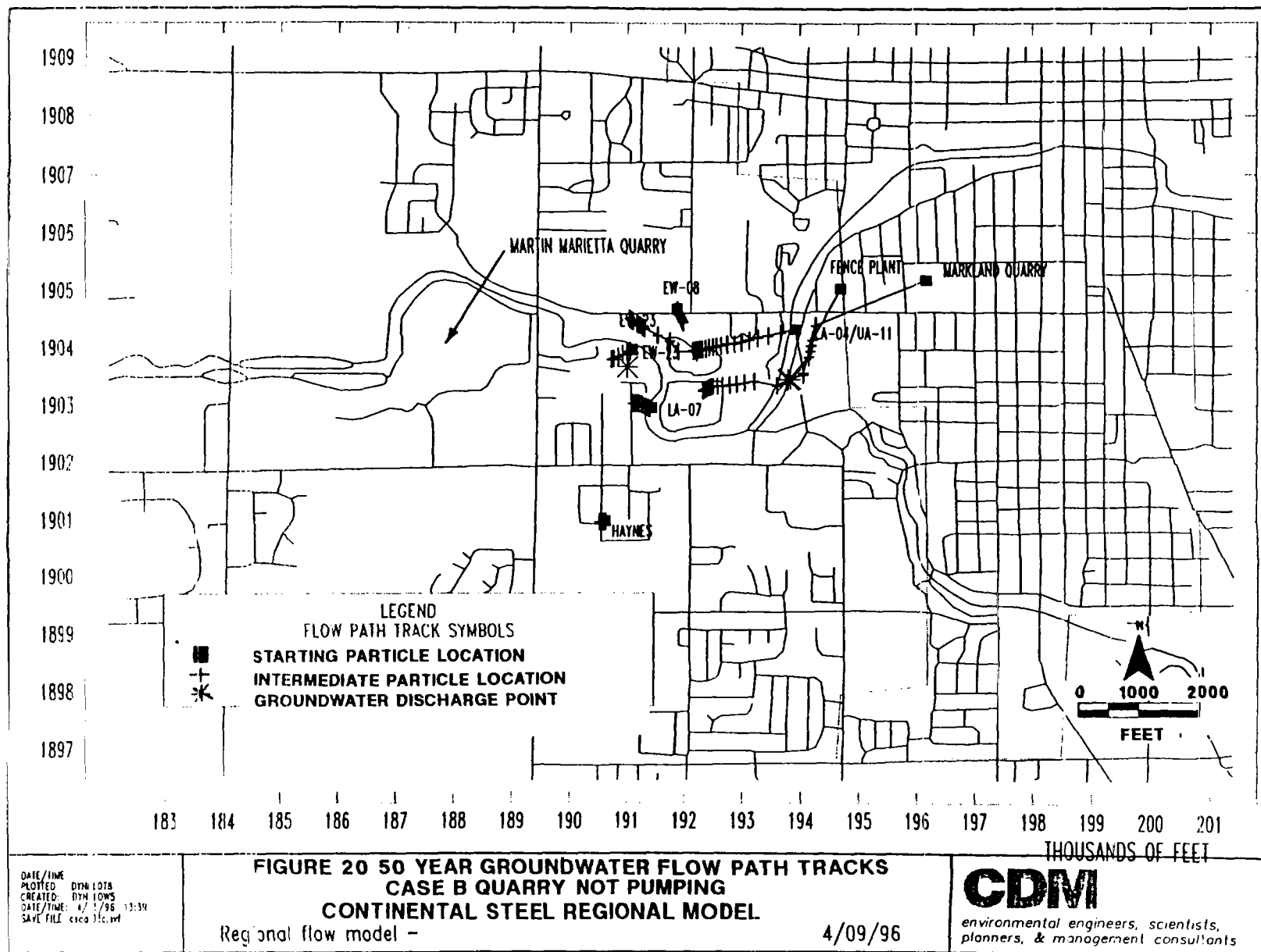
Regional flow model -

4/09/96

CDM

environmental engineers, scientists,
 planners, & management consultants

DATE/TIME:
 PLOTTED: 11/10/96
 CREATED: 11/10/96
 DATE/TIME: 11/15/96 13:39
 SAVE FILE: c:\at\bc.vt



In Case A, all of the simulated particle flow paths move toward the quarry. As observed in the water level contours, the Martin Marietta quarry controls the flow path tracks in the vicinity of the site, (Figure 19). The flow path originating at the well LA-04 location in Case A within Layer 2 moves more directly toward the quarry due to the smaller influence of Wildcat Creek on groundwater flow direction at deeper levels. In Case B, groundwater particles generally do not travel as far as in Case A, due to the lower gradients when the quarry is not pumping, but still follow regional groundwater flow in a generally westward direction, and toward the main channel of Wildcat Creek (Figure 20).

It is noted that contaminant concentrations have been detected in a domestic well, DW-282, located approximately 800 feet north of well EW-09 in the Slag Processing Area. Since well construction information and pumping records were not available for well DW-282, this well was not included as a pumping well in the model. The movement of contamination from known sources to the DW-282 location north of Markland Avenue is not projected by the model. Since this groundwater model is intended to provide a reconnaissance level of detail, this model does not depict localized particle tracking due to potential mounding of the groundwater in the Lagoon Area, preferential flow along localized fractures, and/or influences of pumping from DW-282, all of which may be contributing to the actual detection of contaminants in water samples from this well. Additional modeling undertaken during the FS will include active surface contaminant source terms, which may significantly alter contaminant transport projections for this area.

3.4.2 Contaminant Transport Simulations

Groundwater monitoring results for the CSSS were compiled and tabulated. Values for TCE and PCE for monitoring wells were compiled and identified by model layer (Table 7). These concentrations were contoured using a quadratic interpolation function, with the resulting estimated values used as the initial concentration in the appropriate model layers (Figures 21 through 25b). The initial concentration contour maps were discretized over the model mesh such that individual mesh nodes were assigned initial concentration values. The concentration contour maps generated by the interpolation function are approximate away from the monitoring well data points. Contaminant transport simulations were performed for each of the two compounds using each of the two steady-state flow fields (Cases C through F) over a period of 50 years.

Projected concentrations for each of the contaminant transport simulations after 20 years of simulated contaminant transport are presented in Figures 26 through 35. These figures provide a snapshot of what distributed concentrations of PCE and TCE may prevail in 20 years, assuming source control has been enacted, but no further remedial action has been taken. The time horizon of 20 years was selected as representative of solute transport pathways for the two flow scenarios. In Case C and D, initial TCE and PCE concentrations generally follow advective flow pathways toward the Martin Marietta quarry. Maximum TCE concentrations of approximately 1,020 $\mu\text{g/l}$ are observed in the vicinity of the quarry in Layer 4 after 20 years in Case C (Figure 27). The relatively high projected TCE concentrations in Layer 4 suggest vertical transport of TCE from Layer 5 to Layer 4 is occurring due to the strong vertical downward gradients induced by quarry pumping. Initial TCE concentrations in Layer 2 are advected laterally toward the quarry (Figure 28). The same general trends are observed for PCE in Case D (Figures 29, 30 and 30b). This analysis indicates that

quarry pumping is the dominant process controlling movement of contaminants at the site. Contamination originating in the main plant area and Markland quarry partially flows under Wildcat Creek toward the quarry, with some loss to the creek. Locations which receive discharge from groundwater for the conditions where the quarry is pumping include Wildcat Creek in the reach from the plant site to just below the Haynes International, Inc. facility west of the lagoons, and the Martin Marietta quarry itself. The Martin Marietta quarry is the dominant mechanism for mass removal in the vicinity of the site.

In Cases E and F, initial concentrations of TCE and PCE are generally more dispersed, and do not travel as far from original source areas toward the Martin Marietta quarry, due to the absence of pumping from the pit (Figures 31 through 35). Discharge to Wildcat Creek is the major mechanism controlling movement of contaminants to the surface. Localized areas north and east of the lagoon area shows increased concentrations in model Layer 4 at 20 years, resulting from downward migration in this area (Figure 32). A similar occurrence is observed in this area with respect to PCE concentrations in Layer 4 at 20 years (Figure 35).

All of these simulations assume that no additional source contribution of mass takes place to the aquifer and that advective transport of contaminants currently in groundwater takes place.

Concentrations at potential receptor locations would remain at the peak for a longer period of time if sources continue to contribute.

Additional groundwater quality data is being compiled which will be included in revising the interpretation of the initial concentration plume maps. Future contributions of the source areas will be calculated during the FS.

3.5 Summary of Contaminant Transport Modeling

Based on these simulations, the following conclusions are presented:

- Contaminant transport in the vicinity of the CSSS is controlled by the major hydraulic influences of the Martin Marietta quarry pumping, and Wildcat and Kokomo Creeks.
- Simulated groundwater flow path tracks and dissolved contaminants TCE and PCE are generally confined to a central contaminant transport pathway following the course of Wildcat and Kokomo Creeks in the westerly direction. Transport pathways do not diverge significantly from site source areas to the north or south of this main transport pathway.
- Capture of contaminated groundwater originating on the CSSS by domestic wells in a subdivision located southwest of the site is unlikely under either of the quarry operational scenarios.

The groundwater model as calibrated succeeds in simulating the regional groundwater flow system in the vicinity of the Continental Steel site, including six hydrogeologic units, surface water features, pumping wells, and a heavily pumping quarry pit.

Additional fate and transport analyses will be performed using the model developed as described herein, during the FS. A quantitative risk assessment will also be performed using the model during the time frame of the FS. The model will prove a valuable tool in addressing these key elements of the FS.

Table 7 Initial Solute Concentrations								
Well ID	Easting	Northing	Model Layer	Date	PCE (ug/l)	PCE_qual	TCE (ug/l)	TCE_qual
LA-08E	189971.42	1904277.28	L2	8/14/93	21	U	21	
LA-04E	183942.81	1904305.16	L2	8/20/93	250	U	2830	
LA-08B	189971.42	1904277.28	L4	12/7/95	0	U	110	
LA-02C	195770.37	1905394.65	L4	8/28/93	0	U	12	
LA-02A	195770.37	1905394.65	L4	12/2/95	0	U	15	
EW-17	190864.52	1904055.93	L4	11/30/95	99	E	40	
EW-18	191332.45	1903414.01	L4	11/30/95	0	U	1300	
EW-15	190897.69	1903789.72	L4	11/30/95	0	U	3	
EW-17	190864.52	1904055.93	L4	1/18/93	0		22	
UA-20	188566.89	1903984.82	L4	8/16/93	2		5	
EW-18	191529.93	1903378.76	L5	4/12/93	460		98	
EW-19	190752.77	1903934.36	L5	4/12/93	41700		5400	
EW-20	190862.62	1904053.05	L5	1/8/92	15.5		9.4	
EW-06	191549.16	1903924.34	L5	11/29/95	4		1	
EW-07	191602.15	1904179.51	L5	8/11/93	0	U	3	
EW-09	191026.4	1904252.13	L5	8/11/93	0	U	2	
EW-11	191541.74	1902784.93	L5	11/29/95	0	U	4	
EW-13	188706.14	1904831.38	L5	8/16/93	0.5	J	0.5	
EW-18	191529.93	1903378.76	L5	11/30/95	350	D	140	
EW-19	190752.77	1903934.36	L5	8/3/93	3300	EJBF	1700	
EW-20	190862.62	1904053.05	L5	8/24/93	22		9	
EW-21	191350.21	1903997.25	L5	6/1/93	5	UJBF	5	
EW-23	190886.18	1904072.8	L5	6/1/93	5	UBF	5	
EW-28	192808.64	1904544.69	L5	11/30/95	2		110	
EW-33	194543.96	1903417.86	L5	8/27/93	0	U	3	
LA-06	195055.04	1905329.79	L5	11/29/95	490	E	150	
LA-11	193934.29	1904264.72	L5	8/17/93	290		520	
LA-28	195355.24	1908162.09	L5	11/29/95	600	D	370	D
LA-29	194498.99	1905586.43	L5	11/29/95	48	D	14	
LA-30	194317.54	1905004.46	L5	11/29/95	1900	D	250	D
LA-32	193160.25	1904929.01	L5	12/13/95	0	U	660	D
EW-22	191236.42	1904078.85	L6	6/1/93	410	BF	5	
EW-22	191236.42	1904078.85	L6	4/13/93	100		15	
EW-08	192013.69	1904507.97	L6	11/29/95	0	U	550	
UA-22	196475.54	1905060.57	L6	11/29/95	0	U	440	D
EW-30	193126.15	1902775.28	L6	8/12/93	0	U	3	

B = Indicates the analyte was found in the associated blank as well as the sample.

D = Indicates all compounds identified in an analysis at a secondary dilution factor.

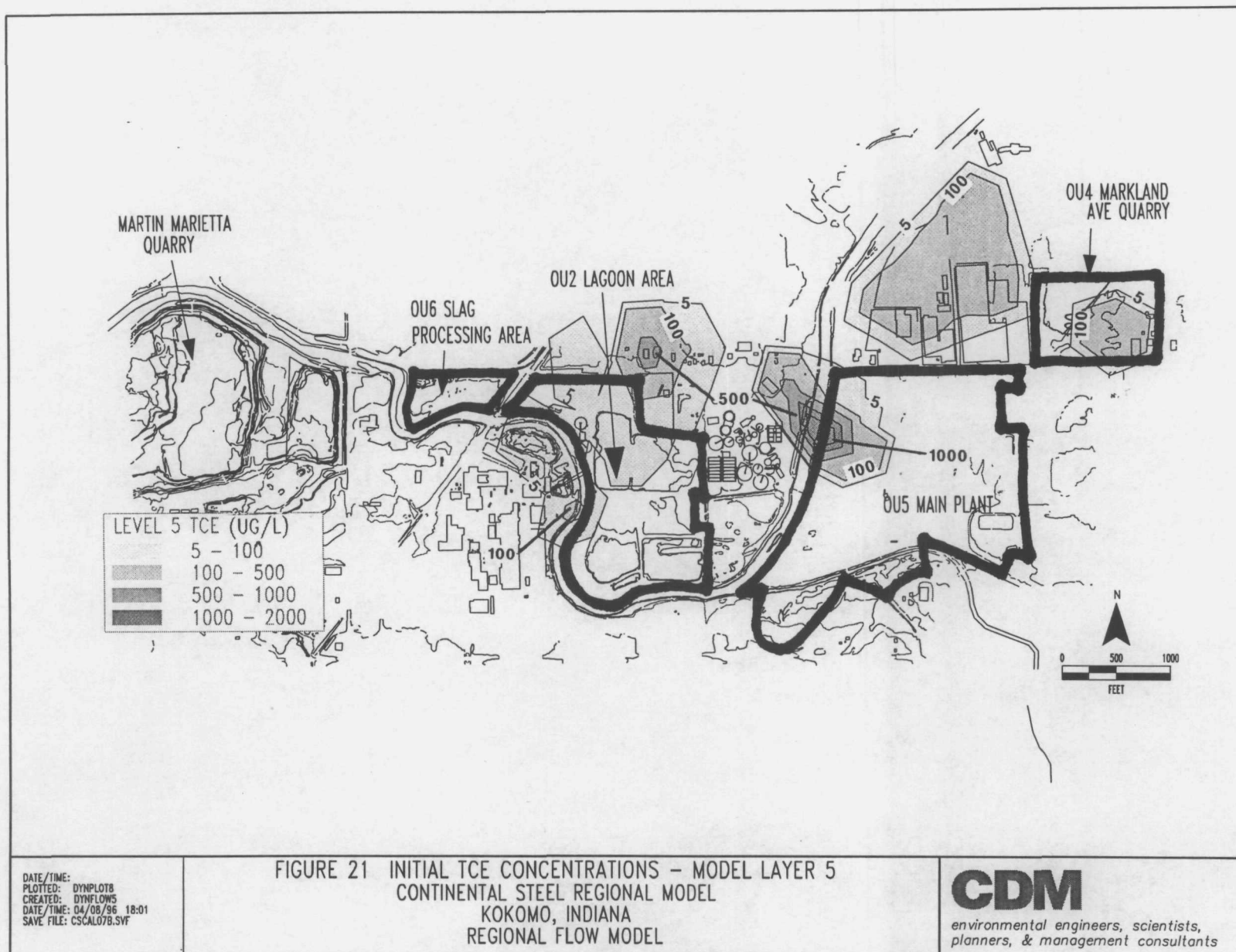
E = Indicates compounds whose concentrations exceed the calibration range of the GC/MS instrument for that specific analysis.

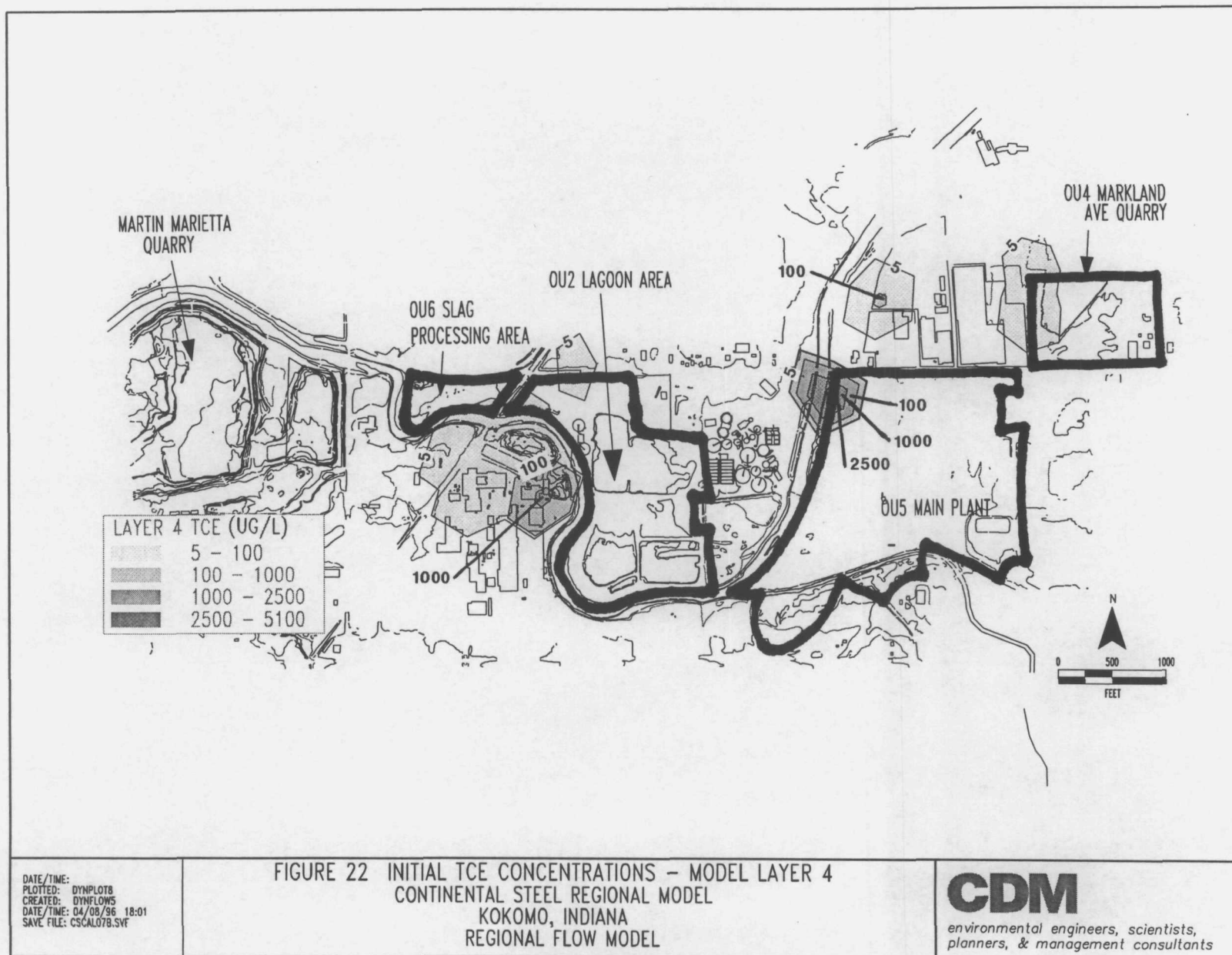
F = Data generated using Field Analytical Services Program using fast analytical methodologies. Analytes are tentatively identified and concentrations are quantitative estimates.

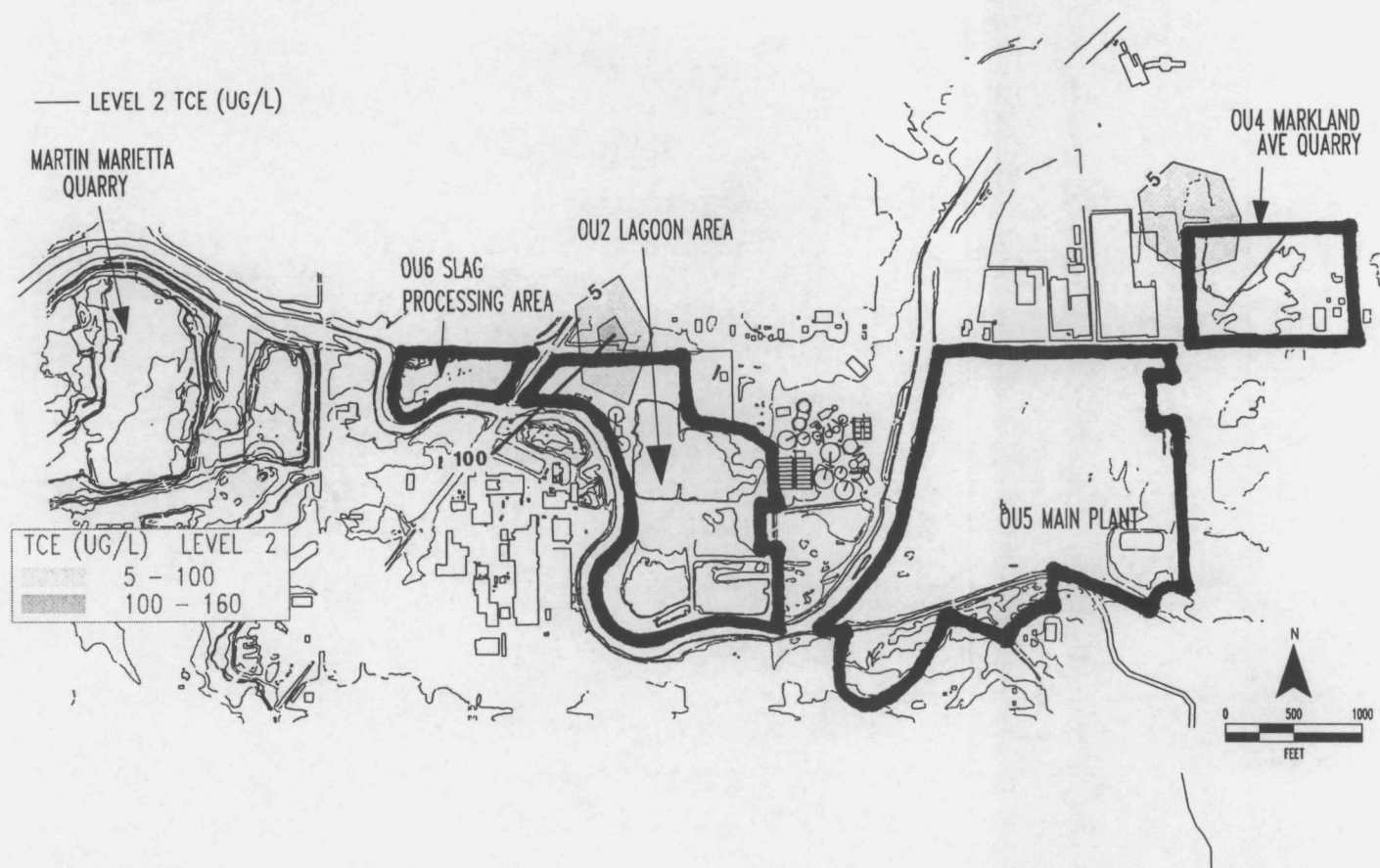
J = Indicates an estimated value.

U = Indicates compound was analyzed for but not detected.

Note: Data compiled prior to 1995 generated by ABB Consultants, and Haynes International





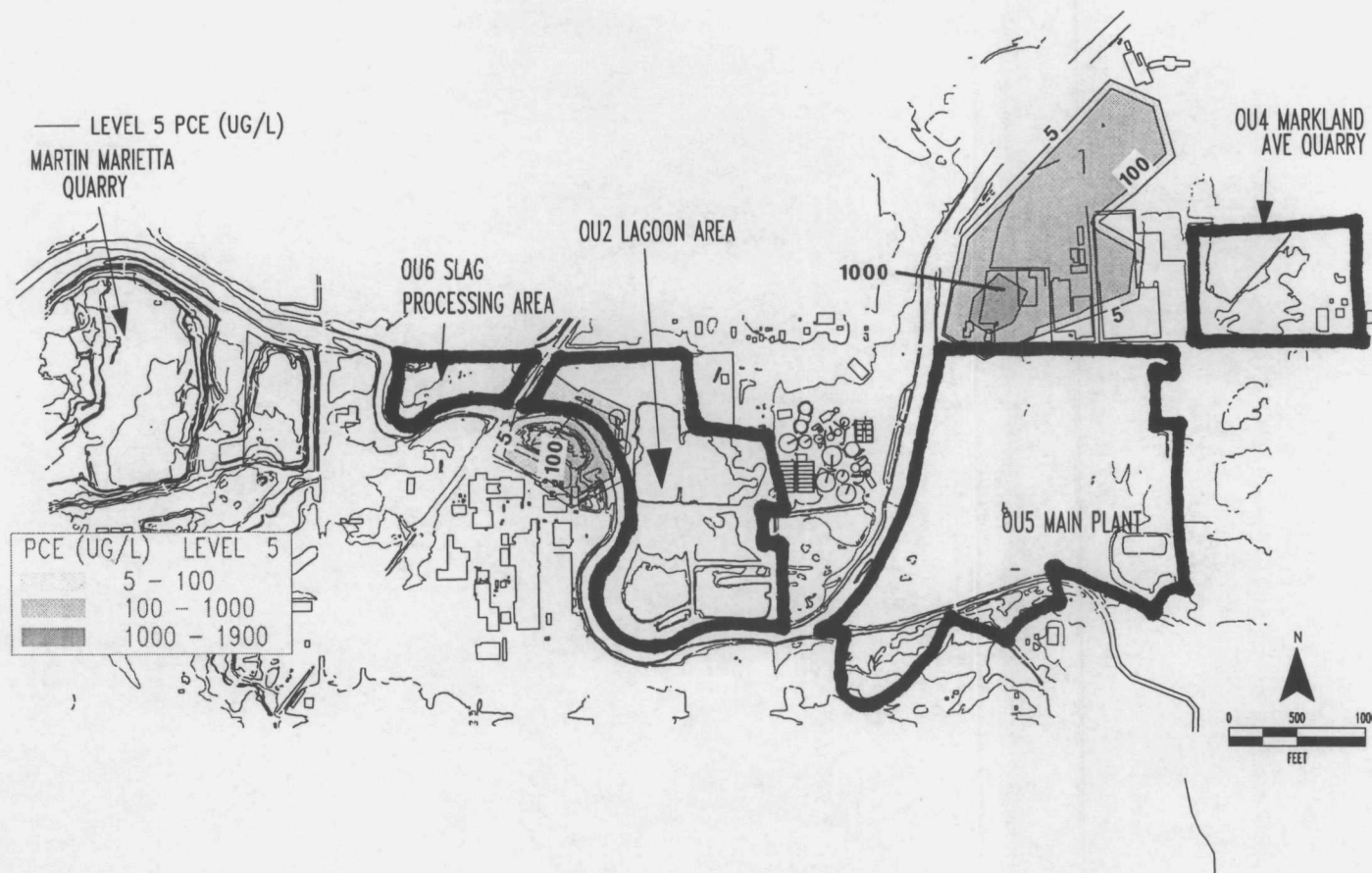


DATE/TIME:
PLOTTED: DYNPLOT8
CREATED: DYNFLOWS
DATE/TIME: 04/08/96 18:01
SAVE FILE: CSCALE07B.SVF

FIGURE 23 INITIAL TCE CONCENTRATIONS - MODEL LAYER 2
CONTINENTAL STEEL REGIONAL MODEL
KOKOMO, INDIANA
REGIONAL FLOW MODEL

CDM

environmental engineers, scientists,
planners, & management consultants

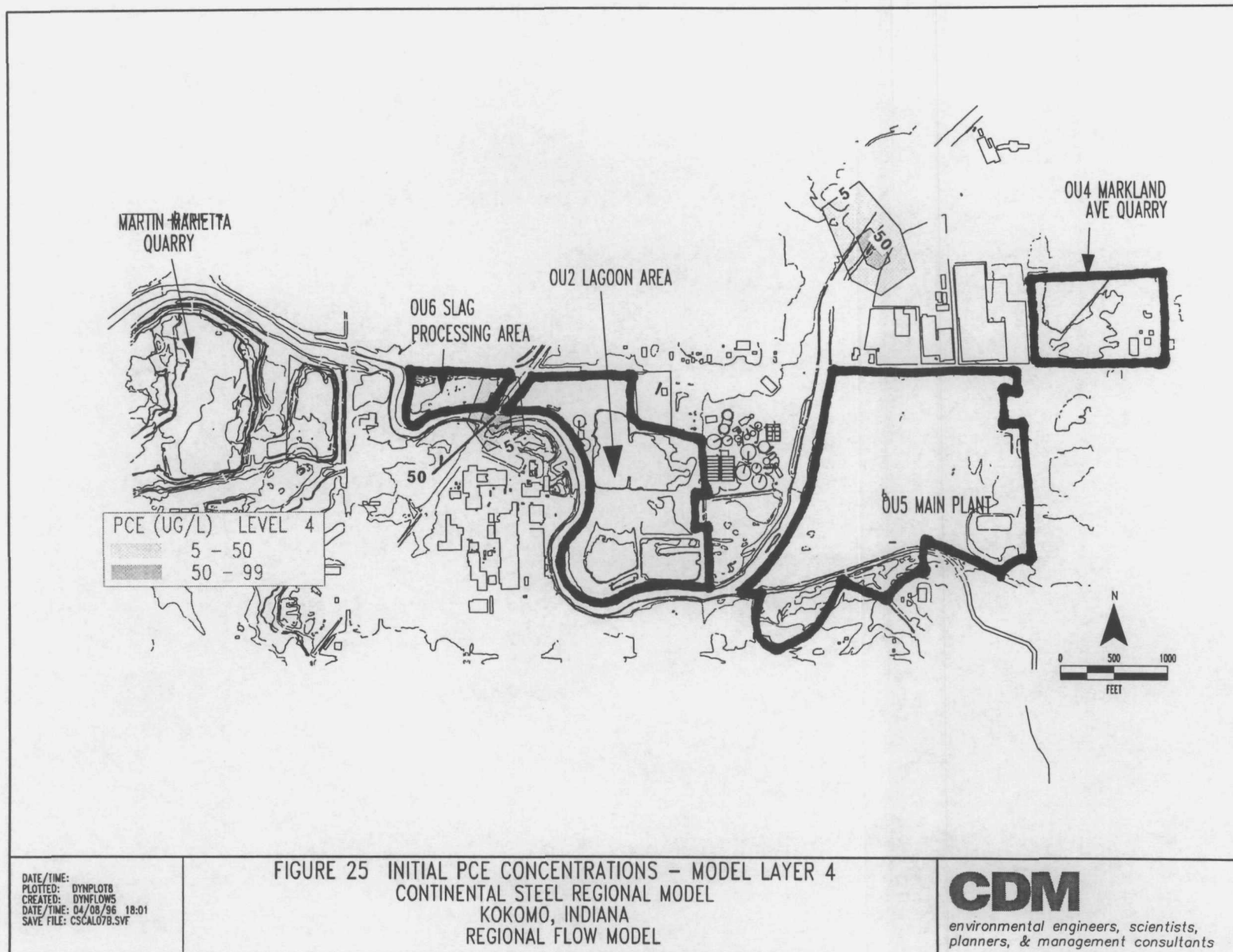


DATE/TIME:
PLOTTED: DYNPLOT8
CREATED: DYNFLOWS
DATE/TIME: 04/08/96 18:01
SAVE FILE: CSCAL07B.SVF

FIGURE 24 INITIAL PCE CONCENTRATIONS - MODEL LAYER 5
CONTINENTAL STEEL REGIONAL MODEL
KOKOMO, INDIANA
REGIONAL FLOW MODEL

CDM

environmental engineers, scientists,
planners, & management consultants



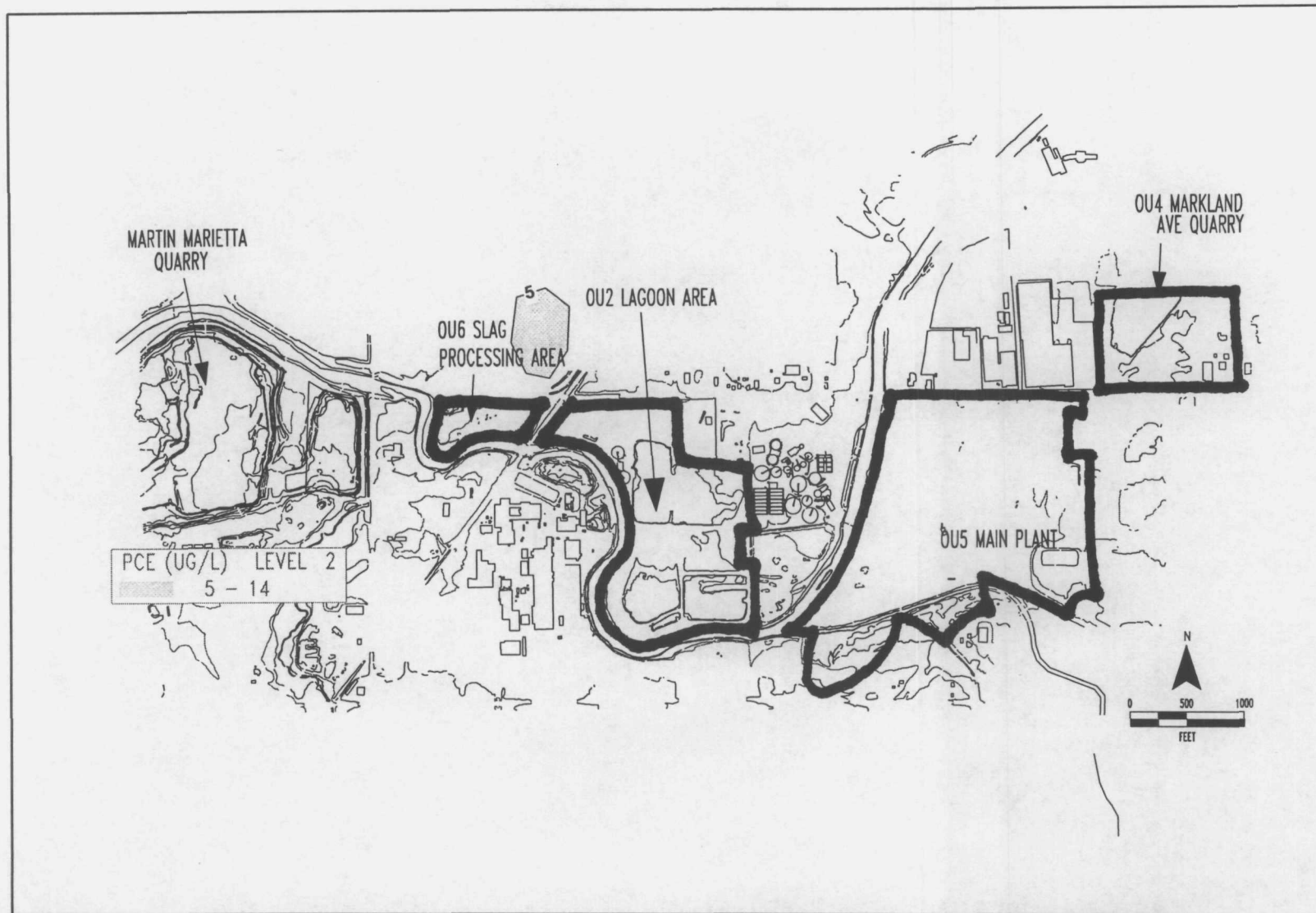
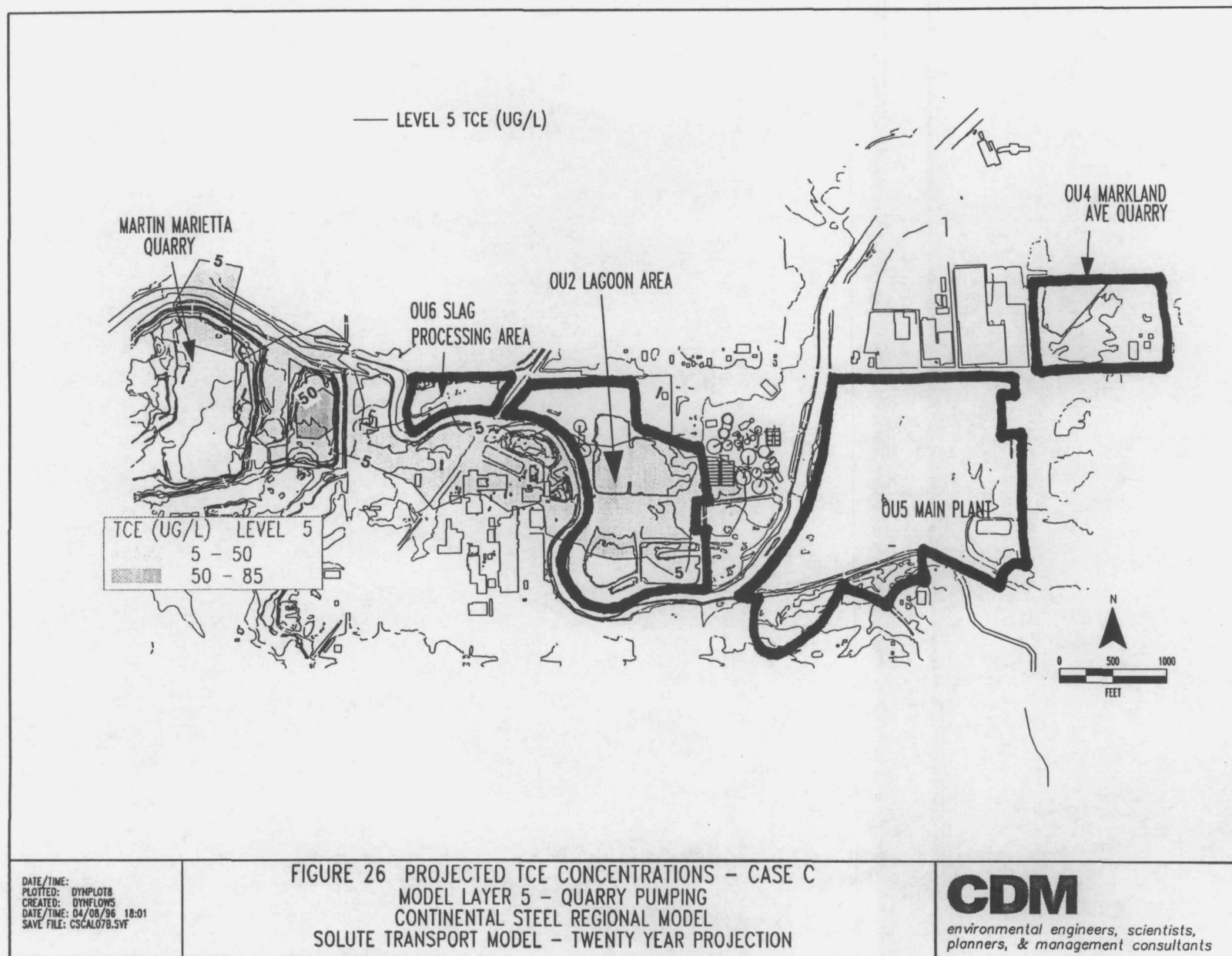


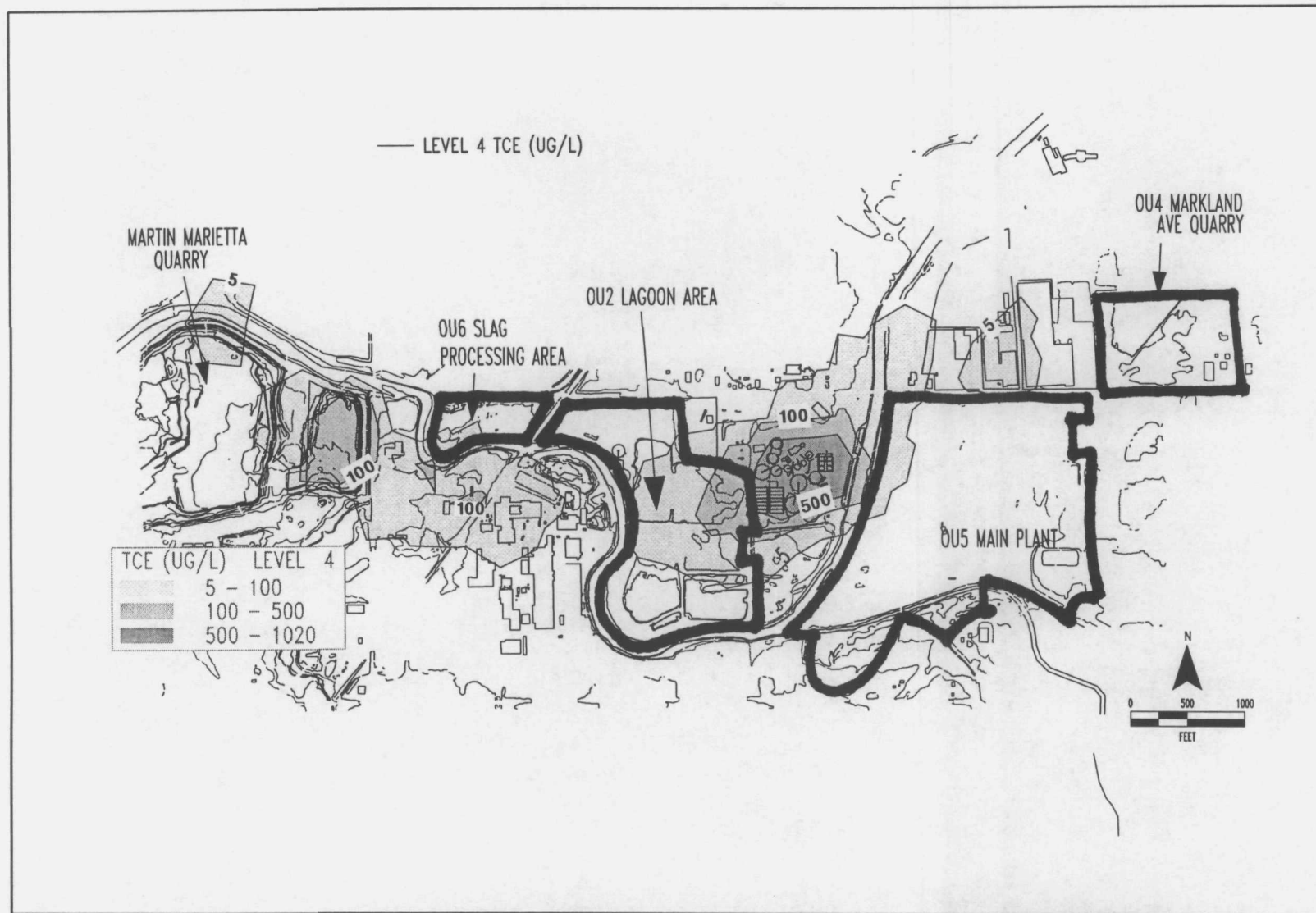
FIGURE 25B INITIAL PCE CONCENTRATIONS - MODEL LAYER 2
CONTINENTAL STEEL REGIONAL MODEL
KOKOMO, INDIANA
REGIONAL FLOW MODEL

DATE/TIME:
PLOTTED: DYNPLOT8
CREATED: DYNFLOWS
DATE/TIME: 04/08/96 18:01
SAVE FILE: CSCAL07B.SVF

CDM

environmental engineers, scientists,
planners, & management consultants



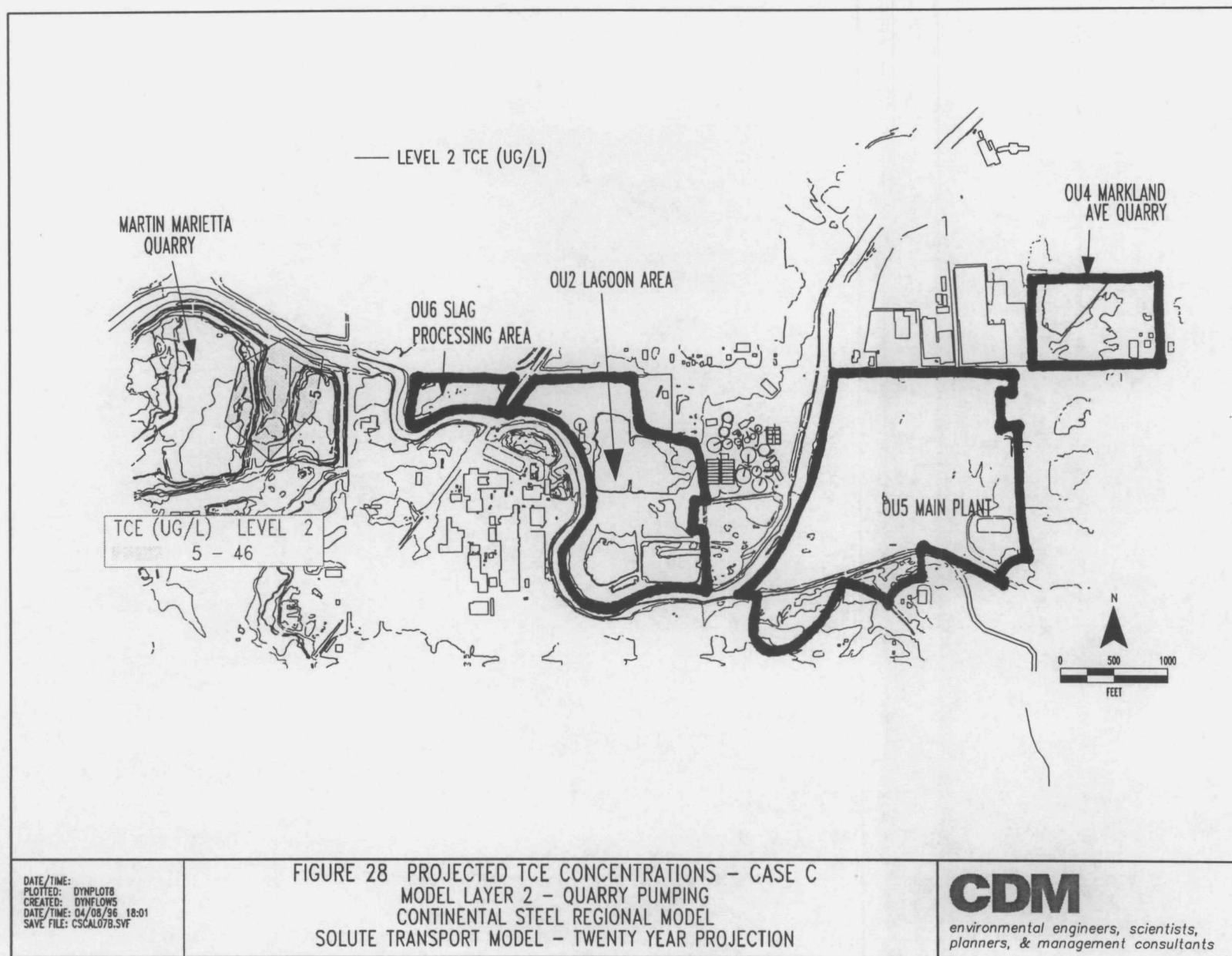


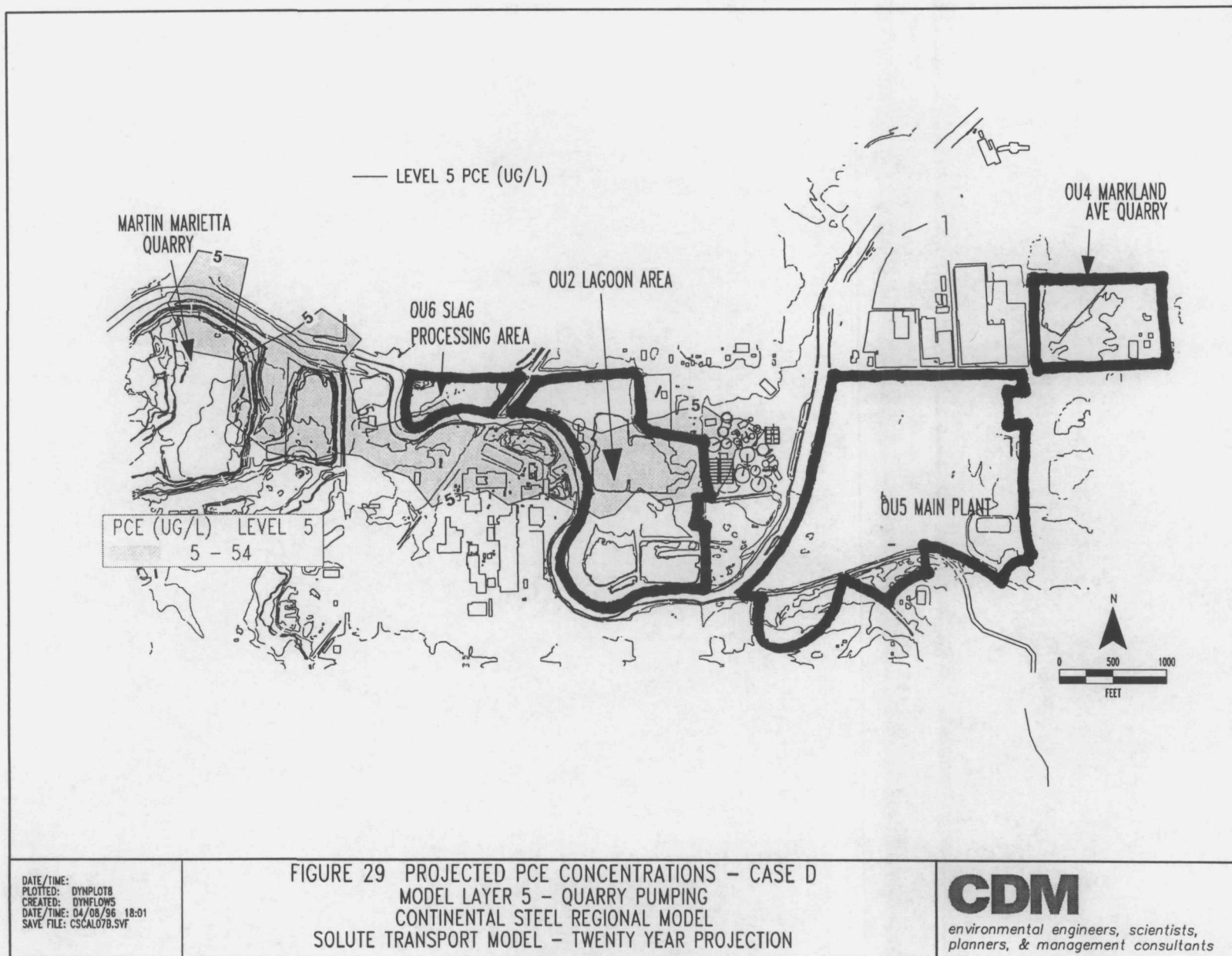
DATE/TIME:
PLOTTED: DYNPLOT8
CREATED: DYNFLOWS
DATE/TIME: 04/08/96 18:01
SAVE FILE: CSCAL07B.SVF

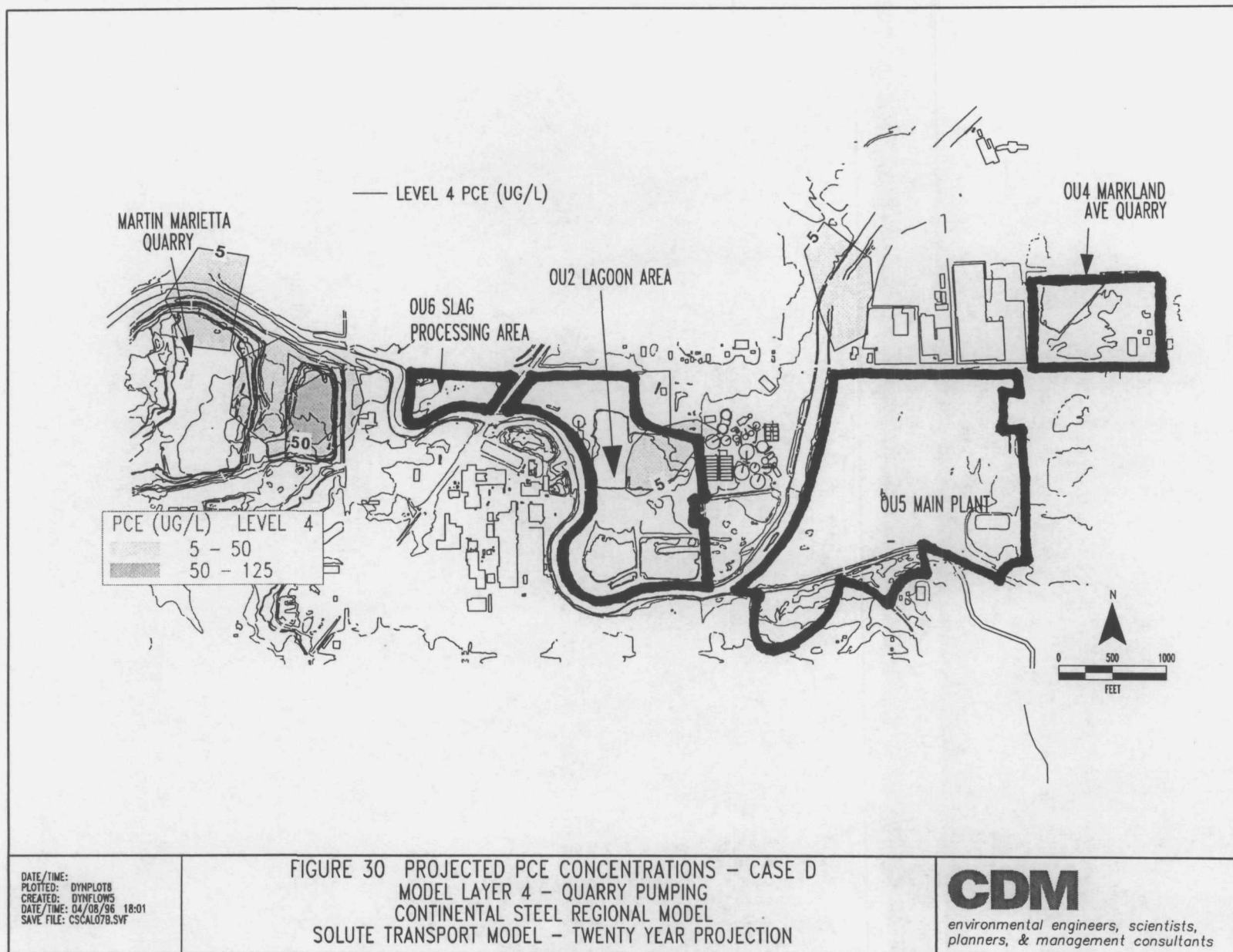
FIGURE 27 PROJECTED TCE CONCENTRATIONS - CASE C
MODEL LAYER 4 - QUARRY PUMPING
CONTINENTAL STEEL REGIONAL MODEL
SOLUTE TRANSPORT MODEL - TWENTY YEAR PROJECTION

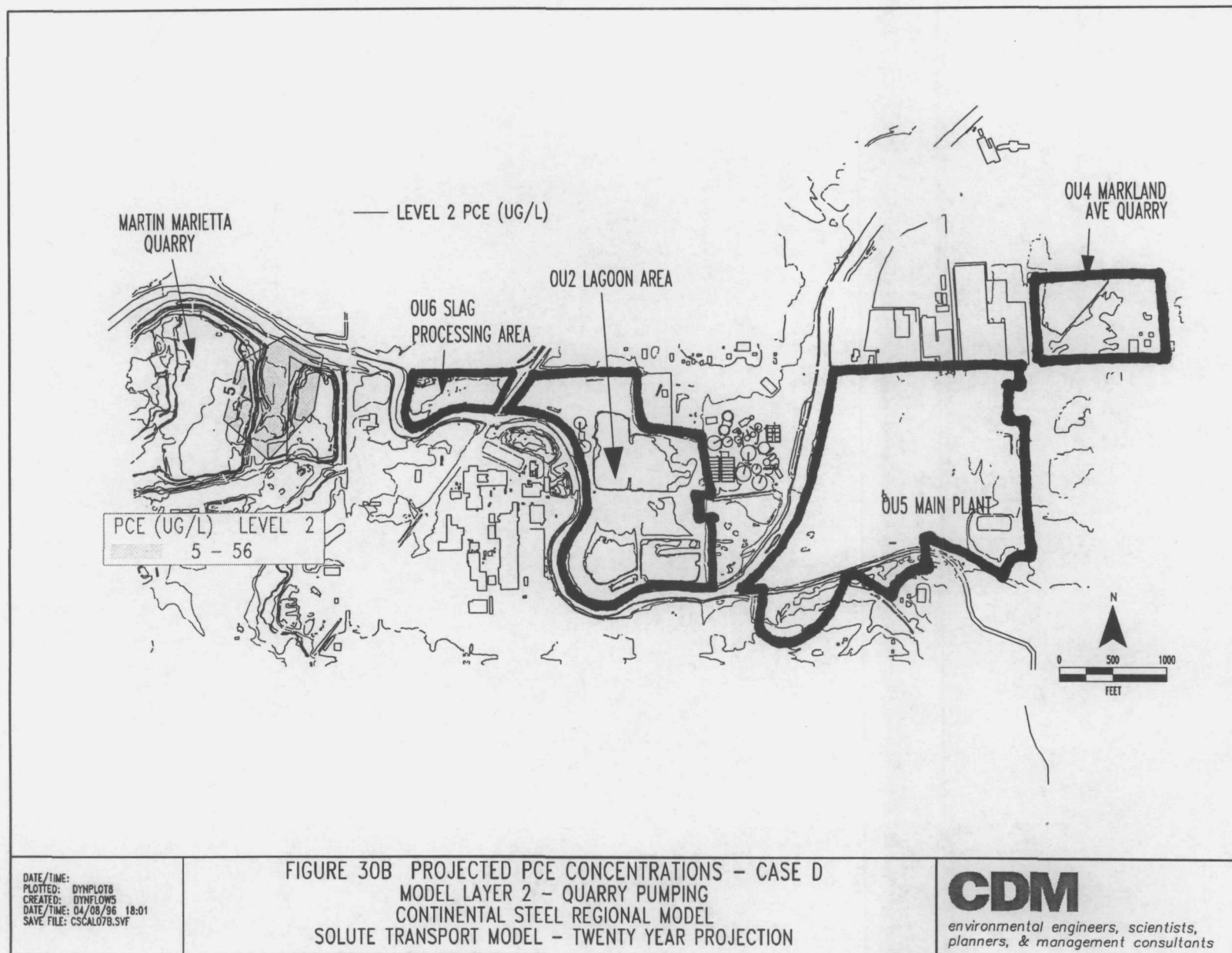
CDM

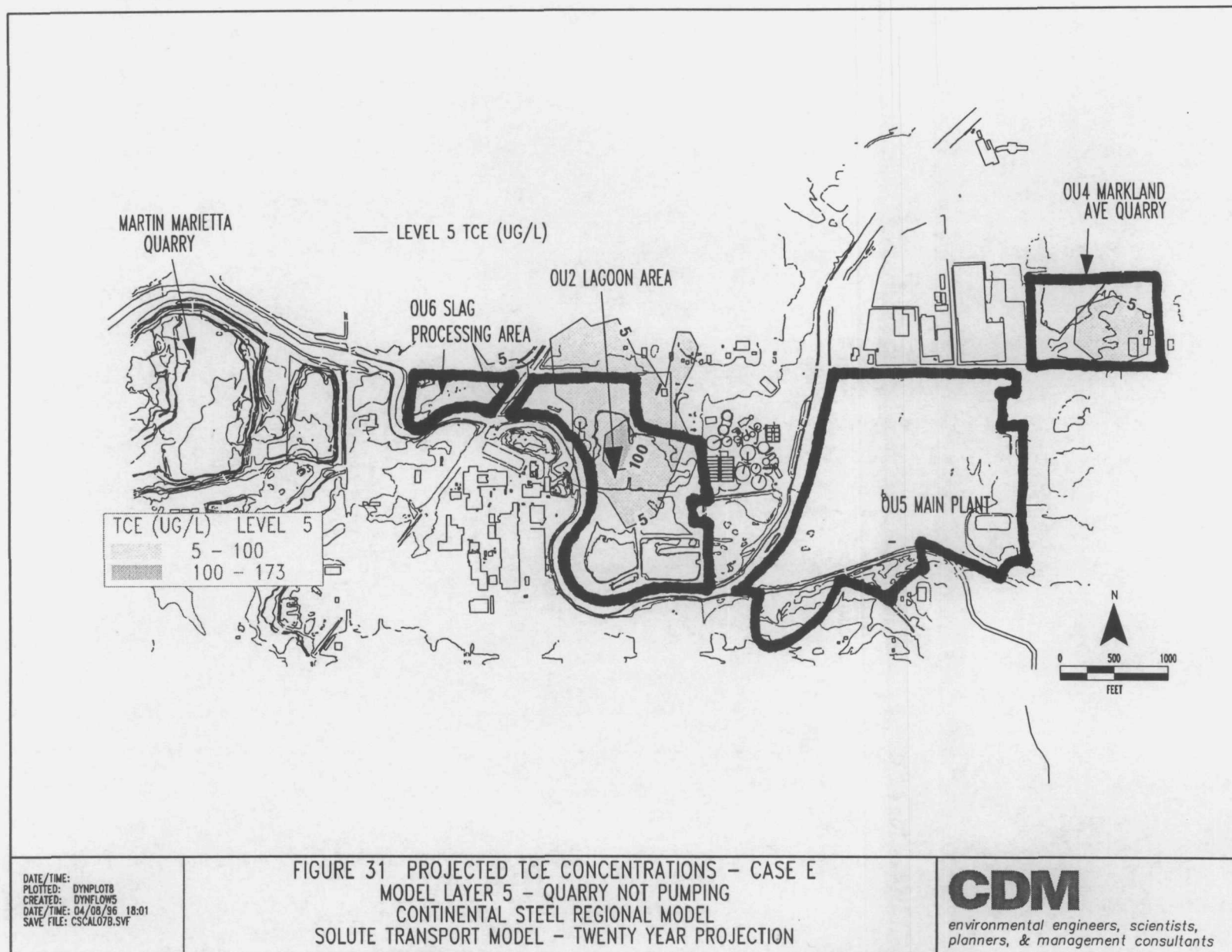
environmental engineers, scientists,
planners, & management consultants

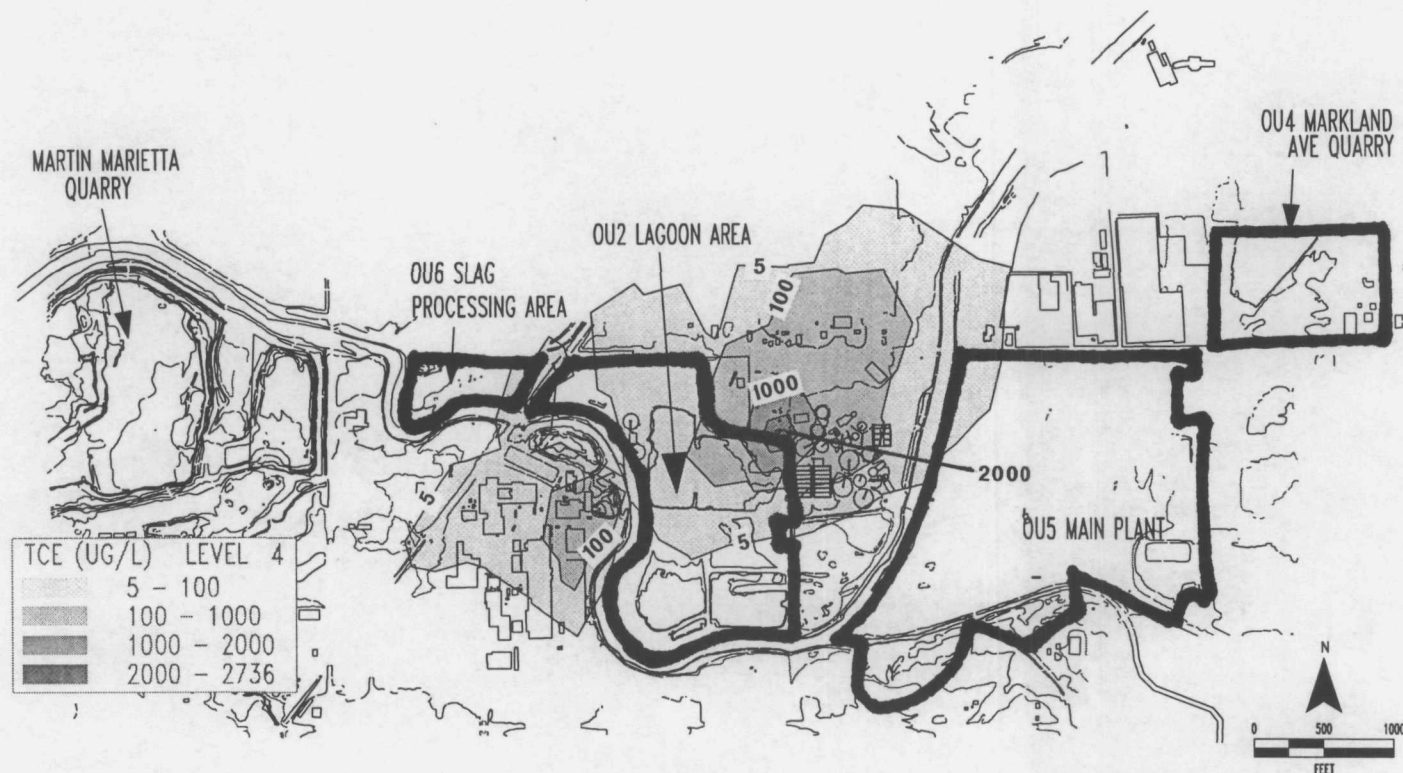










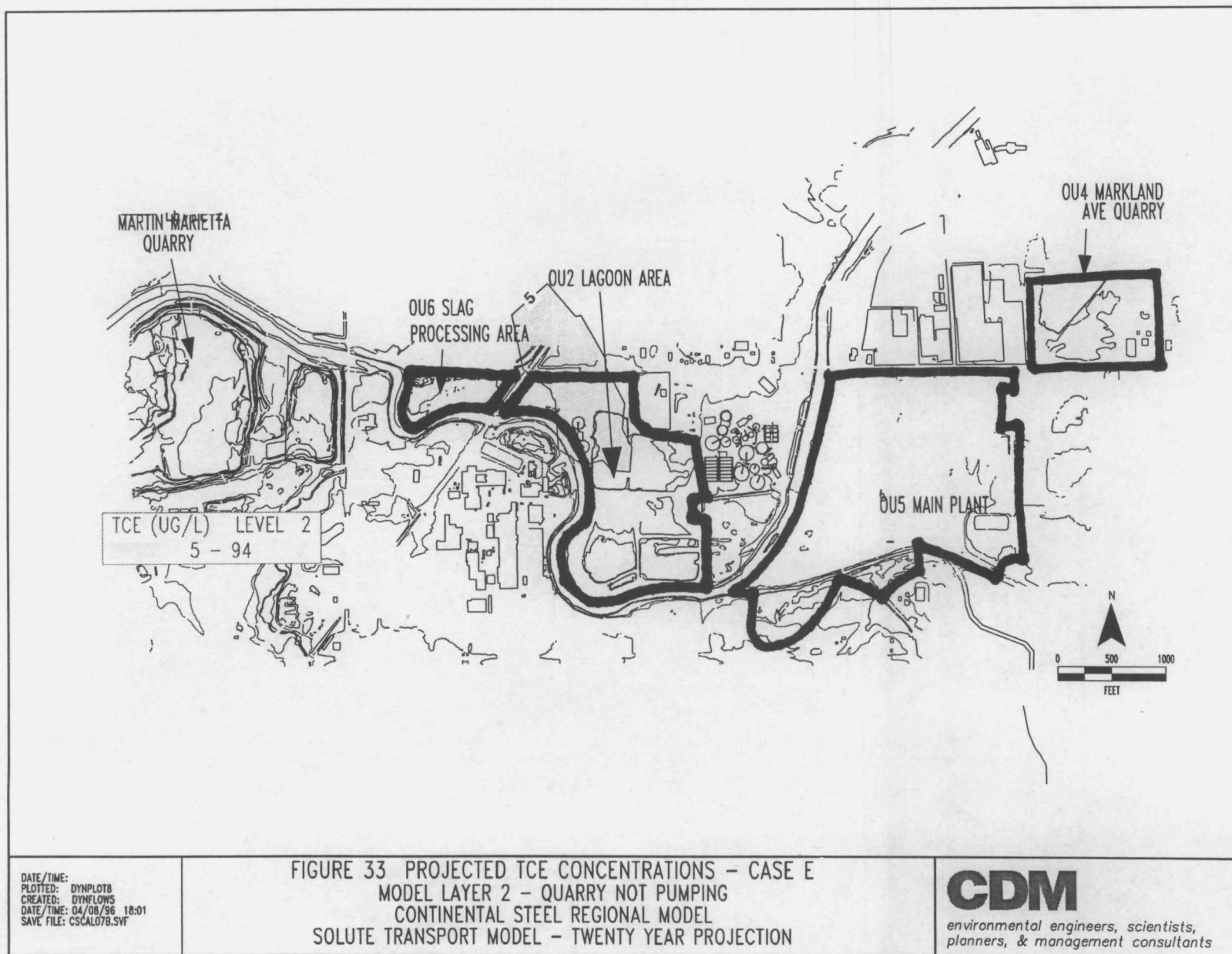


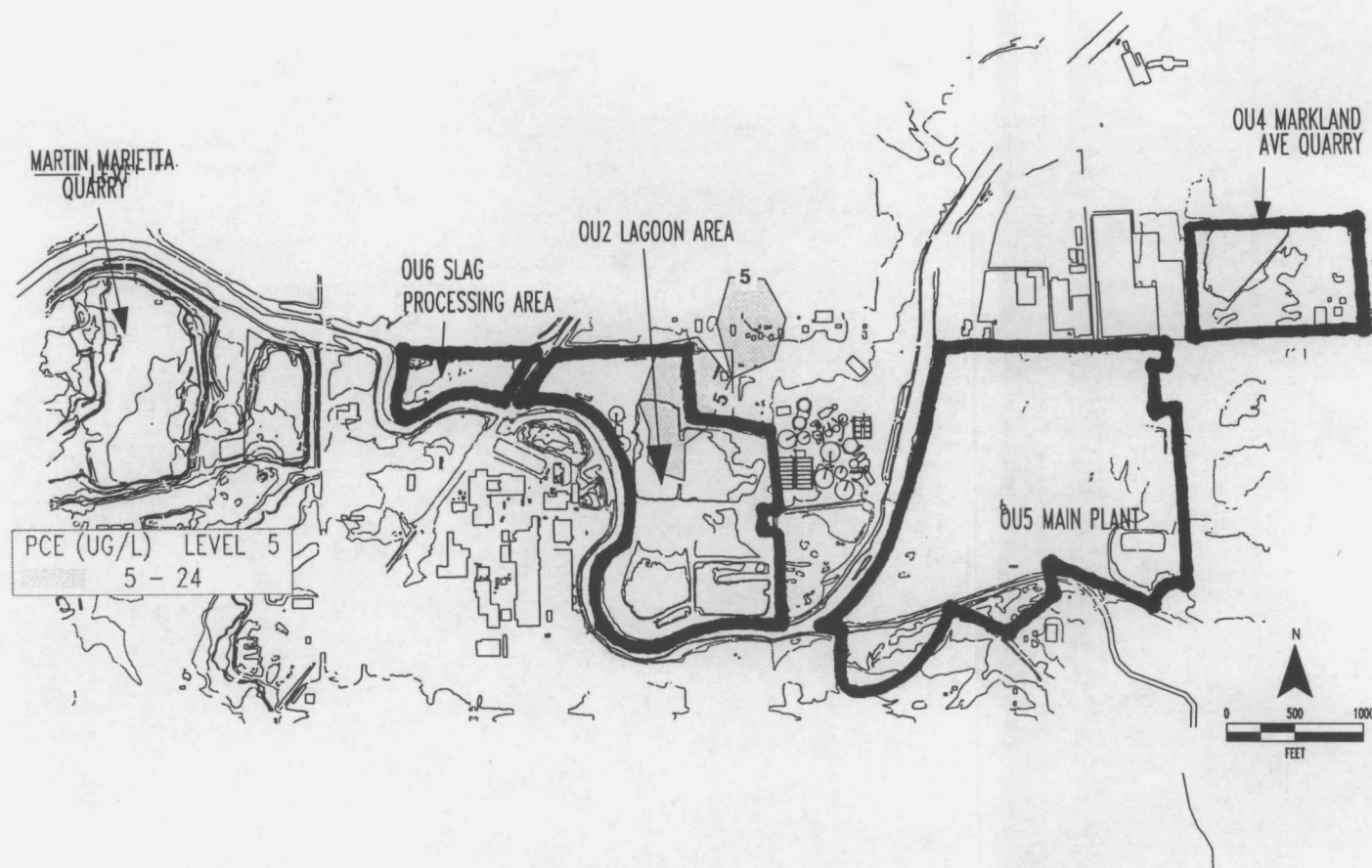
DATE/TIME:
 PLOTTED: DYNPLOT8
 CREATED: DYNFLOWS
 DATE/TIME: 04/08/96 18:01
 SAVE FILE: CSCAL07B.SVF

FIGURE 32 PROJECTED TCE CONCENTRATIONS - CASE E
 MODEL LAYER 4 - QUARRY NOT PUMPING
 CONTINENTAL STEEL REGIONAL MODEL
 SOLUTE TRANSPORT MODEL - TWENTY YEAR PROJECTION

CDM

environmental engineers, scientists,
 planners, & management consultants



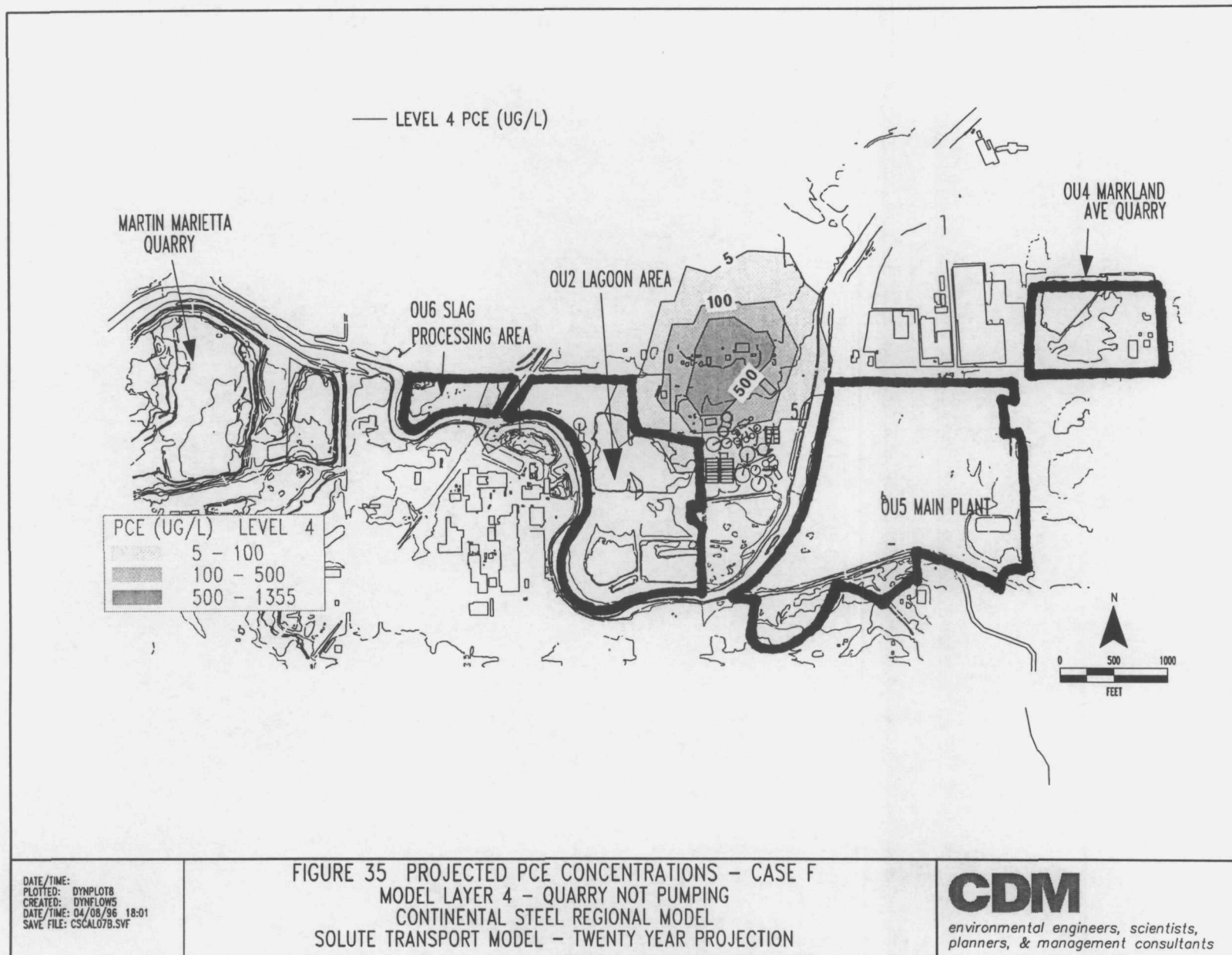


DATE/TIME:
PLOTTED: DYNPLOT8
CREATED: DYNFLOWS
DATE/TIME: 04/08/96 18:01
SAVE FILE: CSCAL078.SVF

FIGURE 34 PROJECTED PCE CONCENTRATIONS - CASE F
MODEL LAYER 5 - QUARRY NOT PUMPING
CONTINENTAL STEEL REGIONAL MODEL
SOLUTE TRANSPORT MODEL - TWENTY YEAR PROJECTION

CDM

environmental engineers, scientists,
planners, & management consultants



4 References

- Bredehoeft, J.D., H.B. Counts, S.G. Robson and J.B. Robertson; 1976. *Solute Transport in Groundwater Systems, in Facets of Hydrology*. Rodda, J.C., Ed, John Wiley and Sons, New York.
- Camp Dresser & McKee Inc. (CDM), 1995. *Continental Steel Superfund Site Focused RI/FS Work Plan*.
- Camp Dresser & McKee Inc. (CDM). 1996. *Continental Steel Superfund Site Remedial Investigation Final Report*.
- Freeze, R.A., and J.A. Cherry. 1979. *Groundwater*. Prentice Hall, Englewood Cliffs, New Jersey.
- Gelhar, Lynn W. 1986. *Stochastic Subsurface Hydrology From Theory to Applications*. Water Resources Research: 22(9), 135S-145S.
- Haynes International Corporation. Selected Water Quality Data. 1995.
- Mercer, J.W., S.D. Thomas, and B. Ross. 1982. *Parameters and Variables Appearing in Repository Siting Models*. Reston, Virginia: GeoTrans, Inc., NUREG/CR-3066.
- National Ground Water Association. 1996. Personal Communication, Dublin Ohio, February 1996.
- Neuman, S.P. 1990. *Universal Scaling of Hydraulic Conductivities and Dispersivities in Geologic Media*. Water Resources Research, 26(8):1, 749-758.
- Pickens, J.F., and G.E. Grisak. 1981a. *Scale-Dependent Dispersion in a Stratified Granular Aquifer*. Water Resources Research 17(4):1, 191-211.
- Pickens, J.F., and G.E. Grisak. 1981b. *Modeling of Scale-Dependent Dispersion in Hydrogeologic Systems*. Water Resources Research 17(6):1, 701-711.
- Smith, Barry S., M.A. Hardy and E.J. Crompton. 1985. *Water Resources of Wildcat and Deer Creek Basins, Howard and Parts of Adjacent Counties, Indiana, 1979-82*.
- United States Geological Survey. 1994. *Hydrogeologic Atlas of Aquifers in Indiana*.
- Wilson, J.L., L.R. Townley, and A.G. Sa Da Costa. 1979. *Mathematical Development and Verification of a Finite Element Aquifer Flow Model AQUIFEM-1*. Department of Civil Engineering, Massachusetts Institute of Technology, TAP Report 79-3, Cambridge, Massachusetts, June 1979.

Groundwater Model - APPENDIX A

GROUNDWATER MODELING NOTES

REVIEW OF DYNFLOW AND DYNTRACK GROUNDWATER
SIMULATION COMPUTER CODES

Report of Findings
by
Paul K.M. van der Heijde

for
U.S. Environmental Protection Agency
Office of Waste Program Enforcement
Washington D.C. 20460

IGWMC 85-17
May 3, 1985

INTERNATIONAL GROUND WATER MODELING CENTER
Holcomb Research Institute
Butler University, 4600 Sunset Avenue
Indianapolis, Indiana 46208

REVIEW OF DYNFLOW AND DYNTRACK GROUNDWATER SIMULATION COMPUTER CODES

Report of Findings, May 3, 1985

by Paul K.M. van der Heijde, Director
International Ground Water Modeling Center
Holcomb Research Institute
Butler University
Indianapolis, IN 46208

Introduction

By request of the Office of Waste Program Enforcement of the U.S. Environmental Protection Agency, the DYNFLOW and DYNTRACK models developed by Camp, Dresser and McKee, Inc., have been reviewed. This document and the opinions expressed herein do not represent the position of the Agency on the issues discussed. For the reasons stated below, this review should not be construed to be a complete or comprehensive peer review.

The review, requested by EPA in support of its involvement in the Price landfill case in New York, is aimed at evaluating the validity of the DYNTRACK solute transport simulation code. As stated in the letter from Johanna Miller, EPA, September 21, 1984, the objective of this review is "to comment on the theoretical base and mathematical framework of the CDM model." Because the heads required as input for the DYNTRACK code are generated by the DYNFLOW groundwater flow code, both DYNFLOW and DYNTRACK are subject to this review. The scope of work for this review is described in a letter by PRC Engineering, Inc., Chicago, Illinois, November 21, 1984, through which organization this review was subcontracted to the Holcomb Research Institute. According to the scope of work described in that letter, the key elements of the review should be:

- (1) Review of all available documentation pertaining to the DYNFLOW and DYNTRACK computer codes;

- (2) Review of modeling theory, the assumptions underlying the models, the equations describing the physics of the real system, the code structures, and the solution techniques;
- (3) Review the exercise of example problems of reviewers' computer facilities; and
- (4) If allotted time allows, develop additional test problems and run them at reviewer's facilities to test the computer codes and to determine their numerical and physical constraints.

The first three of these elements have been completed and are reported in this document. The fourth element could not be carried out because of time constraints.

The definition of the word *model*, as used in this report, includes the mathematical framework and the computer coding. This definition does not include the simulation of any laboratory or field experiment or field problem.

The standard groundwater model review process as carried out by the International Ground Water Modeling Center (IGWMC) comprises evaluation of the underlying theory, review of the user's manuals, and inspection and testing of the computer code. To carry out a complete review, the Center requires detailed documentation of the model, the computer code for implementation on the Center's computer facilities, and a file with the original test data used for the code's verification.

First, the theory underlying the model is reviewed; that is, its mathematical rigor is assessed and an evaluation is made of the correctness of the description of the modeled processes. Additional criteria include evaluation of the numerical method from an application point of view, with respect to the special rules required for proper utilization of the model (e.g., data assignment according to node-centered or block-centered grid structure, shape of elements, grid size variations, treatment of singularities such as wells, approach to vertical averaging in two-dimensional models, or layered three-dimensional models, and treatment of boundary conditions), and evaluation of

the ease with which the mathematical equations, the solution procedures, and the final results can be physically interpreted.

The documentation is then evaluated through visual inspection, comparison with existing documentation standards and guidelines, and through its use as a guide in operating the relevant code at the IGWMC. Good documentation includes a complete treatment of the equations on which the model is based, of the underlying assumptions, of the boundary conditions that can be incorporated in the model, of the method used to solve the equations, and of the limiting conditions resulting from the chosen method. The documentation must also include a user's manual containing example problems complete with input and output, programmer's instructions, operator's instructions, and a report of the initial verification of the code.

The computer code is then reviewed and tested. In the review, attention is given to the manner in which modern programming principles have been applied with respect to code structure, optimal use of the programming language, and internal documentation. To check for correct coding of theoretical principles and for major programming errors ("bugs") in the code, the code is run using problems for which an analytical solution exists. This stage is also used to evaluate the code sensitivity for grid design for various dominant processes and for a wide selection of parameter values. (Due to time constraints, sensitivity testing was not incorporated into this review.)

Although testing numerical computer codes by comparing results for simplified situations with those of analytical models does not guarantee a fully debugged code, a well-selected set of problems ensures that the code's main program and most of its subroutines, including all of the frequently called ones, are being used in the testing.

To test special features that cannot be handled by simple close-form solutions, as in testing irregular boundary conditions and heterogeneous and anisotropic aquifer properties, hypothetical problems are used. Sensitivity analysis is then applied to determine code characteristics. Finally, data from field sites are used (if available) to validate the model. However, for many types of groundwater models, including three-dimensional solute transport simulation codes (as in DYNTRACK), no such complete set of testing techniques

is currently available. Therefore, to test these three-dimensional solute transport simulation codes, one- and two-dimensional analytical solutions are used.

The code testing by the Center is also used to evaluate the user's guide. Special attention is given during the code testing to the rules and restrictions ("tricks") necessary to operate the code.

General Comments on DYNFLOW and DYNTRACK

The DYNFLOW and DYNTRACK computer codes were reviewed by Paul K.M. van der Heijde, at the IGWMC in Indianapolis. P. Srinivasan of the IGWMC assisted in reviewing the codes and in evaluating their documentation. Additional information regarding the operation of the codes was obtained during a meeting with P.J. Riordan, R.P. Schreiber, and B.M. Harley of the Camp, Dresser and McKee model-developing group at the CDM corporate offices in Boston, Massachusetts, December 4-6, 1984 and during a number of telephone conversations in the period December 1, 1984 through February 15, 1985.

Preliminary reporting to EPA took place by letter of December 10, 1984. Some of the reviewed documents were not received until the last week of November 1984, particularly the DYNTRACK user's manual. Upon his arrival at CDM's offices in Boston, Massachusetts on December 4, 1984, the reviewer was provided with a significantly updated version of the DYNTRACK manual. Also, the last two of the reviewed documents listed on p. 2 were first provided during the meeting with the CDM modelers.

After a preliminary evaluation of the findings was reported on December 10, EPA decided to have a more thorough and independent evaluation of the codes undertaken through implementation and test-running of the codes at IGWMC's computer facilities. This code-testing was performed using the complete set of examples presented in the documentation of the codes. To further check the results of the simulations with analytical solutions, programs developed and implemented at IGWMC were used.

As mentioned earlier, well-documented field data sets are scarce and have not yet been developed for the purpose of testing three-dimensional solute

transport models. Testing of the codes was therefore restricted to the simplified hypothetical problems presented in the sample problem set.

The results of the inspection of the DYNFLOW and DYNTRACK source codes and their documentation and of the evaluation of the run-tests of the codes are presented in this report.

Documents Reviewed

Riordan, P.J., B.M. Harley, and R.P. Schreiber, Three-Dimensional Modeling of Flow and Mass Transport Processes in Groundwater Systems. Proceedings NWWA/IGWMC Conf. on Practical Application of Groundwater Models, Columbus, Ohio, August 15-17, 1984, pp. 112-132.

Camp, Dresser and McKee, Inc., Details of the DYNTRACK model. Appendix D of internal report, 1983.

Riordan, P.J., R.P. Schreiber, and B.M. Harley, Three-Dimensional Modeling of Groundwater Flow. Internal report, Camp, Dresser and McKee, Inc., Boston, Mass., 1983.

DYNFLOW A 3-Dimensional Finite-Element Groundwater Flow Model; Description and User's Manual, Version 3.0, (draft), Camp, Dresser and McKee, Inc., Boston, Mass., Nov. 1984.

DYNTRACK, A 3-Dimensional Contaminant Transport Model for Groundwater Studies: Description and User's Manual, Version 1.0 (draft), Camp, Dresser and McKee, Inc., Boston, Mass. November 1984.

Code listings of DYNFLOW and DYNTRACK

Code listing of analytical solutions used to verify the DYNTRACK code

Computer log of test problems for DYNFLOW and DYNTRACK including test data and complete listing of results

DYNFLOW

Description

DYNFLOW is a Galerkin finite-element model for simulation of three-dimensional groundwater flow in saturated porous media. The code uses one-dimensional, planar two-dimensional, and three-dimensional linear elements. The model solves both linear (confined) and nonlinear (phreatic) groundwater flow equations in terms of piezometric head, and it can accommodate changing aquifer conditions during simulation. The code includes options to simulate a hydraulic connection with a stream, dewatering schemes, the effect of ponding, and seepage surfaces. Through use of the model's restart capability, various changes in parameter values, boundary conditions, and stresses can be evaluated during a simulation. The equations are solved by Gaussian elimination or by a block or out-of-core solver.

Evaluation

Computer Code

The DYNFLOW code is based on a well-established quasi-three-dimensional groundwater flow code, AQUIFEM-N. This widely used code is based on a reliable and theoretically well-developed technique. Because of its many options such as the use of various types of elements and its restart capability, the code is quite versatile. To apply the DYNFLOW code to complex problems, a modeler must be familiar with all of DYNFLOW's characteristics and application rules. The application of the current version is somewhat restricted by the limited number of layers in which the vertical dimension can be divided (a maximum of nine layers are hard-wired into the code). However, it is rather simple to modify the code to handle larger problems.

The structure of DYNFLOW is logical and rather efficient. The use of specially defined commands facilitates both interactive program execution and user-friendly updates of data items, simulation parameters, and input-output controls.

The DYNFLOW code is written using modern structured programming principles. All sections of the code are explained internally by COMMENT statements, e.g., the allocation of storage space, the assignment of upper bounds of variables, and the listing of I/O file information. The extensive use of indentation facilitates easy comprehension of the code's segmented structure. There is no apparent misuse of IF/GOTO statements. Except for a few places, the constants are not hard-wired in the subroutines.

The use of ENCODE/DECODE, for processing of the code commands, limits the code to ANSI FORTRAN-77 or extended FORTRAN-66.

The code contains many WRITE statements to log errors and warnings during a run, which is considered good programming practice. Separate I/O files are used to store head, permeability, grid data, etc., a useful adjunct to pre- and postprocessing. Because subroutines are not documented internally and independently, an understanding of previous sections of the code is necessary at all points.

A program of this size should have documentation of its structure, including description of the variables, to assist the user in understanding the workings of the program. This documentation is lacking.

The code has been applied frequently by CDM in recent years. The experience obtained in applying the code has contributed to improvements, updates, and modifications. The final result is a dependable and versatile code, well-suited for use by experienced modelers in the analysis of various groundwater flow problems.

During testing the code performed without problems. CDM provided the reviewer with a complete set of input data and computed results for the given test problems. The data sets provided by CDM were inspected to check the representation of the analytical model. No major differences between the specifications of the test problems and the data used in DYNFLOW were found. The test data were used to run the DYNFLOW code on the reviewer's in-house computer system (DEC Microvax-1). The results of these computations were compared with those provided by CDM and with pertinent analytical solutions. Using the original data set, the reviewer was able to produce the same results

as obtained by the authors. The comparison with analytical solutions was good. However, this analysis showed the need for a thorough understanding of the code's operational characteristics in interpreting computational results. It should be noted that the ponding subroutine has not been tested by the reviewer. Further evaluation of this routine is needed.

Documentation

A complete statement of the objectives of the model must include the basic flow equation and its underlying assumptions. Also necessary is more extensive referencing regarding the derivation of equations, the definition of elements and boundary conditions, and the discussion of the equation solution methods.

The description of the code elements and the definition of the variables (section 3) is too brief. The code structure, especially, needs more in-depth treatment. The interactive commands for running the code and the explanation of individual commands (e.g., reference manual) are detailed and well-written.

The application section should be expanded to contain instructions on grid design, parameter selection, boundary conditions, the use of special elements, calibration techniques, sensitivity analysis, restart capability, and so forth. Such an extension is necessary because many of the situations which can be simulated by the code require instructions on how to combine its advanced features.

Currently lacking in the documentation are the complete input data sets and listings of the results for the given tests. This information is essential to evaluate the author's claims with respect to accuracy of the program. In addition, without such information the user is unable to verify the proper implementation of the code on the user's computer system.

DYNTRACK

Description

DYNTRACK is a computer model for the simulation of three-dimensional solute transport in saturated groundwater systems. The model has two modes of

operation. In the first, or particle tracking mode, it computes the path of a single, conservative particle undergoing advective transport. In the second mode, the model employs the random walk technique to simulate three-dimensional advective-dispersive transport. In this mode, first-order decay and linear adsorption isotherms can be accounted for. The random walk method solves the transport equation indirectly through simulation of an analogous process, tracing the paths of a statistically significant number of particles, each with a predefined mass of the chemical constituent involved. The result of the computations is a distribution of particles and thus of solute mass. The dependent variable in the transport equation (concentration) is then calculated by dividing the total particle mass in a certain volume by the water volume of that total volume. In DYNTRACK the total volume is a volume assigned to each node.

To displace the particles advectively, the velocities in the flow field must be known. In the DYNTRACK code these velocities are generally derived from the nodal heads computed by the DYNFLOW code. Because of this link between the DYNFLOW and the DYNTRACK codes, the computations in the DYNTRACK code generally take place on the same element grid base as in the DYNFLOW code. Also, due to this link, the velocity across an element boundary is discontinuous in the DYNTRACK code.

The displacement of particles moving through more than one element during a certain timestep is not corrected for changing velocity when the particles leave the element where their displacement originated. To prevent cumulative inaccuracies, the code checks for each timestep if at the end of that timestep the particle is in one of the neighboring elements. If the particle is not in this area, the code displays a "particle lost" message and a smaller timestep must be chosen. This feature is also designed to assure conservation of mass in the model.

This approach to displacement accuracy checking is combined with a routine for the simulation of particles bouncing back from a no-flow boundary. It is an efficient routine directly related to the required accuracy for that location through linking to the element configuration (for high accuracy small elements should be used). Although this feature is included in the code, it is not documented in the manuals.

Through use of a retardation factor, the code can handle adsorption. In the code this is an element property. To account for the loss of mass in the liquid phase, the code corrects the calculated concentrations by dividing by the retardation coefficient, resulting in an increase of the apparent volume.

The approximation of adsorptive processes by a retardation coefficient is currently the most widely used approach to incorporate the effects of adsorption into solute transport models. However, desorption cannot be handled by this approach and calls for a more complex representation of the matrix-liquid interactions. The DYNTRACK code does not allow for desorption.

The code can also handle first-order decay. However, this is considered a global property and cannot be assigned to the individual elements.

Fluid density differences resulting from variations in solute concentration are assumed negligible and are therefore not incorporated.

Evaluation

Computer Code

By taking an analogue approach to solving the transport equation, the random walk method distinguishes itself from other numerical methods. Consequently, its strengths and weaknesses differ from the more established finite-difference method and finite-element method, and from the method of characteristics. The strength of the random walk method lies in the analogy used to represent the transport processes. This physically based analogy can be used to analyze the pathways for the solute movement. In addition, the stochastically based random walk representation of dispersion is a generally accepted way of describing this complex phenomenon. The weaknesses of the method are primarily those intrinsic to the use of an analogy and to the discrete nature of the particle mass. Because of the discrete nature of the particles and the application of stochastic principles, a large number of particles is needed to obtain an accurate solute mass distribution. However, no guidelines can be derived for the minimum number of particles theoretically necessary to achieve a certain accuracy. The analogous approach resulting in a solute mass distribution forces the user to interpret the results at the end

of the simulation in terms of concentrations. Various approaches are possible to map the particle mass over each volume element and convert it into a concentration distribution. The approach adopted for the DYNTRACK code results in irregularly patterned concentration distributions. The developers of the DYNTRACK code have therefore added optional routines to smooth the results. However, such techniques might lead to a loss of information in the final results.

For a modeled system in which significant dispersion occurs, back-scatter (negative or upstream random displacement) can cause problems in models based on the random walk method, especially in areas near the solute sources. Also, the use of a finite number of particles can be the cause of scatter in the results.

Finally, the random walk method is not suited for simulation of transport of pollutants from extensive nonpoint sources relative to the scale of modeling. That is, contaminant sources should not exceed an area of a few elements or nodes; otherwise an excessive number of particles would be needed to achieve reasonable accuracy. Therefore, only simulation of distributed sources of limited areal extent can be handled.

The theoretical treatment of the optional nonconservative processes (adsorption and first-order decay) is in accordance with current theory.¹ Further testing of these optional features has not been performed.

Like the DYNFLOW code, DYNTRACK is written using modern structured programming principles. It is internally well "commented." Its flexibility is obtained through use of a set of specially defined commands comparable with DYNFLOW. Extensive use of error messages and debug options makes the code dependable and facilitates its efficient use. Remarks made regarding the programming of the DYNFLOW code also apply to the DYNTRACK code. The built-in random number generator simplifies code transfer to various host computers.

¹Bear, J. (1979). *Hydraulics of Groundwater*. McGraw-Hill, New York, NY, pp. 239-243.

In the testing performed at IGWMC, the code was able, after modification of some of the data sets provided to make them correspond to the input format of the latest version of the code, to simulate various simplified problems accurately. These tests focused on the simulation of advective and dispersive transport processes and showed that the particle tracking routines and the mass-concentration conversions were properly programmed. The analytical solutions used in these test problems were independently programmed and implemented at IGWMC, except for the one in case V.

The six tests performed independently by the reviewer cover four cases presented by the authors of DYNTRACK in the code's documentation. These tests are:

- | | |
|----------------------|--|
| (1) :CDM case I— | Convection and dispersion in one dimension
Contaminant slug transport (SLUG1D-data) |
| (2) :CDM case II(a)— | Convection and dispersion in two dimensions
Slug source (SLUG2D-data) |
| (3) :CDM case II(b)— | Convection and dispersion in two dimensions
Continuous source (CONT2D-data) |
| (4) :CDM case III— | Convection and dispersion in three dimensions
Slug source (SLUG3D-data) |
| (5) :CDM case V(a)— | Two-well pulse test
Orthogonal grid (DOUBL1T-data) |
| (6) :CDM case V(b)— | Two-well pulse test
Bipolar grid (DOUBL3-data) |

The tests (1) through (4) were carried out using the "SOLUTE" package of analytical solution developed at IGWMC. The results of the analytical simulations were compared with the results the reviewer obtained from the DYNTRACK runs on the IGWMC computer system (see appendix).

Tests (5) and (6) were carried out by reviewing the theory as documented by Gelhar² and comparing it with the results provided by CDM as well as with the reviewer's own DYNTRACK simulations (see appendix). These last two tests clearly demonstrate inaccuracies and instabilities which might occur in simulation of extreme hydraulic situations. It is not clear whether these instabilities are a result of the method (e.g., random noise at low concentrations), or a result of grid design (limitation on directions of release of contaminants from source). The case with the octagonal grid (5) shows a close fit between theoretical and numerical results. This is clearly less the case with the orthogonal grid. The shift between values computed at IGWMC and at CDM is probably the result of differences in data sets used.

During the testing it became apparent that proficiency with the theoretical concepts and the structure of the code is prerequisite for a correct representation of the simulated problems in the code's data sets. Thorough understanding of the analogous character of the modeling method used in DYNTRACK is necessary for optimal use of the various options of the code and for adequate interpretation of the simulation results.

Documentation

The latest version of the DYNTRACK documentation contains much of the information necessary to understand the principles on which the model is based. It also contains extensive user's instructions regarding the input data for the computer code. However, the section describing the computer code itself is brief. Because the computer code is not included in the documentation, evaluation of the code structure is not possible. Additional flowcharts and an extended discussion of the subroutines, including the pre- and postsimulation processors, are necessary for such an evaluation.

The verification tests provided in the code documentation are incomplete; little mention is made as to how, or from where, analytical solutions have been obtained, nor does the manual explain how the tests were performed. In some of the test cases, smoothing (moving average, contouring) has been used

²Gelhar, L. (1982). Analysis of two-well tracer tests with a pulse input. RWH-BW-CR-1318, Rockwell International, Hanford, WA.

to represent the results. The effect of such techniques on the accuracy of the results has not been reported by the DYNTRACK authors.

The application sections (modeling strategies and examples) in the user's manual were not included in the version reviewed. Such sections should contain instructions on how to design grids, how to introduce particles, how many particles should be used, how to incorporate boundary conditions (concentrations, solute fluxes), and so forth, and should discuss the relationship between grid design and model accuracy.

APPENDIX

DYNTRACK Test Runs

The results of the DYNTRACK test runs are presented without smoothing or averaging, except in those cases where vertical averaging is mandatory (one- and two-dimensional cases). The test runs were performed using 2,000 particles. Improvement in accuracies is expected when using a larger number of particles (e.g., 10,000).

***** RESULTS *****

-----> distance X CONCENTRATION in mg/l (ppm)
 |
 v time

		source	1.00 m	2.00 m	3.00 m	4.00 m
		0.00 m				
4.00	d	0.9187	3.9491	11.1916	20.9087	25.7516
8.00	d	0.0232	0.1106	0.4282	1.3468	3.4393
		5.00 m	6.00 m	7.00 m	8.00 m	9.00 m
4.00	d	20.9087	11.1916	3.9491	0.9187	0.1409
8.00	d	7.1308	12.0042	16.4078	18.2091	16.4078
		10.00 m	11.00 m	12.00 m	13.00 m	14.00 m
4.00	d	0.0142	0.0009	0.0000	0.0000	0.0000
8.00	d	12.0042	7.1308	3.4393	1.3468	0.4282
		15.00 m	16.00 m	17.00 m	18.00 m	19.00 m
4.00	d	0.0000	0.0000	0.0000	0.0000	0.0000
8.00	d	0.1106	0.0232	0.0039	0.0005	0.0000

DYNTRACK mass per particle .0125

	<u>0.00 m</u>	<u>1.00 m</u>	<u>2.00 m</u>	<u>3.00 m</u>	<u>4.00 m</u>
4 d	0.900	4.650	11.400	20.000	25.750
8 d	-	0.050	0.150	1.300	4.200
	<u>5.00 m</u>	<u>6.00 m</u>	<u>7.00 m</u>	<u>8.00 m</u>	<u>9.00 m</u>
4 d	20.700	11.350	3.850	1.100	0.200
8 d	7.400	12.100	16.950	17.450	16.700

```
*****
*
*   ONE-DIMENSIONAL SOLUTE TRANSPORT EQUATION   *
*   INSTANTANEOUS POINT SOURCE                 *
*
*   MODEL: SLUG1D.BAS                           *
*
*****
```

USER: P.K.M. van der Heijde

LOCATION: IGWMC Indianapolis

DATE: February 10, 1985

INPUT DATA:

TOTAL MASS INJECTED.....:	25.00	kg
DARCY VELOCITY.....:	0.25	m/d
EFFECTIVE POROSITY.....:	.25	
LONGITUDINAL DISPERSIVITY.....:	0.30	m
DECAY CONSTANT (lambda).....:	0.00	1/d
DISTANCE INCREMENT DELX.....:	1.00	m
NUMBER OF DISTANCE INCREMENTS.....:	19	
INITIAL TIME.....:	4.00	d
TIME INCREMENT DELT.....:	4.00	d
NUMBER OF TIME INCREMENTS.....:	1	

```

*****
*
*  SLUG INJECTION IN TWO-DIMENSIONAL UNIFORM FLOW
*
*  MODEL: SLUG.BAS
*
*****

```

USER: P.K.M. van der Heijde

LOCATION: IGWMC Indianapolis

DATE: February 10, 1985

INPUT DATA:

TOTAL SOLUTE MASS INJECTED.....:	25.00 kg
DARCY VELOCITY.....:	0.25 m/d
EFFECTIVE POROSITY.....:	.25
LONGITUDINAL DISPERSIVITY.....:	0.30 m
LATERAL DISPERSIVITY.....:	0.10 m
AQUIFER THICKNESS.....:	1.00 m
X-COORDINATE OF THE GRID ORIGIN.....:	0.00 m
Y-COORDINATE OF THE GRID ORIGIN.....:	0.00 m
DISTANCE INCREMENT DELX.....:	1.00 m
DISTANCE INCREMENT DELY.....:	1.00 m
NUMBER OF NODES IN X-DIRECTION.....:	10
NUMBER OF NODES IN Y-DIRECTION.....:	5
TIME.....:	4.00 d

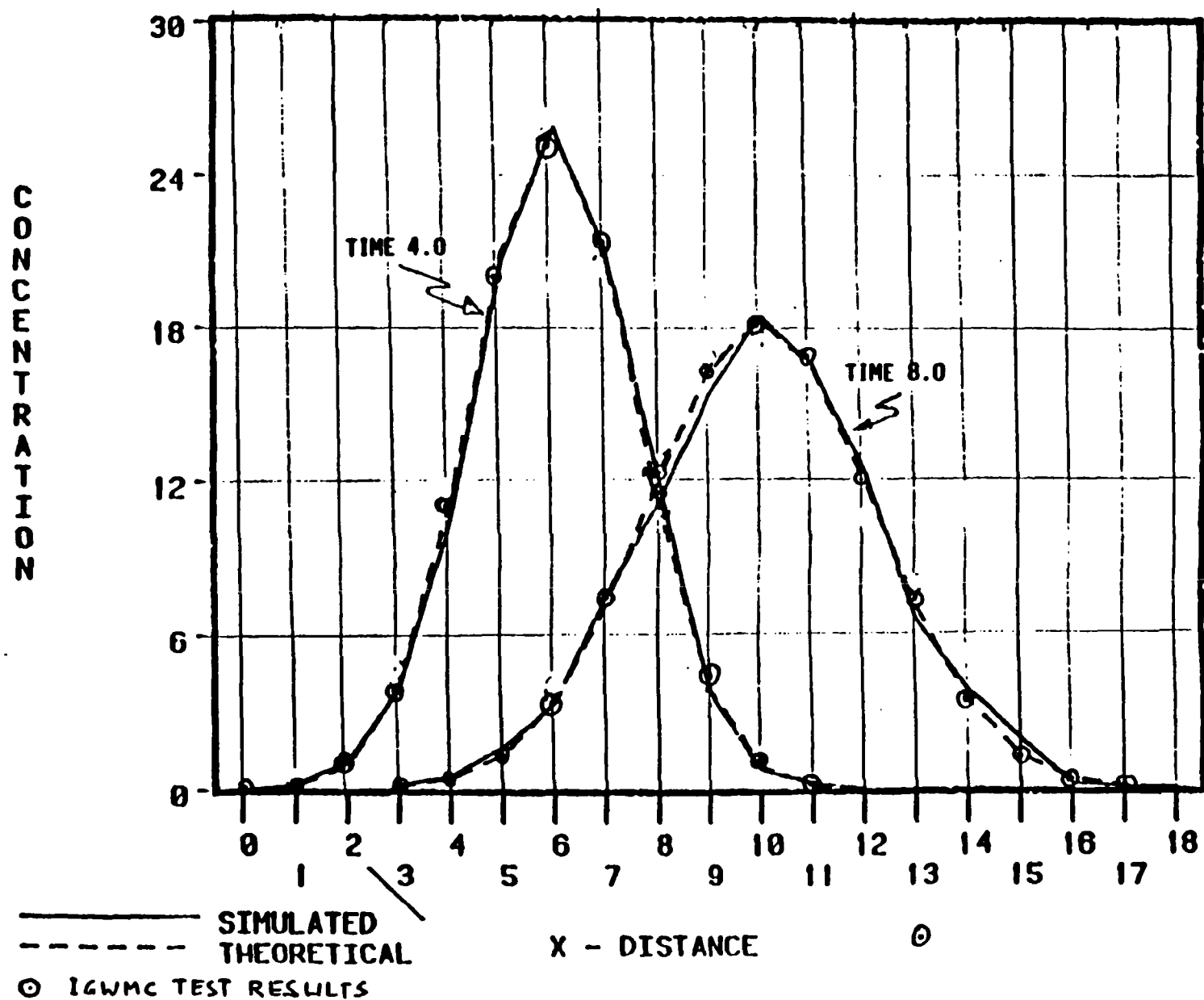


FIGURE 5.1

ONE DIMENSIONAL DISPERSION TEST

SLUG1D Data

***** RESULTS *****

source (0,0)

①-----> x-direction

CONCENTRATION in mg/l (ppm)

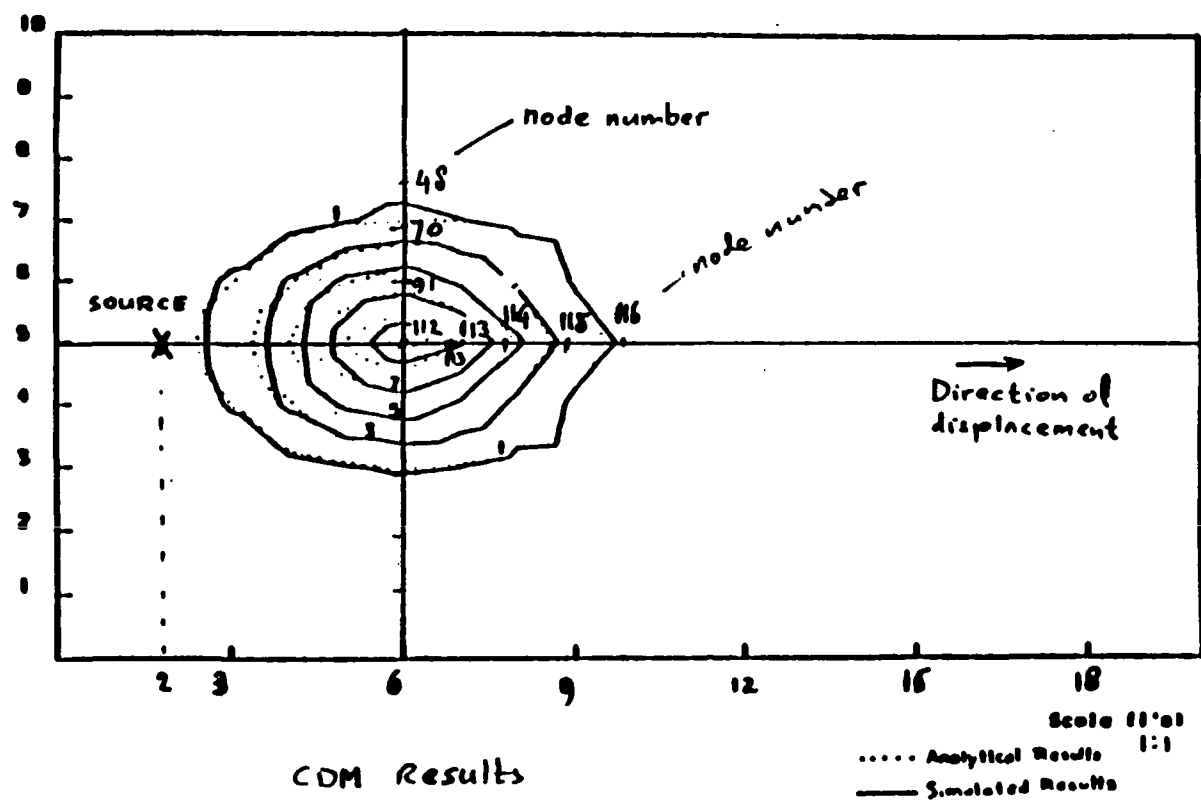
v Y

		0.00 m	1.00 m	2.00 m	3.00 m	4.00 m
0.00	m	409.7524	1761.4380	4991.8030	9325.9140	11486.0200
1.00	m	219.3248	942.8299	2671.9190	4991.8010	6148.0280
2.00	m	33.6345	144.5876	409.7523	765.5178	942.8304
3.00	m	1.4778	6.3527	18.0033	33.6345	41.4251
4.00	m	0.0186	0.0800	0.2266	0.4234	0.5215

		5.00 m	6.00 m	7.00 m	8.00 m	9.00 m
0.00	m	9325.9210	4991.8030	1761.4390	409.7524	62.8377
1.00	m	4991.8020	2671.9200	942.8294	219.3248	33.6346
2.00	m	765.5181	409.7525	144.5876	33.6345	5.1580
3.00	m	33.6345	18.0032	6.3527	1.4778	0.2266
4.00	m	0.4234	0.2266	0.0800	0.0186	0.0029

Results from DYNTRACK are kg/m³ → factor 1000 compared with mg/l. The source is in x=2, y=5. Particle mass: 0.0125

coordinates		concentration			corrected coordinates		node
x	y	level 1	level 2	average	X ₀	Y ₀	
6	8	0.1	0	.05	4	3	49
6	7	1.8	1.0	1.4	4	2	70
6	6	6.2	6.1	6.15	4	1	91
6	5	10.8	9.4	10.1	4	0	112
7	5	8.6	7.3	7.95	5	0	113
8	5	6.1	6.1	6.1	6	0	114
9	5	1.4	1.8	1.6	7	0	115
10	5	0.3	0.4	0.35	8	0	116



PLU A1 . 11/ 4/82 10.8
 PLO1 11:01E . 04-NOV-82 20.41

2-D DISPERSION FROM PLUG SOURCE

T=4d

FIGURE 5.2

SLUG2D data

```
*****
*
*   SLUG INJECTION IN TWO-DIMENSIONAL UNIFORM FLOW   *
*
*   MODEL: SLUG.BAS                                   *
*
*****
```

USER: P.K.M. van der Heijde

LOCATION: IGWMC Indianapolis

DATE: February 10, 1985

INPUT DATA:

TOTAL SOLUTE MASS INJECTED.....:	25.00 kg
DARCY VELOCITY.....:	0.25 m/d
EFFECTIVE POROSITY.....:	.25
LONGITUDINAL DISPERSIVITY.....:	0.30 m
LATERAL DISPERSIVITY.....:	0.10 m
AQUIFER THICKNESS.....:	1.00 m
X-COORDINATE OF THE GRID ORIGIN.....:	0.00 m
Y-COORDINATE OF THE GRID ORIGIN.....:	0.00 m
DISTANCE INCREMENT DELX.....:	1.00 m
DISTANCE INCREMENT DELY.....:	1.00 m
NUMBER OF NODES IN X-DIRECTION.....:	10
NUMBER OF NODES IN Y-DIRECTION.....:	5
TIME.....:	8.00 d

***** RESULTS *****

Source (0,0)

-----> X-direction

CONCENTRATION in mg/l (ppm)

 ↓
 Y

		0.00 m	1.00 m	2.00 m	3.00 m	4.00 m
0.00	m	7.3088	34.8681	135.0626	424.7803	1084.7150
1.00	m	5.3472	25.5100	98.8139	310.7757	793.5943
2.00	m	2.0940	9.9899	38.6961	121.7016	310.7760
3.00	m	0.4389	2.0940	8.1112	25.5100	65.1421
4.00	m	0.0492	0.2349	0.9100	2.8622	7.3088

		5.00 m	6.00 m	7.00 m	8.00 m	9.00 m
0.00	m	2248.9950	3786.0220	5174.8870	5743.0110	5174.8870
1.00	m	1645.4000	2769.9140	3786.0210	4201.6820	3786.0230
2.00	m	644.3478	1084.7160	1482.6280	1645.4000	1482.6280
3.00	m	135.0624	227.3683	310.7758	344.8951	310.7755
4.00	m	15.1536	25.5100	34.8681	38.6961	34.8681

Results from DYNTRACK are $\text{kg/m}^3 \rightarrow$ factor 1000 compared with mg/l

DYNTRACK: source in $x=2, y=5$; particle mass : 0.0125

coord.		corrected coordinates		node	concentration		
x	y	x_0	y_0	#	level 1	level 2	average
6	8	4	3	49	—	—	—
6	7	4	2	70	0.4	0.5	0.45
6	6	4	1	91	1.0	0.9	0.95
6	5	4	0	112	1.2	1.4	1.1
7	5	5	0	113	3.0	1.6	2.3
8	5	6	0	114	2.6	4.1	3.35
9	5	7	0	115	4.8	5.1	4.95
10	5	8	0	116	5.1	5.6	5.35

```

*****
*
*   SOLUTE TRANSPORT FROM POINT SOURCES
*   IN TWO-DIMENSIONAL UNIFORM FLOW
*
*   MODEL: WMPLUME
*
*****

```

USER: P.K.M. van der Heijde

LOCATION: IGWMC Indianapolis

DATE: February 10, 1985

INPUT DATA:

DARCY VELOCITY.....	0.25 m/d
EFFECTIVE POROSITY.....	.25
AQUIFER THICKNESS.....	1.00 m
LONGITUDINAL DISPERSIVITY.....	0.30 m
LATERAL DISPERSIVITY.....	0.10 m
RETARDATION FACTOR.....	1.00
DECAY CONSTANT (lambda).....	0 1/d
NUMBER OF POINT SOURCES.....	1

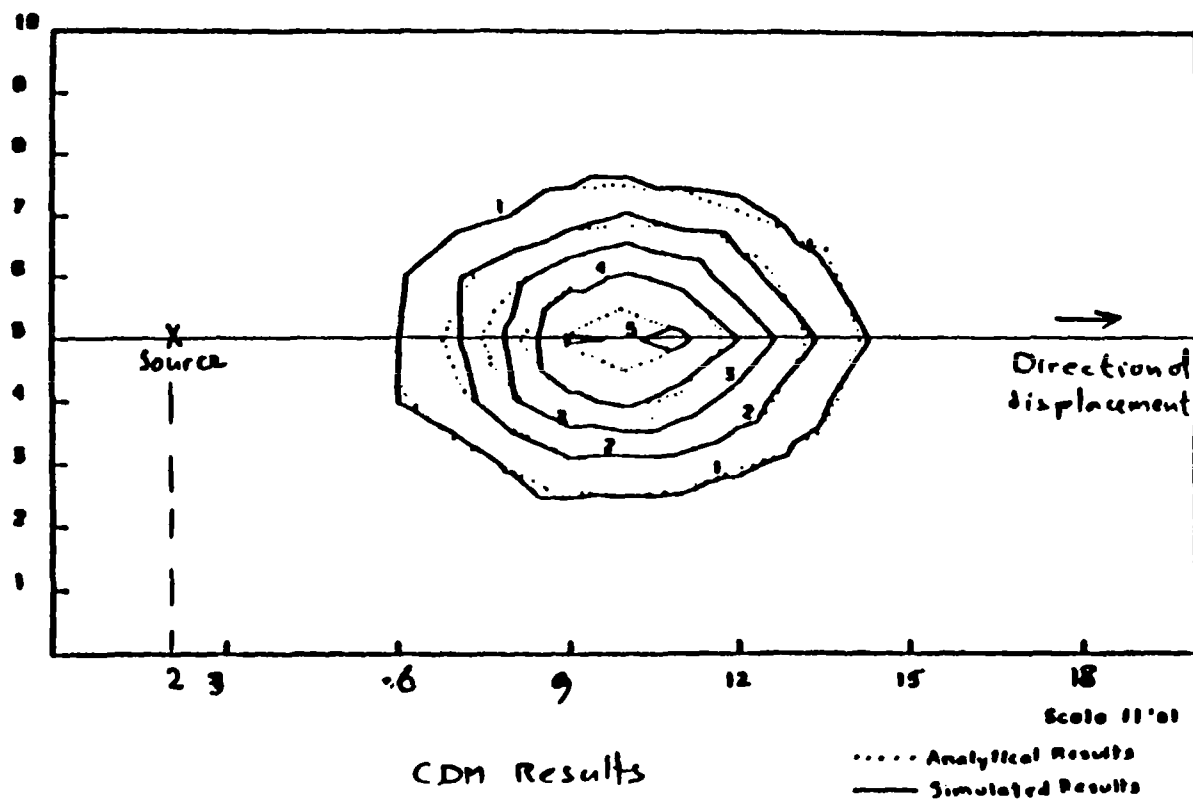
SOURCE DATA:

SOURCE NO. 1

X-COORDINATE OF THE SOURCE.....	0.00 m
Y-COORDINATE OF THE SOURCE.....	0.00 m
THE SOURCE STRENGTH.....	2.50 kg/d
ELAPSED TIME OF THE SOURCE ACTIVITY....	20.00 d

GRID DATA:

X-COORDINATE OF THE GRID ORIGIN.....	0.00 m
Y-COORDINATE OF THE GRID ORIGIN.....	0.00 m
DISTANCE INCREMENT DELX.....	1.00 m
DISTANCE INCREMENT DELY.....	1.00 m
NUMBER OF NODES IN X-DIRECTION.....	20
NUMBER OF NODES IN Y-DIRECTION.....	5



Run #1 11/4/82 10.4
PLD DATE 04-NOV-82 20.47

2-D DISPERSION FROM PLUG SOURCE

$T = 8d$

FIGURE 1

SLUG2D data

***** RESULTS *****

Source

X-direction

CONCENTRATION in mg/l (ppm)

	0.00 m	1.00 m	2.00 m	3.00 m	4.00 m
0.00 m	-1.0000	8920.6210	6307.8320	5150.3210	4460.3020
1.00 m	377.9327	1191.3950	1869.4350	2211.4210	2349.2310
2.00 m	14.9004	61.0869	159.1168	298.0794	450.5890
3.00 m	0.6783	3.0360	9.8881	24.5378	49.0761
4.00 m	0.0328	0.1531	0.5616	1.6523	4.0127

DYNTRACK

0.00 m
2.00 m

	5.00 m	6.00 m	7.00 m	8.00 m	9.00 m
	5.3	7.4 .2	4.7 .3	4.6 .4	3.8 .8

0.00 m	3989.3930	3641.7310	3371.3820	3153.0770	2971.3160
1.00 m	2385.6380	2372.8940	2336.3850	2288.6190	2235.6370
2.00 m	595.1167	721.4293	826.9710	912.8252	981.2449
3.00 m	83.3483	125.3780	172.4102	221.7358	271.0492
4.00 m	8.3009	15.0636	24.5977	36.8998	51.6842

DYNTRACK

0.00 m
2.00 m

	10.00 m	11.00 m	12.00 m	13.00 m	14.00 m
	4.3 .9	4.1 .8	2.3 .7	4.3 .7	2.9 .7

0.00 m	2815.4580	2677.0610	2548.2240	2420.5600	2284.8790
1.00 m	2179.9460	2121.5580	2058.4130	1986.3950	1899.6690
2.00 m	1034.3600	1073.4660	1098.6120	1108.3440	1099.8020
3.00 m	318.4551	362.2535	400.6633	431.5586	452.3850
4.00 m	68.4209	86.3511	104.4720	121.5115	135.9409

DYNTRACK

0.00 m
2.00 m

	15.00 m	16.00 m	17.00 m	18.00 m	19.00 m
	3.0 1.4	1.9 1.0	1.7 1.5	3.0 1.3	2.0 .8

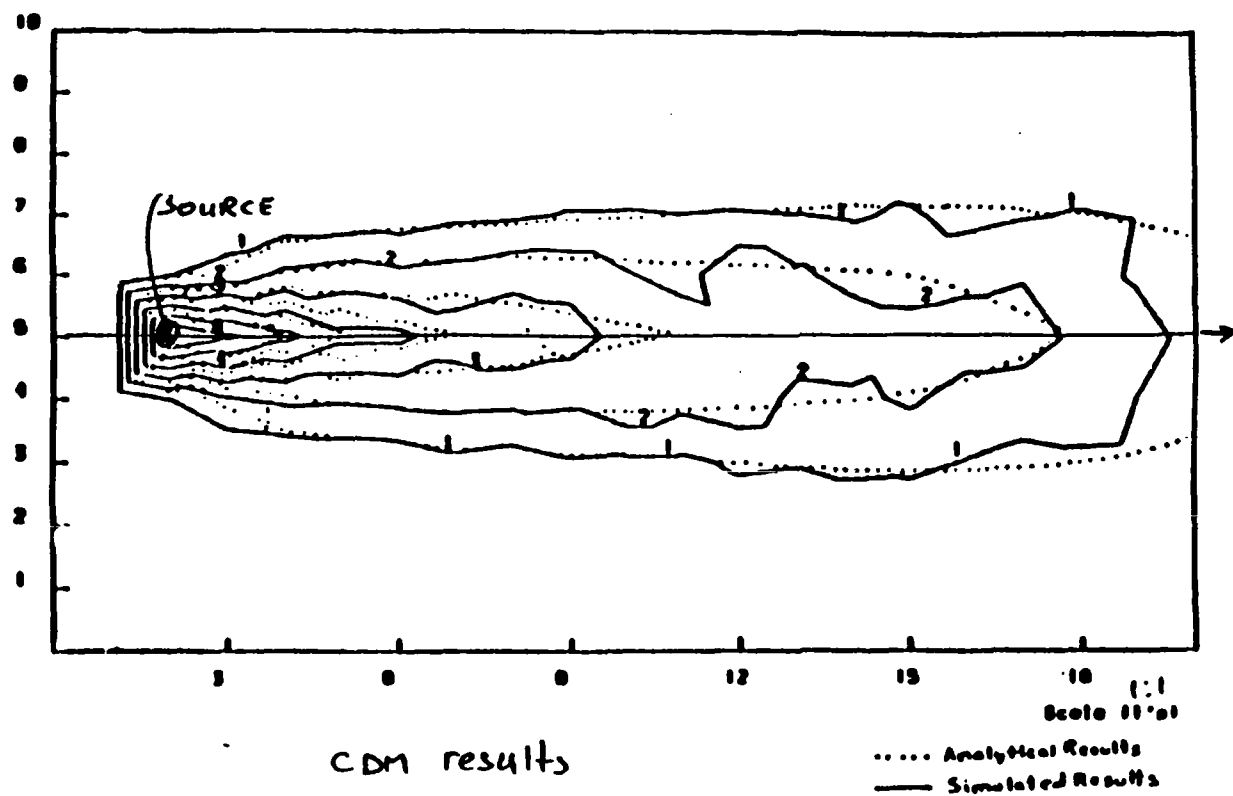
0.00 m	2131.7970	1953.3780	1745.4840	1509.9860	1255.7210
1.00 m	1791.5130	1656.0330	1490.3350	1296.6700	1083.2890
2.00 m	1069.2850	1013.4140	930.7179	823.1512	696.8230
3.00 m	460.3555	453.0024	429.0032	388.9927	335.9920
4.00 m	146.0920	150.4159	147.8525	138.2073	122.3755

DYNTRACK

0.00 m
2.00 m

	2.5	1.2	1.5	0.9	1
	1.5	1.0	1.4	.8	

Particle mass .0125



Run #1 . 11/ 4/02 10.3
 Plot Date . 04-NOV-02 20.02

2-D DISPERSION FROM CONSTANT SOURCE 1-20 d.

FIGURE 5.4

CONT2D data

```

*****
*
* SLUG INJECTION IN THREE-DIMENSIONAL UNIFORM FLOW *
*
* MODEL: SLUG3D.BAS *
*
*****

```

USER: P.K.M. van der Heijde

LOCATION: IGWMC Indianapolis

DATE: February 10, 1985

INPUT DATA:

TOTAL SOLUTE MASS INJECTED.....:	25.00 kg
DARCY VELOCITY.....:	0.25 m/d
EFFECTIVE POROSITY.....:	.25
LONGITUDINAL DISPERSIVITY.....:	0.30 m
LATERAL DISPERSIVITY.....:	0.10 m
VERTICAL DISPERSIVITY.....:	0.03 m
DECAY CONSTANT (lambda).....:	0 1/d
DISTANCE INCREMENT DELX.....:	1.00 m
DISTANCE INCREMENT DELY.....:	1.00 m
DISTANCE INCREMENT DELZ.....:	1.00 m
NUMBER OF NODES IN X-DIRECTION.....:	15
NUMBER OF NODES IN Y-DIRECTION.....:	6
NUMBER OF NODES IN Z-DIRECTION.....:	5
TIME.....:	8.00 d

***** RESULTS *****

+-----> X-direction

CONCENTRATION in mg/l (ppm)

source in [0,0,0]

↓

√ Y

Z = 0 m

		0.00 m	1.00 m	2.00 m	3.00 m	4.00 m
0.00	m	4.6102	21.9942	85.1953	267.9443	684.2196
1.00	m	3.3729	16.0913	62.3302	196.0322	500.5857
2.00	m	1.3209	6.3014	24.4088	76.7673	196.0322
3.00	m	0.2769	1.3209	5.1164	16.0913	41.0906
4.00	m	0.0311	0.1482	0.5740	1.8054	4.6102
5.00	m	0.0019	0.0089	0.0345	0.1084	0.2769

		5.00 m	6.00 m	7.00 m	8.00 m	9.00 m
0.00	m	1418.6280	2388.1610	3264.2290	3622.5930	3264.2290
1.00	m	1037.8900	1747.2160	2388.1610	2650.3460	2388.1610
2.00	m	406.4438	684.2196	935.2172	1037.8900	935.2172
3.00	m	85.1952	143.4202	196.0322	217.5537	196.0322
4.00	m	9.5586	16.0913	21.9942	24.4088	21.9942
5.00	m	0.5740	0.9664	1.3209	1.4659	1.3209

		10.00 m	11.00 m	12.00 m	13.00 m	14.00
0.00	m	2388.1610	1418.6280	684.2196	267.9443	85.1953
1.00	m	1747.2160	1037.8900	500.5857	196.0322	62.3302
2.00	m	684.2196	406.4438	196.0322	76.7673	24.4088
3.00	m	143.4202	85.1952	41.0906	16.0913	5.1164
4.00	m	16.0913	9.5586	4.6102	1.8054	0.5740
5.00	m	0.9664	0.5740	0.2769	0.1084	0.0345

***** RESULTS *****

+-----> X-direction CONCENTRATION in mg/l (ppm)

|

v Y

Z = 2 m

		0.00 m	1.00 m	2.00 m	3.00 m
0.00	m	0.0311	0.1482	0.5740	1.8054
1.00	m	0.0227	0.1084	0.4200	1.3209
2.00	m	0.0089	0.0425	0.1645	0.5173
3.00	m	0.0019	0.0089	0.0345	0.1084
4.00	m	0.0002	0.0010	0.0039	0.0122
5.00	m	0.0000	0.0000	0.0002	0.0007

		5.00 m	6.00 m	7.00 m	8.00 m
0.00	m	9.5586	16.0913	21.9942	24.4088
1.00	m	6.9933	11.7726	16.0913	17.8579
2.00	m	2.7386	4.6102	6.3014	6.9933
3.00	m	0.5740	0.9664	1.3209	1.4659
4.00	m	0.0644	0.1084	0.1482	0.1645
5.00	m	0.0039	0.0065	0.0089	0.0099

		10.00 m	11.00 m	12.00 m	13.00 m
0.00	m	16.0913	9.5586	4.6102	1.8054
1.00	m	11.7726	6.9933	3.3729	1.3209
2.00	m	4.6102	2.7386	1.3209	0.5173
3.00	m	0.9664	0.5740	0.2769	0.1084
4.00	m	0.1084	0.0644	0.0311	0.0122
5.00	m	0.0065	0.0039	0.0019	0.0007

***** RESULTS *****

+-----> X-direction CONCENTRATION in mg/l (ppm)

↓
Y

Z = 1 m

		0.00 m	1.00 m	2.00 m	3.00 m	4.00 m
0.00	m	1.3209	6.3014	24.4088	76.7673	196.0322
1.00	m	0.9664	4.6102	17.8579	56.1642	143.4202
2.00	m	0.3784	1.8054	6.9933	21.9942	56.1642
3.00	m	0.0793	0.3784	1.4659	4.6102	11.7726
4.00	m	0.0089	0.0425	0.1645	0.5173	1.3209
5.00	m	0.0005	0.0025	0.0099	0.0311	0.0793

		5.00 m	6.00 m	7.00 m	8.00 m	9.00 m
0.00	m	406.4438	684.2196	935.2172	1037.8900	935.2172
1.00	m	297.3606	500.5857	684.2196	759.3368	684.2196
2.00	m	116.4481	196.0322	267.9443	297.3606	267.9443
3.00	m	24.4088	41.0906	56.1641	62.3302	56.1641
4.00	m	2.7386	4.6102	6.3014	6.9933	6.3014
5.00	m	0.1645	0.2769	0.3784	0.4200	0.3784

		10.00 m	11.00 m	12.00 m	13.00 m	14.00 m
0.00	m	684.2196	406.4438	196.0322	76.7673	24.4088
1.00	m	500.5857	297.3606	143.4202	56.1642	17.8579
2.00	m	196.0322	116.4481	56.1642	21.9942	6.9933
3.00	m	41.0906	24.4088	11.7726	4.6102	1.4659
4.00	m	4.6102	2.7386	1.3209	0.5173	0.1645
5.00	m	0.2769	0.1645	0.0793	0.0311	0.0099

***** RESULTS *****

+-----> X-direction CONCENTRATION in mg/l (ppm)

↓
Y

Z = 4 m

		0.00 m	1.00 m	2.00 m	3.00 m	4.00 m
0.00	m	0.0000	0.0000	0.0000	0.0000	0.0000
1.00	m	0.0000	0.0000	0.0000	0.0000	0.0000
2.00	m	0.0000	0.0000	0.0000	0.0000	0.0000
3.00	m	0.0000	0.0000	0.0000	0.0000	0.0000
4.00	m	0.0000	0.0000	0.0000	0.0000	0.0000
5.00	m	0.0000	0.0000	0.0000	0.0000	0.0000

		5.00 m	6.00 m	7.00 m	8.00 m	9.00 m
0.00	m	0.0000	0.0000	0.0000	0.0000	0.0000
1.00	m	0.0000	0.0000	0.0000	0.0000	0.0000
2.00	m	0.0000	0.0000	0.0000	0.0000	0.0000
3.00	m	0.0000	0.0000	0.0000	0.0000	0.0000
4.00	m	0.0000	0.0000	0.0000	0.0000	0.0000
5.00	m	0.0000	0.0000	0.0000	0.0000	0.0000

		10.00 m	11.00 m	12.00 m	13.00 m	14.00 m
0.00	m	0.0000	0.0000	0.0000	0.0000	0.0000
1.00	m	0.0000	0.0000	0.0000	0.0000	0.0000
2.00	m	0.0000	0.0000	0.0000	0.0000	0.0000
3.00	m	0.0000	0.0000	0.0000	0.0000	0.0000
4.00	m	0.0000	0.0000	0.0000	0.0000	0.0000
5.00	m	0.0000	0.0000	0.0000	0.0000	0.0000

***** RESULTS *****

+-----> X-direction CONCENTRATION in mg/l (ppm)

↓

v Y

Z = 3 m

		0.00 m	1.00 m	2.00 m	3.00 m	4.00 m
0.00	m	0.0000	0.0003	0.0011	0.0035	0.0089
1.00	m	0.0000	0.0002	0.0008	0.0025	0.0065
2.00	m	0.0000	0.0000	0.0003	0.0010	0.0025
3.00	m	0.0000	0.0000	0.0000	0.0002	0.0005
4.00	m	0.0000	0.0000	0.0000	0.0000	0.0000
5.00	m	0.0000	0.0000	0.0000	0.0000	0.0000

		5.00 m	6.00 m	7.00 m	8.00 m	9.00 m
0.00	m	0.0185	0.0311	0.0425	0.0471	0.0425
1.00	m	0.0135	0.0227	0.0311	0.0345	0.0311
2.00	m	0.0053	0.0089	0.0122	0.0135	0.0122
3.00	m	0.0011	0.0019	0.0025	0.0028	0.0025
4.00	m	0.0001	0.0002	0.0003	0.0003	0.0003
5.00	m	0.0000	0.0000	0.0000	0.0000	0.0000

		10.00 m	11.00 m	12.00 m	13.00 m	14.00 m
0.00	m	0.0311	0.0185	0.0089	0.0035	0.0011
1.00	m	0.0227	0.0135	0.0065	0.0025	0.0008
2.00	m	0.0089	0.0053	0.0025	0.0010	0.0003
3.00	m	0.0019	0.0011	0.0005	0.0002	0.0000
4.00	m	0.0002	0.0001	0.0000	0.0000	0.0000
5.00	m	0.0000	0.0000	0.0000	0.0000	0.0000

NODE NUMBERS		NODAL COORDINATES	
INT.	EXT.	X	Y
=====			
1	1	0.00000000	10.00000000
2	2	1.00000000	10.00000000
3	3	2.00000000	10.00000000
4	4	3.00000000	10.00000000
5	5	4.00000000	10.00000000
6	6	5.00000000	10.00000000
7	7	6.00000000	10.00000000
8	8	7.00000000	10.00000000
9	9	8.00000000	10.00000000
10	10	9.00000000	10.00000000
11	11	10.00000000	10.00000000
12	12	11.00000000	10.00000000
13	13	12.00000000	10.00000000
14	14	13.00000000	10.00000000
15	15	14.00000000	10.00000000
16	16	15.00000000	10.00000000
17	17	16.00000000	10.00000000
18	18	17.00000000	10.00000000
19	19	18.00000000	10.00000000
20	20	19.00000000	10.00000000
21	21	20.00000000	10.00000000
22	22	0.00000000	9.00000000
23	23	1.00000000	9.00000000
24	24	2.00000000	9.00000000
25	25	3.00000000	9.00000000
26	26	4.00000000	9.00000000
27	27	5.00000000	9.00000000
28	28	6.00000000	9.00000000
29	29	7.00000000	9.00000000
30	30	8.00000000	9.00000000
31	31	9.00000000	9.00000000
32	32	10.00000000	9.00000000
33	33	11.00000000	9.00000000
34	34	12.00000000	9.00000000
35	35	13.00000000	9.00000000
36	36	14.00000000	9.00000000
37	37	15.00000000	9.00000000
38	38	16.00000000	9.00000000
39	39	17.00000000	9.00000000
40	40	18.00000000	9.00000000
41	41	19.00000000	9.00000000
42	42	20.00000000	9.00000000
43	43	0.00000000	8.00000000
44	44	1.00000000	8.00000000
45	45	2.00000000	8.00000000
46	46	3.00000000	8.00000000
47	47	4.00000000	8.00000000
48	48	5.00000000	8.00000000
49	49	6.00000000	8.00000000
50	50	7.00000000	8.00000000

NODE NUMBERS		NODAL COORDINATES	
INT.	EXT.	X	Y
=====			
1	1	0.00000000	10.00000000
2	2	1.00000000	10.00000000
3	3	2.00000000	10.00000000
4	4	3.00000000	10.00000000
5	5	4.00000000	10.00000000
6	6	5.00000000	10.00000000
7	7	6.00000000	10.00000000
8	8	7.00000000	10.00000000
9	9	8.00000000	10.00000000
10	10	9.00000000	10.00000000
11	11	10.00000000	10.00000000
12	12	11.00000000	10.00000000
13	13	12.00000000	10.00000000
14	14	13.00000000	10.00000000
15	15	14.00000000	10.00000000
16	16	15.00000000	10.00000000
17	17	16.00000000	10.00000000
18	18	17.00000000	10.00000000
19	19	18.00000000	10.00000000
20	20	19.00000000	10.00000000
21	21	20.00000000	10.00000000
22	22	0.00000000	9.00000000
23	23	1.00000000	9.00000000
24	24	2.00000000	9.00000000
25	25	3.00000000	9.00000000
26	26	4.00000000	9.00000000
27	27	5.00000000	9.00000000
28	28	6.00000000	9.00000000
29	29	7.00000000	9.00000000
30	30	8.00000000	9.00000000
31	31	9.00000000	9.00000000
32	32	10.00000000	9.00000000
33	33	11.00000000	9.00000000
34	34	12.00000000	9.00000000
35	35	13.00000000	9.00000000
36	36	14.00000000	9.00000000
37	37	15.00000000	9.00000000
38	38	16.00000000	9.00000000
39	39	17.00000000	9.00000000
40	40	18.00000000	9.00000000
41	41	19.00000000	9.00000000
42	42	20.00000000	9.00000000
43	43	0.00000000	8.00000000
44	44	1.00000000	8.00000000
45	45	2.00000000	8.00000000
46	46	3.00000000	8.00000000
47	47	4.00000000	8.00000000
48	48	5.00000000	8.00000000
49	49	6.00000000	8.00000000
50	50	7.00000000	8.00000000

NODE NUMBERS		NODAL COORDINATES	
INT.	EXT.	X	Y
101	101	16.00000000	6.00000000
102	102	17.00000000	6.00000000
103	103	18.00000000	6.00000000
104	104	19.00000000	6.00000000
105	105	20.00000000	6.00000000
106	106	0.00000000	5.00000000
107	107	1.00000000	5.00000000
108	108	2.00000000	5.00000000
109	109	3.00000000	5.00000000
110	110	4.00000000	5.00000000
111	111	5.00000000	5.00000000
112	112	6.00000000	5.00000000
113	113	7.00000000	5.00000000
114	114	8.00000000	5.00000000
115	115	9.00000000	5.00000000
116	116	10.00000000	5.00000000
117	117	11.00000000	5.00000000
118	118	12.00000000	5.00000000
119	119	13.00000000	5.00000000
120	120	14.00000000	5.00000000
121	121	15.00000000	5.00000000
122	122	16.00000000	5.00000000
123	123	17.00000000	5.00000000
124	124	18.00000000	5.00000000
125	125	19.00000000	5.00000000
126	126	20.00000000	5.00000000
127	127	0.00000000	4.00000000
128	128	1.00000000	4.00000000
129	129	2.00000000	4.00000000
130	130	3.00000000	4.00000000
131	131	4.00000000	4.00000000
132	132	5.00000000	4.00000000
133	133	6.00000000	4.00000000
134	134	7.00000000	4.00000000
135	135	8.00000000	4.00000000
136	136	9.00000000	4.00000000
137	137	10.00000000	4.00000000
138	138	11.00000000	4.00000000
139	139	12.00000000	4.00000000
140	140	13.00000000	4.00000000
141	141	14.00000000	4.00000000
142	142	15.00000000	4.00000000
143	143	16.00000000	4.00000000
144	144	17.00000000	4.00000000
145	145	18.00000000	4.00000000
146	146	19.00000000	4.00000000
147	147	20.00000000	4.00000000
148	148	0.00000000	3.00000000
149	149	1.00000000	3.00000000
150	150	2.00000000	3.00000000

NODE NUMBERS		NODAL COORDINATES	
INT.	EXT.	X	Y
51	51	8.00000000	8.00000000
52	52	9.00000000	8.00000000
53	53	10.00000000	8.00000000
54	54	11.00000000	8.00000000
55	55	12.00000000	8.00000000
56	56	13.00000000	8.00000000
57	57	14.00000000	8.00000000
58	58	15.00000000	8.00000000
59	59	16.00000000	8.00000000
60	60	17.00000000	8.00000000
61	61	18.00000000	8.00000000
62	62	19.00000000	8.00000000
63	63	20.00000000	8.00000000
64	64	0.00000000	7.00000000
65	65	1.00000000	7.00000000
66	66	2.00000000	7.00000000
67	67	3.00000000	7.00000000
68	68	4.00000000	7.00000000
69	69	5.00000000	7.00000000
70	70	6.00000000	7.00000000
71	71	7.00000000	7.00000000
72	72	8.00000000	7.00000000
73	73	9.00000000	7.00000000
74	74	10.00000000	7.00000000
75	75	11.00000000	7.00000000
76	76	12.00000000	7.00000000
77	77	13.00000000	7.00000000
78	78	14.00000000	7.00000000
79	79	15.00000000	7.00000000
80	80	16.00000000	7.00000000
81	81	17.00000000	7.00000000
82	82	18.00000000	7.00000000
83	83	19.00000000	7.00000000
84	84	20.00000000	7.00000000
85	85	0.00000000	6.00000000
86	86	1.00000000	6.00000000
87	87	2.00000000	6.00000000
88	88	3.00000000	6.00000000
89	89	4.00000000	6.00000000
90	90	5.00000000	6.00000000
91	91	6.00000000	6.00000000
92	92	7.00000000	6.00000000
93	93	8.00000000	6.00000000
94	94	9.00000000	6.00000000
95	95	10.00000000	6.00000000
96	96	11.00000000	6.00000000
97	97	12.00000000	6.00000000
98	98	13.00000000	6.00000000
99	99	14.00000000	6.00000000
100	100	15.00000000	6.00000000

NODE NUMBERS		NODAL COORDINATES	
INT.	EXT.	X	Y
201	201	11.00000000	1.000000000
202	202	12.00000000	1.000000000
203	203	13.00000000	1.000000000
204	204	14.00000000	1.000000000
205	205	15.00000000	1.000000000
206	206	16.00000000	1.000000000
207	207	17.00000000	1.000000000
208	208	18.00000000	1.000000000
209	209	19.00000000	1.000000000
210	210	20.00000000	1.000000000
211	211	0.000000000	0.000000000E+00
212	212	1.000000000	0.000000000E+00
213	213	2.000000000	0.000000000E+00
214	214	3.000000000	0.000000000E+00
215	215	4.000000000	0.000000000E+00
216	216	5.000000000	0.000000000E+00
217	217	6.000000000	0.000000000E+00
218	218	7.000000000	0.000000000E+00
219	219	8.000000000	0.000000000E+00
220	220	9.000000000	0.000000000E+00
221	221	10.00000000	0.000000000E+00
222	222	11.00000000	0.000000000E+00
223	223	12.00000000	0.000000000E+00
224	224	13.00000000	0.000000000E+00
225	225	14.00000000	0.000000000E+00
226	226	15.00000000	0.000000000E+00
227	227	16.00000000	0.000000000E+00
228	228	17.00000000	0.000000000E+00
229	229	18.00000000	0.000000000E+00
230	230	19.00000000	0.000000000E+00
231	231	20.00000000	0.000000000E+00

NODE NUMBERS		NODAL COORDINATES	
INT.	EXT.	X	Y
151	151	3.00000000	3.00000000
152	152	4.00000000	3.00000000
153	153	5.00000000	3.00000000
154	154	6.00000000	3.00000000
155	155	7.00000000	3.00000000
156	156	8.00000000	3.00000000
157	157	9.00000000	3.00000000
158	158	10.00000000	3.00000000
159	159	11.00000000	3.00000000
160	160	12.00000000	3.00000000
161	161	13.00000000	3.00000000
162	162	14.00000000	3.00000000
163	163	15.00000000	3.00000000
164	164	16.00000000	3.00000000
165	165	17.00000000	3.00000000
166	166	18.00000000	3.00000000
167	167	19.00000000	3.00000000
168	168	20.00000000	3.00000000
169	169	0.00000000	2.00000000
170	170	1.00000000	2.00000000
171	171	2.00000000	2.00000000
172	172	3.00000000	2.00000000
173	173	4.00000000	2.00000000
174	174	5.00000000	2.00000000
175	175	6.00000000	2.00000000
176	176	7.00000000	2.00000000
177	177	8.00000000	2.00000000
178	178	9.00000000	2.00000000
179	179	10.00000000	2.00000000
180	180	11.00000000	2.00000000
181	181	12.00000000	2.00000000
182	182	13.00000000	2.00000000
183	183	14.00000000	2.00000000
184	184	15.00000000	2.00000000
185	185	16.00000000	2.00000000
186	186	17.00000000	2.00000000
187	187	18.00000000	2.00000000
188	188	19.00000000	2.00000000
189	189	20.00000000	2.00000000
190	190	0.00000000	1.00000000
191	191	1.00000000	1.00000000
192	192	2.00000000	1.00000000
193	193	3.00000000	1.00000000
194	194	4.00000000	1.00000000
195	195	5.00000000	1.00000000
196	196	6.00000000	1.00000000
197	197	7.00000000	1.00000000
198	198	8.00000000	1.00000000
199	199	9.00000000	1.00000000
200	200	10.00000000	1.00000000

101	0.0000E+00	0.0000E+00	0.5000E-01	0.0000E+00	0.0000E+00
110	0.0000E+00	0.0000E+00	0.1000	0.5000E-01	0.0000E+00
111	0.0000E+00	0.0000E+00	0.4000	0.1000	0.0000E+00
112	0.0000E+00	0.4500	0.5000	0.5000E-01	0.0000E+00
113	0.0000E+00	0.4500	1.000	0.6000	0.1000
114	0.3000	0.5000	2.800	1.000	0.0000E+00
115	0.0000E+00	1.050	2.550	0.7000	0.0000E+00
116	0.0000E+00	0.8000	2.800	1.300	0.0000E+00
117	0.1000	0.8000	3.450	0.9500	0.0000E+00
118	0.0000E+00	0.6500	2.050	0.8000	0.0000E+00
119	0.0000E+00	0.4000	1.450	0.3500	0.0000E+00
120	0.0000E+00	0.1500	1.050	0.2000	0.0000E+00
121	0.0000E+00	0.0000E+00	0.1500	0.5000E-01	0.0000E+00
122	0.1000	0.0000E+00	0.5000E-01	0.0000E+00	0.0000E+00
123	0.0000E+00	0.0000E+00	0.0000E+00	0.5000E-01	0.0000E+00
124	0.0000E+00	0.0000E+00	1.5000E-01	0.5000E-01	0.0000E+00
132	0.0000E+00	0.1500	0.1500	0.5000E-01	0.0000E+00
131	0.0000E+00	0.2500	0.3000	0.1500	0.0000E+00
134	0.0000E+00	0.5000E-01	1.050	0.3500	0.0000E+00
135	0.1000	0.7000	1.400	0.4000	0.0000E+00
136	0.1000	0.8500	2.650	0.7000	0.2000
137	0.1000	1.000	2.100	1.350	0.0000E+00
138	0.0000E+00	0.9500	2.250	0.9000	0.0000E+00
139	0.1000	0.6000	1.100	0.3500	0.1000
140	0.0000E+00	0.3000	0.6000	0.5000	0.1000
141	0.0000E+00	0.5000E-01	0.2000	0.2500	0.0000E+00
142	0.0000E+00	0.1000	0.1000	0.5000E-01	0.0000E+00
143	0.0000E+00	0.5000E-01	0.0000E+00	0.0000E+00	0.0000E+00
144	0.0000E+00	0.5000E-01	0.0000E+00	0.5000E-01	0.0000E+00
152	0.0000E+00	0.0000E+00	0.0000E+00	0.5000E-01	0.0000E+00
153	0.0000E+00	0.5000E-01	0.5000E-01	0.0000E+00	0.0000E+00
154	0.0000E+00	0.5000E-01	0.5000E-01	0.5000E-01	0.0000E+00
155	0.0000E+00	0.2000	0.4500	0.5000E-01	0.0000E+00
156	0.0000E+00	0.1000	0.4500	0.1000	0.0000E+00
157	0.0000E+00	0.0000E+00	0.8500	0.3000	0.0000E+00
158	0.0000E+00	0.5000	0.9500	0.3500	0.0000E+00
159	0.0000E+00	0.4000	1.150	0.4000	0.2000
160	0.1000	0.2000	0.6000	0.1500	0.0000E+00
161	0.0000E+00	0.2000	0.4000	0.1500	0.0000E+00
162	0.0000E+00	0.5000E-01	0.4000	0.1000	0.0000E+00
163	0.0000E+00	0.0000E+00	0.5000E-01	0.5000E-01	0.0000E+00
164	0.0000E+00	0.0000E+00	0.0000E+00	0.0000E+00	0.1000
174	0.0000E+00	0.0000E+00	0.5000E-01	0.5000E-01	0.0000E+00
175	0.0000E+00	0.5000E-01	0.5000E-01	0.0000E+00	0.0000E+00
176	0.0000E+00	0.0000E+00	0.0000E+00	0.1000	0.0000E+00
177	0.0000E+00	0.0000E+00	0.1000	0.0000E+00	0.0000E+00
178	0.0000E+00	0.0000E+00	0.1500	0.5000E-01	0.0000E+00
179	0.0000E+00	0.1000	0.1500	0.1500	0.0000E+00
180	0.0000E+00	0.0000E+00	0.4000	0.5000E-01	0.0000E+00
181	0.0000E+00	0.5000E-01	0.2000	0.1000	0.0000E+00
182	0.0000E+00	0.5000E-01	0.0000E+00	0.5000E-01	0.0000E+00
184	0.0000E+00	0.5000E-01	0.0000E+00	0.0000E+00	0.0000E+00
194	0.0000E+00	0.0000E+00	0.0000E+00	0.5000E-01	0.0000E+00
197	0.0000E+00	0.0000E+00	0.5000E-01	0.5000E-01	0.0000E+00
200	0.0000E+00	0.0000E+00	0.5000E-01	0.0000E+00	0.0000E+00
202	0.0000E+00	0.0000E+00	0.0000E+00	0.5000E-01	0.0000E+00

CONTAMINANT MASS LEFT SYSTEM

=====

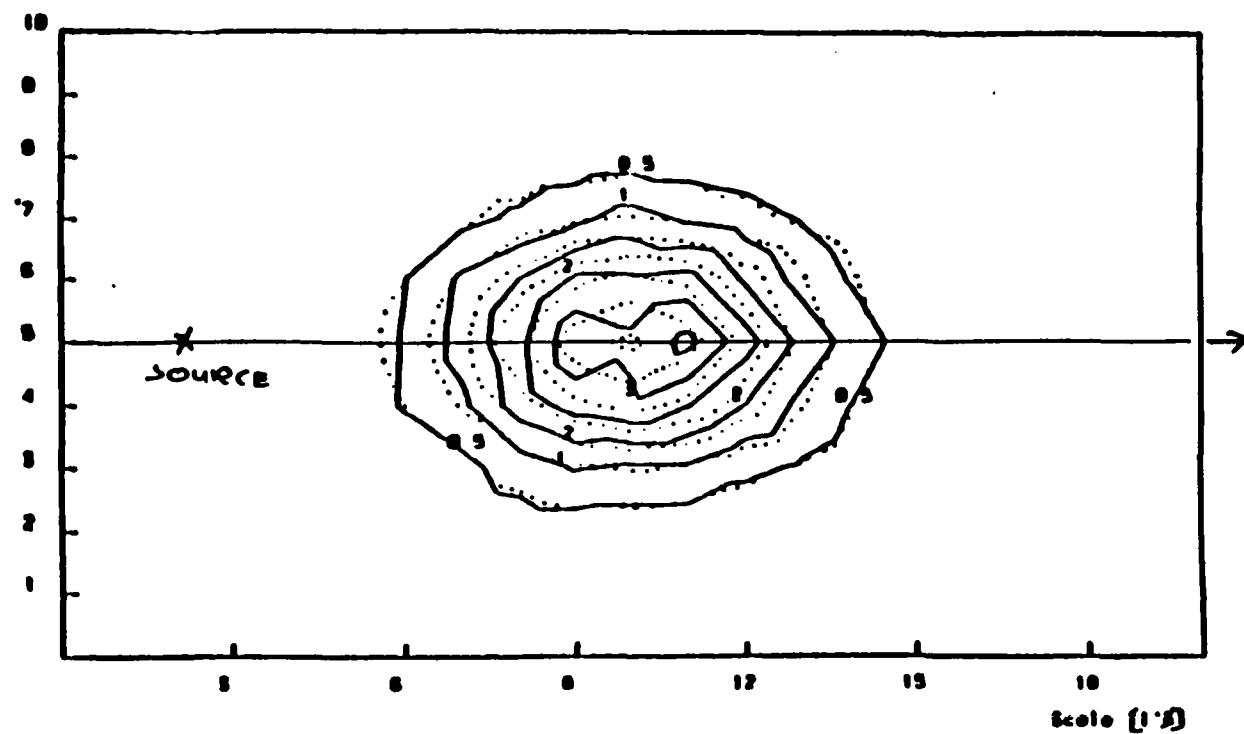
DYNIRA RUN OF 4/26/85 AT 17:00:07

SLUGGED THREE DIMENSIONAL DISPERSION TEST CASE; 2000 PART.
 UNIFORM FLOW FIELD, $v=1.0$ - INJECTED MASS = 25 AT (2.0,5.0,2.0)
 LONG DISP = .3, VERT DISP = .1, AZ/AY FACTOR = .5, EFF POROS = .25

TIME : 8.0000

CONCENTRATIONS
 =====

	LEVEL				
TIME	1	2	3	4	5
----	---	---	---	---	---
10	0.0000E+00	0.1000	0.0000E+00	0.0000E+00	0.0000E+00
20	0.0000E+00	0.0000E+00	0.5000E-01	0.0000E+00	0.0000E+00
30	0.0000E+00	0.0000E+00	0.0000E+00	0.5000E-01	0.0000E+00
40	0.0000E+00	0.0000E+00	0.1000	0.0000E+00	0.0000E+00
45	0.0000E+00	0.0000E+00	0.5000E-01	0.0000E+00	0.0000E+00
48	0.0000E+00	0.0000E+00	0.0000E+00	0.5000E-01	0.0000E+00
50	0.0000E+00	0.1500	0.0000E+00	0.0000E+00	0.0000E+00
51	0.0000E+00	0.5000E-01	0.2500	0.5000E-01	0.0000E+00
52	0.0000E+00	0.0000E+00	0.1500	0.0000E+00	0.0000E+00
53	0.0000E+00	0.1000	0.2000	0.1000	0.0000E+00
54	0.0000E+00	0.5000E-01	0.1500	0.0000E+00	0.0000E+00
55	0.1000	0.5000E-01	0.1000	0.5000E-01	0.0000E+00
56	0.0000E+00	0.0000E+00	0.1000	0.5000E-01	0.0000E+00
57	0.0000E+00	0.0000E+00	0.1500	0.0000E+00	0.0000E+00
58	0.0000E+00	0.0000E+00	0.0000E+00	0.1000	0.0000E+00
63	0.0000E+00	0.0000E+00	0.1000	0.0000E+00	0.0000E+00
69	0.0000E+00	0.5000E-01	0.0000E-01	0.0000E+00	0.0000E+00
70	0.0000E+00	0.2500	0.1000	0.1500	0.0000E+00
71	0.0000E+00	0.5000E-01	0.3000	0.1000	0.0000E+00
72	0.0000E+00	0.2500	0.7500	0.3500	0.0000E+00
73	0.1000	0.1500	0.8500	0.5000	0.1000
74	0.0000E+00	0.4000	1.200	0.5000	0.0000E+00
75	0.0000E+00	0.5500	1.100	0.2000	0.0000E+00
76	0.0000E+00	0.1500	0.6500	0.3000	0.0000E+00
77	0.0000E+00	0.2000	0.4500	0.1500	0.0000E+00
78	0.0000E+00	0.5000E-01	0.1000	0.1500	0.0000E+00
79	0.0000E+00	0.1000	0.1000	0.0000E+00	0.0000E+00
80	0.0000E+00	0.5000E-01	0.5000E-01	0.0000E+00	0.0000E+00
81	0.0000E+00	0.5000E-01	0.0000E+00	0.0000E+00	0.0000E+00
89	0.0000E+00	0.0000E+00	0.1000	0.0000E+00	0.0000E+00
90	0.0000E+00	0.0000E+00	0.2500	0.1000	0.0000E+00
91	0.1000	0.2000	0.6500	0.2000	0.0000E+00
92	0.0000E+00	0.3500	1.100	0.4000	0.0000E+00
93	0.1000	0.5500	2.000	0.4500	0.0000E+00
94	0.0000E+00	0.6500	2.350	1.050	0.0000E+00
95	0.2000	0.9000	2.150	0.9000	0.0000E+00
96	0.0000E+00	0.5500	1.800	0.7500	0.2000
97	0.0000E+00	0.5500	1.600	0.5000	0.2000
98	0.2000	0.1000	0.8500	0.3000	0.0000E+00
99	0.0000E+00	0.2000	0.6500	0.2500	0.0000E+00
100	0.0000E+00	0.1000	0.5000E-01	0.5000E-01	0.0000E+00



MINI 01 11/ 4/82 10.3
 PLOT DATE 04-NOV-82 20.00

3-D DISPERSION SECTION WITH Z=2 T=8
 Z=2. T=8

FIGURE 5.5 CDM results SLUG3D data

	LEVEL				
NODE	1	2	3	4	5
----	---	---	---	---	---
64	0.0000E+00	0.1250E-01	0.0000E+00	0.0000E+00	0.0000E+00

MASS SUMMARY
=====

INITIAL TOTAL NUMBER OF PARTICLES: 2000
PRESENT TOTAL NUMBER OF PARTICLES: 1999
TOTAL NUMBER OF PARTICLES LEFT SYSTEM : 1
TOTAL NUMBER OF PARTICLES LOST: 0

INITIAL TOTAL PARTICLE MASS: 25.00
PRESENT TOTAL PARTICLE MASS: 24.99
TOTAL PARTICLE MASS LEFT SYSTEM: 0.1250E-01
TOTAL PARTICLE MASS LOST: 0.0000E+00

REPORT OF RELATIVE PARTICLES LOSS
=====

	LEVEL			
ELEMENT	1	2	3	4
-----	---	---	---	---

END

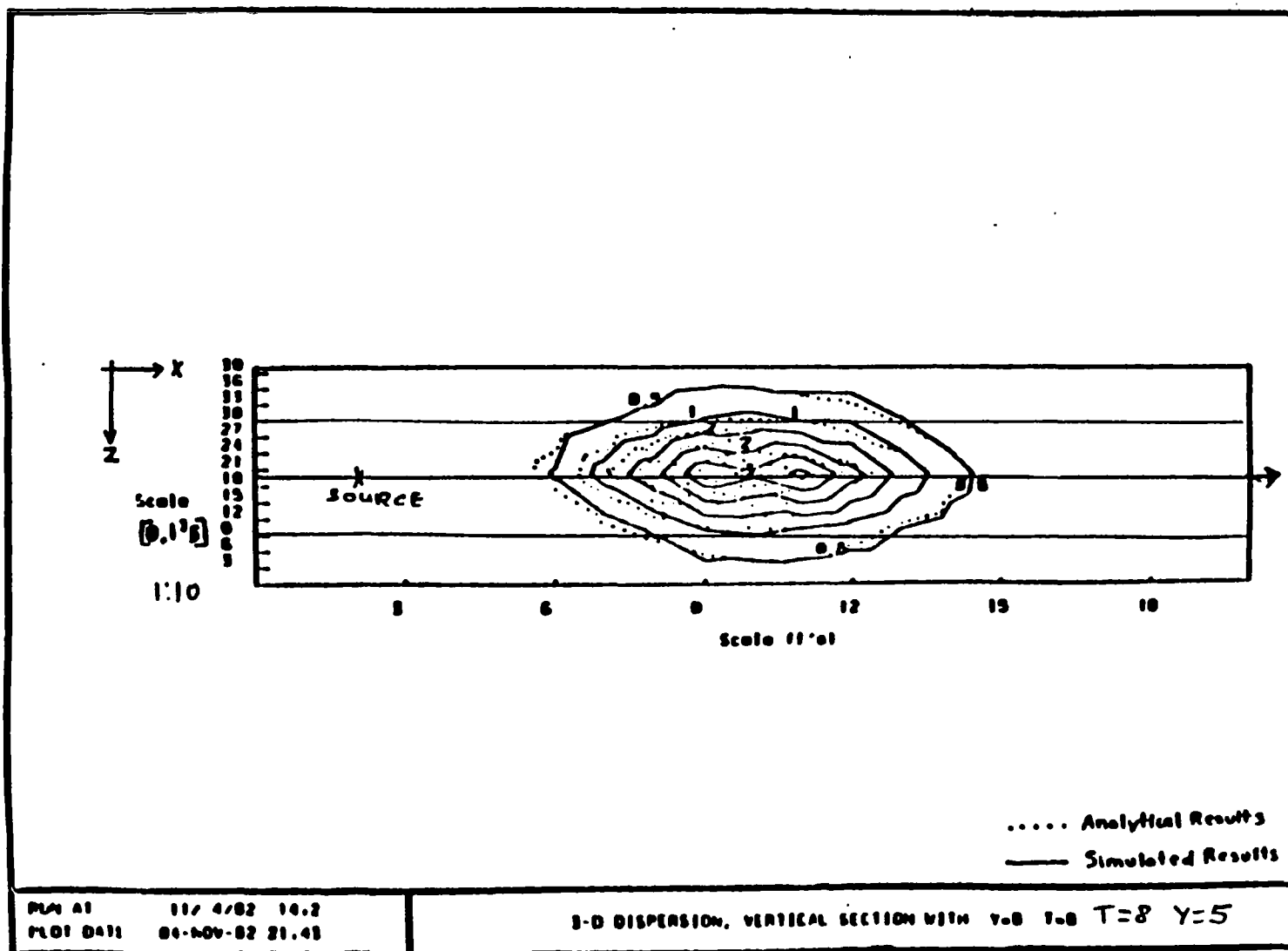
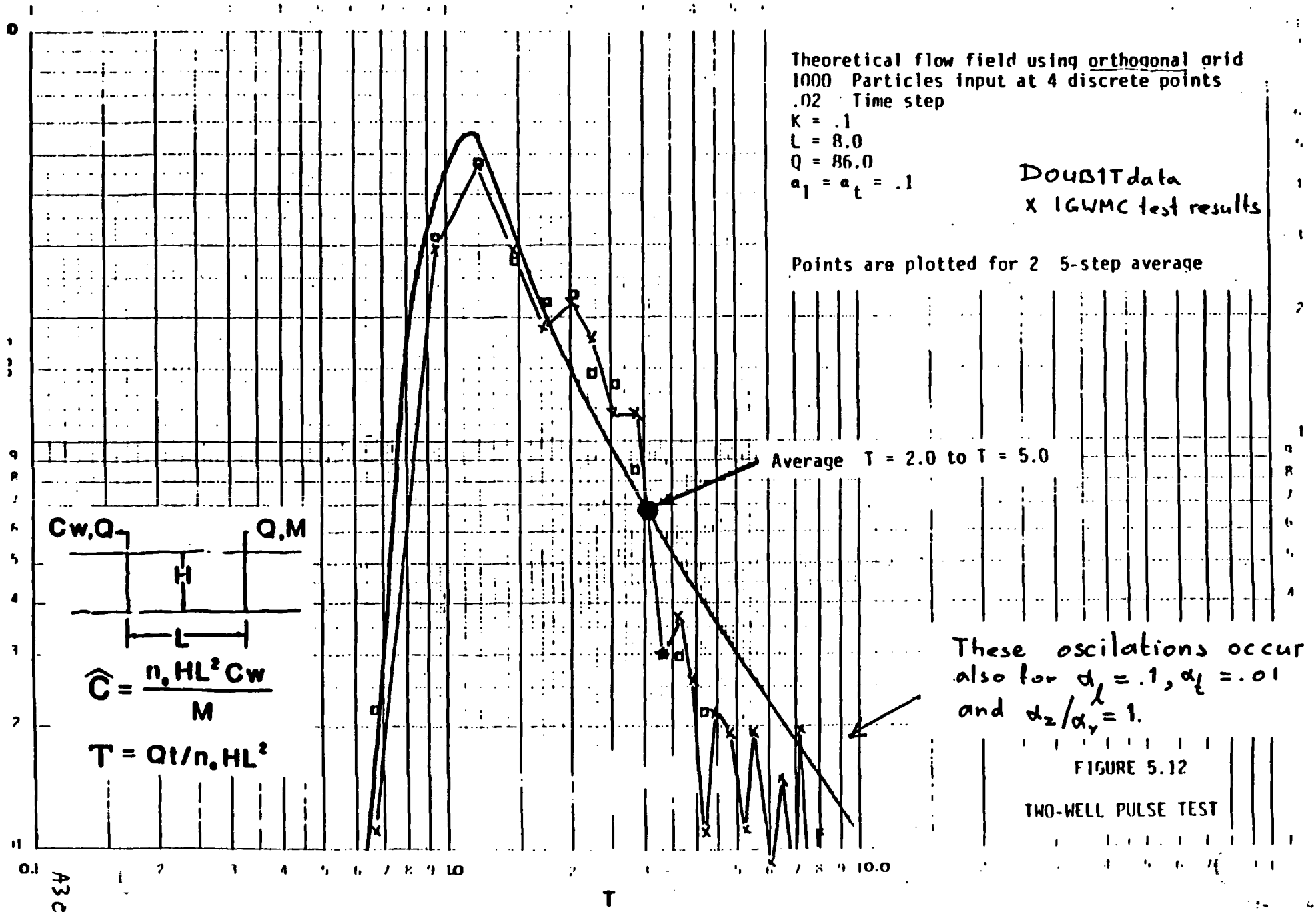
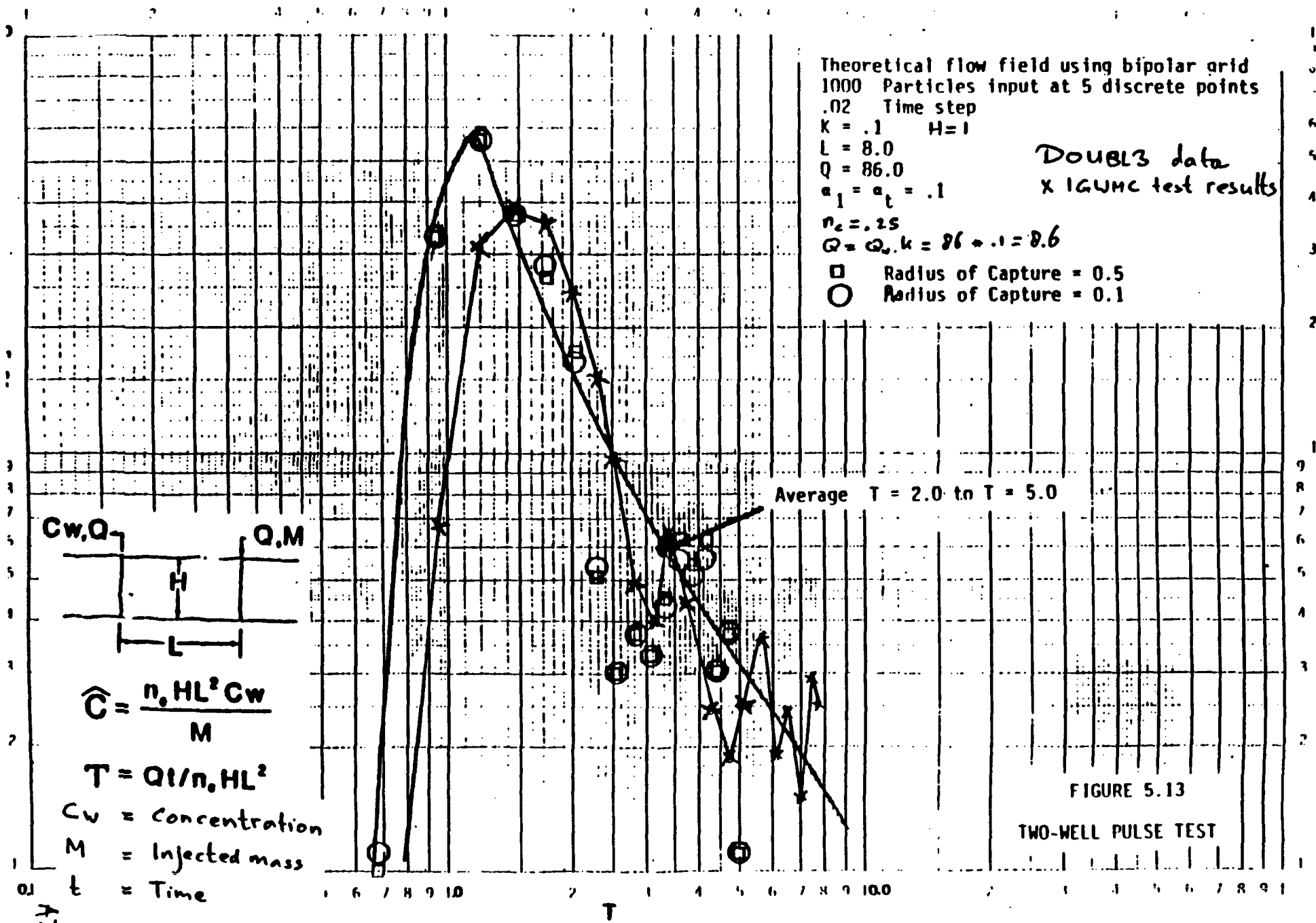


FIGURE 5.6 CDN results slug3D data





Groundwater Model - APPENDIX B

SECTION 2

MODEL FORMULATION

2.1 General Introduction

One form of the governing equations for three-dimensional ground water flow is [Bear, 1972]:

$$S_s \frac{\partial H}{\partial t} = \frac{\partial}{\partial x} \left(K_x \frac{\partial H}{\partial x} \right) + \frac{\partial}{\partial y} \left(K_y \frac{\partial H}{\partial y} \right) + \frac{\partial}{\partial z} \left(K_z \frac{\partial H}{\partial z} \right) \quad (2-1)$$

Where H represents the piezometric head; K_x , K_y , and K_z represent the hydraulic conductivity in the principal orthogonal coordinate directions; S_s is the specific storativity; and t is time.

H has the units of length (L), x, y, z have units of length, K_x , K_y , K_z have units of length per unit time (L/T). Hydraulic conductivity can also be described as a flow per unit area $[(L^3/T)/L^2]$ which reduces to L/T. The time, t, has units of time (T). The specific storativity has units of (1/L) and can be described as the volume of water released (or stored) per unit volume of aquifer per unit change in head $[(L^3/L^3)/L]$ which reduces to 1/L.

Equation (2-1) results directly from the generalized Darcy equation:

$$q_i = -K_i \frac{\partial H}{\partial x_i}; \quad (i,j=1,2,3) \quad (2-2)$$

and the continuity equation:

$$\frac{\partial q_i}{\partial x_i} = -S_s \frac{\partial H}{\partial t}; \quad (i=1,2,3) \quad (2-3)$$

In the case of equation (2-1), $k_i = 0$ for $i \neq j$.

Many methods of solving this equation exist. The finite element method, which is used by the method described in this manual, provides a general solution that offers variable boundary conditions, aquifer properties and geometry. It has proven to be a robust and flexible method with a wide range of applications.

Applications of the finite element method involves the following steps:

- a) Divide the region under consideration into a finite number of discrete sub-regions (elements) with simple geometries (e.g., prism, tetrahedra, prismoids).
- b) Assume the manner in which the piezometric head, H , can vary throughout each element (i.e., linear variation, quadratic variation, etc.).
- c) Based on the element geometry, and on the assumption of the head variation, write linear (local) equations for nodal point flux in terms of the piezometric head at the nodes defining the element.
- d) Assemble the local equations for each element into a global system of linear equations, assuming continuity of heads from one element to the next.
- e) Solve the global system of equations for the unknown piezometric head or flux at each node.

2.2 Structure of the Finite Element Equations

The global system of finite element equations can be written in the form:

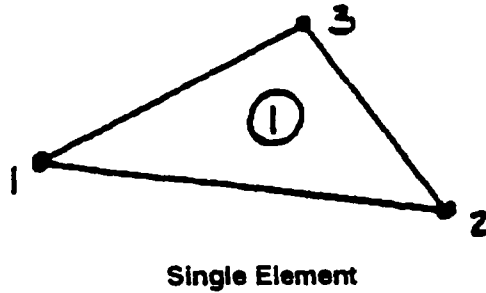
$$Q_i = S_i \cdot H_i \quad (2-4)$$

Where:

Q_i = the nodal point flux,
 H_i = the nodal point head, and
 S_i = the coefficient matrix relating the two.

Furthermore, it can be shown that equations developed by other numerical techniques such as the finite difference method or integrated finite difference method have the same general form. Only the values of the coefficient matrix terms will differ from case to case. Therefore the following discussion is generic to numerical methods in general. Details of the derivation of the finite element equations and the comparison between the finite element equations and the finite difference equations are presented in Appendix A.

Consider the simplest level of discretization, that of one element as shown below.



The element is triangular and is numbered 1. There are three nodes, one at each corner. The three nodes are sufficient to uniquely define a plane, and thus the head can be defined over the element in terms of nodal point heads (H_i) if it is assumed that the head variation is linear (the gradient is constant).

The gradient can be determined from the nodal point heads, and once the gradient is found, the specific discharge (Darcy velocity) can be found by the Darcy Equation (2-2). Integrating the specific discharge over the portions of the boundary contributing to each node results in expressions for nodal point flux Q_i in terms of nodal point head.

A natural conclusion from the equation is that the only way in which flow can enter the element is via the nodes as a node point flux. The equations do not represent flux across the boundary.

The finite element equations represent a series of linear simultaneous equations in this form:

$$\begin{aligned} Q_1' &= S_{11}' \cdot H_1 + S_{12}' \cdot H_2 + S_{13}' \cdot H_3 \\ Q_2' &= S_{21}' \cdot H_1 + S_{22}' \cdot H_2 + S_{23}' \cdot H_3 \\ Q_3' &= S_{31}' \cdot H_1 + S_{32}' \cdot H_2 + S_{33}' \cdot H_3 \end{aligned} \quad (2-5)$$

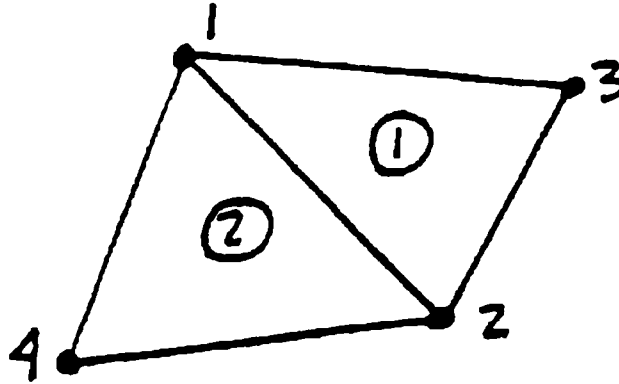
These equations can be solved if and only if either the head or the flux is known in each equation. That is, at any node either the head or the flux must be specified, otherwise there will be too many unknowns, or the problem will be over-specified with too many equations.

Implications of Boundary Conditions

Specification of the head at a node is called a first-type, or Dirichlet, boundary condition. Specification of the flux at a node is called a second type, or Neumann, boundary condition.

Assembly

Consider a two-element grid.



Finite element equations can be written for both elements individually. Adding both sets of equations results in a new set of assembled simultaneous equations as follows:

$$\begin{aligned}
 Q_1^1 + Q_1^2 &= (S_{11}^1 + S_{11}^2) \cdot H_1 + (S_{12}^1 + S_{12}^2) \cdot H_2 + S_{13}^1 \cdot H_3 + S_{14}^2 \cdot H_4 \\
 Q_2^1 + Q_2^2 &= (S_{21}^1 + S_{21}^2) \cdot H_1 + (S_{22}^1 + S_{22}^2) \cdot H_2 + S_{23}^1 \cdot H_3 + S_{24}^2 \cdot H_4 \\
 Q_3^1 &= (S_{31}^1) \cdot H_1 + (S_{32}^1) \cdot H_2 + S_{33}^1 \cdot H_3 \\
 Q_4^2 &= (S_{41}^2) \cdot H_1 + (S_{42}^2) \cdot H_2 + S_{44}^2 \cdot H_4
 \end{aligned} \tag{2-6}$$

There are four equations with four unknowns, and again either the head or the flux is specified at each node. There will always be only one equation for each node in the assembled equations.

Note first that there are no terms relating the flux at node 4 to the head at node 3 and vice versa. This is because there are no elements directly connecting these nodes. Thus, unless two nodes are connected, the S_{ij} terms will be zero. If they are connected, the S_{ij} terms will be the sum of the individual terms from each element which connects them. In the example given, for nodes 1 and 2, there are two elements (1 and 2), while for nodes 2 and 3 there is only one element (1). Thus, for a complex system of discretization, the Coefficient Matrix, S_{ij} , will be sparsely populated and will, in general, be banded, that is all terms beyond the maximum node number difference in any element will be zero. This latter feature of the equations is used to develop efficient solving routines for large matrices.

Nature of Fluxes

The net nodal point flux will be the sum of the individual element contributions. Thus, the nodal point flux at node 1 will be the sum of the contributions from elements 1 and 2. If for the simple two-element system described above, there is no externally applied flux and the head is unknown, the net flux will be zero. That is, the flux out of element 1 through node 1 will equal the flux into element 2 through node 1 or vice versa depending on the direction of flow. For complex systems, this would be the most common situation and therefore, a second-type boundary with a flux of zero is the default boundary condition at each node. This is typical for most finite element and finite difference codes.

The nodal point flux can be the sum of several different fluxes. For instance, it can include recharge, Q_r , storage flux, Q_s , pumping flux, Q_p , and many others.

$$Q_i = Q_p + Q_r + Q_s \quad (2-7)$$

Many codes, including DYNFLOW, permit specification of recharge as a unit flux. However no code, finite element or finite difference, can use such a flux directly in the equations.

In DYNFLOW for instance, the recharge flux for a given element is multiplied by one third of the plan area of each element and added as a nodal point flux to each of the appropriate nodal equations. Similar computations are made in all numerical codes.

Evaporation terms are tabulated in the same manner as recharge terms.

The storage flux term would be included only in transient cases. The storage flux is the instantaneous storage flux at the time being simulated, and transient simulations are actually a series of steady state simulations (or snap shots of the system) with varying storage fluxes at each time. The storage flux will in general be a function of both the head at the previous time step and the current time. At any node where the current head is unknown, the storage flux term must be broken up, with the known portion remaining on the left and the unknown portion added to the appropriate S_i terms on the right.

Preservation of Mass

For groundwater flow in general, the simplest of all cases is that of no flow, that is, all heads are equal. Considering the single element equations originally introduced, this case results in the following:

$$\begin{aligned}Q_1 &= (S_{11} + S_{12} + S_{13}) \cdot H \\Q_2 &= (S_{21} + S_{22} + S_{23}) \cdot H \\Q_3 &= (S_{31} + S_{32} + S_{33}) \cdot H\end{aligned}\tag{2-8}$$

Where $H_1 = H_2 = H_3 = H$. Since there is no flow, $Q_1 = Q_2 = Q_3 = 0$. Therefore the sum of the coefficient matrix rows ($S_{11} + S_{12} + S_{13}$ etc.) must also sum to zero. If indeed the coefficient matrix terms in each row sum to zero, then each nodal point flux equals zero and the case is correctly represented.

It can be shown that each column of the coefficient matrix sums to zero since the integration for nodal point fluxes, when taken together, is simply the integration of a scalar around the boundary of the element. Therefore, the limits of the integration are the same points, and the definite integral will be zero.

It can also be shown that the coefficient matrix is symmetric; that is $S_{ij} = S_{ji}$. The physical implication of this feature is that the influence of a unit flux at node i on the head at node j is the same as the influence of a unit flux at node j on the head at node i . This is to be expected for a linear system. As a consequence of symmetry, all rows in the coefficient matrix will also sum to zero, thus meeting the requirements for the simplest case noted above.

In general, the criteria that the coefficient matrix sums to zero is the guarantee that the method preserves mass. Mass is preserved, therefore, in terms of nodal point flux; nodal point flux is the only flux computed by the finite element (or finite difference) method which is consistent with the derivation.

Existence of Solution

Since the matrix sums to zero, its determinant will also be zero. Therefore, the matrix cannot be inverted. However, the matrix must be inverted in one fashion or another to solve the linear system of equations. The physical implication of this feature are as follows. Consider the single element as before, and assume that fluxes are applied at each node such that, in preserving mass, $Q_1 + Q_2 + Q_3 = 0$. Since we are dealing with a linear system of equations, any set of heads, H_i ,

which produce the required gradient for these fluxes is a solution to the equations. Therefore there is no unique solution in this case.

To obtain a unique solution, at least one value of head must be specified. In doing so, the equations will be altered as follows:

(assuming H_3 is specified)

$$\begin{aligned} Q_1 &= S_{11} H_1 + S_{12} H_2 + S_{13} H_3 \\ Q_2 &= S_{21} H_1 + S_{22} H_2 + S_{23} H_3 \\ H_3 &= -(S_{31}/S_{33}) H_1 - (S_{32}/S_{33}) H_2 + Q_3/S_{33} \end{aligned} \quad (2-9)$$

with all known values of the equations now on the left side. New coefficients now appear in the third row of the equations which cause the matrix columns to no longer sum to zero, which eliminates symmetry (assuming that S_{33} does not equal -1.0). It can be shown that the diagonal coefficient terms must always be greater than zero for any real problem. To be negative, the volume or the hydraulic conductivity would have to be less than zero.

Thus to solve the equations, at least one value of head must be specified. This is true for any equilibrium solution and any transient case where explicit storage flux terms are used (i.e. storage flux at previous time steps).

For the transient case where implicit or trapezoidal storage fluxes are used, coefficients of the current head will be added to the coefficient matrix terms, and thus the matrix will no longer sum to zero. Viewed another way, the heads at the previous time step serve the same function as first type boundaries in this case.

Non-Linear Case

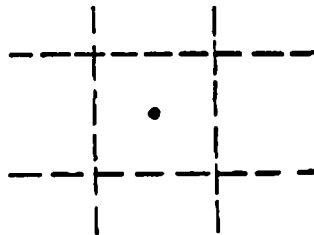
Whenever a phreatic surface occurs, the equations become non-linear: that is, the coordinates on the upper boundary are a function of the head. In three dimensions, there is a geometric non-linearity, while for vertically integrated (2-dimensional) problems, it is a physical (or parametric) non-linearity with the Transmissivity a function of the head. In finite element and finite difference solutions, this non-linearity is approximated with a series of successive linear solutions, each using the latest computed value of head to determine the aquifer geometry. In some cases, relaxation coefficients are used in the iteration process to hasten convergence, but in all cases, the process is continued until some pre-set convergence tolerance is met. While in theory, a unique solution exists for the non-linear case where only flux is known, since the non-linear case is approximated by a series of linear cases, at least one value of head must be specified for the non-linear case as well.

Computation of Fluxes

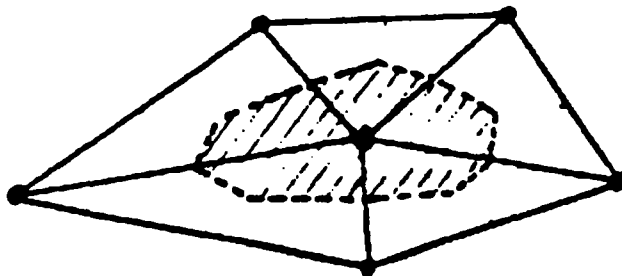
Since nodal point fluxes are the only fluxes consistent with the form of the equations, use of nodal point fluxes is the only consistent way in which to determine if a solution preserves mass. It is also the only consistent way in which to determine fluxes across internal boundaries. Since however, such fluxes are not explicitly computed in the solution, a second step is necessary to compute such fluxes. The step involves partitioning the grid to provide the required boundary, use of computed heads as input, and treating the boundaries as first-type (fixed head) boundaries. The nodal fluxes calculated as a result will be the fluxes across the boundary. Details of the method are provided in later sections of the manual.

While it might appear to be sufficient to integrate specific discharge along a boundary, such a procedure can lead to significant mass balance errors.

These points apply equally well to finite element or finite difference methods. At this point, it is instructive to compare the two methods to demonstrate this point. Consider first a block centered finite difference scheme in two dimensions:



The node is at the center of the cell, and is connected to neighboring nodes by flow links which can be shown to be nothing more than one-dimensional elements. Integration of specific discharge along a cell boundary is appropriate since the assumption of a constant specific discharge in the one-dimensional element holds. The resultant flux is the flux from one node to its neighbor. The finite element equivalent to the finite difference cell is shown below for a single node:



The finite element cell is simply the contributory area to the node identical to the finite difference cell. Integration of specific discharge along cell boundaries is also appropriate since, in the formulation, the specific discharge is also constant. Again the resultant flux is the flux from one node to another within the element. In neither case, however, can the specific discharge be integrated along an element boundary to determine the flux from one element to another, and the procedures described above must be used.

2.3 Implementation Aspects of DYNFLOW

The DYNFLOW code implements the simple mathematical relationships described in the previous section for ground water flow. Written in FORTRAN, it consists of a core computational program and associated data processing programs. The program has the ability to simulate ground water flow using one-, two-, and three-dimensional elements, or any combination of the three types.

Discretization

DYNFLOW discretizes a three-dimensional region in two steps: first, the horizontal plan area is discretized by creating a grid of triangular elements. The vertices of the triangular elements (points where multiple elements join) are called nodes. This discretization in plan view is held constant in the vertical direction: thus, the second step in discretization is to define the number of node levels/element layers in the vertical. Each element in plan view will therefore represent a series of overlying layers with the same plan view expression but with variable thicknesses. The layers in the vertical are defined by levels of nodes underlying the plan view nodes. The nodes within any given level do not however have to have the same elevation. The resultant discretization is a series of triangular prisms as shown in Figure 2-6. These are the working elements defined by the user using the following DYNFLOW commands:

GRID	Defines number of nodes, elements, nodal point coordinates in plan view, and nodes defining each element;
LEVE(L)	Defines the number of levels and layers (one less than the number of levels);
ELEV(ation)	Defines the vertical coordinate of each node/level.

Each node and element in the grid is assigned an external number which becomes the 'name' of the node/element which is used in addressing the node/element using DYNFLOW commands. The node/element also will carry an internal number which is defined by the order in which the node is input. The internal number defines the order in which the nodes appear in the coefficient matrix (used for minimizing band width) and all data is stored in DYNFLOW by internal number. Since there will be in general fewer levels, and because the minimum bandwidth vertically is

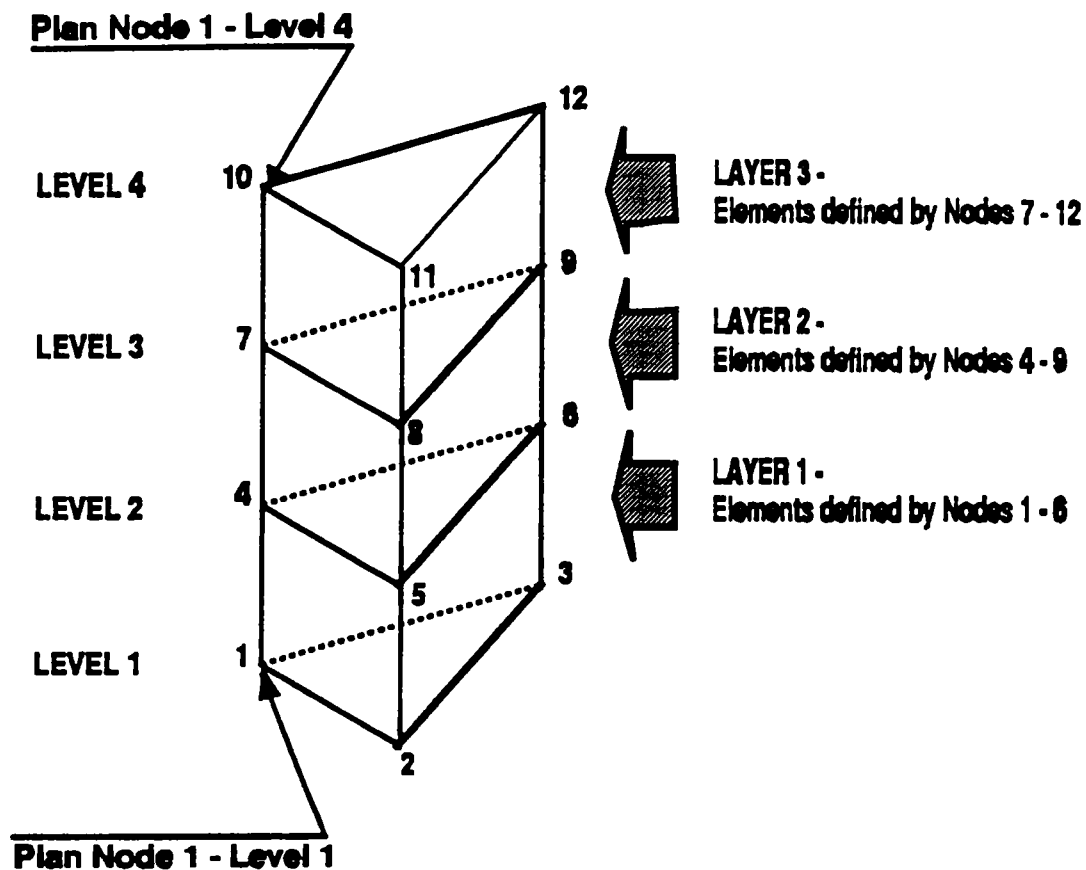


Figure 2-1: Finite Element Stack

predetermined by the structure of the discretization, no external/internal differentiation is made for levels.

Properties

Each element will have an assigned property set which defines the hydraulic properties which are held constant in each element, but can vary from element to element. These properties are set with the following commands:

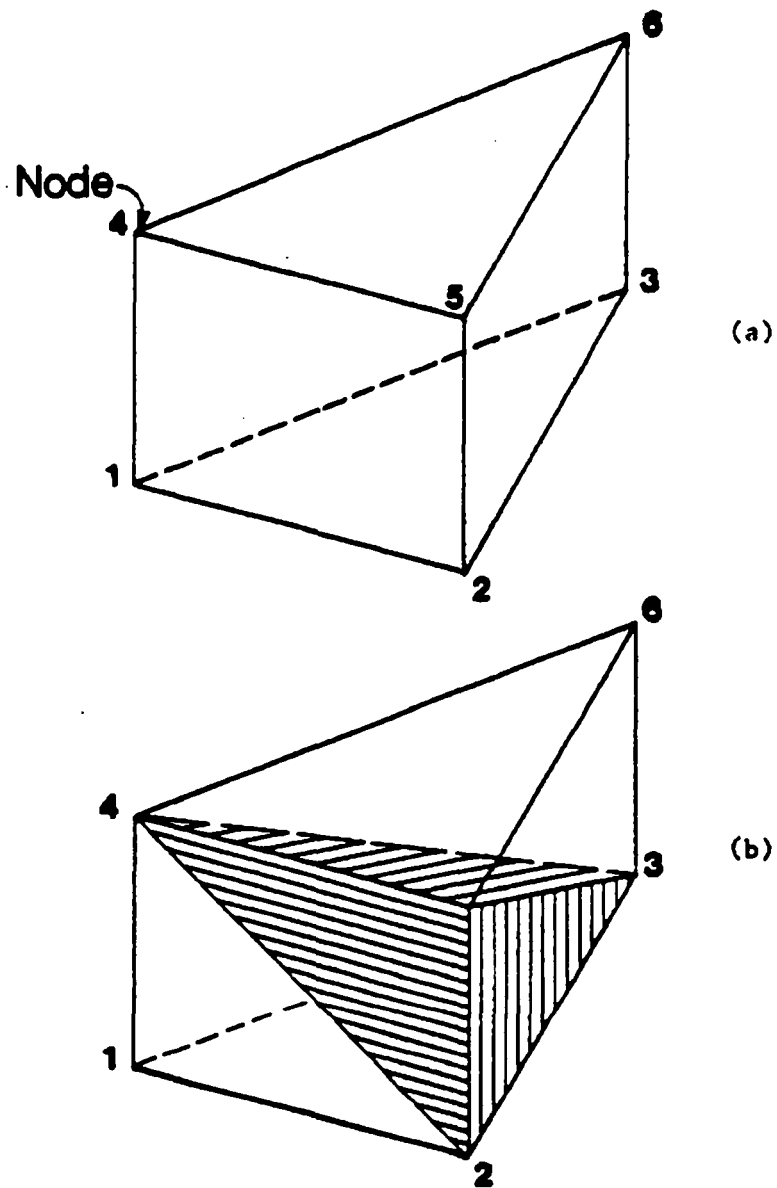
MATN(umber) Sets element type and property set number.

PROP(erty) Assigns values to property sets.

The property sets are assigned an external number from zero to 99, which is the number referenced by the **MATNumber** command. The property set includes the following:

- Hydraulic Conductivity in the first principal direction (default = x-direction)
- Hydraulic Conductivity in the second principal direction (default = y-direction)
- Hydraulic Conductivity in the third principal direction (default = z-direction)
- Specific storativity
- Specific yield
- Recharge rate (applied only at the water table)
- Rotation angle of the principal directions about the z-axis
- Rotation angle of the principal directions about the y-axis
- Bulk specific gravity of overburden
- Effective stress at which assigned properties are valid

In general, a porous medium will be represented by three-dimensional elements using the basic working element in three dimensions (vertical triangular prism with six nodes as shown in Figure 2-2(a)). Using methods presented by Huang, et al. [1979], the working element is subdivided within the DYNFLOW code into three computational elements (tetrahedra) as shown in Figure 2-2(b). The coefficient matrix for each tetrahedron is then computed using the working element properties and the assumption of a constant gradient. The coefficient matrix for the tetrahedron is then assembled into the global coefficient matrix.



- (a) - The Basic Element
- (b) - The Three Tetrahedral Computational Elements

Figure 2-2

A Three-Dimensional Working Element

Figure 2-3: Property Averaging (WPG File: C:\dr11\avg.wpg)

Phreatic Surface

DYNFLOW can treat phreatic, confined or mixed conditions, with the phreatic surface occurring at any node level, or moving between node levels in a transient case. DYNFLOW can treat only one phreatic surface (except for specified phreatic surfaces above the water table - see **FIX** and **POND** commands). The phreatic surface can occur at any level in the model. The phreatic surface is treated as a geometric non-linearity in that the elevation of all nodes above the phreatic surface (and below any specified head nodes) are temporarily moved vertically to the phreatic surface as shown on figure 2-3. As noted above, specified head nodes above the phreatic surface are held and leakage fluxes are calculated from the specified head nodes and applied at the water table. The method of calculating the leakage flux is discussed below under boundary conditions.

Transients

In the transient case, either the trapezoidal (Crank-Nickolson) or implicit time stepping scheme can be used, and storage terms can be lumped at nodes or distributed in one of several different ways (see **STORE** command, and theoretical background in Appendix A).

Two types of storage terms can be applied, specific storativity (units 1/L) and specific yield (dimensionless). The storage terms for specific storativity (represented elastic storage) are calculated by multiplying the tetrahedron volume times the specific storativity and distributing the terms to the tetrahedron nodes as appropriate to the storage distribution scheme being used.

The storage terms for specific yield (drainable yield at the water table) are calculated by multiplying the specific yield times the plan view area of the element and distributing the terms to three water table nodes, regardless of the level in which the water table resides. The calculations for the specific yield are made at the end of the individual working element calculations for each element in plan view.

Where the water table spans the uppermost level within an element (one or two nodes are confined), the specific yield storage fluxes are proportioned on the basis of the relative percent of the element which is phreatic and the storage terms distributed as follows (see Figure 2-4):

Figure 2-4: Temporal Averaging of Storage Terms
(WPG File: C:\DR11\TRAN.WPG)

$$Q_{s,i} = A_{ij} \times pct_j \times H_j$$

Where:

A_{ij} = the storage distribution array

pct_j = the percent of the head change at each node which is phreatic

Boundary Conditions

Either the head or flux can be specified at any node. The code calculates the head at all nodes where the flux is specified and the flux at all nodes where the head is specified. Distributed flux (recharge or evaporation) or nodal point flux can be used. The boundary conditions are set with the following commands:

FIX, HEAD, FIXH	Sets a first type boundary (specified head)
FREE, FLUX	Sets a second type boundary (specified flux)
RISI(<i>ng</i>)	Sets a 'Rising Water' boundary (conditional)
DRY	Sets a 'Dry' boundary (conditional)
RECH(<i>arge</i>), FLRE	Sets distributed recharge
EVAP, DEPTH, FLEV	Assigns evaporation potential, and extinction depth

Of the two conditional boundaries that can be specified, the first, called "The Rising Water Condition", specifies that the head be fixed at the elevation of the node at any node where the head tends to rise above the elevation of the node. Once set, the rising water condition is released when the calculated flux is positive (into the aquifer). The checks on rising water are made throughout the iteration process, and are not carried forward in time based solely on the first estimate of head during a time step.

The second conditional boundary, called the "Dry Condition" specifies that the head be held at the elevation of the node at any node where the head tends to fall below the elevation of the node. Once set, the dry condition is held until either:

- a) The flux becomes positive in which case the specified head is released and the discharge fluxes deleted; or,
- b) The calculated discharge flux exceeds the specified discharge flux in which case the specified head is released but the discharge flux maintained.

As with the rising water case, the check for the dry condition is made throughout the iteration process.

The values of specified flux can be assigned directly (FLUX) or can be specified as a distributed flux at the water table (RECH,EVAP). Distributed fluxes are assigned only at phreatic nodes and are otherwise neglected.

The evaporation loss is calculated as a linear function of the depth to ground water, with the loss set to zero when the water level is at or below the extinction depth, and the loss equal to the total potential if the water level is at the ground surface.

Boundary condition types and values can be updated at any time in a transient simulation to account for temporal variations in these parameters.

The default condition in DYNFLOW is a specified flux of zero everywhere except the uppermost level of nodes where a rising water condition is assigned at all phreatic nodes, and at the lowest level where a dry condition is specified at all nodes. This means that the user must specify a first type boundary in the aquifer to obtain a solution unless there will be an invoked rising water or dry condition in the initial conditions. All default conditions can be changed in DYNFLOW to any other condition prior to a simulation except that the dry condition at level 1 can only be overridden by a specified head at an elevation above the base of the model. Discharge fluxes would of course be applied at level 1 until such time as the dry condition were invoked.

Groundwater Model - APPENDIX C

SECTION 2

MODEL FORMULATION

2.1 Mathematical Background

The differential equation describing transport of conservative contaminants in a groundwater flow field is (Bear, 1979):

$$\theta \frac{\partial C}{\partial t} = \frac{\partial}{\partial x_i} \left(\theta D_{ij} \frac{\partial C}{\partial x_j} \right) - q_i \frac{\partial C}{\partial x_i} \quad (1)$$

where C is the concentration at any point, θ is the effective porosity, q_i is the specific discharge, and D_{ij} is the dispersion coefficient matrix. The first term on the right-hand side of Equation 1 represents the dispersive flux as embodied by Fick's law; the second represents the convective flux.

Many methods for solving this equation exist. Finite element or finite difference schemes have been applied to this equation (Pinder & Gray, 1977; Bear 1979); however, as noted in Section 1, these methods are subject to numerical dispersion and overshoot resulting from the approximations introduced in the process of discretization.

Bear (1979) notes that numerical dispersion is a truncation error resulting from the fact that the term proportional to the second derivative is neglected in the convective terms in Equation 1. Overshoot results from oscillation of the solution at a fixed point beyond physical limits as a result of the limited ability of interpolation schemes to represent rapidly changing concentration gradients while at the same time preserving mass.

Pinder and Gray (1977) note that overshoot can be controlled only at the expense of numerical dispersion and vice versa.

Because of the above problems associated with the convective terms in Equation (1), engineers have sought other methods of solving this equation for complex flow systems. The Lagrangian approach is described below. The process utilizes the random walk method for statistically significant numbers of particles wherein each particle is convected with the mean velocity and then randomly dispersed according to the specified dispersion parameters. Bear (1979) demonstrates that this numerical analogue satisfies Equation (1).

2.2 Velocity Field

The first task of transport modeling is to determine mean flow velocity in each component direction within each element. This is computed from element geometry, material properties and nodal point heads using Darcy's Law, which expresses flow rate as a function of the hydraulic gradient.

Piezometric heads used in the DYNTRACK model are generally computed by DYNFLOW (see DYNFLOW User's Manual). From a computed set of heads, the specific discharge vector is computed as follows for each tetrahedron in a working element:

$$q_i = k_{ij} \cdot C_{jk} \cdot H_k \quad (2)$$

where q is the specific discharge, k is the hydraulic conductivity, C is the matrix that transforms heads to gradients, and H is the piezometric head.

For each working element, a weighted average of the specific discharge vector in each contributing tetrahedron is then computed. The velocity vector is unaffected by the contaminant concentrations in this case, and thus, density differences are not considered.

2.3 Single Particle Tracking

In the simplest analysis, mass is assumed to be convected in groundwater at the rate of the local mean seepage velocity. If a tracer particle is injected in a flow field at point x, y, z at a time t , after period of time t , its new location will be:

$$\begin{aligned}x_t + \Delta t &= x_t + \frac{q_x}{n_e} \Delta t = x_t + \Delta x_v \\y_t + \Delta t &= y_t + \frac{q_y}{n_e} \Delta t = y_t + \Delta y_v \\z_t + \Delta t &= z_t + \frac{q_z}{n_e} \Delta t = z_t + \Delta z_v\end{aligned}\tag{3}$$

where the seepage velocities, $v = q/n_e$, are those computed for the element in which it was initially located. If the new location is in a different element, the seepage velocities computed for the new element will be applied to compute particle displacement for the next time step.

Single particle tracking is a means of forecasting the mean path and time of transport from a particular point in an aquifer under given hydraulic conditions. By using a negative time step, it can also be used in a "hindcasting" mode, whereby possible source areas of contaminants reaching a particular point in an aquifer are suggested. However, single particle tracking does not account for the dispersion of contaminant plumes observed in nature.

2.4 Dispersion

Dispersion phenomena in flow through porous media occur at three scales of observation. The smallest scale is molecular diffusion due to the random collisions and displacements of individual molecules. At the laboratory scale, dispersion is observed in a uniform medium due to the many different tortuous flow paths followed. In the field, due to limited sampling and the variable, "interbedded" nature of aquifer materials, porous media which can be considered homogeneous for flow purposes will be heterogeneous in their ability to transport contaminants. Dispersion occurs in all three cases because different fractions of a tracer mass are transported within the medium at different velocities.

Dispersion observed at the field scale is much greater than that observed at laboratory or molecular scale, and it is most relevant to contaminant transport studies of field situations. The magnitude of field dispersion is a function not only of soil types and flow velocities, but also of the scale and precision of study. Other things being equal, contaminant transport in a large aquifer which is approximately represented will appear to be governed more by random dispersion than will contaminant transport in a small aquifer which is very precisely represented.

Various studies (Bear, 1972) have shown that dispersion in the direction of mean flow tends to be greater, usually by an order of magnitude, than dispersion transverse to the mean direction of flow. Therefore, when simulating dispersion in any element, a local orthogonal coordinate system with the principal axes aligned parallel (x') and perpendicular (y' , z') to the velocity vector is used. Separate coefficients are applied to longitudinal and transverse dispersion. It has also been shown that dispersion coefficients are proportional to the magnitude of the resultant seepage velocity.

In DYNTRACK a contaminant mass is represented by many particles. The dispersion process is simulated by adding to each particle random dispersive displacements in addition to the convective displacements described for single particle tracking. It can be shown that the dispersion process applied to a given mass injected at a point, will lead to a normal distribution of mass in any of the principal directions (see Model Verification -- Section 5). The standard deviation, σ , of the distribution, or the average displacement, will be:

$$\sigma = \sqrt{2D\Delta t} \quad (4)$$

where D (L^2/t), the dispersion coefficient is given by:

$$D = \alpha |v| = \alpha L/\Delta t$$

and α is the dispersivity (L), $|V|$ is the absolute value of the resultant velocity vector (L/T) and L (L) is the distance traveled. In three dimensional porous media, it has been generally observed that the dispersivity in the direction of flow is greater than the dispersivity normal to it (Ahlstrom et al, 1977; Bear 1979). This gives rise to two companion relationships for longitudinal and transverse dispersion:

$$\begin{aligned} \sigma_L &= \sqrt{2\alpha_L L} \\ \sigma_T &= \sqrt{2\alpha_T L} \end{aligned} \quad (5)$$

where σ_L , α_L and σ_T , α_T are the standard deviation and dispersivity in the longitudinal and transverse directions, respectively.

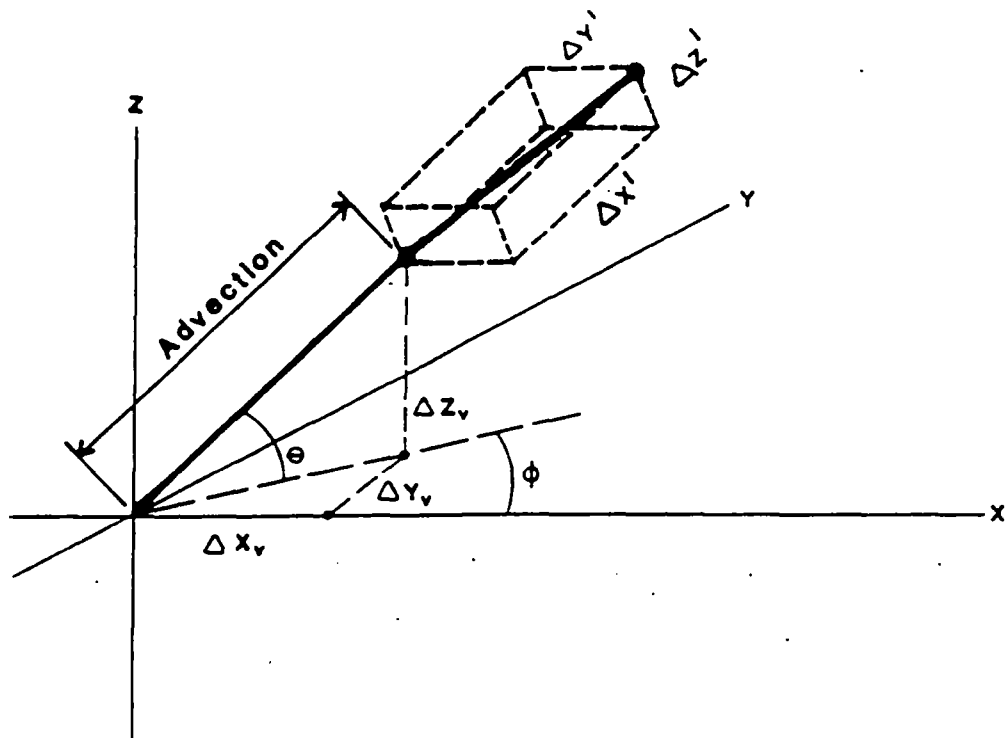


Figure 2.1

COORDINATE TRANSFORMATION FOR DISPERSIVE MOVEMENT

For any individual particle of mass, the dispersive displacements take the form:

$$\begin{aligned}\Delta x' &= \sqrt{2a_L} L \cdot (\sqrt{12}) \cdot 0.5 - R_1 \Big|_0^1 \\ \Delta y' &= \sqrt{2a_L} L \cdot (\sqrt{12}) \cdot 0.5 - R_2 \Big|_0^1 \\ \Delta z' &= \sqrt{2a_L} L \cdot (\sqrt{12}) \cdot 0.5 - R_3 \Big|_0^1\end{aligned}\quad (6)$$

where x' , y' and z' are the local velocity vector coordinates as shown in Figure 2.1, R_n are random numbers ranging from 0 to 1, and the term $\sqrt{12}$ converts the range of the random number function to the value necessary to preserve the statistics implied by Equation (4). Note that to preserve the statistics of Equation (4) the range of allowable displacements can be defined by a random number with a range of $\pm\sqrt{6a} L$.

The random displacements given by Equation (6) must now be converted to the global coordinate system x, y, z . Again, referring to Figure 2.1, the conversion takes the form:

$$\begin{aligned}\Delta x_d &= x' \cdot \cos \theta \cos \phi + y' \sin \phi + z' \cdot \sin \theta \cdot \cos \phi \\ \Delta y_d &= x' \cos \theta \cdot \sin \phi + y' \cos \phi + z' \sin \theta \cdot \sin \phi \\ \Delta z_d &= x' \sin \theta + z' \cos \theta\end{aligned}\quad (7)$$

The total displacement for an individual particle for a time step is then the sum of the advective and dispersive motions:

$$\begin{aligned}\Delta x &= \Delta x_v + \Delta x_d \\ \Delta y &= \Delta y_v + \Delta y_d \\ \Delta z &= \Delta z_v + \Delta z_d\end{aligned}\quad (8)$$

Where the bedded nature of soil deposits results in significantly reduced vertical flow conductance compared to horizontal conductance, observed vertical dispersion may be considerably suppressed. DYNTRACK allows for the specification of an anisotropy ratio by which vertical dispersion is suppressed with respect to horizontal dispersion in a given element. Note, however, that suppression does not affect the convective movement in which flow field anisotropy is implicit.

The suppression is implemented by application of the anisotropy ratio to the vertical dispersive displacement such that Equation (8) becomes:

$$\begin{aligned}\Delta x &= \Delta x_v + \Delta x_d \\ \Delta y &= \Delta y_v + \Delta y_d \\ \Delta z &= \Delta z_v + S \Delta z_d\end{aligned}\tag{9}$$

where 'S' is the anisotropy ratio. In DYNTRACK, specification of a value of 0.0 for S results in no vertical suppression.

2.5 Decay

The total mass of a contaminant which enters an aquifer may be reduced by various decay mechanisms. Reduction of mass can be simulated in DYNTRACK as a simple first order decay process. In this case, the mass assigned to each particle is adjusted at each time step according to the relationship:

$$W_{t + \Delta t} = W_t \cdot \exp(-\lambda \Delta t) \quad (10)$$

where:

W_t = particle mass at time t

λ = first order decay coefficient

\exp = natural logarithmic base

2.6 Adsorption

The process of adsorption/desorption of dissolved solute on soil grains can change the concentration of solute in water. This process results in an apparent movement of solute which is slower than water. This phenomena is described by the retardation equation (Freeze & Cherry, 1979):

$$V/V_a = 1 + \frac{P_b}{n_e} \cdot k_d = R \quad (11)$$

where:

V is the mean velocity of water

V_a is the apparent mean velocity of solute

n_e is the effective porosity

P_b is the bulk dry density of the soil fraction

k_d is the distribution coefficient

R is the retardation factor

The distribution coefficient is a function of the soil and solute chemistry. For volatile organic constituents, it is a function of the organic carbon content of the soil. The distribution coefficient is defined by:

$$k_d = c_s/c_w \quad (12)$$

where c_s is the concentration by weight on the soil and c_w is the concentration by volume in water. Equations (11) and (12) assume rapid reversible adsorption with a linear isotherm (Freeze & Cherry, 1979).

The movement of solute whose behavior is approximated by the retardation equation, can be simulated in the random walk method by simply reducing the velocity of any particle by the retardation factor. This will reduce the distance travelled in any time step and thus the dispersive displacements will be likewise reduced.

The concentration of solute in the aqueous phase can be determined as follows (Gelhar, 1984). Considering first the phase diagram as shown in Figure 2.2 and assuming that the soil is saturated and the volume of solute is negligible, yields:

$$V_c \approx 0$$

$$V_w \approx V_v$$

$$V_w + V_s \approx V_t \quad (13)$$

$$W_w + W_s \approx W_t$$

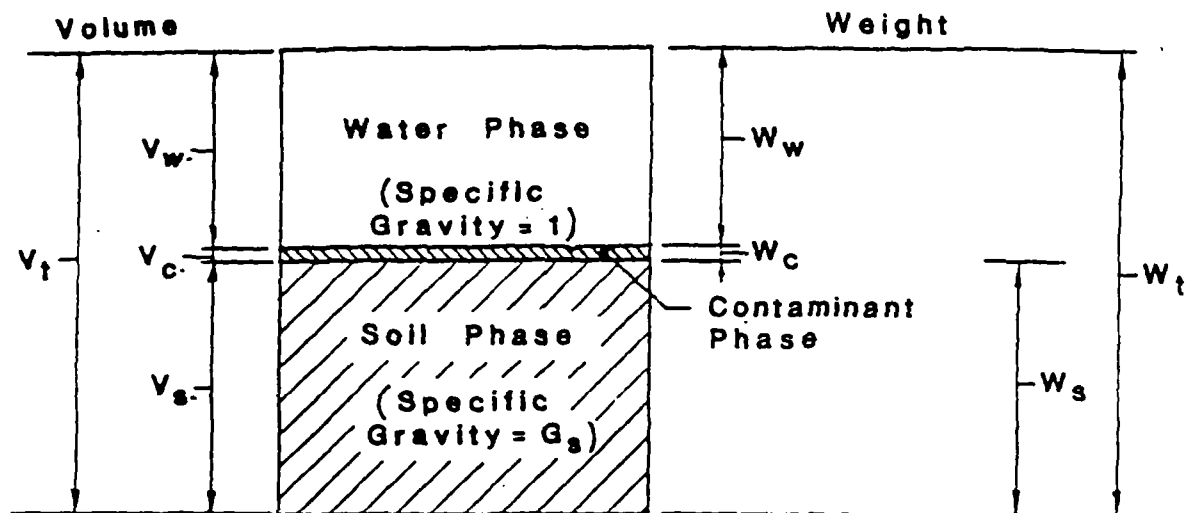
The bulk dry density of the soil matrix can therefore be defined as follows:

$$P_t = \frac{W_s}{V_t} = \frac{G_s \cdot V_s}{V_t} = \frac{G_s}{V_t} [V_t - V_w] = (1-n) \cdot G_s \quad (14)$$

where n is the total porosity (V_v/V_t).

The concentration in water can be defined as:

$$C_w = \frac{W_{cw}}{V_w} = \frac{W_c - W_{cs}}{nV_t} \quad (15)$$



$$\begin{aligned}
 V_t &= V_c + V_s + V_w \\
 W_t &= W_w + W_c + W_s \\
 V_s &= W_s / G_s \\
 V_w &= W_w
 \end{aligned}$$

Figure 2.2
PHASE DIAGRAM

DYNFLOW uses the same properties within each element of the triangular prism except for the non-linear case where the phreatic surface spans two working elements in the vertical direction. For this case, averaging of properties for each tetrahedron is done based on the relative portion of the tetrahedron in each originally defined working element. The proportioning is done on the basis of the total vertical distance spanned in each layer and is shown in Figure 2-3 for a 2 layer system. The result is as follows:

For hydraulic conductivities in all directions:

$$K_{avg} = \frac{\sum L_j}{\sum \left(\frac{L_j}{K_j} \right)}, \quad j = 1, \text{ number of levels spanned}$$

Where:

L_j = min[HMAX, ELEV(j+1)] - max[HMIN, ELEV(j)]

K_j = Hydraulic conductivity of layer

HMAX = the highest head at phreatic surface within the plan element

HMIN = the lowest head in the plan element

j = layer, level number

For storage properties and angles of anisotropy:

$$P_{avg} = \frac{\sum K_j \times L_j}{\sum L_j}$$

Where:

P_{avg} = 'Property' being averaged

and the other variables are defined as above

The stress dependent parameters, γ , and σ , are not averaged.

and the concentration on the soil

$$C_s = \frac{W_{cs}}{V_s G_s} \quad (16)$$

therefore:

$$\begin{aligned} C_w &= \frac{W_c - G_s \cdot V_s \cdot C_s}{nV_t} \\ &= \frac{W_c}{nV_t} - \frac{G_s (V_t - V_w) k_p \cdot C_w}{nV_t} \\ &= \frac{W_c}{nV_t} - \frac{G_s (1-n) k_p \cdot C_w}{n} \\ &= \frac{W_c}{nV_t} - \frac{P_b}{n} k_p C_w \end{aligned} \quad (17)$$

Rearranging terms and solving for C_w yields

$$C_w = \frac{W_c}{R \cdot nV_t} \quad (18)$$

In DYNTRACK, it is assumed that the total porosity and effective porosity are the same ($n = n_e$), which for practical engineering considerations is an acceptable assumption. Thus, by use of an equivalent effective porosity of $R \cdot n_e$, the velocity will be appropriately reduced in Equation (3) and the concentration in the aqueous phase will be appropriately reduced in Equation (18).

2.7 Computation of Concentration

Each particle is assigned a mass which is held constant throughout the simulation except for the case of decay as described in Section 2.5. At any point in space or time, the concentration of solute can be computed by selecting a volume and summing the mass of all particles within the volume. The concentration then becomes:

$$C_w = \frac{W_c}{nV_t} \quad (19)$$

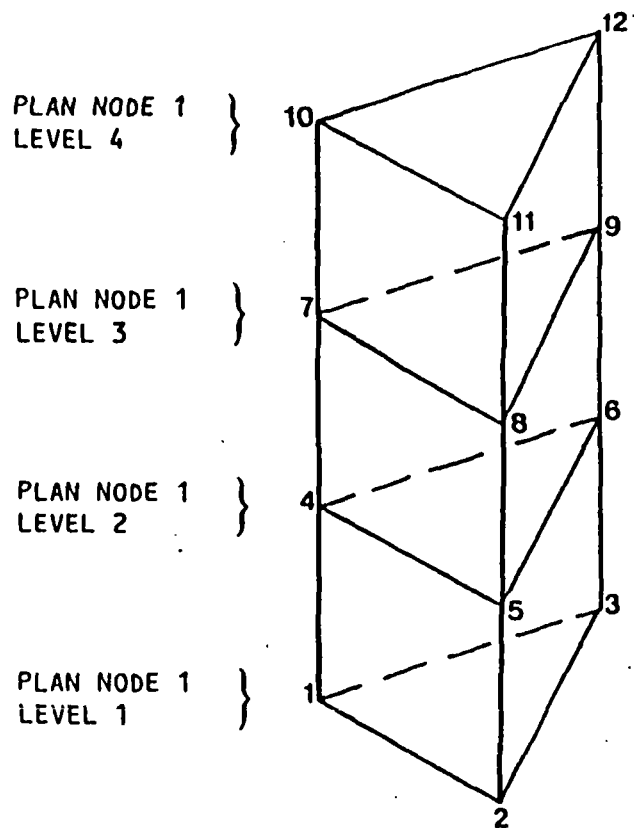
where W_c is the total particle mass within the total volume V_T , and n is the total porosity. In DYNTRACK, as noted above, the total porosity and effective porosity are assumed equal, which is adequate for most engineering applications.

In DYNTRACK, concentrations can be calculated using two basic methods. The first method computes concentrations at all nodes in the finite element grid used by the flow and contaminant transport models. Particles are assigned to nodes using the appropriate geometric relationships which define the contributing volume to each node. The porosity for each segment of the contributing volume is used to calculate the volume of water contributing to the node.

A variation on this concept is the calculation of vertically averaged concentrations at the plan location of all node columns in the flow model. In this case the contributing volume to the plan node consists of the entire vertical column as shown in Figure 2.3. The volume of water in the column is calculated by multiplying the volume of each layer within the column times the effective porosity of the layer. The vertically averaged concentration then becomes the total particle mass in the column divided by the total volume of water in the column.

Both individual node concentrations and vertically averaged concentrations can be directly contoured using companion plotting routines with either linear or logarithmic/linear interpolation functions.

The second basic method of calculating concentrations is to specify at any point an associated cylindrical volume centered about a point. The particle mass within the cylinder divided by the pore volume of the cylinder yields the concentration at the point. This method of computation permits direct comparison to field data points which do not lie at the flow model nodes, and permits the computation of spatial moving averages by overlapping the cylinders.



LEVEL 4

LAYER 3 : ELEMENT DEFINED BY NODES
7 - 12

LEVEL 3

LAYER 2 : ELEMENT DEFINED BY NODES
4 - 9

LEVEL 2

LAYER 1 : ELEMENT DEFINED BY NODES
1 - 6

LEVEL 1

FIGURE 2.3 ASSEMBLY OF 3-D WORKING ELEMENTS
FROM PLAN GRID.

2.8 Plume Modeling

To model the passage of a contaminant plume through an aquifer, thousands of individual particles are utilized. Convective and dispersive displacements are computed repeatedly for each particle for each time step of the simulation. The particles, as a whole, represent the entire contaminant mass, with a small, discrete portion of that mass assigned to each particle.

Results from multiple simulations can be added, with relative weighting, to represent multiple sources, or to improve the accuracy of a single simulation by increasing the number of particles. Where multiple sources are simulated during the calibration step, this additive capacity of simulation readily permits the use of influence matrices to assess the relative weights of various sources. This is done by simulation of each source using unit source loading. If there are N sources, then these sources can be related to N points of observation as follows:

$$C_i = u_{ij} \cdot w_j$$

where C_i is the observed contamination at point i, u_{ij} is the simulated concentration at point i from unit source j, and w_j is the weight of source j. This equation can be solved directly for the weights or bounded optimization techniques can be used. This approach can be extended to multiple sets of N observed data as validation, or to incorporate the effects of not only source weight but also source duration or other source unknowns.

APPENDIX I

ABB-ES Data

4.3 OU2 - LAGOON AREA

This section discusses the nature and extent of contaminants in lagoon surface water, lagoon sludge, soils underlying and adjacent to the lagoons, waste piles, sludge within mixing and clarifier tanks at the treatment building, and water in the basement of the treatment building.

4.3.1 Lagoon Operational History

The Lagoon Area is about 45 acres in size and includes 10 lagoons. When operational, spent pickle liquor generated at the Main Plant was transferred into two hazardous waste storage (or acid) lagoons, labelled Lagoons 1 and 2 on Figure 4-7. The pickle liquor, which had a pH of approximately 2, was pumped to a Treatment Building and neutralized using lime. The Treatment Building includes a lime hopper, three mixing tanks, two clarifier tanks, and two filter presses. Neutralization involve adding lime to the liquid in the mixing tanks. The mixture would be transferred to clarifier tanks where sludge would precipitate and be separated. Sludges were sent through filter presses for dewatering and then transferred to sludge drying beds (Lagoons 8, 9 and 10 on Figure 4-7). The treated liquid is thought to have been discharged to polishing Lagoon 3 and then transferred through polishing Lagoons 4, 6, and 7 during which solids suspended within the liquid would settled to the bottom of these lagoons. After polishing, the liquid was stored in Lagoon 5 and then discharged to Wildcat Creek through outfall CS-04.

Based upon aerial photographs, it appears that the acid and polishing lagoons were constructed in the late 1930's and the sludge drying beds were constructed in the late 1960's or early 1970's (USEPA, May 1990). Aerial photographs indicate that a meander in the Wildcat Creek channel may have been filled and the creek diverted as part of the construction (USEPA, March 1992). The approximate location of the channel is shown on Figure 4-7.

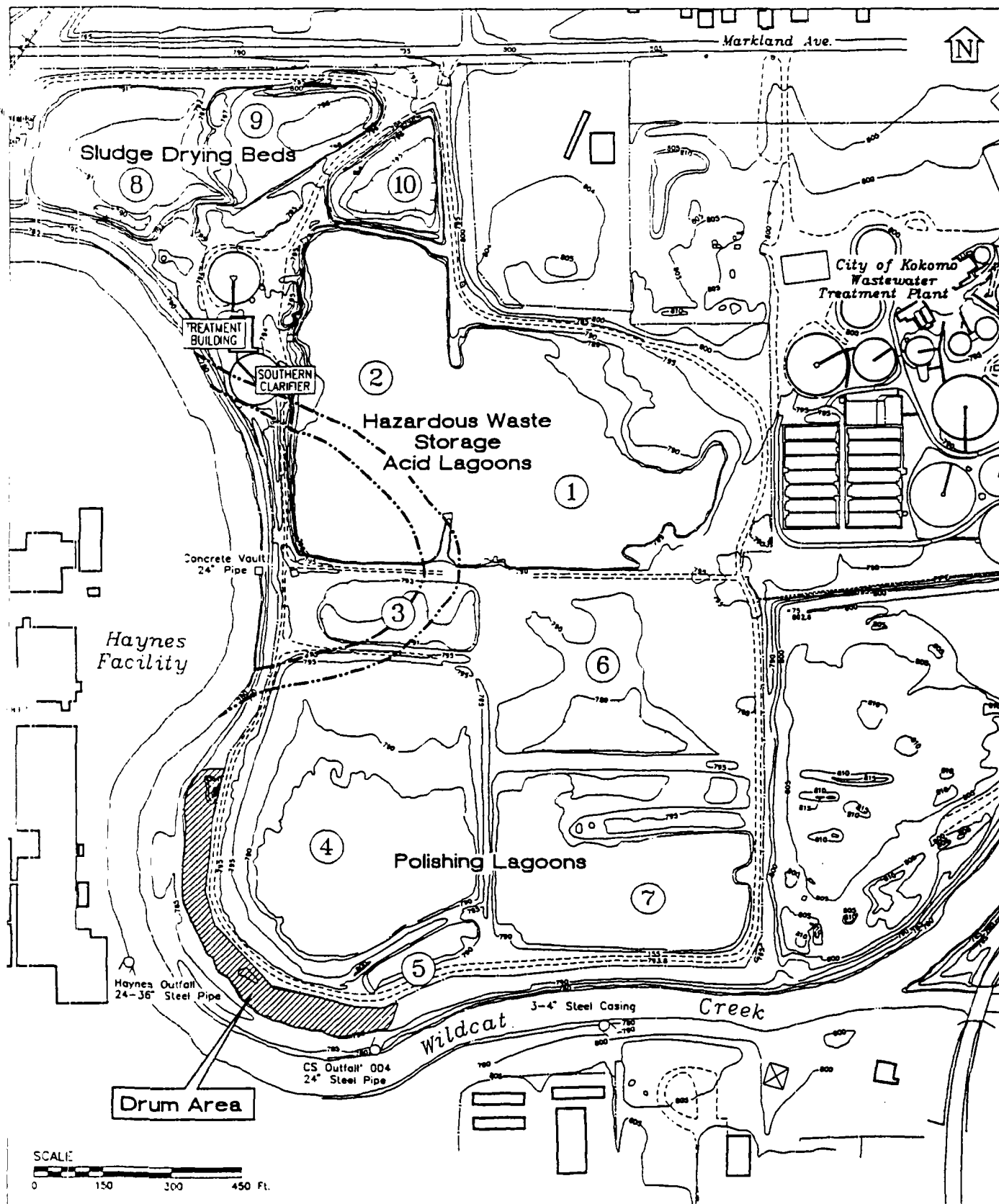


FIGURE 4-7
LAGOON SURFACE WATER SAMPLING LOCATIONS
CONTINENTAL STEEL RI
KOKOMO, INDIANA

ABB Environmental Services, Inc.

Available documentation for the site provided little information on the methods used to construct the lagoons. Soil boring data combined with the information provided in the historical aerial photographs provided some indications of the types of materials used to construct the lagoons. This interpretation is provided in Section 4.2.3.

4.3.2 Surface Water Quality

The untreated and treated pickle liquor has been removed from the lagoons. At the time of the study, rainwater was present in the areas shown on Figure 4-7. Surface water areas vary seasonally dependant upon precipitation and evaporation. Mud cracks in the sludges of Lagoons 4 and 7 indicate that these areas are not always covered with water.

Field screening and laboratory results for general surface water chemistry are summarized on Table 4-11 and 4-12. The water chemistry was fairly similar between lagoons with two notable exceptions. First, water in the acid lagoons was slightly acid with a mean pH of 4.8 while water in the polishing lagoons was nearly neutral, with the pH ranging from 6.3 to 6.9. Also, ammonia concentrations in the acid lagoons averaged 3.7 mg/L, while concentrations in the polishing lagoons were 0.15 mg/L or less.

Detected organic compounds in lagoon surface waters are summarized on Table 4-13. Detected compounds were acetone in seven samples with concentrations ranging from 5 ug/L to 8 ug/L, bis (2-Ethylhexyl)phthalate in three samples with concentrations ranging from 3 ug/L to 8 ug/L, Endosulfan I in three samples with concentration ranging from 0.004 ug/L to 0.014 ug/L, and Endosulfan II in one sample at a concentration of 0.004 ug/L.

Inorganic compounds detected in the lagoon surface waters are summarized on Table 4-14. With the exception of calcium and magnesium, inorganic concentrations are considerable higher in the acid lagoons than in the polishing lagoons. For example, aluminum was detected in all eleven unfiltered acid lagoon surface water samples with an average concentration of 3,180 mg/L. In the polishing lagoons, aluminum

TABLE 4-11
FIELD SCREENING RESULTS OF GENERAL CHEMISTRY
LAGOON SURFACE WATER
CONTINENTAL STEEL RI
Kokomo, Indiana

Sample Location	Temperature (Deg. C.)	pH (units)	Specific Conductance (uS/cm)	Dissolved Oxygen (mg/L)
ACID LAGOON #1/#2				
SW-11	28.0	4.7	850	7.2
SW-12	28.0	5.2	810	3.2
SW-13	29.0	5.9	945	8.7
SW-14	26.5	4.3	890	8.1
SW-15	28.0	5.8	950	7.0
SW-16 (3 ft)	28.5	4.6	910	6.1
SW-16 (9 ft)	28.0	4.6	900	4.0
SW-17	26.0	4.5	880	7.8
SW-18	28.0	4.4	955	6.5
SW-19	27.5	4.2	940	6.8
SW-20	32.0	4.7	1,080	7.0
Arithmetic Mean	28.1	4.8	919	6.6
POLISHING LAGOON #4				
SW-03	27.5	6.9	1,020	7.3
SW-04	34.0	6.8	900	7.2
SW-05	27.0	6.3	1,015	6.9
SW-06	21.0	6.4	900	6.9
Arithmetic Mean	27.4	6.6	959	7.1
POLISHING LAGOON #5				
SW-01	31.0	6.5	820	8.2
SW-02	31.0	6.4	930	5.1
Arithmetic Mean	31.0	6.5	875	6.7
POLISHING LAGOON #7				
SW-07	22.0	6.7	860	7.8
SW-08	26.5	6.9	875	7.0
SW-09	30.0	6.8	920	7.0
SW-10	26.5	7.0	885	7.0
Arithmetic Mean	26.3	6.9	885	7.2

Deg. C. - Degrees celcius

mg/L - Milligrams per liter

uS/cm - Microsiemens per centimeter at 25 degrees celcius

TABLE 4-12
LABORATORY RESULTS OF GENERAL CHEMISTRY
LAGOON SURFACE WATER
(CLP Results in mg/L)
CONTINENTAL STEEL SITE
Kokomo, Indiana

SAMPLE LOCATION	LAGOON	CaCo ₃	NH ₃ -N	Cl	N+N	O&G	P	SO ₄	TDS	TOC	TSS	BOD
SW-1	Polishing Lagoon #5	31.90	ND	33.10	0.33 J	R	ND	1,430	2,590 J	ND	ND	1.1
SW-4	Polishing Lagoon #4	28.20	ND	30.10	0.28 J	R	ND	1,740	2,170 J	ND	ND	ND
SW-9	Polishing Lagoon #7	49.60	0.15 J	18.80	ND	R	ND	1,670	2,400 J	5.2	ND	2.0
SW-9 (DUP)		48.80	0.10 J	18.90	ND	R	0.050 J	1,640	2,350 J	5.32	3.0 J	1.4
SW-11	Acid Lagoon #1	ND	3.6 J	28.70	0.21 J	R	ND	1,410	2,150 J	ND	ND	0.40
SW-20	Acid Lagoon #2	ND	3.8 J	28.50	0.19 J	R	ND	1,390	2,120 J	ND	ND	ND

NOTES:

BOD = Biological Oxygen Demand
CaCo₃ = Alkalinity
Cl = Chloride
J = Concentration is estimated
ND = Not detected

NH₃-N = Ammonia as nitrogen
N+N = Nitrate plus nitrite
O&G = Oil and grease
P = Phosphorus
R = Rejected during validation

SO₄ = Sulfate
TDS = Total Dissolved Solids
TOC = Total Organic Carbons
TSS = Total Suspended Solids

TABLE 4-13
DETECTED ORGANIC COMPOUNDS IN LAGOON SURFACE WATER
(CLP Results in ug/Kg)
CONTINENTAL STEEL RI
Kokomo, Indiana

		LAGOON #1/#2										LAGOON #4				LAGOON #5		LAGOON #7				
COMPOUND	CRQL	SW-11	SW-12	SW-13	SW-14	SW-15	SW-16 (3 ft)	SW-16 (9 ft)	SW-17	SW-18	SW-19	SW-20	SW-03	SW-04	SW-05	SW-06	SW-01	SW-02	SW-07	SW-08	SW-09	SW-10
Acetone	5	R	R	6 J	5/R	7 J	R	R	7 J	7 J	8 J/6 J	R	R	R	R	4 J	R	R	R	R	R/R	R
bis(2-Ethylhexyl)phthalate	5	-	-	-	-/-	-	-	-	3 J	-	-/-	8	-	-	-	-	-	-	3 J	-	-/-	-
Endosulfan I	0.01	-	-	-	-/-	-	-	-	-	-	-/-	-	0.004 J	-	0.014	0.004 J	-	-	-	-	-/-	-
Endosulfan II	0.02	-	-	-	-/-	-	-	-	-	-	-/-	-	-	-	0.004 J	-	-	-	-	-	-/-	-
Total TICs for SVOCs	-	-	-	-	-/-	-	-	-	-	-	-/-	45	-	-	-	-	-	-	-	-	-/-	-

NOTES:

S/R - Sample concentration/duplicate concentration

CLP - Contract laboratory program

CRQL - Contact required quantitation limits

J - Concentration is estimated

ug/Kg - Micrograms per kilograms

R - Lab rejected sample

-/- - Not detected

TABLE 4-14
DETECTED INORGANIC COMPOUNDS IN LAGOON SURFACE WATER
(CLP Results in mg/Kg)
CONTINENTAL STEEL RI
Kokomo, Indiana

		LAGOON #1/2																							
		SW-11		SW-12		SW-13		SW-14		SW-15		SW-16 (3 h)		SW-16 (9 h)		SW-17		SW-18		SW-19		SW-20			
COMPOUND	CRQL	F	UF	F	UF	F	UF	F	UF	F	UF	F	UF	F	UF	F	UF	F	UF	F	UF	F	UF		
Aluminum	100	3,200	3,370 J	3,000	3,200 J	2,710	2,900 J	2,920/3,100	3,070/3,080	3,050	3,230 J	3,170	3,250 J	3,000	3,230 J	3,060	3,050	3,020	3,230 J	3,120/3,130	3,140/3,200 J	3,180	3,250 J		
Barium	20	16.6 J	19.9 J	16.7 J	18.9 J	16.6 J	20.8 J	17.8 J/18.4 J	18.3 J/17.8 J	16.3 J	19.7 J	16.2 J	18.3 J	16 J	19.2 J	18 J	18 J	16.5 J	19.1 J	17.8 J/17.7 J	20.2 J/20 J	18.9 J	19.1 J		
Beryllium	1	-	-	-	-	-	-	-	-	-	-	-	-	-	-	-	-	-	-	-	-	-			
Cadmium	1	3.6 J	2.8 J	3.4 J	3.4 J	3.2 J	2.2 J	3.8/2 J	2.2 J/2.1 J	2.8 J	2.9 J	3.4 J	2.8 J	3.3 J	5.3 J	1.6 J	1.9 J	-	3.6 J	-	3 J	-	2.8 J		
Calcium	500	484,000	507,000	477,000	485,000	482,000	480,000	455,000/472,000	468,000/474,000	457,000	506,000	445,000	494,000	477,000	488,000	471,000	473,000	449,000	501,000	468,000/464,000	497,000/494,000	479,000	498,000		
Chromium	10	-	-	-	-	-	-	-	-	-	-	-	-	-	-	-	-	-	-	-	-	-			
Cobalt	10	60.2 J	65.1 J	66.2 J	64.4 J	64.9 J	73 J	58.4/59.6	62.7/56.3	61.5 J	61.2 J	66.5 J	67.5 J	63.3 J	66.7 J	63.3	62	69.6 J	58 J	68.1 J/63.7 J	71.1/67.2 J	65.4 J	67.6 J		
Copper	10	94.8	102	93	102	89.9	95.4	94.5/95	98.8/94.4	95.1	103	95.8	102	92.2	101	95.2	92	97.4	101	95.3/100	104/102	100	102		
Iron	100	553	645	592	653	588	764	655/654	702/707	610	755	614	677	619	688	663	702	724	828	705/679	816/816	611	656		
Lead	2	783 J	917	826 J	820	767 J	719	967/952	649/786	844 J	782	920 J	881	839 J	790	925	833	910 J	769	902 J/822 J	801/858	990 J	820		
Magnesium	500	37,500	40,200	37,800	39,800	36,500	37,600	37,600/38,000	39,400 J/38,800 J	36,100	39,200	38,100	39,100	37,700	39,500	36,400	38,700 J	36,300	39,500	36,800/36,200	39,700/39,400	38,800	38,800		
Manganese	10	9,130	9,600	9,450	9,750	9,350	9,690	8,820/8,960	9,170/9,150	9,230	9,810	9,490	9,520	9,330	9,610	9,290	9,100	9,140	10,100	9,290/9,340	10,000/10,300	9,600	9,690		
Nickel	20	647	707	675	689	658	666	646/651	682/671	665	713	664	690	666	697	650	670 J	678	707	680/664	702/716	647	688		
Potassium	750	4,020	4,210	5,920	5,690	5,990	5,610	4,250/4,420	6,640/4,430	4,110	5,770	6,190	5,470	6,010	5,920	6,560	6,010	6,420	6,030	6,380/6,450	5,930/5,820	6,520	6,040		
Selenium	3	1.5 J	-	1	-	-	-	-	R/R	-	-	-	-	-	-	-	-	-	-	-	-	13.3	-		
Silver	10	-	-	-	-	-	-	-	-	-	-	-	-	-	-	-	-	-	-	-	-	-	-		
Thallium	10	-	-	-	-	-	2.2	2.4/2	2.7 J	-	-	-	-	-	-	-	-	-	-	-	-	-	-		
Sodium	500	13,500 J	14,000	13,800 J	14,400	14,000	13,900 J	13,300/13,600	13,800 J/13,600 J	14,000	14,300 J	14,000	13,500	13,600 J	13,900	13,400	13,600 J	13,800	13,900 J	14,000/14,100	14,700 J/14,200 J	14,100 J	13,800		
Zinc	20	13,900	14,300	13,800	13,800	13,300	13,500	13,400/13,300	13,900/13,800	13,600	14,200	14,100	13,500	13,700	13,900	13,700	13,900	13,600	16,500	13,800/13,500	14,400/14,200	14,000	13,800		

		LAGOON #4								LAGOON #5				LAGOON #7								
		SW-03		SW-04		SW-05		SW-06		SW-01		SW-02		SW-07		SW-08		SW-09		SW-10		
COMPOUND	CRQL	F	UF	F	UF	F	UF	F	UF	F	UF	F	UF	F	UF	F	UF	F	UF	F	UF	
Aluminum	100	-	75.4 J	74.1 J	147 J	78.6 J	96 J	65.9 J	153	134	96.4 J	40.9 J	76.7 J	120	-	96	33.4 J	59.2 J/55.6	81.4 J/60.8 J	81.3	92.7	
Barium	20	-	21.1 J	-	2.9 J	1.7 J	2.4 J	2.5 J	2.4 J	15.7 J	18.2 J	16.7 J	18 J	10.6 J	10.3 J	10.4 J	11.4 J	9.7 J/9.3 J	11.8 J/11.5 J	11 J	10.9 J	
Beryllium	1	-	-	-	-	-	-	-	-	-	-	-	-	-	-	-	-	-	-	-	-	
Cadmium	1	-	-	-	-	-	-	-	-	-	-	-	-	-	-	-	-	-	-	-	-	
Calcium	500	529,000	565,000	547,000	563,000	523,000	550,000	519,000	537,000	585,000	601,000	557,000	572,000	496,000	511,000	510,000	510,000	523,000/511,000	520,000/513,000	506,000	500,000	
Chromium	10	-	-	-	-	-	-	-	-	-	-	-	-	-	-	-	-	-	-	-	-	
Cobalt	10	-	-	-	-	-	-	-	-	-	-	-	-	-	-	-	-	-	-	-	-	
Copper	10	-	-	-	-	-	-	-	-	5.4 J	-	-	-	-	-	-	-	-	-	-	-	
Iron	100	-	1690	-	244	-	141	-	844	-	382	-	65.9 J	-	145	-	64.9 J	-	67.4 J/64.6 J	-	14 J	121
Lead	2	-	-	-	-	-	-	-	-	-	-	-	-	-	-	-	-	-	-	-	-	
Magnesium	500	99,700	107,000	105,000	109,000	101,000	104,000	102,000	106,000 J	18,300	18,700	17,100	17,900	96,100	99,700 J	101,000	103,000 J	97,400/96,200	99,700/100,000	100,000	99,700 J	
Manganese	10	5.4 J	15.5	2.4 J	6.5 J	2 J	2.8 J	2.1 J	9.2 J	6.1 J	17.3	3.1 J	11.7	3.5 J	17.9	2.4 J	14.2	6.1 J/5.6 J	16.3 J/11.5 J	3.8 J	15.1	
Nickel	20	-	-	-	-	-	-	-	20.4	-	-	-	-	-	-	-	-	-	-	-	20.5	
Potassium	750	3,420	2,820	3,380	2,990	3,280	2,900	3,600	3,230	6,700	6,210	6,390	6,370	4,440	4,040	3,750	3,900	4,300/4,190	3,670/3,470	4,050	4,070	
Selenium	3	-	-	-	-	-	-	-	-	-	-	-	-	-	-	-	-	-	-	-	R	
Silver	10	-	-	-	-	-	-	-	-	-	-	-	-	-	-	-	-	-	-	-	-	
Thallium	10	-	-	-	-	-	-	-	-	-	-	-	-	-	-	-	-	-	-	-	-	
Sodium	500	16,200	16,300 J	16,300 J	16,300	15,500 J	15,500	15,500	15,600 J	20,100 J	19,800	19,100 J	19,500	15,600	15,400 J	15,700 J	16,100	15,600 J/15,600 J	15,500/16,000	15,300 J	15,700	
Zinc	20	-	36	-	-	-	-	-	22.3	9 J	-	-	-	-	-	-	-	-	-	-	-	

NOTES:

2,920/3,100 - Sample concentration/duplicate concentration
CLP - Contract laboratory program
CRQL - Contract required quantitation limits
J - Concentration is estimated

F - Field Filtered
UF - Unfiltered

mg/Kg - Milligrams per kilogram

R - Lab rejected sample

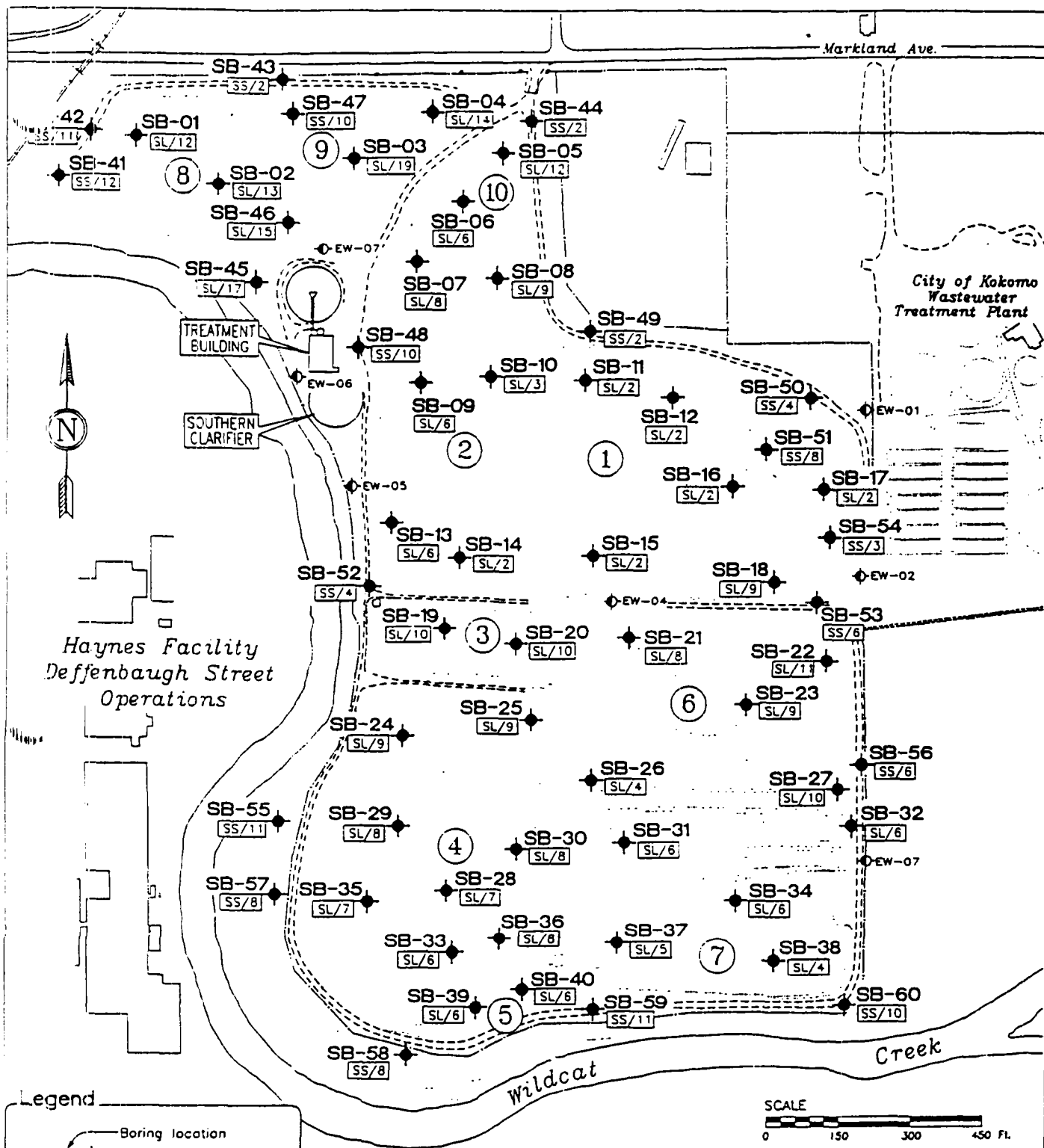
- - - Not detected

was detected 9 of 10 unfiltered samples with an average concentration of 80 mg/L. Zinc was detected in all eleven unfiltered acid lagoon samples with an average concentration of 14,000 mg/L. In the polishing lagoons, zinc was detected 2 of 10 unfiltered samples with an average concentration of 29.2 mg/L. Calcium and magnesium concentration were higher in the polishing lagoon surface waters, most likely a result of the use of lime (calcium magnesium carbonate) during the neutralizing process.

4.3.3 Sludges and Soils

Three soil units are present in the Lagoon Area: (1) surficial soils, (2) intermediate soils, and (3) basal soils. The surficial unit consists of sludge inside of the lagoons and a mixture of slag and fill soils outside of the lagoons. Areas and thicknesses of the sludges and the slag/soil mixtures are shown on Figure 4-8. In the acid lagoons, sludge is generally 2-foot thick, excluding the northern portion of Lagoon No. 2 where the sludge thickness ranged from 6 to 8 feet. The sludge thickness ranged from 4 to 11 feet in the polishing lagoons. In the sludge drying beds, the sludge thickness ranged from 12 to 19 feet. The slag/soil mixture was 2- to 4-feet thick along the northern and eastern boundary of the Lagoon Area. Along the southern and western boundaries of the Lagoon Area, the slag/soil mixture was 8- to 11-feet thick.

In some areas, a clayey fill was encountered below the sludge or slag/soil mixture. The clayey fill generally consisted of silty or sandy clay. This intermediate soil layer is interpreted to be fill due to its lower density when compared to the glacial silts and clay (generally 10 blows per foot verses 40 blows per foot). Figure 4-9 illustrates the areas and thickness of the clayey fill. The clay fill is not present across the entire Lagoon Area. The clayey fill is absent over the majority of the acid lagoons and polishing lagoons. Where present, the thickness varies from 1 foot to 14 feet. The clayey fill averages 3-foot thick where it overlies the lagoons.



Legend

SB-58 Boring location

Thickness
 Soil unit

KEY TO SOIL UNITS

SL Sludge
 SS Slag/soil mixture

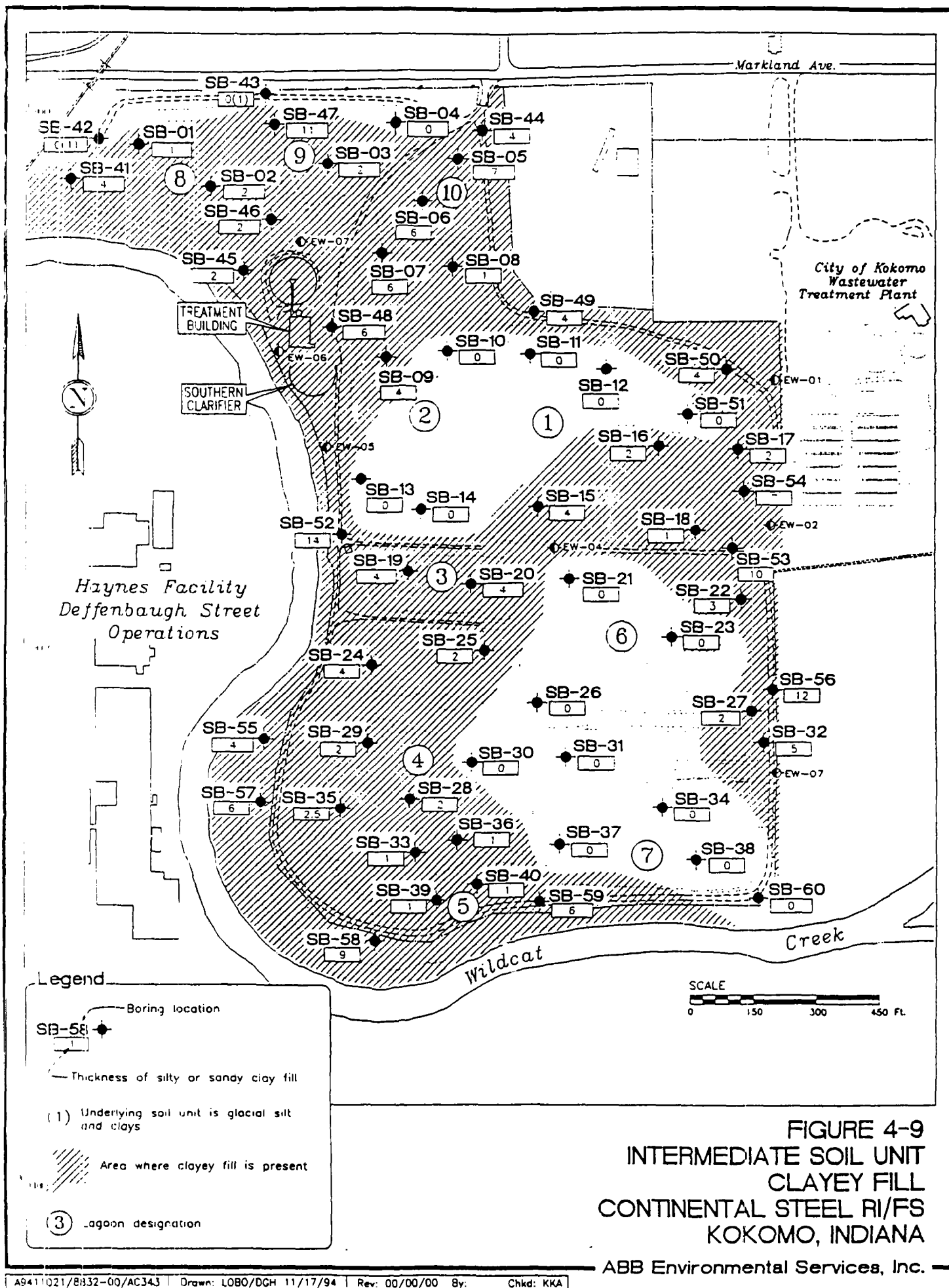
Lagoon designation

NOTE:

At SL/SB-08, SL/SB-04, SL/SB-05, SL/SB-06, SL/SB-18, SL/SB-22 sludge and slag existed in alternating layers. For mapping purposes, these alternating layers were considered sludge.

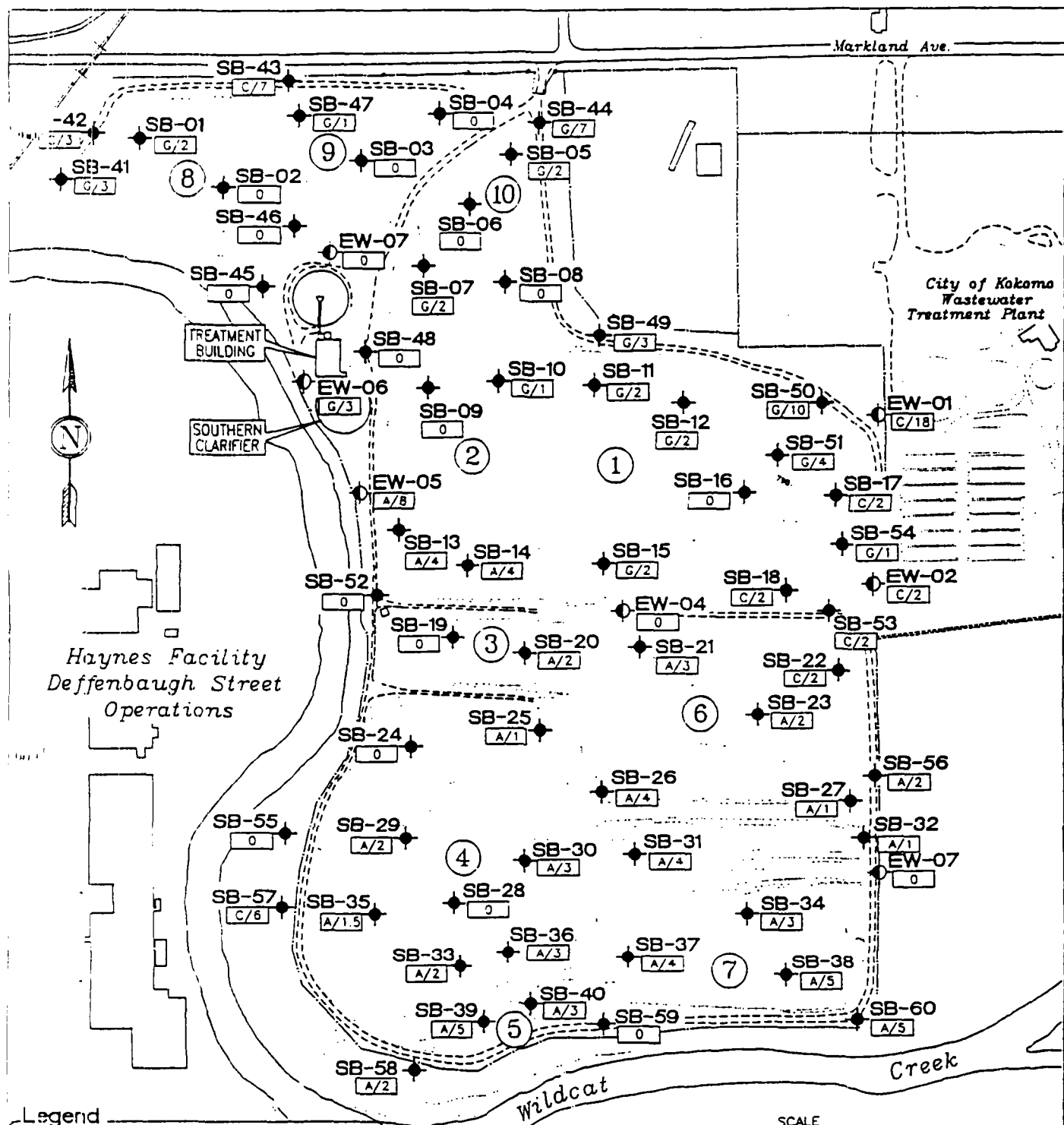
FIGURE 4-8
SURFICIAL UNIT
SLUDGE AND SLAG/SOIL FILL
CONTINENTAL STEEL RI/FS
KOKOMO, INDIANA

ABB Environmental Services, Inc.



Where the intermediate clayey fill is not present, the sludge or slag/soil mixture directly overlies glacial sands and gravels and/or alluvial silts and sand. Both of these soil types are suspected to be relatively permeable. The glacial sands and gravels and alluvial silts and sands, along with glacial silts and clays, are interpreted to be the native soils in this area. They are termed the basal soil unit because they are encountered directly above the bedrock limestone. The areas in which each of these soils were encountered and the thickness at each boring location is shown on Figure 4-10. Glacial silts and clays were encountered in the northwestern and eastern portions of the lagoons. These soils ranged from 1- to 18-foot thick and were predominantly encountered in bedrock channels. Glacial sands and gravels were encountered primarily in the northern half of the Lagoon Area, with thicknesses of 1-foot to 7-feet. Alluvial silts and sands were present in the throughout the polishing bed area. The alluvial deposits were 1- to 8-feet thick. It is interpreted that the alluvial deposits may have been removed along the eastern boundary of Lagoon Nos. 2, 3, and 4, possibly during the diversion of the creek channel. In the area of Lagoons No. 4 and No.7, the alluvial deposits appeared to overly glacial sands and gravels.

The soil units describe above give some indications as to the construction of the lagoons. It does not appear that the lagoons were lined as part of the construction because the clayey fill is absent over the majority of the acid lagoons and polishing lagoons. It appears that a mixture of slag, bricks, concrete, sand and clay was used to create berms around each lagoon and fill low lying areas. Fill was encountered between sludge layers at boring locations SL/SB-01, SL/SB-03, SL/SB-05, and SB-45. These borings are located in the Sludge Drying Bed Area. Also, fill was encountered between sludge layers at boring locations SL/SB-18 and SL/SB-22. These borings are located near the southeast corner of Lagoon No. 1. In these areas, sludge and fill (e.g., slag, bricks) were most likely disposed in alternating layers as they were generated by the Lagoon Treatment Building processes (for sludge) or processes at the Main Plant (for fill).



Legend

- Boring location
 SB-58
 A/2
 Thickness of Soil Unit
 Soil type overlying bedrock

KEY TO SOIL TYPES

- [A] Glacial sand and gravel
 [C] Glacial silts and clays
 [S] Alluvial deposits
 [] indicates soil unit was not encountered
 (3) Lagoon designation

NOTE:

Detailed soils descriptions were provided on boring logs for wells EW-01 through EW-06 (installed by others), therefore, these data was included in the interpretation.

Soils descriptions on boring logs for wells EW-08 through EW-12 (installed by others) were non-descriptive, therefore these data were not included in this interpretation.

FIGURE 4-10
 BASAL SOIL UNIT - NATURAL SOILS
 CONTINENTAL STEEL RI/FS
 KOKOMO, INDIANA

ABB Environmental Services, Inc.

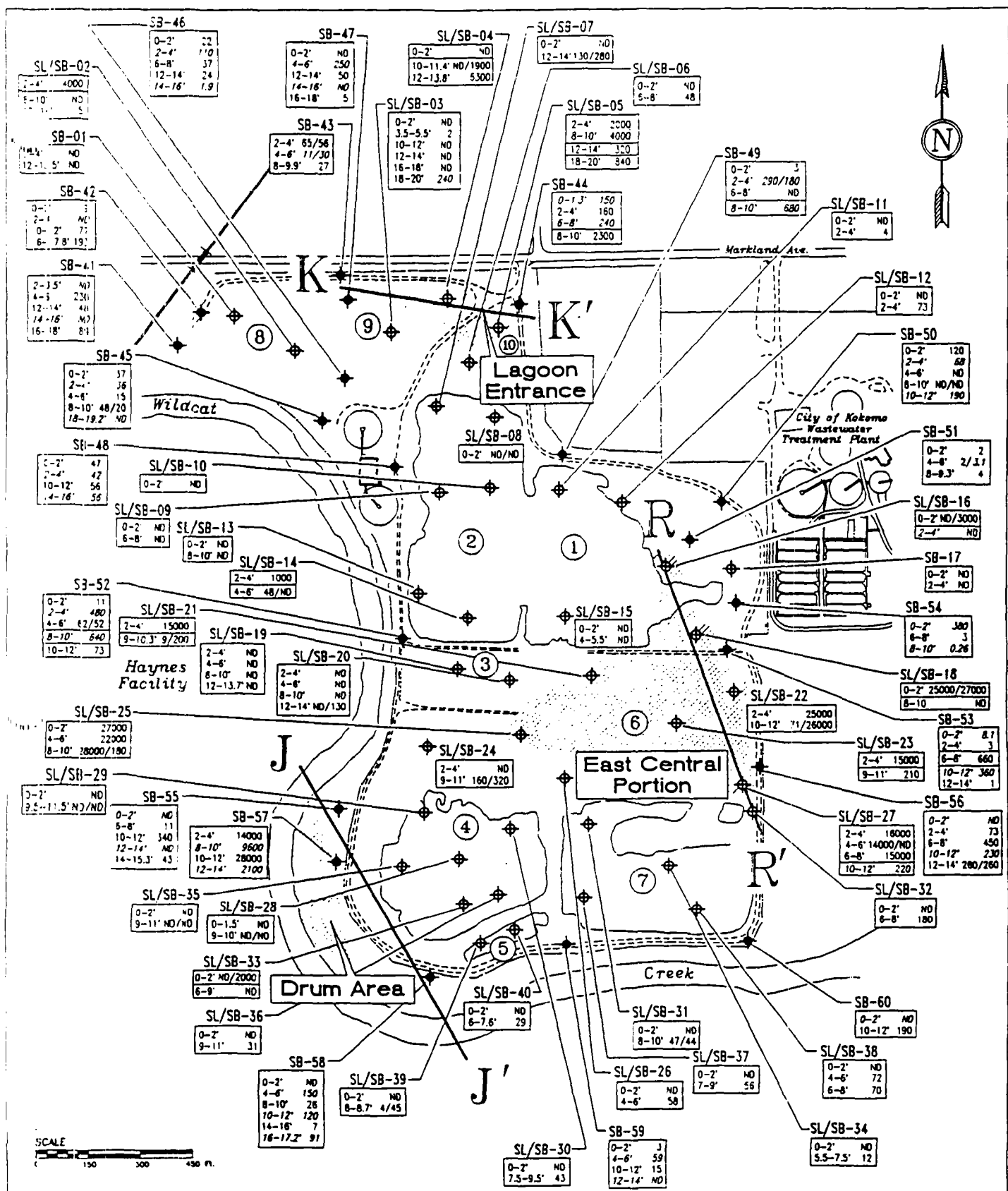
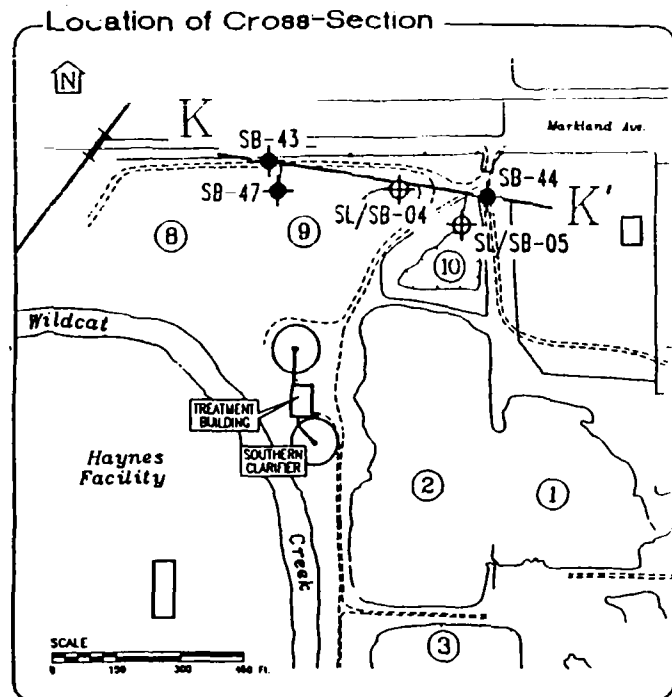


FIGURE 4-11
DISTRIBUTION OF VOCs
IN LAGOON SLUDGES AND SOILS
CONTINENTAL STEEL RI
KOKOMO, INDIANA

ABB Environmental Services, Inc.



Legend

- SB-47 Soil boring
- SL/SB-04 Soil boring
- 160 CLP Analysis (ug/Kg)
- 250 Field Analysis (ug/Kg)
- ND/ND Duplicate sample
- ND Not Detected
- J Estimated
- Approximate location of concentrations greater than 500 ug/Kg
- Split spoon sampling interval
- Water level in lagoon
- Approximate boundary of lagoon

K
Northwest

K'
Southeast

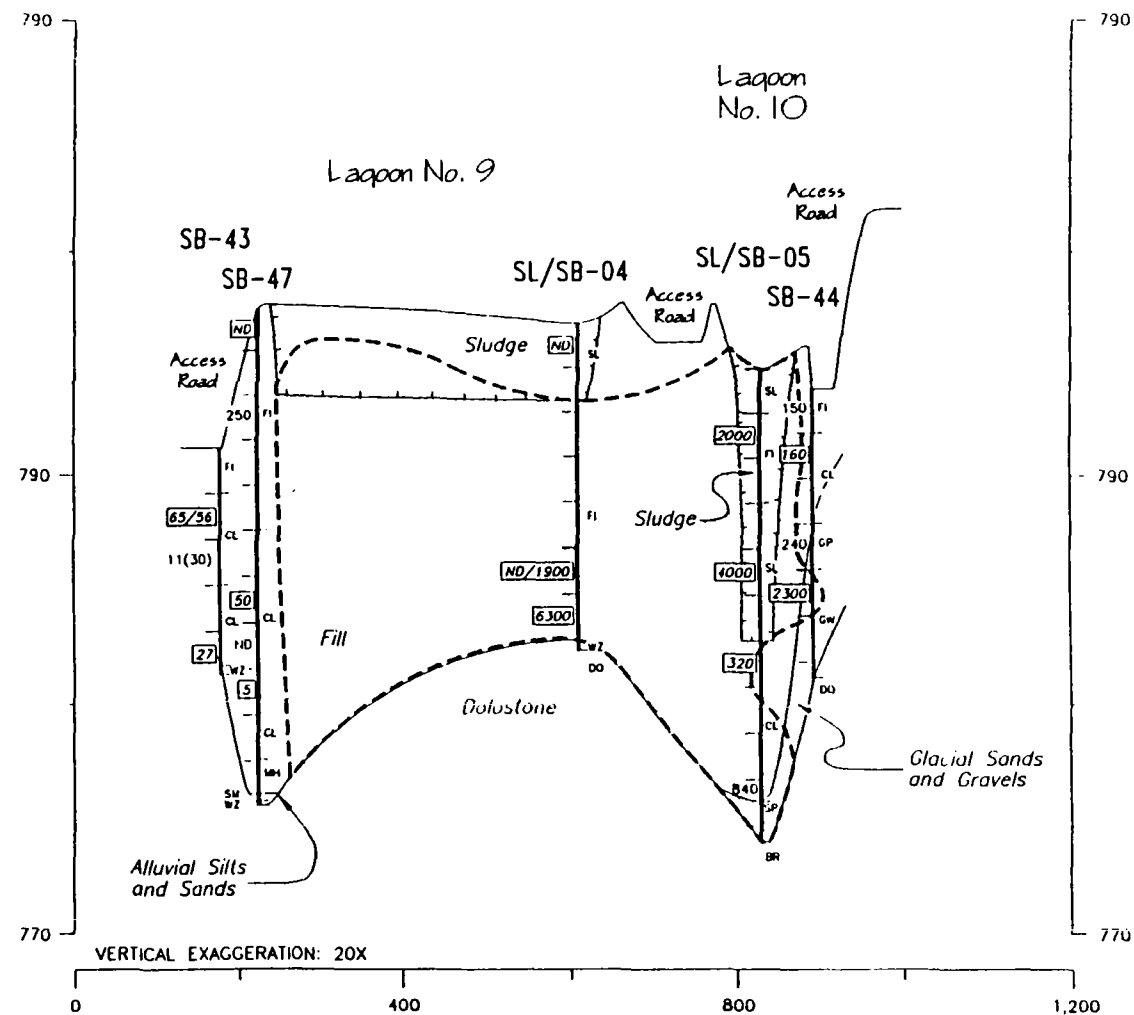


FIGURE 4-12
VERTICAL DISTRIBUTION OF VOCs
LAGOON AREA ENTRANCE
CONTINENTAL STEEL RI
KOKOMO, INDIANA

ABB Environmental Services, Inc. -

TABLE 4-15
SUMMARY OF DETECTED VOCs IN LAGOON SLUDGE AND SOILS
(CLP Results in ug/Kg)
CONTINENTAL STEEL RI
Kokomo, Indiana

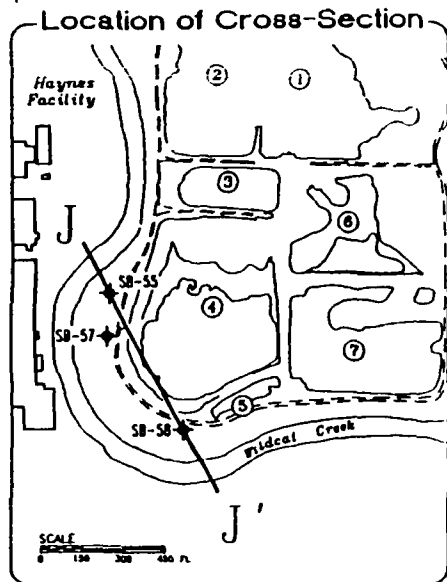
AREA/MEDIA		FREQUENCY OF DETECTION	MINIMUM DETECTED CONCENTRATION	MAXIMUM DETECTED CONCENTRATION	ARITHMETIC MEAN ¹ OF DETECTS
LAGOON ENTRANCE					
SLUDGE	Methylene Chloride	2/4	2,000	4,000	3,000
SOIL	Acetone	3/6	18	220	98
	Benzene	1/6	2.0	2.0	2.0
	2-Butanone	4/6	14	76	31
	1,1-Dichloroethene	2/6	3.0	7.0	5.0
	1,2-Dichloroethene (total)	5/6	14	540	210
	Ethylbenzene	1/6	5.0	5.0	5.0
	Tetrachloroethene	2/6	690	1,200	950
	Toluene	1/6	9.0	9.0	9.0
	Trichloroethene	6/6	11	5,100	1,400
	Vinyl Chloride	1/6	3.0	3.0	3.0
	Total Xylenes	1/6	26	26	26
DRUM AREA					
SOIL	Acetone	3/8	11	240	94
	2-Butanone	3/8	4.0	89	35
	Carbon Disulfide	1/8	4.0	4.0	4.0
	1,2-Dichloroethene (total)	3/8	5.0	6,300	2,200
	Toluene	3/8	1.0	12	5.0
	Trichloroethene	4/8	3.0	22,000	9,000
EAST CENTRAL PORTION OF LAGOONS					
SLUDGE	Acetone	1/18	2,800	2,800	2,800
	2-Butanone	1/18	5.0	5.0	5.0
	Carbon Disulfide	1/18	59	59	59
	Methylene Chloride	11/18	8,000	28,000	20,000
	Tetrachloroethene	1/18	3.0	3.0	3.0
	Toluene	1/18	4.0	4.0	4.0
SOIL	Acetone	2/6	68	210	139
	Carbon Disulfide	2/6	55	200	130
	Toluene	1/6	1.0	1.0	1.0
OTHER SLUDGE²					
Acetone		8/50	13	2,300	440
Benzene		1/50	13	13	13
2-Butanone		7/50	9.0	34	19
Carbon Disulfide		2/50	3.0	3.0	3.0
1,1-Dichloroethene		1/50	3.0	3.0	3.0
Ethylbenzene		1/50	4.0	4.0	4.0
Methylene Chloride		1/50	4,000	4,000	4,000
Toluene		3/50	3.0	6.0	4.5
Trichloroethene		2/50	2.0	2.0	2.0
Total Xylenes		1/50	2.0	2.0	2.0
OTHER SOILS					
Acetone		25/75	9.0	520	110
Benzene		6/75	1.5	12	4.3
2-Butanone		23/75	3.0	140	27
Carbon Disulfide		16/75	1.0	51	11
Chlorobenzene		1/75	4.0	4.0	4.0
1,1-Dichloroethene		1/75	3.0	3.0	3.0
1,2-Dichloroethene (total)		4/75	3.0	8.0	4.5
Ethylbenzene		2/75	0.70	3.0	1.9
2-Hexanone		1/75	48	48	48
Methylene Chloride		3/75	6.0	120	63
4-Methyl-2-Pentanone		1/75	59	59	59
Toluene		38/75	1.0	29	6.5
Trichloroethene		6/75	2.0	220	49
Total Xylenes		9/75	1.0	19	4.1

¹ In calculating the mean, duplicate values were averaged and then the average was used in the calculation. Non-detects were not used in the calculation except when averaging a duplicate results where one of the two samples is non-detect. In this case, half the undetected value was used.

² In soil borings 03, 05, 06, 18, 22, 45; where there were alternating layers of fill and sludge, the fill was included with the sludge calculation.

³ For the calculations, all samples from SB-46 were considered sludge.

⁴ Where sludge and soil are mixed in a sample, the sample is calculated as a sludge.



Legend

- SB-55 Soil boring
- [J40] CLP Analysis (ug/Kg)
- 9800 Field Analysis (ug/Kg)
- ND/ND Duplicate sample
- ND Not Detected
- J Estimated
- Approximate location of concentrations greater than 500 ug/Kg
- Split spoon sampling interval
- Water level in lagoon
- Approximate boundary of lagoon

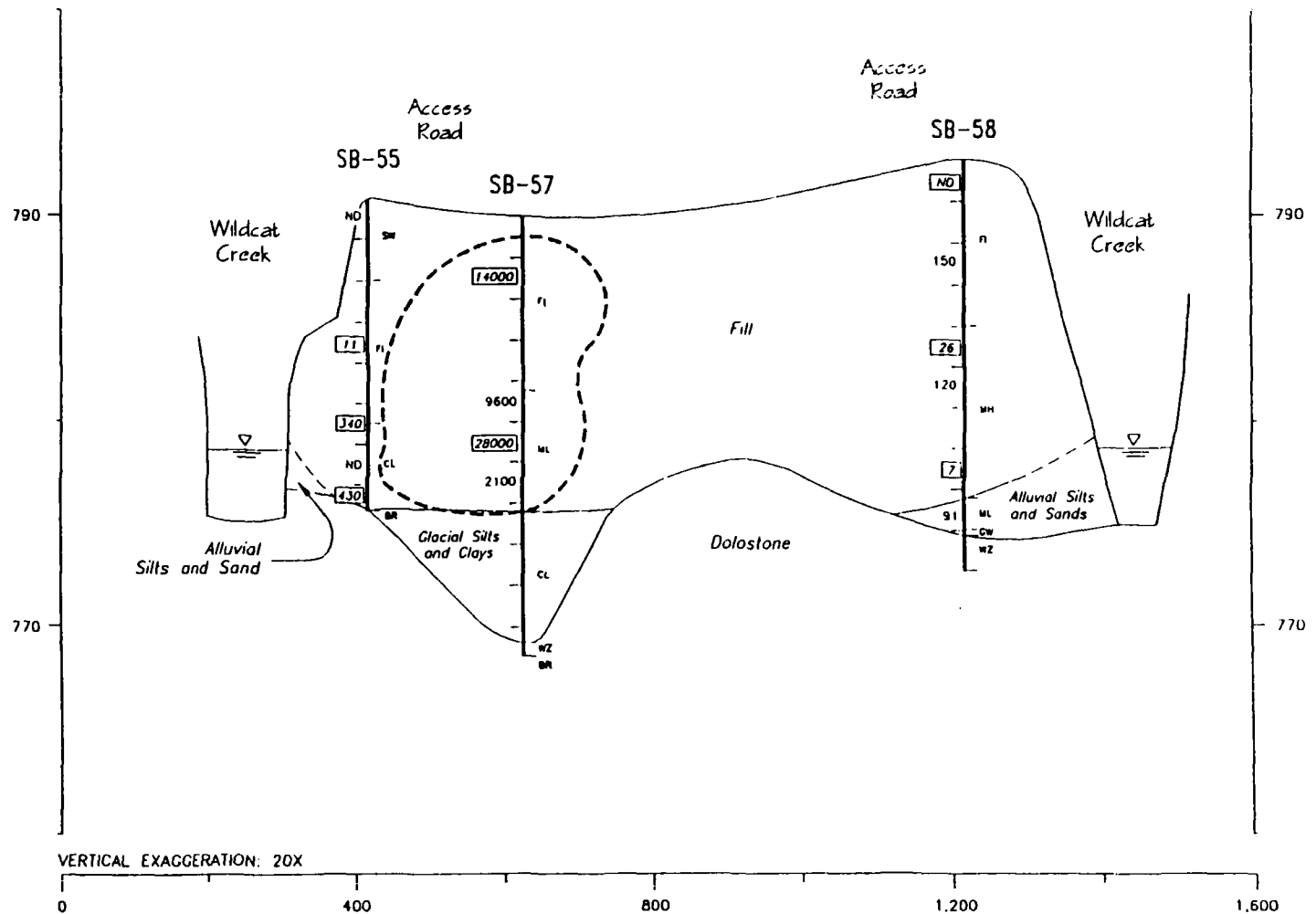


FIGURE 4-13
VERTICAL DISTRIBUTION OF VOCs
LAGOON DRUM AREA
CONTINENTAL STEEL RI
KOKOMO, INDIANA

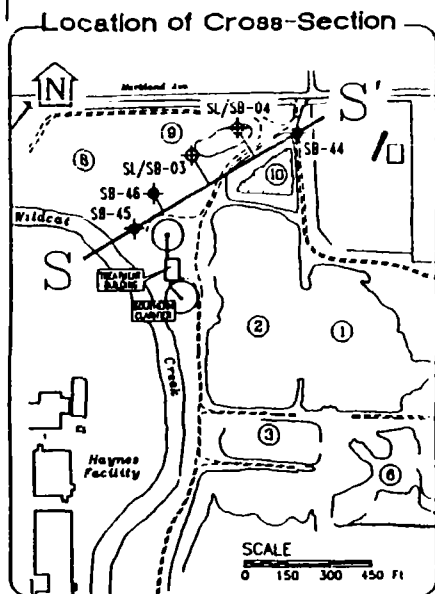
ABB Environmental Services, Inc.

In this area, several drums of TCE and TCE-contaminated soils were removed by the USEPA (USEPA, 1993). USEPA reported that, during the excavation activities, the concentration of organic vapors increased with depth until the clay layer was encountered. Once the clay layer was encountered, the concentration decreased significantly. This indicates that the silty clay *may be inhibiting the downward migration of the chemicals.*

Figure 4-14 is a geologic cross-section through the east-central portion of the lagoons. The VOC concentration which exceed 500 ug/kg appear to exist only within the sludge layer. As shown on Table 4-15, methylene chloride was detected in 11 of 18 sludge samples with a mean concentration of 20,000 ug/kg. Maximum concentrations in the underlying soils were less than 210 ug/kg.

4.3.3.2 Polynuclear Aromatic Hydrocarbons - The distribution of total PAHs in sludge and soils is shown on Figure 4-15. The figure includes both CLP and field laboratory results. Table 4-16 summarizes the individual compounds and their concentration. PAHs were non-detectable in the majority of the acid and polishing lagoons (excluding a detection of 9,900 ug/kg in a soil sample from SL/SB-14). PAHs were consistently detected in the other portions of the Lagoon Area. Total PAH concentrations exceeded 500 ug/kg in three main areas. These areas, illustrated by the shading on Figure 4-15, are: (1) the Sludge Drying Beds, (2) the Drum Area, and (3) the east-central boundary of the lagoons.

Figure 4-16 is a cross-section through the Sludge Drying Beds. The areas where the total PAH concentration exceed 500 ug/kg appear to be discontinuous and are present within both the upper and lower portions of the sludge/fill. As shown on Table 4-16, fluoranthene, phenanthrene, and pyrene were detected in 25 percent of the CLP samples collected from this area. These compounds had mean concentrations greater than 1,000 ug/kg.



Legend

- SB-44 Soil boring
- SL/SB-45 Sludge/soil boring
- [100] CLP Analysis (ug/Kg)
- 2800 Field Analysis (ug/Kg)
- ND/ND Duplicate sample
- ND Not Detected
- J Estimated
- (Dashed line) Approximate location of concentrations greater than 500 ug/Kg
- E Split spoon sampling interval
- ▽ Water level in lagoon
- V Approximate boundary of lagoon

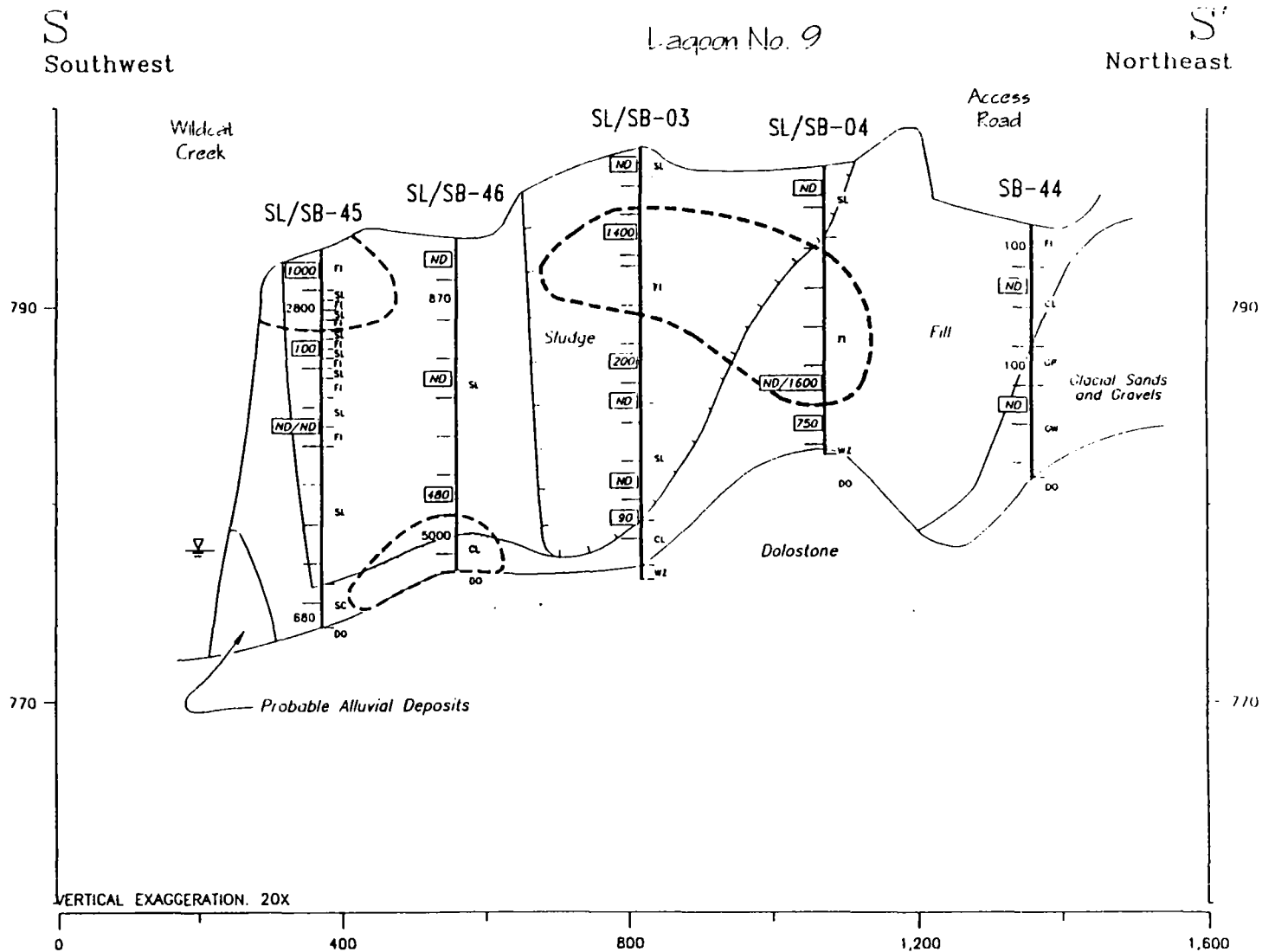


FIGURE 4-16
VERTICAL DISTRIBUTION OF PAHs
SLUDGE DRYING BEDS
CONTINENTAL STEEL RI
KOKOMO, INDIANA

ABB Environmental Services, Inc. —

SUMMARY OF DETECTED PAHs IN LAKEON SLUDGE AND SOILS
(CLP Results in $\mu\text{g/Kg}$)
CONTINENTAL STEEL RI
Kokomo, Indiana

AREA/MEDIA		FREQUENCY OF DETECTION	MINIMUM DETECTED CONCENTRATION	MAXIMUM DETECTED CONCENTRATION	ARITHMETIC MEAN ¹ OF DETECTS
SLUDGE DRYING BEDS					
SLUDGE	Benzo(a)Anthracene	2/12	95	130	110
	Benzo(a)Pyrene	2/12	83	120	100
	Benzo(b)Fluoranthene	2/12	180	200	190
	Benzo(g,h,i)perylene	1/12	61	61	61
	Benzo(k)Fluoranthene	1/12	160	160	160
	Chrysene	2/12	110	180	150
	Dibenz(a,h)Anthracene	1/12	47	47	47
	Fluoranthene	4/12	58	280	150
	Indeno(1,2,3-cd)Pyrene	1/12	180	180	180
	Phenanthrene	5/12	58	240	110
	Pyrene	5/12	31	190	110
DRUM AREA					
SLUDGE	Pyrene	1/2	7,000	7,000	7,000
SOIL	Anthracene	2/13	58	970	510
	Benzo(a)Anthracene	4/13	220	2,800	1,100
	Benzo(a)Pyrene	4/13	210	3,800	1,400
	Benzo(b)Fluoranthene	4/13	250	5,500	1,800
	Benzo(g,h,i)Perylene	3/13	340	3,700	1,800
	Benzo(k)Fluoranthene	3/13	230	1,400	640
	Chrysene	4/13	250	3,200	1,300
	Dibenz(a,h)Anthracene	3/13	92	530	350
	Fluoranthene	4/13	330	2,600	1,100
	Fluorene	1/13	290	290	290
	Indeno(1,2,3-cd)Pyrene	4/13	330	2,500	1,100
	Naphthalene	1/13	300	300	300
	Phenanthrene	3/13	270	1,600	840
	Pyrene	4/13	220	4,000	1,500
EAST CENTRAL BOUNDARY					
SLUDGE	Acenaphthene	3/9	1,000	8,000	3,300
	Anthracene	1/9	1,000	1,000	1,000
	Benzo(a)Anthracene	1/9	2,000	2,000	2,000
	Benzo(a)Pyrene	1/9	2,000	2,000	2,000
	Chrysene	2/9	5,000	5,000	5,000
	Fluoranthene	1/9	2,000	2,000	2,000
	Fluorene	1/9	6,000	6,000	6,000
	Phenanthrene	4/9	64	9,000	4,500
	Pyrene	3/9	2,000	7,000	5,300
SOIL	Acenaphthylene	1/8	81	81	81
	Anthracene	2/8	19	86	53
	Benzo(a)Anthracene	5/8	40	390	170
	Benzo(a)Pyrene	5/8	33	350	170
	Benzo(b)Fluoranthene	6/8	19	330	140
	Benzo(g,h,i)perylene	3/8	53	310	140
	Benzo(k)Fluoranthene	6/8	23	240	110
	Chrysene	5/8	49	530	230
	Dibenz(a,h)Anthracene	1/8	88	88	88
	Fluoranthene	6/8	26	420	170
	Indeno(1,2,3-cd)Pyrene	3/8	59	340	180
	Naphthalene	1/8	44	44	44
	Phenanthrene	5/8	48	300	130
	Pyrene	7/8	29	540	190
OTHER SLUDGE²					
	Benzo(a)Anthracene	2/43	48	55	52
	Benzo(a)Pyrene	2/43	50	73	62
	Benzo(b)Fluoranthene	2/43	46	46	46
	Benzo(g,h,i)perylene	1/43	55	55	55
	Benzo(k)Fluoranthene	2/43	45	66	58
	Chrysene	2/43	61	61	61
	Fluoranthene	2/43	75	100	88
	Fluorene	1/43	42	42	42
	Indeno(1,2,3-cd)Pyrene	1/43	66	66	66
	Phenanthrene	2/43	50	140	95
	Pyrene	2/43	73	92	83
OTHER SOILS					
	Benzo(a)Anthracene	7/57	26	830	170
	Benzo(a)Pyrene	7/57	31	1,200	230
	Benzo(b)Fluoranthene	5/57	30	140	76
	Benzo(g,h,i)perylene	1/57	420	420	420
	Benzo(k)Fluoranthene	4/57	32	550	180
	Chrysene	8/57	35	1,300	230
	Fluoranthene	7/57	51	1,300	270
	Fluorene	1/57	170	170	170
	Phenanthrene	5/57	83	940	280
	Pyrene	9/57	44	2,000	320

¹ In calculating the mean, duplicate values were averaged and then the average was used in the calculation. Non-detects were not in the calculation except when averaging duplicate results where one of the two samples is non-detect. In this case, half the undetected value was used.

² In soil borings SL/SB 03, 05, 06, 18, 22, 45; where there were alternating layers of fill and sludge, the fill was included with the sludge calculation.

³ For these calculations, all samples from SB-46 were considered sludge.

⁴ Where sludge and soil are mixed in a sample, the sample is calculated as a sludge.

Figure 4-17 is a cross-section through the Drum Area. As illustrated, total PAHs appear to exceed 500 ug/kg primarily in the upper 5- to 10-feet of the fill soils. As shown on Table 4-16, benzo(a)anthracene, benzo(a)pyrene, benzo(b)fluoranthene, chrysene, fluoranthene, indeno(1,2,3-cd)pyrene, and pyrene were detected in more than 25 percent of the CLP samples collected from the Drum Area. These samples had mean concentrations greater than 1,000 ug/kg.

Figure 4-18 is a cross-section through the east-central boundary of the Lagoon Area. In northern portion of the cross-section (at the northeast corner of Lagoon No. 1), the total PAH concentration exceeded 500 ug/kg in the upper 10 feet of the fill soils. In the central portion of the cross-section (along the eastern boundary of Lagoon No. 6), the total PAH concentrations exceeded 500 ug/kg in 6-foot thick lower portion of the sludge. As shown on Table 4-16, acenaphthene, phenanthrene, and pyrene were detected in more than 25 percent of the sludge samples analyzed by the CLP laboratory. These compounds had mean concentrations greater than 1,000 ug/kg. Several other PAHs were detected in sludge at concentrations greater than 1,000 ug/kg. In soils, the mean PAH concentrations for individual compounds were less than 230 ug/kg.

4.3.3.3 Polychlorinated Biphenyls - The distribution of total PCBs in sludge and soils is shown on Figure 4-19. The figure includes both CLP and field laboratory results. Table 4-17 summarizes the individual compounds and their concentration. The table also provides a comparison to maximum background soils concentrations.

PCBs were consistently detected near the Lagoon Entrance, illustrated by the shading on Figure 4-19. In other areas of the lagoons, the detection of PCBs was sporadic.

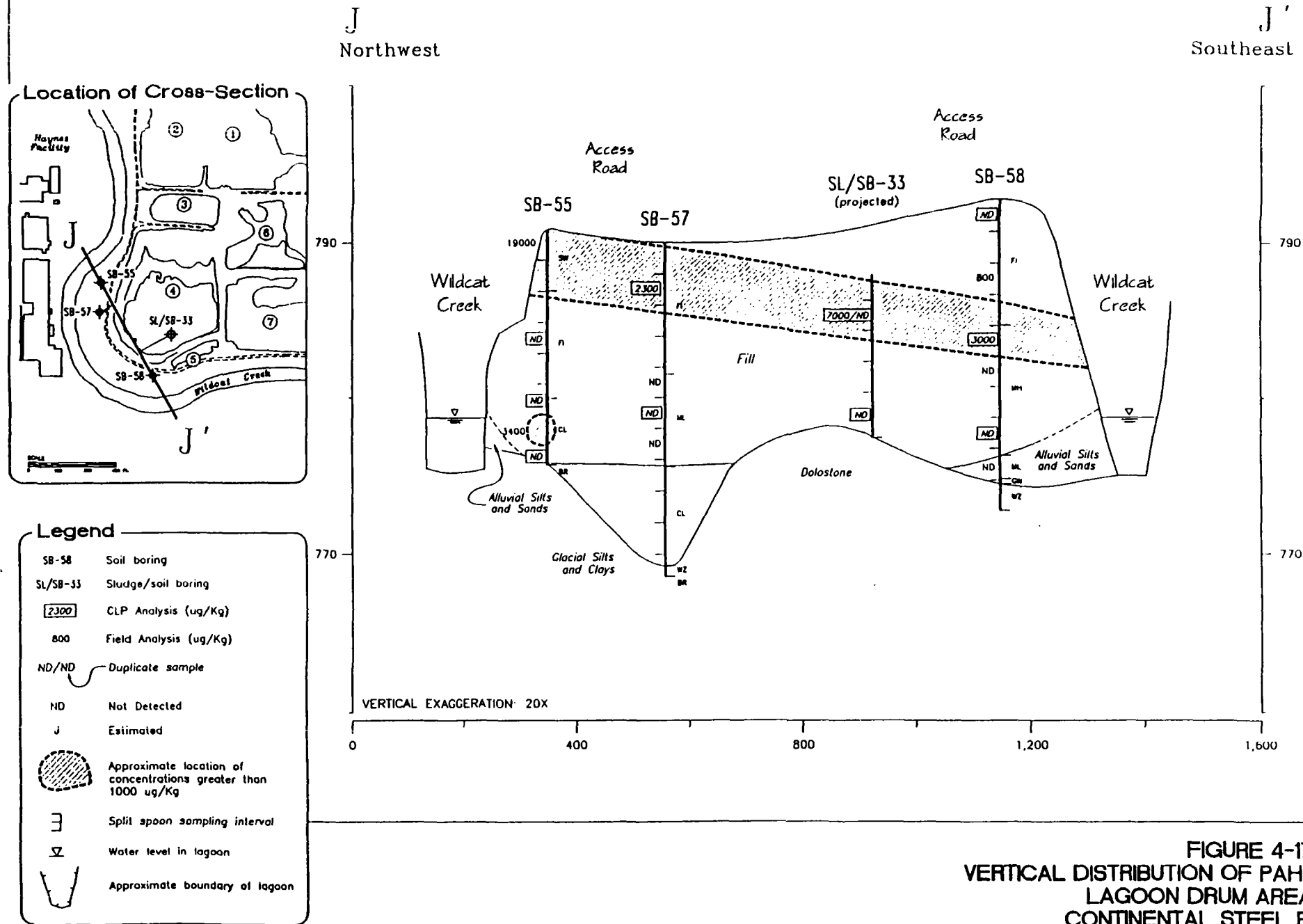


FIGURE 4-17
VERTICAL DISTRIBUTION OF PAHs
LAGOON DRUM AREA
CONTINENTAL STEEL RI
KOKOMO, INDIANA

ABB Environmental Services, Inc.

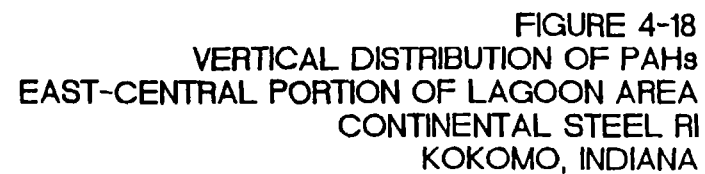


TABLE 4-17
SUMMARY OF DETECTED PCBs IN LAGOON SLUDGE AND SOILS
(CLP Results in ug/Kg)
CONTINENTAL STEEL RI
Kokomo, Indiana

AREA/MEDIA		FREQUENCY OF DETECTION	MINIMUM DETECTED CONCENTRATION	MAXIMUM DETECTED CONCENTRATION	ARITHMETIC MEAN ¹ OF DETECTS
LAGOON ENTRANCE					
SLUDGE	Aroclor-1232	1/12	6,000	6,000	6,000
	Aroclor-1242	3/12	240	2,100	1,100
	Aroclor-1248	3/12	81	52,000	17,000
	Aroclor-1254	2/12	110	130	120
SOIL	Aroclor-1242	2/9	1,200	1,200	1,200
	Aroclor-1248	5/9	240	16,000	4,500
	Aroclor-1254	1/9	260	260	260
	Aroclor-1260	1/9	140	140	140
OTHER SLUDGE²					
Aroclor-1248		2/60	74	8,000	4,037
OTHER SOILS					
Aroclor-1242		1/87	220	220	220
Aroclor-1248		8/87	37	3,800	880
Aroclor-1254		2/87	69	110	90
Aroclor-1260		1/87	45	45	45

¹ In calculating the mean, duplicate values were averaged and then the average was used in the calculation. Non-detects were not used in the calculation except when averaging duplicate results where one of the two samples is non-detect. In this case, half the undetected value was used.

² In soil borings 03, 05, 06, 18, 22, 45; where there were alternating layers of fill and sludge, the fill was included with the sludge calculation.

³ Soil boring 46 was misidentified as a soil, it is a sludge.

⁴ Where sludge and soil are mixed in a sample, the sample is calculated as a sludge.

Figure 4-20 is a cross-section through the Lagoon Entrance. The figure illustrates that the PCB concentrations were primarily encountered in the upper 6 to 10 feet of the sludge/fill. In the sludge, Aroclor-1242 and Aroclor-1248 were detected in 25 percent of the CLP sludge samples. The mean concentrations of these aroclors in sludge were 1,100 ug/kg and 17,000 ug/kg, respectively. Aroclor-1248 was also detected in 5 of 9 CLP samples collected from the underlying soils.

4.3.3.4 Other Semi-Volatile Organics - Other semi-volatile compounds were sporadically detected in the Lagoon Area sludges and soils. Table 4-18 provide a summary of these compounds. Detected compounds included pesticides, phenol, and phthalates.

4.3.3.5 Inorganics - Table 4-19 provides a summary of the metals detected in the lagoon sludge and soil. The distribution of the metals concentration is described below.

The vertical distribution of the metals in the sludge drying bed area is shown on Figure 4-21. Chromium, copper, nickel, lead and zinc were consistently detected at concentrations three time above the UTL.

Figure 4-22 is a geologic cross-section through the acid lagoons. Chromium, copper, nickel, lead, and zinc were consistently detected at concentrations three or more time above the UTL.

Figure 4-23 is a geologic cross-section through Polishing Lagoons 3 and 6. Chromium, copper, nickel, lead, and zinc were consistently detected at concentrations three or more time above the UTL.

Figure 4-24 is a geologic cross-section through Polishing Lagoons 4 and 7. Chromium and zinc were consistently detected at concentrations three or more time above the UTL.

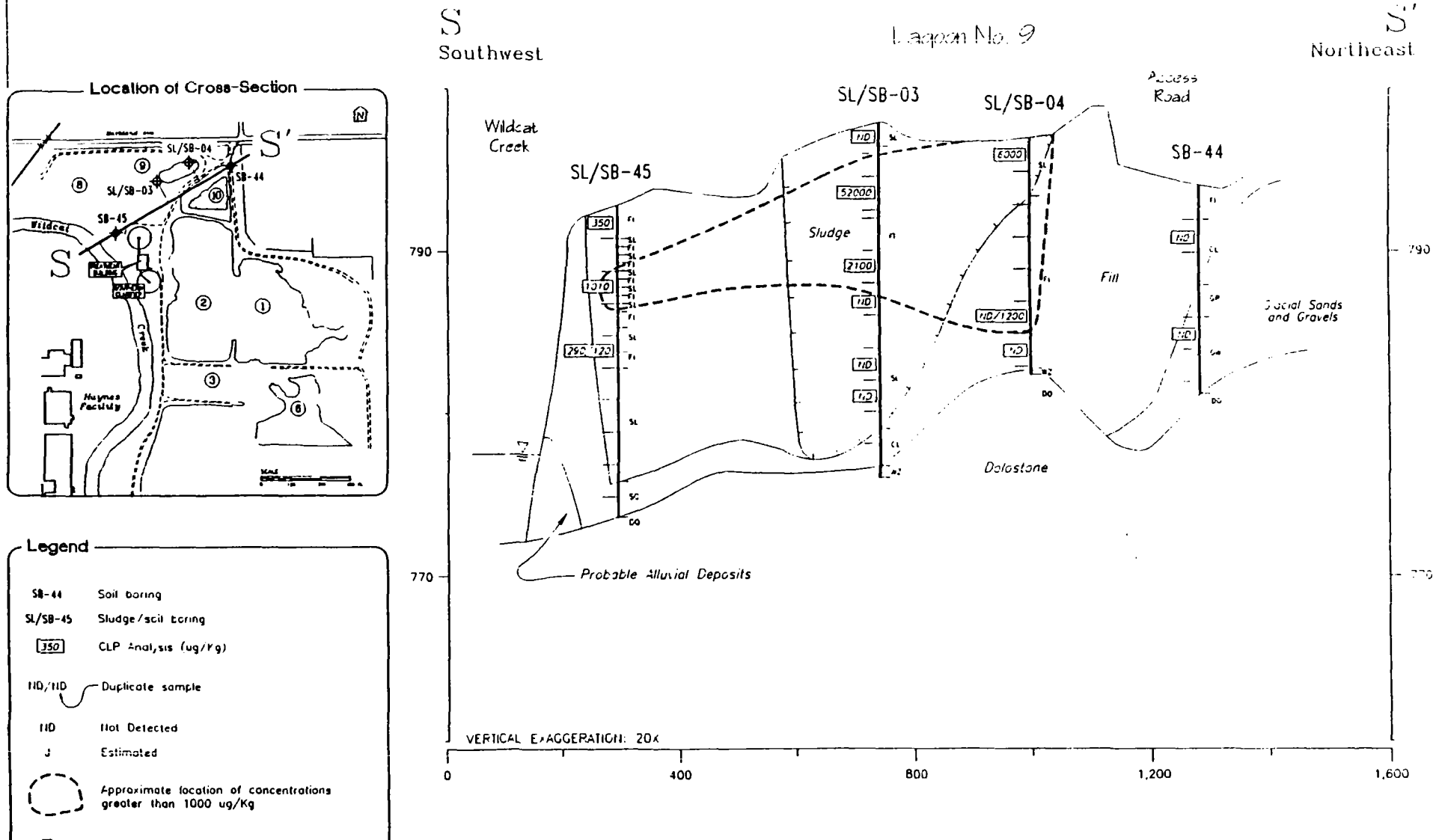


FIGURE 4-20
VERTICAL DISTRIBUTION OF PCBs
LAGOON AREA ENTRANCE
CONTINENTAL STEEL RI
KOKOMO, INDIANA

ABB Environmental Services, Inc.

TABLE 4-18
SUMMARY OF OTHER DETECTED ORGANICS IN LAGOON SLUDGE AND SOILS
(CLP Results in ug/Kg)
CONTINENTAL STEEL RI
Kokomo, Indiana

AREA/MEDIA	FREQUENCY OF DETECTION	MINIMUM DETECTED CONCENTRATION	MAXIMUM DETECTED CONCENTRATION	ARITHMETIC MEAN ¹ OF DETECTS
SLUDGES				
Aldrin	1/77	0.077	0.077	0.077
4,4'-DDD	2/77	0.35	0.41	0.38
4,4'-DDT	2/77	7.8	26	16.9
Dieldrin	4/77	0.73	4.3	2.5
Endosulfan II	3/77	0.65	2.0	1.1
Endosulfan Sulfate	2/77	0.34	0.45	0.40
Endrin	2/77	0.64	0.73	0.69
Endrin Ketone	2/77	1.7	7.0	4.4
Endrin Aldehyde	3/77	1.5	30	12
Heptachlor	1/77	1.6	1.6	1.6
Heptachlor Epoxide	3/77	0.69	1.2	0.92
Methoxychlor	1/77	3.8	3.8	3.8
SOILS				
Alpha-BHC	1/95	0.36	0.36	0.36
Aldrin	3/95	1.0	3.6	2
4,4'-DDD	8/95	0.25	18	3.7
4,4'-DDE	5/95	2.0	240	62
4,4'-DDT	9/95	0.21	42	12
Delta-BHC	1/95	19	19	19
Dieldrin	9/95	0.25	11	3.0
Endosulfan I	4/95	0.064	12	5.2
Endosulfan II	5/95	0.23	6.1	3.5
Endosulfan Sulfate	6/95	0.19	7.6	2.5
Endrin	9/95	0.32	76	15
Endrin Ketone	4/95	0.24	8.6	2.8
Endrin Aldehyde	7/95	1.7	20	9.7
Gamma-BHC (Lindane)	3/95	0.098	0.19	0.14
Gamma-Chlordane	4/95	0.075	61	17
Heptachlor	1/95	42	42	42
Heptachlor Epoxide	7/95	0.13	24	5.4
Methoxychlor	10/95	0.13	57	10

¹ In calculating the mean, duplicate values were averaged and then the average was used in the calculation. Non-detects were not used in the calculation except when averaging duplicate results where one of the two samples is non-detect. In this case, half the undetected value was used.

² In soil borings 03, 05, 06, 18, 22, 45; where there were alternating layers of fill and sludge, the fill was included with the sludge calculation.

³ Soil boring 46 was misidentified as a soil, it is a sludge.

⁴ Where sludge and soil are mixed in a sample, the sample is calculated as a sludge.

TABLE 4-18
SUMMARY OF OTHER DETECTED ORGANICS IN LAGOON SLUDGE AND SOILS
(CLP Results in ug/Kg)
CONTINENTAL STEEL RI
Kokomo, Indiana

AREA/MEDIA	FREQUENCY OF DETECTION	MINIMUM DETECTED CONCENTRATION	MAXIMUM DETECTED CONCENTRATION	ARITHMETIC MEAN ¹ OF DETECTS
SLUDGES				
Bis(2-Ethylhexyl)phthalate	8/77	49	6,000	2,200
Dibenzofuran	3/77	49	11,000	4,000
Pentachlorophenol	1/77	2,000	2,000	2,000
Phenol	1/77	150	150	150
SOILS				
Bis(2-Ethylhexyl)phthalate	19/95	23	580	110
Carbazole	1/95	200	200	200
Dibenzofuran	3/95	22	150	86
Di-n-butylphthalate	3/95	52	110	81
Di-n-octylphthalate	2/95	86	86	86
2-Methylnaphthalene	6/95	35	1,200	390
Phenol	2/95	120	150	135

¹ In calculating the mean, duplicate values were averaged and then the average was used in the calculation. Non-detects were not used in the calculation except when averaging duplicate results where one of the two samples is non-detect. In this case, half the undetected value was used.

² In soil borings 03, 05, 06, 18, 22, 45; where there were alternating layers of fill and sludge, the fill was included with the sludge calculation.

³ Soil boring 46 was misidentified as a soil, it is a sludge.

⁴ Where sludge and soil are mixed in a sample, the sample is calculated as a sludge.

SUMMARY OF DETECTED METALS IN LAGOON SLUDGE AND SOILS
(CLP Results in mg/Kg)
CONTINENTAL STEEL RI
Kokomo, Indiana

AREA/MEDIA	FREQUENCY OF DETECTION	MINIMUM DETECTED CONCENTRATION	MAXIMUM DETECTED CONCENTRATION	ARITHMETIC MEAN ¹ OF DETECTS
SLUDGE^{2,3}				
Aluminum	67/72	275	22,400	2,040
Antimony	5/72	10.5	30.8	20
Arsenic	30/72	1.20	49.3	9.28
Barium	48/72	2.50	439	76.7
Beryllium	15/72	0.29	1.6	0.80
Cadmium	6/72	0.70	6.6	3.1
Calcium	61/71	1440	200,000	79,700
Chromium	68/72	4.40	4,210	215
Cobalt	58/72	3.50	47.7	11.4
Copper	57/72	4.70	972	161
Iron	67/72	942	374,000	105,000
Lead	64/72	14.1	10,200	710
Magnesium	62/72	204	31,200	4,260
Manganese	68/72	16.0	33,200	1,600
Mercury	12/72	0.18	4.2	0.78
Nickel	62/72	6.10	458	97.5
Potassium	5/72	453	3,170	1,350
Selenium	2/72	0.76	1.3	1.0
Silver	7/72	1.1	31	6.3
Sodium	15/72	109	868	261
Thallium	9/72	0.83	6.4	3.0
Vanadium	47/72	2.80	136	17.1
Zinc	68/72	11.4	3,630	1,160
Cyanide	5/72	1.40	187	48.9
SOIL BENEATH SLUDGE				
Aluminum	33/47	160	13,400	3,770
Antimony	1/47	5.10	5.10	5.10
Arsenic	33/47	0.64	101	11.4
Barium	33/47	6.5	362	83.2
Beryllium	12/47	0.075	0.74	0.35
Cadmium	14/47	1.1	22	6.4
Calcium	33/47	1,130	162,000	31,300
Chromium	33/47	2.20	3580	281
Cobalt	10/47	0.310	19.3	4.53
Copper	26/47	3.50	410	65.6
Iron	33/47	486	230,000	43,300
Lead	33/47	4.70	857	124
Magnesium	31/47	57.2	37,000	3,810
Manganese	29/47	10.3	45,300	2,770
Mercury	18/47	0.070	3.2	0.61
Nickel	24/47	0.72	146	26.4
Potassium	32/47	98.5	1750	619
Selenium	12/47	0.12	1.7	0.60
Silver	7/47	0.48	2.4	1.3
Sodium	27/47	49.1	2,330	490
Thallium	5/47	0.21	0.36	0.28
Vanadium	33/47	1.2	351	33.4
Zinc	25/47	6.18	4,590	419
Cyanide	10/47	0.710	71.2	13.6
SOIL OUTSIDE OF LAGOON AREAS				
Aluminum	43/48	813	24,300	8,690
Antimony	15/48	6.20	470	60.0
Arsenic	43/48	1.20	193	18.3
Barium	43/48	19.3	720	142
Beryllium	28/48	0.27	1.5	0.63
Cadmium	29/48	0.50	470	26.0
Calcium	43/48	891	223,000	59,400
Chromium	43/48	4.60	5,510	625
Cobalt	36/48	1.30	62.4	9.80
Copper	43/48	6.90	4,680	352
Iron	42/47	4750	613,000	79,600
Lead	43/48	4	19,300	829
Magnesium	43/48	290	47,300	10,800
Manganese	42/47	17.5	39,800	6,040
Mercury	10/48	0.065	1.8	0.40
Nickel	37/48	7.8	861	104
Potassium	38/48	129	2,960	936
Selenium	10/48	0.51	1.3	0.79
Silver	14/48	0.52	67	8.3
Sodium	28/48	124	1,120	399
Thallium	4/48	0.79	0.90	0.85
Vanadium	43/48	5.70	381	59.0
Zinc	43/48	10.2	249,000	8,440
Cyanide	4/48	0.67	1.40	0.983

¹ In calculating the mean, duplicate values were averaged and then the average was used in the calculation. Non-detects were not used in the calculation except when averaging a duplicate results where one of the two samples was non-detect. In this case, half the undetected value was used for the non-detect

² Where there were alternating layers of fill and sludge, the fill was included with the sludge calculation.

³ Where sludge and soil are mixed in a sample, the sample was calculated as a sludge.

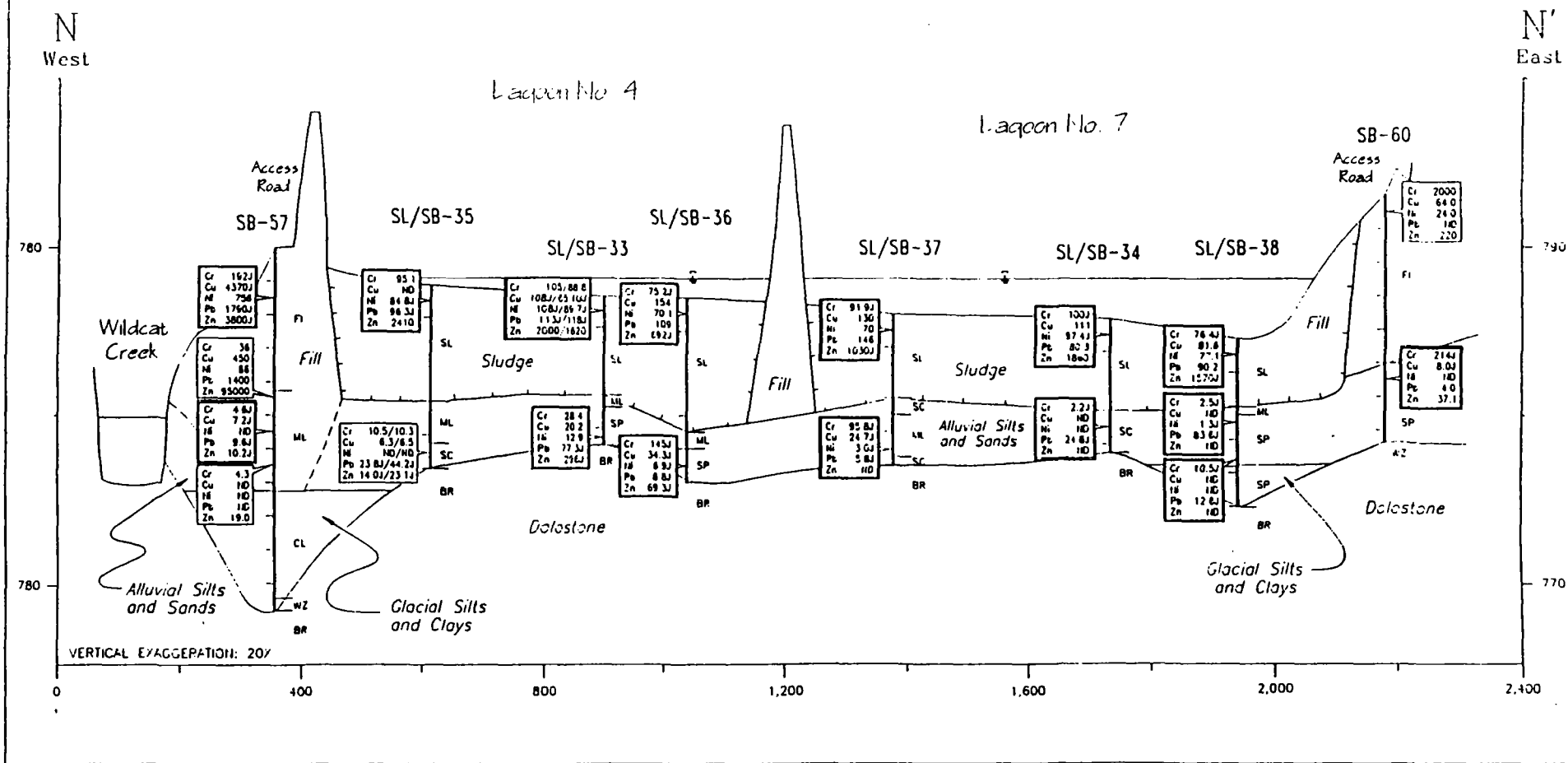


FIGURE 4-24
VERTICAL DISTRIBUTION OF METALS
POLISHING LAGOONS 4 AND 7
CONTINENTAL STEEL RI
KOKOMO, INDIANA

ABB Environmental Services, Inc.

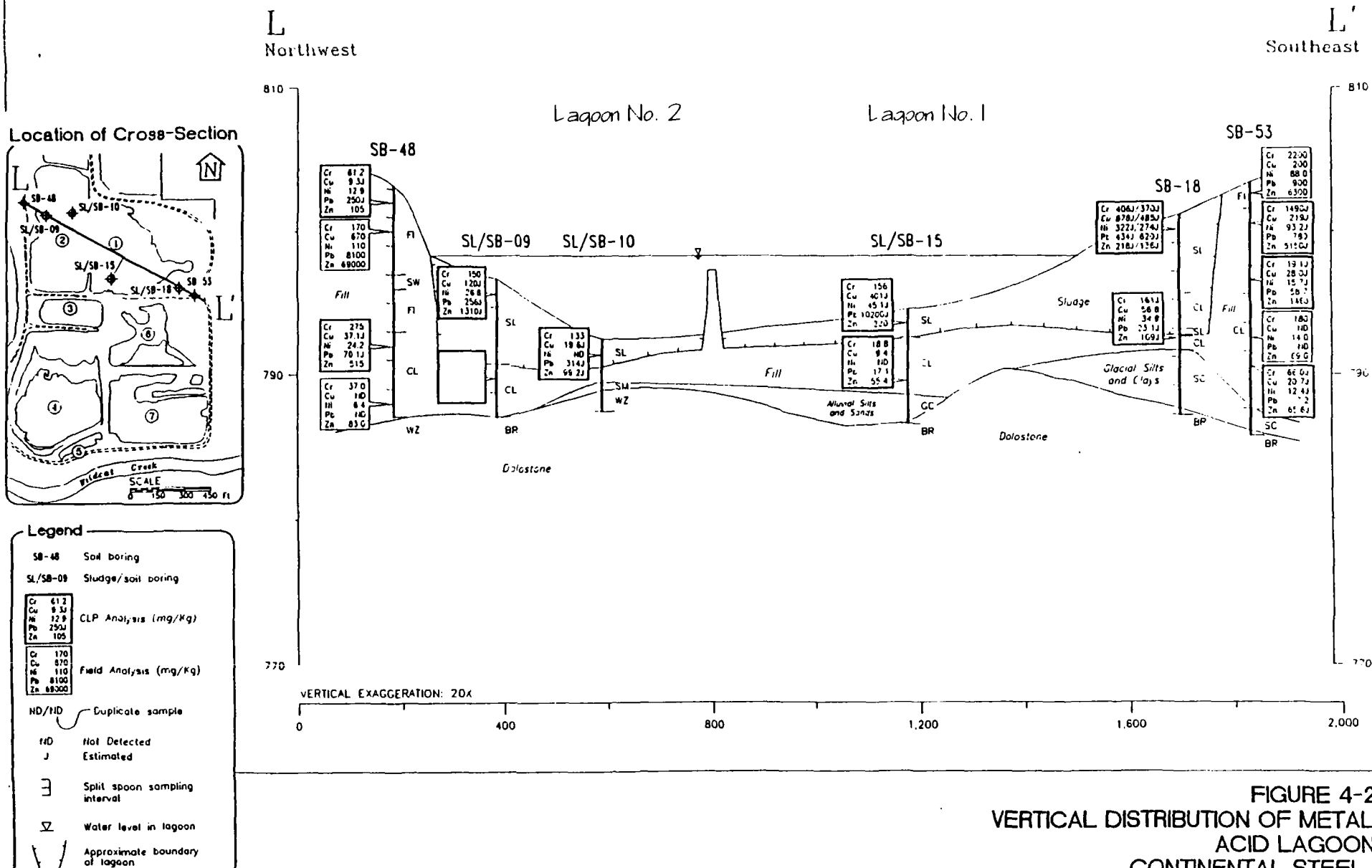


FIGURE 4-22
VERTICAL DISTRIBUTION OF METALS
ACID LAGOONS
CONTINENTAL STEEL RI
KOKOMO, INDIANA

ABB Environmental Services, Inc. -

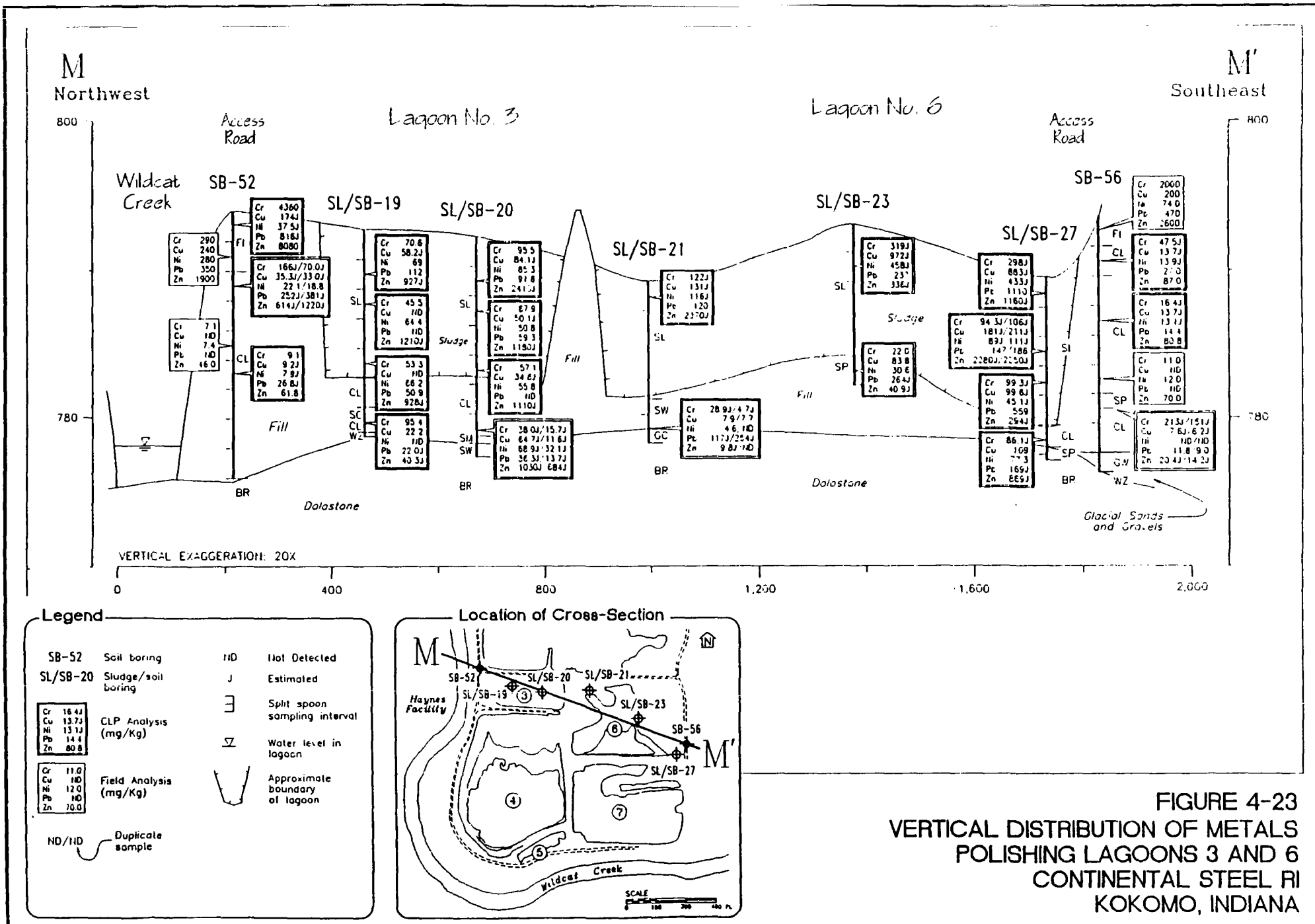


FIGURE 4-23
VERTICAL DISTRIBUTION OF METALS
POLISHING LAGOONS 3 AND 6
CONTINENTAL STEEL RI
KOKOMO, INDIANA

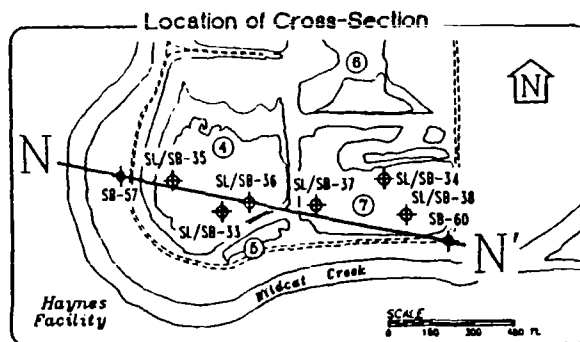
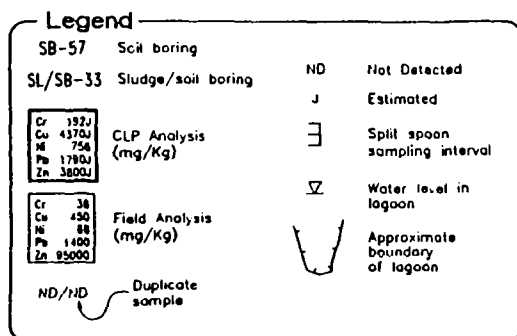
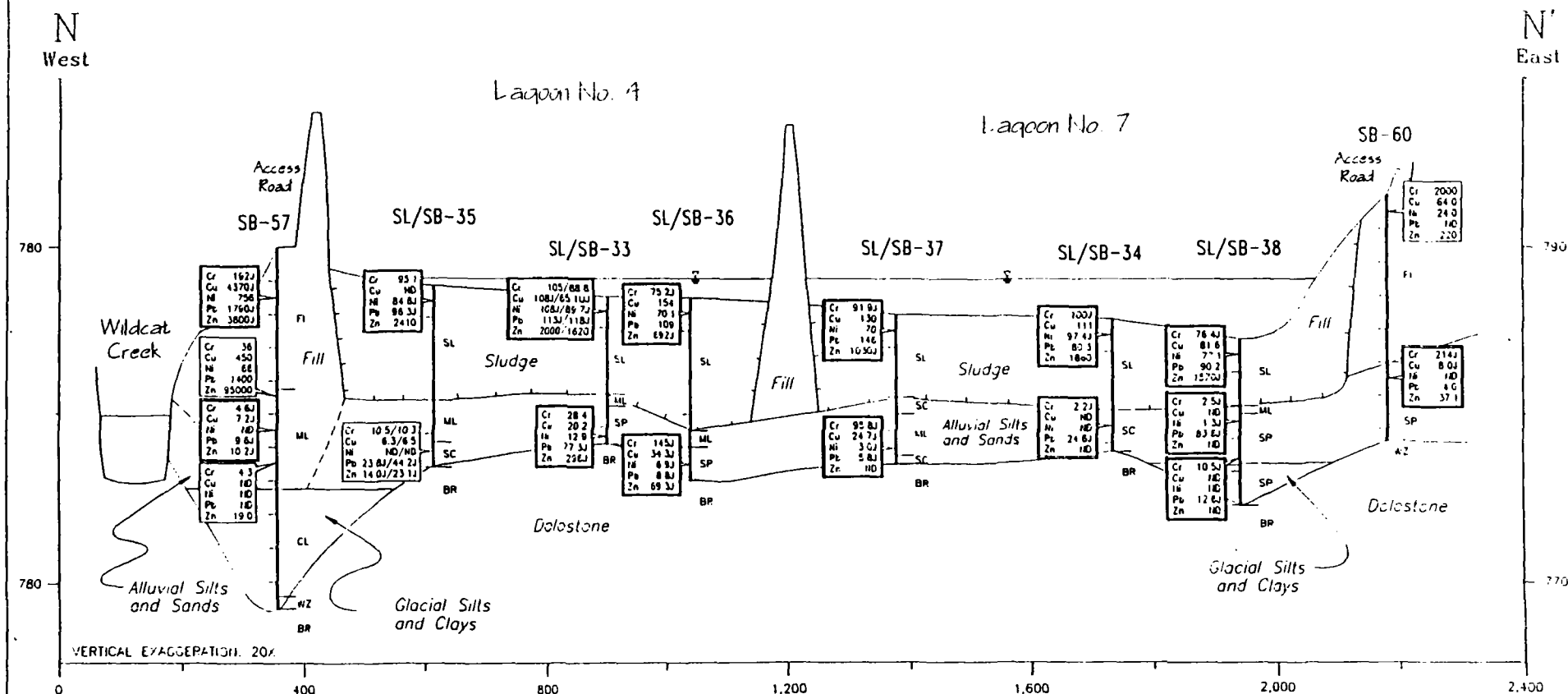
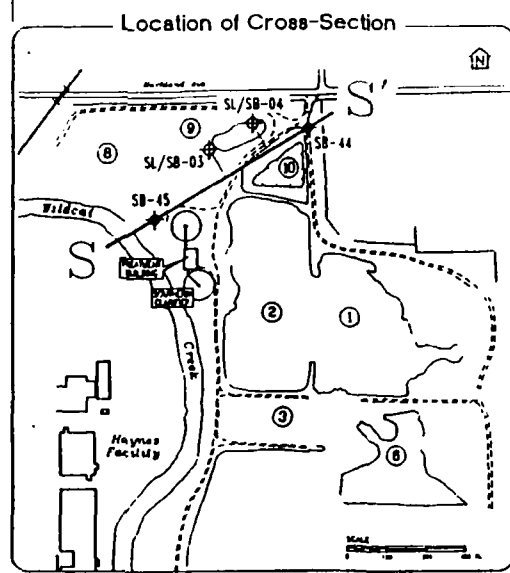


FIGURE 4-24
VERTICAL DISTRIBUTION OF METALS
POLISHING LAGOONS 4 AND 7
CONTINENTAL STEEL RI
KOKOMO, INDIANA



Legend

- SB-44 Soil boring
- SL/SB-45 Sludge/soil boring
- [350] CLP Analysis (ug/Kg)
- 11D/11D Duplicate sample
- 11D Not Detected
- J Estimated
- Approximate location of concentrations greater than 1000 ug/Kg
- [] Split spoon sampling interval
- ▽ Water level in lagoon
- U Approximate boundary of lagoon

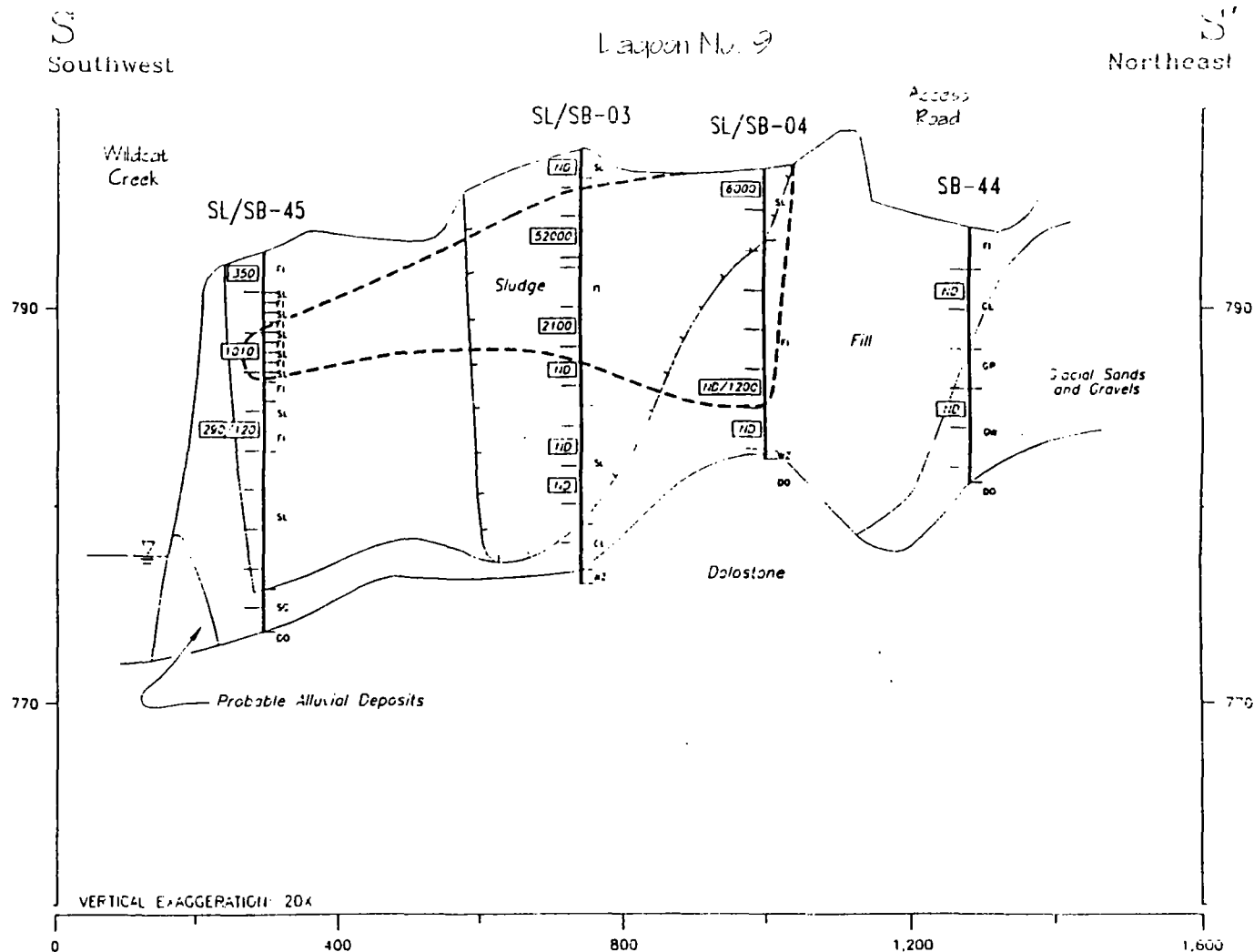


FIGURE 4-20
VERTICAL DISTRIBUTION OF PCBs
LAGOON AREA ENTRANCE
CONTINENTAL STEEL RI
KOKOMO, INDIANA

ABB Environmental Services, Inc.

TABLE 4-18
SUMMARY OF OTHER DETECTED ORGANICS IN LAGOON SLUDGE AND SOILS
(CLP Results in ug/Kg)
CONTINENTAL STEEL RI
Kokomo, Indiana

AREA/MEDIA	FREQUENCY OF DETECTION	MINIMUM DETECTED CONCENTRATION	MAXIMUM DETECTED CONCENTRATION	ARITHMETIC MEAN ¹ OF DETECTS
SLUDGES				
Aldrin	1/77	0.077	0.077	0.077
4,4'-DDD	2/77	0.35	0.41	0.38
4,4'-DDT	2/77	7.8	26	16.9
Dieldrin	4/77	0.73	4.3	2.5
Endosulfan II	3/77	0.65	2.0	1.1
Endosulfan Sulfate	2/77	0.34	0.45	0.40
Endrin	2/77	0.64	0.73	0.69
Endrin Ketone	2/77	1.7	7.0	4.4
Endrin Aldehyde	3/77	1.5	30	12
Heptachlor	1/77	1.6	1.6	1.6
Heptachlor Epoxide	3/77	0.69	1.2	0.92
Methoxychlor	1/77	3.8	3.8	3.8
SOILS				
Alpha-BHC	1/95	0.36	0.36	0.36
Aldrin	3/95	1.0	3.6	2
4,4'-DDD	8/95	0.25	18	3.7
4,4'-DDE	5/95	2.0	240	62
4,4'-DDT	9/95	0.21	42	12
Delta-BHC	1/95	19	19	19
Dieldrin	9/95	0.25	11	3.0
Endosulfan I	4/95	0.064	12	5.2
Endosulfan II	5/95	0.23	6.1	3.5
Endosulfan Sulfate	6/95	0.19	7.6	2.5
Endrin	9/95	0.32	76	15
Endrin Ketone	4/95	0.24	8.6	2.8
Endrin Aldehyde	7/95	1.7	20	9.7
Gamma-BHC (Lindane)	3/95	0.098	0.19	0.14
Gamma-Chlordane	4/95	0.075	61	17
Heptachlor	1/95	42	42	42
Heptachlor Epoxide	7/95	0.13	24	5.4
Methoxychlor	10/95	0.13	57	10

¹ In calculating the mean, duplicate values were averaged and then the average was used in the calculation. Non-detects were not used in the calculation except when averaging duplicate results where one of the two samples is non-detect. In this case, half the undetected value was used.

² In soil borings 03, 05, 06, 18, 22, 45; where there were alternating layers of fill and sludge, the fill was included with the sludge calculation.

³ Soil boring 46 was misidentified as a soil, it is a sludge.

⁴ Where sludge and soil are mixed in a sample, the sample is calculated as a sludge.

TABLE 4-18
SUMMARY OF OTHER DETECTED ORGANICS IN LAGOON SLUDGE AND SOILS
(CLP Results in ug/Kg)
CONTINENTAL STEEL RI
Kokomo, Indiana

AREA/MEDIA	FREQUENCY OF DETECTION	MINIMUM DETECTED CONCENTRATION	MAXIMUM DETECTED CONCENTRATION	ARITHMETIC MEAN ¹ OF DETECTS
SLUDGES				
Bis(2-Ethylhexyl)phthalate	8/77	49	6,000	2,200
Dibenzofuran	3/77	49	11,000	4,000
Pentachlorophenol	1/77	2,000	2,000	2,000
Phenol	1/77	150	150	150
SOILS				
Bis(2-Ethylhexyl)phthalate	19/95	23	580	110
Carbazole	1/95	200	200	200
Dibenzofuran	3/95	22	150	86
Di-n-butylphthalate	3/95	52	110	81
Di-n-octylphthalate	2/95	86	86	86
2-Methylnaphthalene	6/95	35	1,200	390
Phenol	2/95	120	150	135

¹ In calculating the mean, duplicate values were averaged and then the average was used in the calculation. Non-detects were not used in the calculation except when averaging duplicate results where one of the two samples is non-detect. In this case, half the undetected value was used.

² In soil borings 03, 05, 06, 18, 22, 45; where there were alternating layers of fill and sludge, the fill was included with the sludge calculation.

³ Soil boring 46 was misidentified as a soil, it is a sludge.

⁴ Where sludge and soil are mixed in a sample, the sample is calculated as a sludge.

TABLE 4-19
SUMMARY OF DETECTED METALS IN LAGOON SLUDGE AND SOILS
(CLP Results in mg/Kg)
CONTINENTAL STEEL RI
Kokomo, Indiana

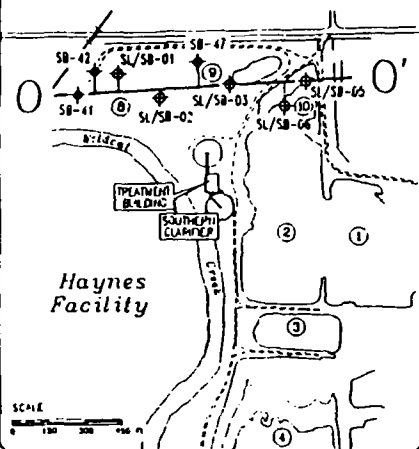
AREA/MEDIA	FREQUENCY OF DETECTION	MINIMUM DETECTED CONCENTRATION	MAXIMUM DETECTED CONCENTRATION	ARITHMETIC MEAN* OF DETECTS
SLUDGE^{2,3}				
Aluminum	67/72	275	22,400	2,040
Antimony	5/72	10.5	30.8	20
Arsenic	30/72	1.20	49.3	9.28
Barium	48/72	2.50	439	76.7
Beryllium	15/72	0.29	1.6	0.80
Cadmium	6/72	0.70	6.6	3.1
Calcium	61/71	1440	200,000	79,700
Chromium	68/72	4.40	4,210	215
Cobalt	58/72	3.50	47.7	11.4
Copper	57/72	4.70	972	161
Iron	67/72	942	374,000	105,000
Lead	64/72	14.1	10,200	710
Magnesium	62/72	204	31,200	4,260
Manganese	68/72	16.0	33,200	1,600
Mercury	12/72	0.18	4.2	0.78
Nickel	62/72	6.10	458	97.5
Potassium	5/72	453	3,170	1,350
Selenium	2/72	0.76	1.3	1.0
Silver	7/72	1.1	31	6.3
Sodium	15/72	109	568	261
Thallium	9/72	0.83	6.4	3.0
Vanadium	47/72	2.80	136	17.1
Zinc	68/72	11.4	3,630	1,160
Cyanide	5/72	1.40	187	48.9
SOIL BENEATH SLUDGE				
Aluminum	33/47	160	13,400	3,770
Antimony	1/47	5.10	5.10	5.10
Arsenic	33/47	0.64	101	11.4
Barium	33/47	6.5	362	83.2
Beryllium	12/47	0.075	0.74	0.35
Cadmium	14/47	1.1	22	6.4
Calcium	33/47	1,130	162,000	31,300
Chromium	33/47	2.20	3580	281
Cobalt	10/47	0.310	19.3	4.53
Copper	26/47	3.50	410	65.6
Iron	33/47	486	230,000	43,300
Lead	33/47	4.70	857	124
Magnesium	31/47	57.2	37,000	3,810
Manganese	29/47	10.3	45,300	2,770
Mercury	18/47	0.070	3.2	0.61
Nickel	24/47	0.72	146	26.4
Potassium	32/47	98.5	1750	619
Selenium	12/47	0.12	1.7	0.60
Silver	7/47	0.48	2.4	1.3
Sodium	27/47	49.1	2,330	490
Thallium	5/47	0.21	0.36	0.28
Vanadium	33/47	1.2	351	33.4
Zinc	25/47	6.18	4,590	419
Cyanide	10/47	0.710	71.2	13.6
SOIL OUTSIDE OF LAGOON AREAS				
Aluminum	43/48	813	24,300	8,690
Antimony	15/48	6.20	470	60.0
Arsenic	43/48	1.20	193	18.3
Barium	43/48	19.3	720	142
Beryllium	28/48	0.27	1.5	0.63
Cadmium	29/48	0.50	470	26.0
Calcium	43/48	891	223,000	59,400
Chromium	43/48	4.60	5,510	625
Cobalt	36/48	1.30	62.4	9.80
Copper	43/48	6.90	4,680	352
Iron	42/47	4750	613,000	79,600
Lead	43/48	4	19,300	829
Magnesium	43/48	290	47,300	10,800
Manganese	42/47	17.5	39,800	6,040
Mercury	10/48	0.065	1.8	0.40
Nickel	37/48	7.8	861	104
Potassium	38/48	129	2,960	936
Selenium	10/48	0.51	1.3	0.79
Silver	14/48	0.52	67	8.3
Sodium	28/48	124	1,120	399
Thallium	4/48	0.79	0.90	0.85
Vanadium	43/48	5.70	381	59.0
Zinc	43/48	10.2	249,000	8,440
Cyanide	4/48	0.67	1.40	0.983

¹ In calculating the mean, duplicate values were averaged and then the average was used in the calculation. Non-detects were not used in the calculation except when averaging a duplicate results where one of the two samples was non-detect. In this case, half the undetected value was used for the non-detect

² Where there were alternating layers of fill and sludge, the fill was included with the sludge calculation.

³ Where sludge and soil are mixed in a sample, the sample was calculated as a sludge.

Location of Cross-Section



Legend

- SB-42 Soil Entry
- SL/SB-01 Sludge/sow boring
- CLP Analysis (mg/kg)
- Field Analysis (mg/kg)
- HD/HD Duplicate sample
- ND Not Detected
- J Estimated
- Split spoon sampling interval
- Water level in lagoon
- Approximate boundary of lagoon

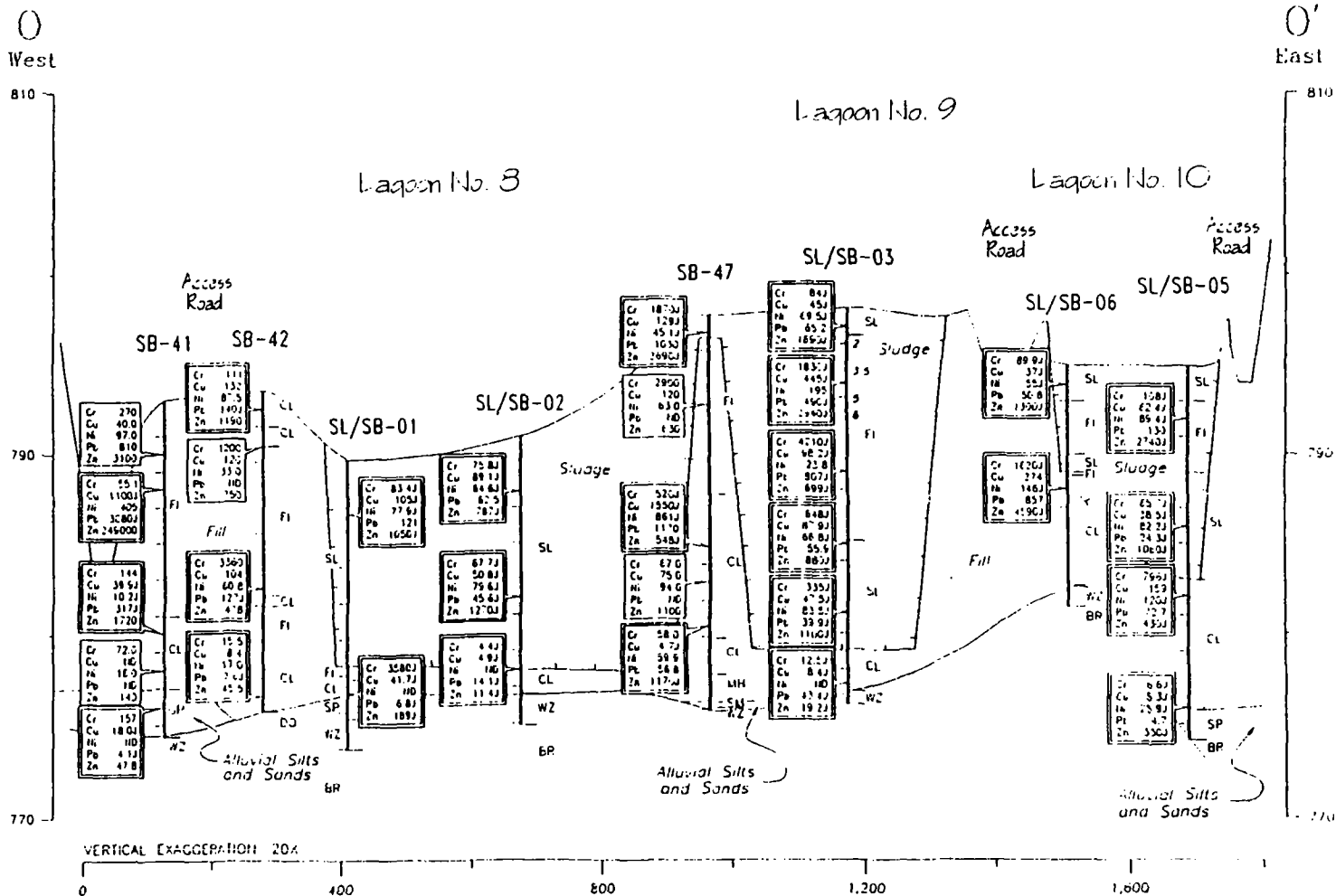


FIGURE 4-21
VERTICAL DISTRIBUTION OF METALS
SLUDGE DRYING BEDS
CONTINENTAL STEEL RI
KOKOMO, INDIANA

ABB Environmental Services, Inc.



An estimate 1,350 buried drums were removed from the southwest side of the Lagoon Area (see Figure 4-7). The drums contained TCE, oil, grease, slag, scale, dirt and garbage. It is interpreted that the drums, along with slag fill, were pushed over the high bank created by the Wildcat Creek floodplain. The processes resulted in the filling of this low lying area.

Results of the laboratory analyses of sludge and soils are described below by chemical group.

4.3.3.1 Volatile Organic Compounds - The distribution of total VOCs in sludge and soils is shown on Figure 4-11. The figure includes both CLP and field laboratory results. Table 4-15 summarizes the individual compounds and their concentration. The table also provides a comparison to maximum background soils concentrations.

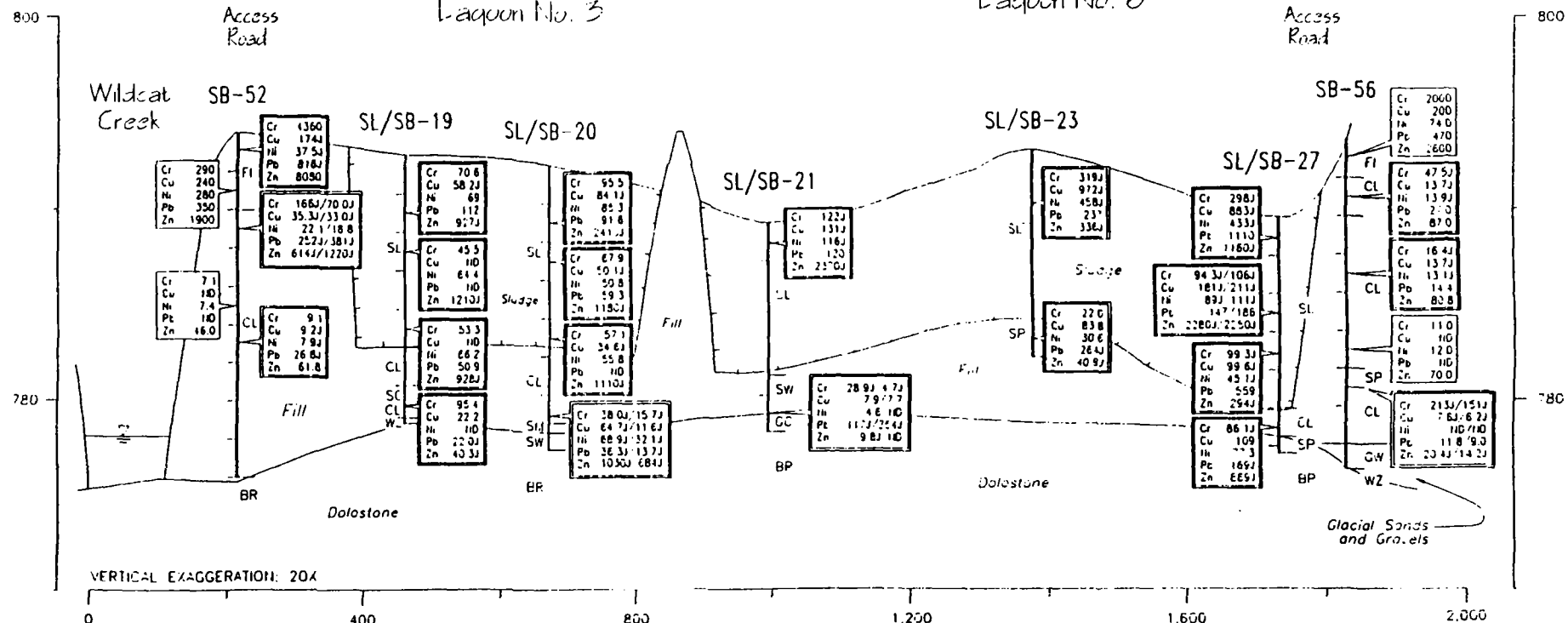
VOCs were detected above the maximum background levels across the entire Lagoon Area. Total VOCs exceeded 500 ug/kg in three main areas. These areas, illustrated by the shading on Figure 4-11, are: (1) the Lagoon Entrance, (2) the Drum Area, and (3) the east-central portion of the lagoons.

Figure 4-12 is a cross-section through the Lagoon Entrance. The figure indicates that total VOCs exceeded 500 ug/kg from just below the ground surface to the top of bedrock. Methylene chloride was detected in two of four CLP sludge samples from this area with a mean concentration of 3,000 ug/kg (see Table 4-15). In the soils below the sludge, acetone, 2-butanone, 1,1-DCE, 1,2-DCE, PCE, and TCE were detected in more than 25 percent of the CLP samples. PCE and TCE had mean concentrations near or greater than 1,000 ug/kg (see Table 4-15).

Figure 4-13 is a cross-section through the Drum Area. VOCs were detected above 500 ug/kg from just below the ground surface to the top of a silty clay (encountered at a depth of approximately 14 feet). Acetone, 2-butanone, 1,2-DCE, toluene, and TCE were detected in more than 25 percent of the CLP soil samples. PCE and TCE had concentrations greater than 1,000 ug/kg (see Table 4-15).

M
Northwest

M'
Southeast



Legend

- SB-52 Soil boring
- SL/SB-20 Sludge/soil boring
- CLP Analysis (mg/Kg)
- Field Analysis (mg/Kg)
- ND/ND Duplicate sample
- ND Not Detected
- J Estimated
- Split spoon sampling interval
- Water level in lagoon
- Approximate boundary of lagoon

Location of Cross-Section

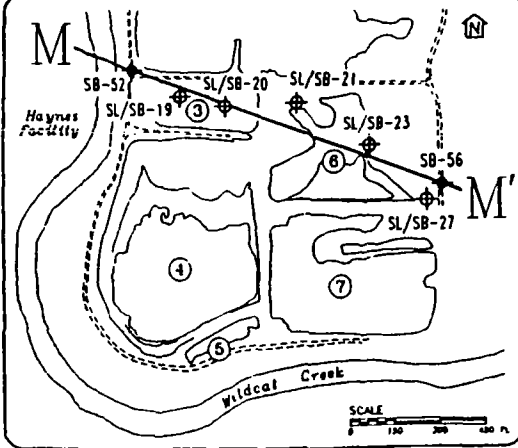


FIGURE 4-23
VERTICAL DISTRIBUTION OF METALS
POLISHING LAGOONS 3 AND 6
CONTINENTAL STEEL RI
KOKOMO, INDIANA

ABB Environmental Services, Inc.

4.3.4 WASTE PILES

As shown on Figure 2-8, waste piles are present throughout the Lagoon Area. The waste piles were inventoried and eight different waste pile types were noted. Table 4-20 provides a summary of the waste pile types and the total estimated volume for each type. The total estimated volume is 349 cubic yards.

A samples was collected from one of each of the waste pile types. Detected constituents are shown on Table 4-21. Constituents detected above the maximum background are indicated with an asterisk. Detected organic compound were below the maximum background in all samples. Chromium, copper, lead, nickel and zinc were detected above the maximum background in four or more of the waste piles.

4.3.5 Treatment Building/Clarifier Tanks

As shown on Figure 2-7, samples of mixing tanks sludge, basement water and clarifier tank sludge were collected from the Treatment Building. The results of these analyses are discussed in this section.

4.3.5.1 Mixing Tank Sludge Samples - Two mixing tanks are located in the Treatment Building. The tanks have diameters of 15 foot 10 inches and heights of 20 feet 3 inches. Each tank is coated with a hardened sludge. The sludge thickness is variable up to 1.5 feet. Organics and inorganics detected during field screening of the mixing tank sludge are shown on Table 4-22. The sludge appears to consist primarily of calcium, iron, and magnesium.

4.3.5.2 Basement Water Samples - Table 4-22 provides a summary of the analytical results for the field screening of water samples collected from the Treatment Building basement. Methylene chloride and 1,1-DCA were detected at low concentrations along with several metals.

TABLE 4-20
LAGOON AREA WASTE PILE DESCRIPTIONS AND VOLUMES
CONTINENTAL STEEL RI/FS
Kokomo, Indiana

WASTE PILE ID	DESCRIPTION	ESTIMATED ¹ VOLUME (cyd)
02WP01	White, brittle, powdery, blocky	110
02WP02	Orange, powdery, loose	9
02WP03	Light grey, powdery, loose (with nails throughout)	12
02WP04	Grey, fine-grained, white mottling	58
02WP05	Black, metallic, fine-grained, powdery	21
02WP06	Orange, soft, fine sludge	2
02WP07	Black, hard, fine-grained, consolidated	100
02WP08	Black, fine-grained, semi-consolidated	6
Two additional piles near the Treatment Building were a mixture of WP-02 and WP-07.		31
TOTAL ESTIMATED VOLUME		349

cyd = cubic yards

max 4-20-21
DETECTED ORGANICS AND INORGANICS IN WASTE PILES
(CLP RESULTS)
CONTINENTAL STEEL RI
Kokomo, Indiana

max 50K

SAMPLE LOCATION:	CRQL	BKG SOIL MAX UTL	WP-01	WP-02	WP-03	WP-04	WP-05	WP-06	WP-07	WP-08
ORGANICS (µg/Kg)										
Acetone	5	<5	-	-	- / -	-	-	-	2 J	-
Anthracene	20	<33	R	-	- / -	3 J	-	-	-	R
bis(2-Ethylhexyl)phthalate	20	<33	R	-	- / -	R	-	3 J	-	R
Chrysene	20	32	R	-	- / -	R	-	-	2 J	R
Pyrene	20	33	R	-	- / -	1 J	-	-	2 J	R
Toluene	2.5	52	-	-	- / -	-	0.5 J	-	-	-
Total Xylenes	2.5	4	-	0.5 J	- / -	-	-	-	-	-
Total TICs for VOCs	-	25	130 J	70 J	110 J / 150 J	120 J	130 J	130 J	560 J	14 J
METALS (mg/Kg)										
Aluminum	80	33300	-	5500 J	4490 J / 4700 J*	1420 J	-	3290 J	1790 J	-
Antimony	20	14	-	-	- / -	-	-	-	-	84.8 *
Arsenic	10	28.2	-	1.8 J	4.5 J / 11.3 J	2.8 J	31.1 *	2.7 J	24.6	17
Barium	80	270	-	146	215 / 226	4.6 J	5.7 J	46.4 J	18.6 J	12.1 J
Beryllium	10	1.5	0.64 J	1.6 J*	1.2 J / -	1.4 J	-	0.96 J	-	-
Cadmium	10	1.3	-	-	4.6 J / 9.3 J*	-	-	-	-	-
Calcium	80	188000	275000 J*	213000 J*	173000 J / 1220	211000 J*	1500 J	167000 J	5780 J	1530 J
Chromium	10	36.4	-	18.2	546 / 537 *	103 *	437 *	340 *	3760 *	165
Cobalt	20	25.3	-	-	10.4 J / 11.6 J	-	35.8 *	13.7 J	132 *	16.7 J
Copper	40	32.9	3.6 J	17.4 J	194 / 228 *	53.8 *	1110 J*	120 *	377 *	1080 *
Iron	20	17900	287	20400	60000 / 63300*	35400	363000	134000 *	324000 *	154000 *
Lead	50	42.9	-	-	803 / 1140*	27.6 J	-	340 *	171 *	2000 *
Magnesium	80	46700	1400	8920	21300 / 18800	96200 *	407	12500	2490	319
Manganese	10	3050	12	142	7530 / 8450*	1240	1840	2600	1910	1350
Mercury	0.3	<0.12	R	R	R / 0.73 J*	R	R	R	R	R
Nickel	20	48.9	-	-	115 J / 130 J*	40.4 J	564 J*	118 J*	7490 J*	309 J*
Thallium	100	<0.70	4 J*	-	- / -	-	-	-	-	-
Vanadium	20	59.2	3.7 J	9 J	32.1 / 32.4	34.7	8.3 J	30.1	15.4 J	8.9 J
Zinc	10	260	15.9	306 J*	13200 J / 25700	352 *	1790 *	3290 *	7850 *	120

NOTES:

B = Compound was found in associated blank

CLP = Contract Laboratory Program

J = Concentration is estimated

MAX = Maximum

mg/Kg = milligrams per kilogram

R = Rejected

TICs = Tentatively Identified Compounds

µg/Kg = Micrograms per kilogram

UTL = Upper tolerance limit (mean plus three times the standard deviation)

- = Not detected

* = Exceeds maximum or UTL

TABLE 4-22
DETECTED ORGANICS AND INORGANICS IN TREATMENT BUILDING SAMPLES
(Field Analytical Results)
CONTINENTAL STEEL RI
Kokomo, Indiana

		BACKGROUND	MIXING TANK SLUDGE SAMPLES		
COMPOUNDS	CROL	MAX/SOIL	SL-61	SL-62	SL-63
ORGANICS (ug/Kg)					
t-1,2-Dichloroethene	-		NA	47 B	-/-
Pyrene	0.45		0.36 J	-	-/0.27 J
Benzo(a)Anthracene	0.45		-	0.14 J	-/-
INORGANICS (mg/Kg)					
Aluminum	-		240	1,800	330/260
Barium	-		4.9	15	6.8/5.6
Calcium	-		140,000 J	170,000 J	160,000 J/160,000 J
Chromium	-		14	28	13/11
Copper	-		-	22	-/25 J
Iron	-		20,000	35,000	19,000/23,000
Magnesium	-		1,300	9,500	1,100/1,100
Manganese	-		160	250	160/190
Nickel	-		18	31	21/25
Potassium	-		180	2,900	210 J/350 J
Sodium	-		930	3,000	1,900/1,800
Zinc	-		450	440	300/320

		BACKGROUND MAX/GROUND- WATER	BASEMENT WATER SAMPLES			
COMPOUND	CROL		WW-01 (0-1 ft)	WW-01 (2-3 ft)	WW-02 (0-1 ft)	WW-03 (0-1 ft)
ORGANICS (ug/L)						
Methylene Chloride	5.0		—	0.35 J	0.33 J/—	0.54 J
1,1-Dichloroethane	5.0		1.8 JF	6.1	0.32 J/0.49 J	—
INORGANICS (mg/L)						
Calcium	0.5		560	380	370/430	580
Chromium	0.02		—	0.05	0.05/0.06	—
Magnesium	0.5		8.3	4.2	3.5/3.6	7.8
Potassium	0.5		89	28	27/29	84
Sodium	1.0		100	29	29/29	94

NOTES:

NA - Not analysed. Sample was sent to field lab for volatiles analyses but the field lab did not analyze the sample.

MAX - Maximum

mg/Kg - Micrograms per kilograms

mg/L - Micrograms per liter

ug/Kg - Millograms per kilograms

ug/L - Millograms per liter

UTL - Upper tolerance limit

TABLE 4-23
DETECTED INORGANICS IN CLARIFIER TANK SLUDGE SAMPLES
(CLP Results in mg/Kg)
CONTINENTAL STEEL RI
Kokomo, Indiana

COMPOUND	CRQL	BACKGROUND MAX SOIL.	SL-64 (2-3 ft)	SL-64 (3-4 ft)	SL-65 (1-2 ft)	SL-65 (2-3 ft)	SL-66 (1-2 ft)	SL-66 (2-3 ft)
Aluminum	80	33,300	1,650 J	846 J	1,220 J/2,560 J	1,230 J	3,130 J	998 J
Barium	80	270	20.1 J	15 J	13.3 J/47.8 J	13.3 J	18.8 J	15.1 J
Beryllium	10	1.5	0.72 J	0.61 J	-/-	-	0.46 J	-
Calcium	80	188,000	65,300 J	74,200 J	45,500 J/85,900 J	46,200 J	101,000 J	55,500 J
Chromium	10	36.4	91.7 *	107 *	136 J/73.9 J *	139 *	48.3 *	153 *
Cobalt	20	25.3	8.8 J	12.3 J	13.1 J/7.4 J	14.3 J	3.6 J	13 J
Copper	40	32.9	94.8 *	83.2 *	146 J/113 J *	147 J *	55.8 J *	97.9 J *
Iron	20	37,900	109,000 J *	123,000 J *	166,000 J/100,000 J *	168,000 *	56,900 *	175,000 *
Lead	50	42.9	101 *	145 *	263 J/125 J *	259 *	35.8 J	173 *
Magnesium	80	46,700	7,300	6,160	5,480 J/12,800 J	5,580	9,850	6,920
Manganese	10	3,050	800 J	1,060 J	1,490 J/726 J	1,510	587	1,640
Nickel	20	48.9	74.2 J *	85.8 J *	131 J/46.1 J *	136 *	29.9	129 *
Sodium	80	<122	640 *	465 *	-/-	-	-	-
Vanadium	20	59.2	12.8 J	12.4 J	17.8 J/18.5 J	17.6 J	6.7 J	15.4 J
Zinc	10	260	2,080 J *	2,860 J *	5,950 J/1,630 J *	6,090 J *	1,230 J *	5,040 J *

NOTES:

CLP - Contract laboratory program

CRQL - Contract required quantitation limits

ft - Feet

MAX - Maximum

mg/Kg - Milligrams per kilograms

** - Exceeds maximum or UTL

4.3.5.3 Clarifier Tank Sludge Samples - Two clarifier tanks are located at the Treatment Building. One tank is located on the north end of the building. This tank is empty. The other tank is located on the south end of the building. This tank contained a 4- to 6-foot thick layer of sludge.

Sludge samples were collected at three locations in the souther clarifier tank. At each location, samples were collected near the middle and bottom of the tank. (see Figure 2-7). Constituents detected within the sludge are summarized on Table 4-23.

4.4 OU3 - Kokomo and Wildcat Creeks

The nature and extent of contamination in creek sediments and surface water are discussed in this section.

4.4.1 Sediments

Creek sediment samples were collected in three rounds of sampling for field analyses and one round of sampling for CLP analyses. Field analytical data from the first two rounds of sampling were used to identify these areas of possible contamination and evaluate the extent of contamination. Samples were then collected from potentially contaminated areas, uncontaminated areas, and background locations for CLP analyses. The CLP data provided an identification and quantification of the compounds within these areas. The results of these analyses are discussed by chemical group in this section.

For each chemical group, analytical results are compared to background sediment quality. Sediment samples SD-01, SD-41, SD-45, SD-46, SD-103, and SD-104 were selected as background sediment sampling locations (see Figure 2-9). Analytical results indicated that background sediment quality in each creek was similar; therefore, the data from each creek were combined into one data set. The background samples consisted of one silty clay, one silt, three well-graded sands, and one well-graded sand and gravel. These sediment types were considered representative of the range in grain sizes observed in the creeks.

3.4.3 Outfalls

Figure 3-4 illustrates outfalls identified during the field work. These include outfalls at the Continental Steel plant, the two Haynes facilities, the Martin Marietta Quarry, and the City of Kokomo Wastewater Treatment Plant. These outfalls are discussed in the following paragraphs. The discussions are based upon a review of each facilities' NPDES permit.

Wastewater from Continental Steel was discharged through five outfalls, designated CS-01 through CS-05 (ISPCB, 1985). Outfall CS-01, which has not been located, was previously the main processing outfall before the installation of the Filter Plant. Upon installation of the plant, this outfall was eliminated. The locations of outfalls CS-02 through CS-05 are shown on Figure 3-4. Discharge at outfall CS-02 included non-contact cooling water from annealing, galvanizing, and wire tinning; some process water from galvanizing; stormwater; and cooling tower water from the Melt Shop. In 1984, a lift station was

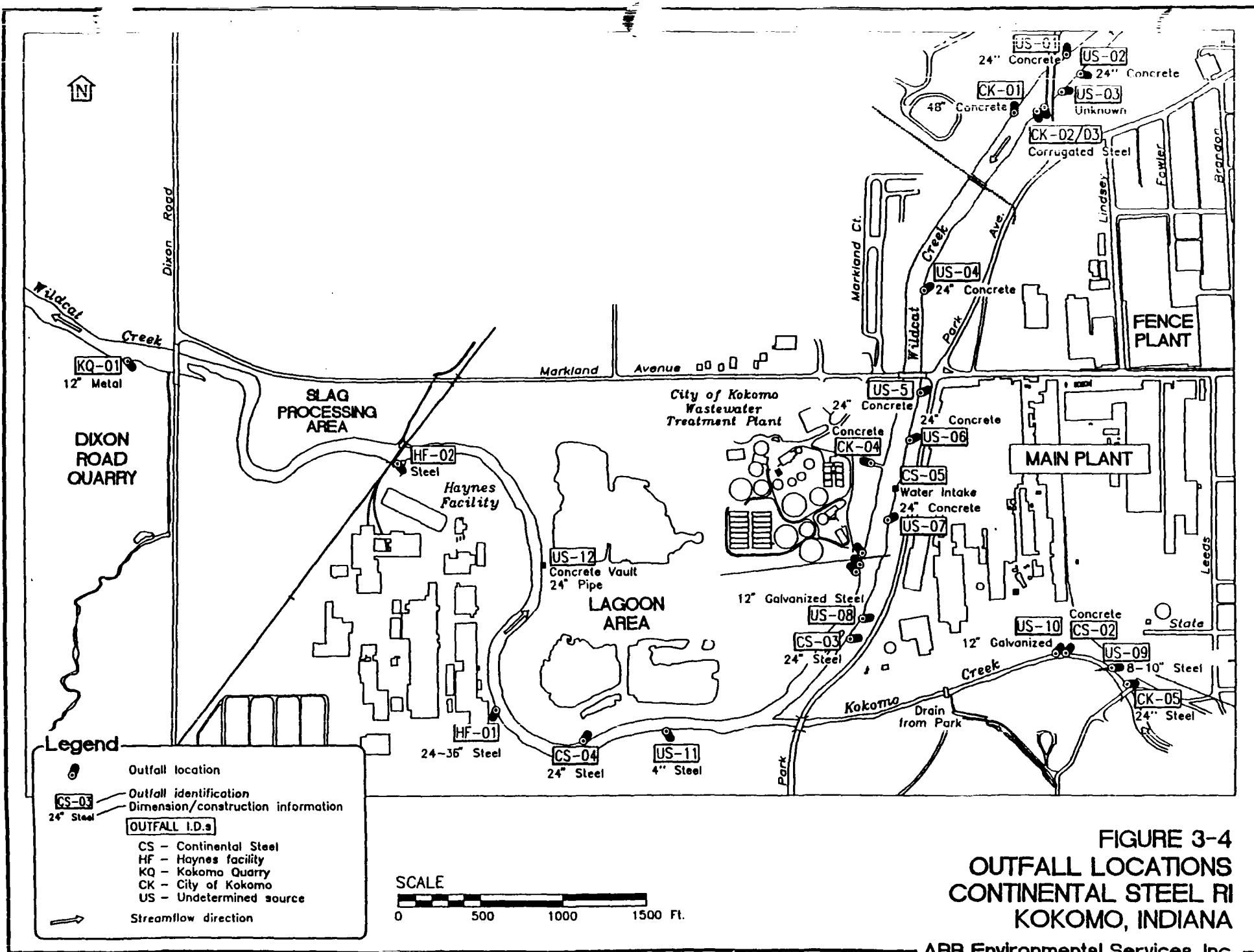


FIGURE 3-4
OUTFALL LOCATIONS
CONTINENTAL STEEL RI
KOKOMO, INDIANA

ABB Environmental Services, Inc.

apparently installed which pumped the wastewater from this line to the Filter Plant. Outfall CS-02 then discharged to Kokomo Creek only during times when excessive quantities of stormwater caused an overflow. Outfall CS-03 was an emergency overflow for untreated wastewater. Outfall CS-04 discharged wastewater from the Lagoon Area. Acid-pickling wastewater was transferred to the Lagoon Area where these wastewaters were neutralized, run through clarifiers and polishing lagoons, and then discharged. Structure CS-05 served as both an outfall and a water intake. As an outfall, it was the discharge point for filtered, non-contact cooling waters and process waters from rolling, drawing, and annealing operations. As an intake, water was withdrawn daily from Wildcat Creek.

Wastewater from the Haynes facilities are discharged through six outfalls (IDEM, 1990). Stormwater that does not contact plant processes is discharged through four outfalls. Stormwater and non-contact cooling water is discharged through outfall HF-01 (shown on Figure 3-4). Outfall HF-02 is the discharge point for the facilities' landfill stormwater retention pond which discharges 0.4 million gallons per day once or twice per year.

Martin Marietta Quarry has three outfalls for the discharge of water generated during pit dewatering (Stanifer, M.W., 1985). Discharge occurs irregularly at quantities as high as much as 5 million gallons per day. The water is not treated before discharge. One of these outfalls was identified during the field work and is shown on Figure 3-4 as KQ-01.

Treated domestic and industrial wastewater from the City of Kokomo's 30 million-gallon-per-day wastewater treatment plant is discharged to Wildcat Creek through a single outfall. The outfall is designated CK-04 and its location is shown on Figure 3-4 (IDEM, 1988). Various combined sewer overflow, bypass, and storm-water discharge points constructed by the city are located along much of the study area.



9406014.WP/TN039
6802-08

June 8, 1994

Mr. Art Garceau
IDEM-OER, Superfund Section
100 N. Senate Avenue
P.O. Box 6015
Indianapolis, IN 46206-6015

Subject: OU1/Task 3M, Aquifer Testing

Dear Mr. Garceau:

Enclosed are memoranda on the in-situ hydraulic conductivity (slug) testing and the stepped-discharge and constant-discharge aquifer pumping tests conducted as part of OU1/Task 3M, Aquifer Testing. These memoranda have been revised to reflect the agency comments provided in the May 4, 1994 letter from Indiana Department of Environmental Management. As you may recall, ABB Environmental Services, Inc. received a letter from you dated May 20, 1994 requesting that these documents be resubmitted.

Please call Don Walsh at (317) 871-8074 if you have any questions as you review the memoranda.

Respectfully,

ABB ENVIRONMENTAL SERVICES, INC.

A handwritten signature in black ink that reads 'Brenda K. Lonowski'. The signature is written in a cursive, flowing style.

Brenda K. Lonowski
Project Assistant

enclosures

cc: Don Walsh, ABB-ES Site Manager
Kim Kesler-Arnold, ABB-ES Program Manager

ABB Environmental Services, Inc.



MLMS Zones

The zones tested are as follows:

<u>MLMS. NO.</u>	<u>MONITORING ZONE DEPTH (feet)</u>	<u>MONITORING ZONE ELEVATION (feet Mean Sea Level)</u>
LA-02	45 - 57	743 - 755
LA-02	60 - 72	728 - 740
LA-02	112 - 132	668 - 688
LA-03	27 - 39	752 - 764
LA-03	42 - 54	737 - 7493
LA-03	107 - 130	661 - 684
LA-05	110 - 131	662 - 683

Conductivity testing in the MLMS zones was performed using Westbay equipment. Prior to conducting the test, a pressure profile was obtained from the zone to be tested. This involved installing the pressure probe to the desired depth, and obtaining pressure readings inside and outside the casing to determine the head differential. A head differential of 3 feet or greater was considered adequate for testing. The pressure probe was then removed from the MLMS and the open/close tool installed to the desired pumping port depth. The pressure probe was then reinstalled above the tested port. The pumping port was then opened using the open/close tool and the water level was continuously recorded using a field computer in communication with the pressure probe. The opening of the pumping port acted as a "slug", with the pressure equilibrating between the inside and the outside of the casing according to the initial head differential. In all but two of the tests, the pressure was greater inside the casing than outside, resulting in a falling-head test. At LA-02 (60 to 72 feet) and LA-05 (110 to 131 feet), rising-head tests were performed since the pressure was lower inside the casing than outside. The water level data were recorded until pressure equilibration.

ANALYSIS

Existing and Shallow Monitoring Wells

The resulting time-recovery data were analyzed using conventional variable-head (e.g., slug) test methods based upon Hvorslev's methodology and described in Cedergren, 1977. These methods of analysis account for differences in well-construction features, aquifer characteristics (i.e., unconfined versus confined), and assume that the aquifer near the screen is homogeneous and isotropic. The influence of the filter pack zone on the cross-sectional area was considered in the equations when the well screen straddled the water table.

Test results were plotted on a semi-logarithmic graph (with drawdown on the log scale) and a "best fit" straight line was generated by computer through the data points (see Attachment A). Two points were chosen from the straight line, and the values of time and drawdown at these points were entered into the appropriate equation. At a number of locations, especially in those wells screened across



the water table, a double straight line effect was observed. The later data were used in the equation when this was observed (Bouwer, 1989). It is believed that the first straight line reflects the influence of the draining sand pack around the well screen.

Selected test results were also analyzed using Bouwer and Rice, 1976, for comparative purposes. This method can be used for completely or partially penetrating wells in unconfined or confined aquifers. The solution is based on the assumption that the aquifer is homogeneous and isotropic. The influence of the filter pack zone on the cross-sectional area was considered in the equations when the well screen straddled the water table.

The Bouwer and Rice method was applied through the computer code AQTESOLV™. Test results for UA-05, UA-16, and UA-18 were plotted on a semi-logarithmic graph (with drawdown on the log scale) and a "best fit" straight line was generated by computer through the data points (see Attachment B). The "best fit" line was adjusted as necessary for a better fit and a hydraulic conductivity value was obtained. The later data were used in the equation when the double straight line effect was observed.

MLMS Zones

All of the MLMS hydraulic conductivity tests were analyzed using the method presented by Cooper et al., 1967. Cooper et al. assumes that the well is fully penetrating and that the aquifer is confined. The data for the shallow bedrock zones was also analyzed according to Bouwer and Rice for comparative purposes. Both methods were applied through the computer code AQTESOLV™.

For the Cooper analysis, the time-recovery data were plotted on a semi-logarithmic graph (with time on the logarithmic scale) and a type curve was generated by computer through the data points (see Attachment C). The type curve was adjusted as necessary for a better fit, and a transmissivity value obtained from the type curve match. The Bouwer and Rice analysis was performed as described above.

TEST RESULTS

The results of the in-situ hydraulic conductivity tests performed are intended to represent the bulk hydraulic conductivity of the bedrock. The hydraulic conductivity, and the resulting groundwater flow velocity, of an individual fracture may be significantly higher than the value obtained for the overall section of rock tested.

Existing and Shallow Monitoring Wells

The hydraulic conductivity values obtained from the time-recovery analyses are listed on Table 1. The calculated hydraulic conductivity values varied greatly within the upper bedrock aquifer across the site. Values ranged from 1.7×10^{-2} cm/sec at UA-16 to 2.0×10^{-5} at UA-18. The results between multiple tests at UA-5 and UA-14 were consistent, indicating that the testing procedure did not significantly affect the test results. As shown in Table 1, the monitoring well screens straddle soil and bedrock units with varying permeabilities. Therefore, the permeability results may represent a combination of these hydraulic conductivities or may almost totally represent the hydraulic conductivity of the more permeable unit depending on their relative values. The data obtained during these tests are thought to represent the general variability of hydraulic conductivity across the site.



TABLE 1
HYDRAULIC CONDUCTIVITY RESULTS

LOCATION	ZONE/SCREEN DEPTH (ft)	ZONE/SCREEN ELEVATION (ft MSL)	FORMATION TESTED	HYDRAULIC CONDUCTIVITY		ANALYTICAL METHOD
				(ft/day)	(cm/sec)	
EW-03	16 - 26	777 - 767 ¹	KL	1.8	6.4X10 ⁻⁴	HVORSLEV
EW-10	18 - 20	772 - 774	KL	3.7	1.3X10 ⁻³	HVORSLEV
UA-05	4 - 19	782 - 797	F/KL	2.8 3.1 3.4 2.6	1.0X10 ⁻³ 1.1X10 ⁻³ 1.2X10 ⁻³ 9.3X10 ⁻⁴	HVORSLEV HVORSLEV HVORSLEV BOUWER/RICE
UA-07	6 - 16	783 - 793	F/KL	7.1X10 ⁻²	2.5X10 ⁻⁵	HVORSLEV
UA-12	34 - 44	748 - 758	GT/KL/LCUA	5.7	2.0X10 ⁻³	HVORSLEV
UA-14	31 - 41	757 - 767	KL	1.2 9.3X10 ⁻¹ 1.0	4.2X10 ⁻⁴ 3.3X10 ⁻⁴ 3.6X10 ⁻⁴	HVORSLEV HVORSLEV HVORSLEV
UA-16	22 - 32	763 - 773	MA/KL	48 42	1.7X10 ⁻² 1.5X10 ⁻²	HVORSLEV BOUWER/RICE
UA-18	34 - 54	738 - 758	KL	5.9X10 ⁻² 5.7X10 ⁻²	2.1X10 ⁻⁵ 2.0X10 ⁻⁵	HVORSLEV BOUWER/RICE
LA-02	45 - 57	743 - 755	KL/LCUA	1.6 2.3	5.5X10 ⁻⁴ 8.0X10 ⁻⁴	COOPER ET AL BOUWER/RICE
LA-02	60 - 72	728 - 740	LCUA	1.2X10 ⁻¹	4.4X10 ⁻⁵	COOPER ET AL
LA-02	112 - 132	668 - 688	LCUB/MF	1.5	5.2X10 ⁻⁴	COOPER ET AL
LA-03	27 - 39	752 - 764	KL/LCUA	5.9 8.2	2.1X10 ⁻³ 2.9X10 ⁻³	COOPER ET AL BOUWER/RICE
LA-03	42 - 54	737 - 749	LCUA	3.2 4.0	1.1X10 ⁻³ 1.4X10 ⁻³	COOPER ET AL BOUWER/RICE

Notes:

¹Approximated from soil boring record

ft = Feet

ft/day = Feet per day

cm/sec = Centimeters per second

F = Fill

GT = Glacial Till

KL = Kokomo Limestone

LCUA = Liston Creek Unit A

LCUB = Liston Creek Unit B

MA = Martinsville Alluvium

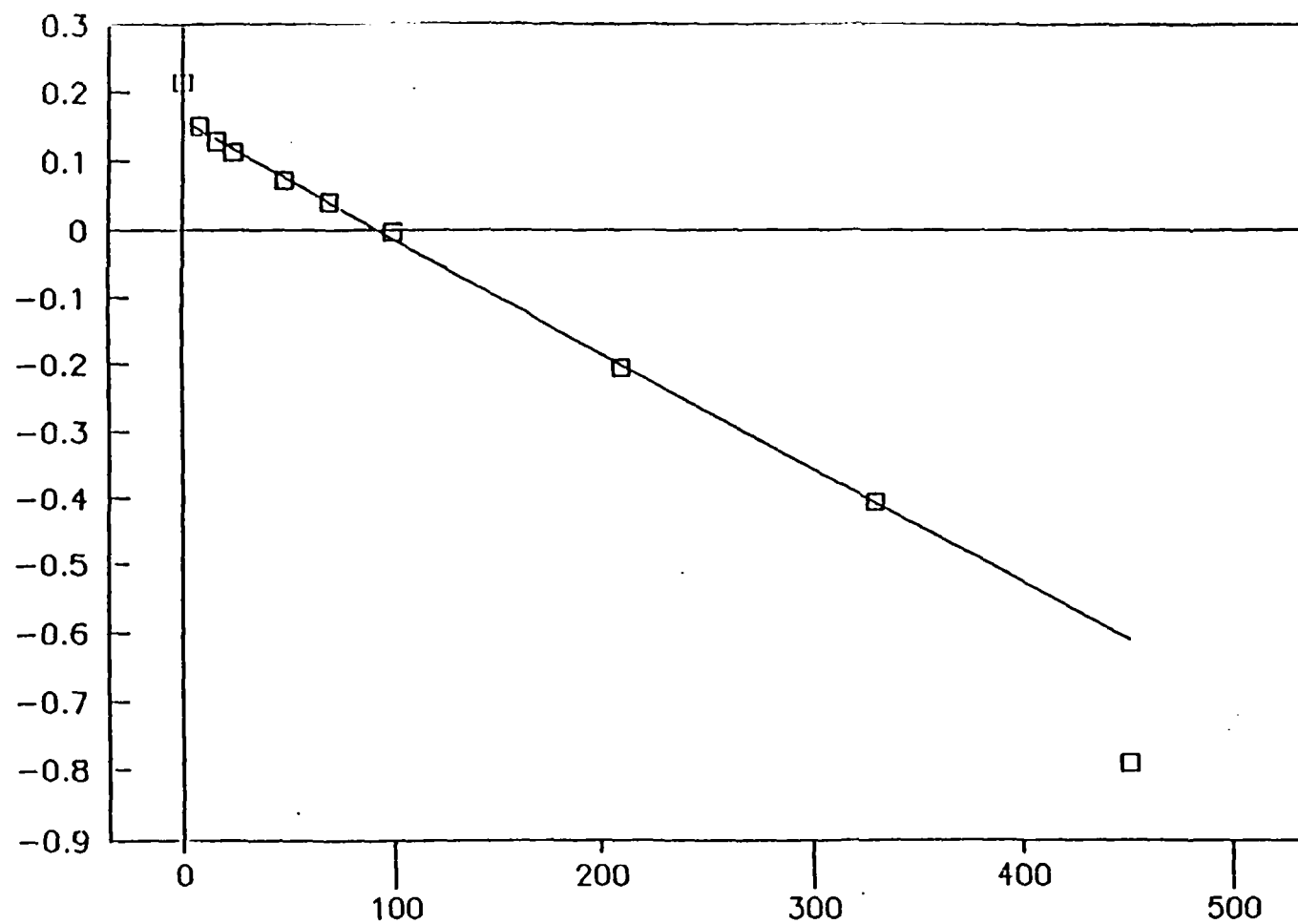
MSL = Mean sea level

MF = Mississinewa Formation

ATTACHMENT A
EXISTING AND SHALLOW MONITORING WELLS
HVORSLEV RESULTS

TIME VS. LOG DRAWDOWN

EW-03 TEST 1



TIME (SECONDS)

□ DRAWDOWN DATA

— BEST FIT LINE

WELL NO: EW-03
 TEST NO: 1
 TEST DATE: 6-30-93

JOB NO: 6802-02
 JOB NAME: CONTINENTAL STEEL
 DATE: 1-18-94

RESULTS OF IN-SITU HYDRAULIC CONDUCTIVITY TEST

COMMENTS: BAIL TEST

TIME (seconds)	Ho	ht	DRAWDOWN (feet)	LOG drawdown
0	76.2	62.0	1.64	0.21449415
8	76.2	64.0	1.41	0.14856564
16	76.2	64.6	1.34	0.12666380
24	76.2	65.0	1.29	0.11142383
48	76.2	66.0	1.18	0.07080598
70	76.2	66.7	1.10	0.03992941
100	76.2	67.6	0.99	-0.00329574
210	76.2	70.8	0.62	-0.20540043
330	76.2	72.8	0.39	-0.40631527
450	76.2	74.8	0.16	-0.79166616

COORDINATES OF BEST FIT LINE (Y=A+BX)

Regression Output		X COORD	Y COORD
Constant	0.157459554	0	0.15745955
Std Err of Y Est	0.005836927	8	0.14378909
R Squared	0.999221860	16	0.13011863
No. of Observations	8	24	0.11644816
Degrees of Freedom	6	48	0.07543677
		70	0.03784300
X Coefficient(s)	-0.001708	100	-0.01342124
Std Err of Coef.	0.0000194	210	-0.20139012
		330	-0.40644707
		450	-0.61150403

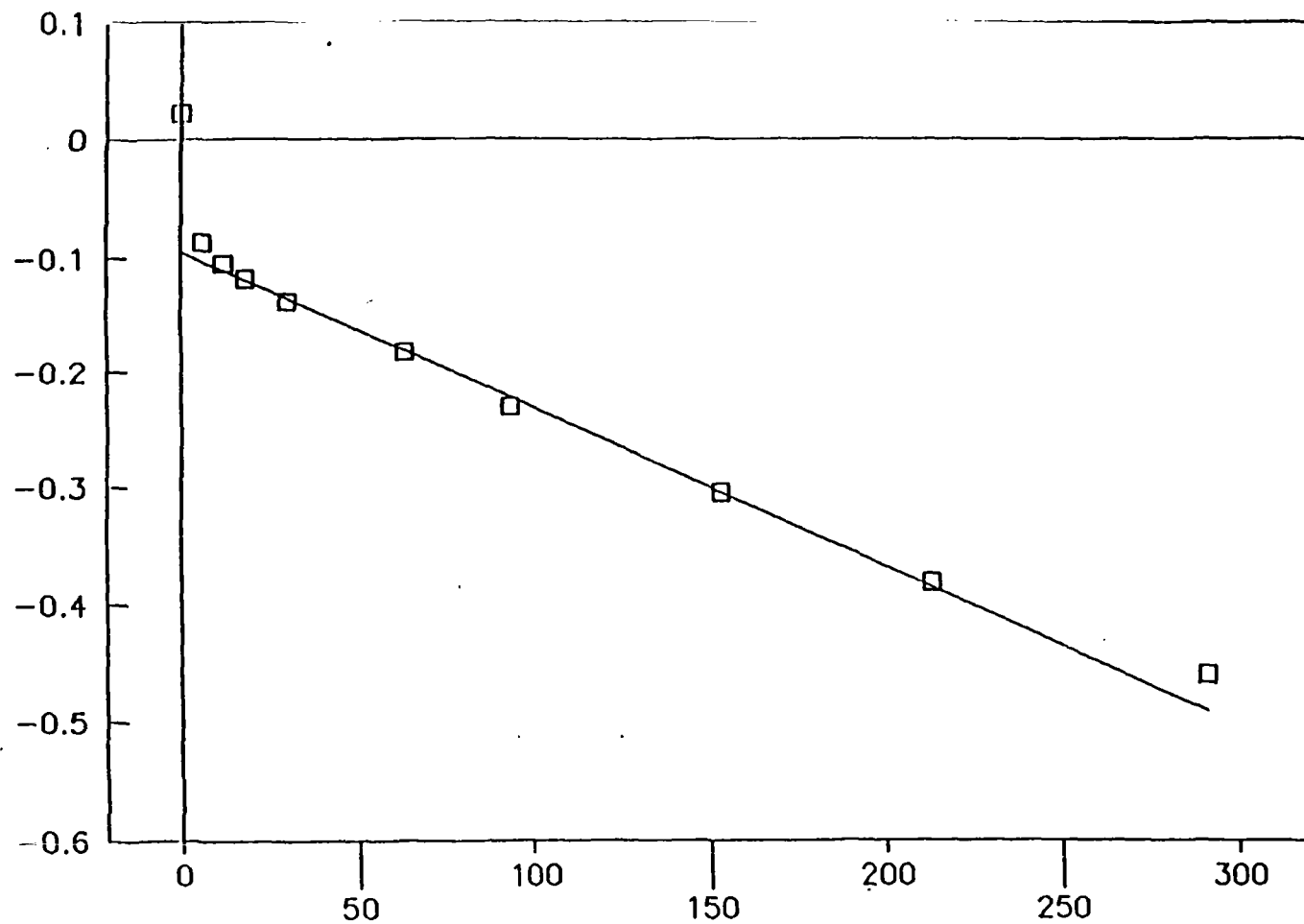
SCREEN LENGTH (L) = 120.00 INCHES
 CASING RADIUS (r) = 2.00 INCH
 BOREHOLE RAD. (R) = 2.50 INCHES
 H1 = 1.19 FEET
 T1 = 48.00 SECONDS
 H2 = 1.09 FEET
 T2 = 70.00 SECONDS

$$\text{HYDRAULIC CONDUCTIVITY} = \frac{(r^2) \ln(L/R) \ln(H1/H2) * 2.54}{2L(T2-T1)} \text{---[CEDERGREN, 1977]}$$

HYDRAULIC CONDUCTIVITY = 6.4E-04 CM/SEC

TIME VS. LOG DRAWDOWN

EW-10 TEST 1



TIME (SECONDS)

□ DRAWDOWN DATA

— BEST FIT LINE

WELL NO: EW-10
 TEST NO: 1
 TEST DATE: 6-30-93

JOB NO: 6802-02
 JOB NAME: CONTINENTAL STEEL
 DATE: 1-18-94

RESULTS OF IN-SITU HYDRAULIC CONDUCTIVITY TEST

COMMENTS: BAIL TEST

TIME (seconds)	Ho	ht	DRAWDOWN (feet)	LOG drawdown
0	75.1	66.0	1.05	0.02124720
6	75.1	68.0	0.82	-0.08653584
12	75.1	68.3	0.78	-0.10528528
18	75.1	68.5	0.76	-0.11825026
30	75.1	68.8	0.73	-0.13845364
63	75.1	69.4	0.66	-0.18191934
93	75.1	70.0	0.59	-0.23022402
153	75.1	70.8	0.50	-0.30432574
213	75.1	71.5	0.42	-0.38149169
291	75.1	72.1	0.35	-0.46067294

COORDINATES OF BEST FIT LINE (Y=A+BX)

Regression Output:		X COORD	Y COORD
Constant	-0.09524173	0	-0.09524174
Std Err of Y Est	0.005151616	6	-0.10341965
R Squared	0.997926367	12	-0.11159757
No. of Observations	7	18	-0.11977548
Degrees of Freedom	5	30	-0.13613131
		63	-0.18110985
X Coefficient(s)	-0.001362	93	-0.22199943
Std Err of Coef.	0.0000277	153	-0.30377858
		213	-0.38555774
		291	-0.49187064

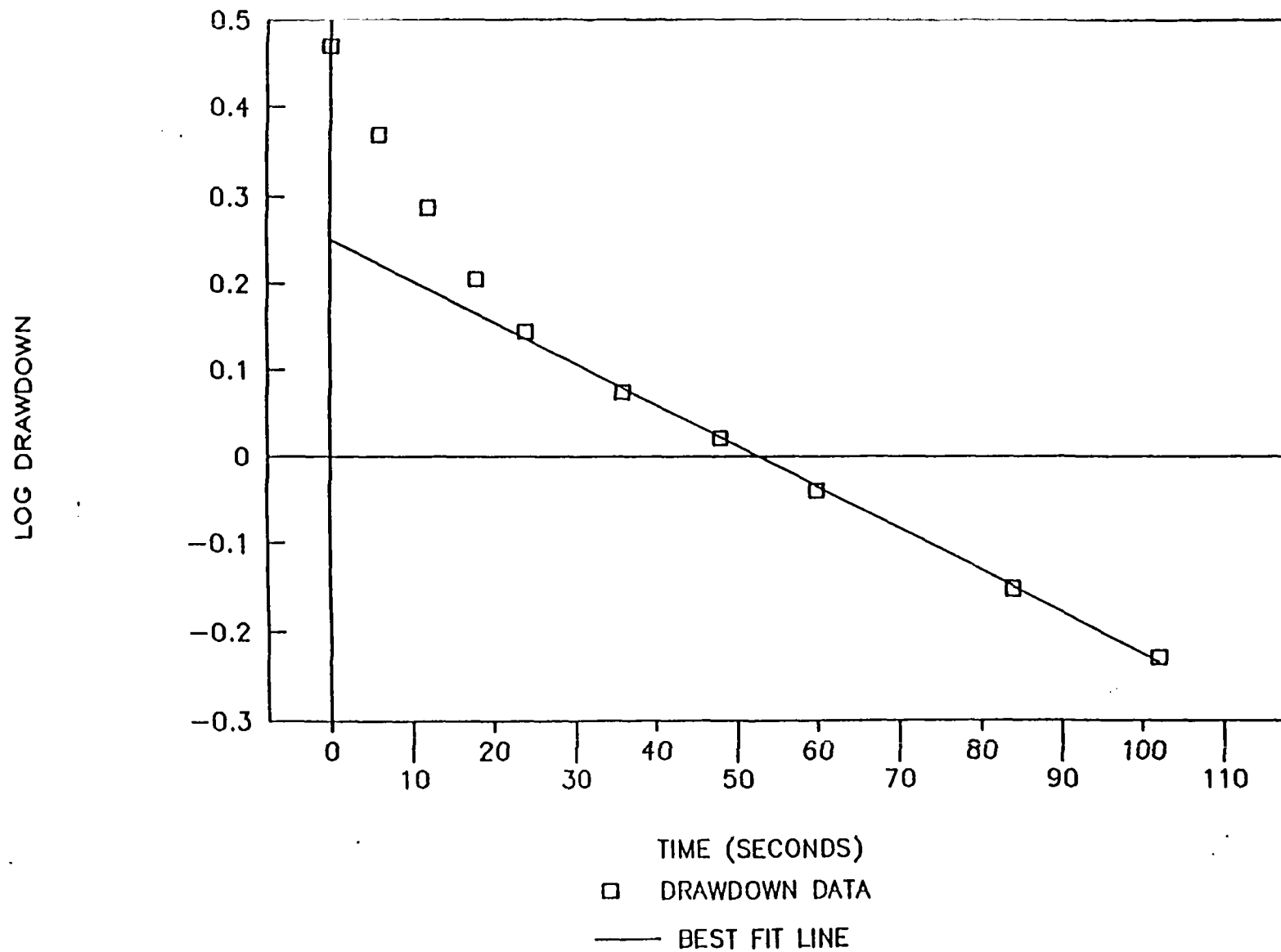
SCREEN LENGTH (L) = 24.00 INCHES
 CASING RADIUS (r) = 2.00 INCH
 BOREHOLE RAD. (R) = 3.50 INCHES
 H1 = 0.73 FEET
 T1 = 30.00 SECONDS
 H2 = 0.66 FEET
 T2 = 63.00 SECONDS

$$\text{HYDRAULIC CONDUCTIVITY} = \frac{(r^2) \ln(L/R) \ln(H1/H2) * 2.54}{2L(T2-T1)} \text{---[CEDERGREN, 1977]}$$

HYDRAULIC CONDUCTIVITY = 1.3E-03 CM/SEC

TIME VS. LOG DRAWDOWN

UA-05 TEST 1



WELL NO: UA-05
 TEST NO: 1
 TEST DATE: 6-29-93

JOB NO: 6802-02
 JOB NAME: CONTINENTAL STEEL
 DATE: 1-18-94

RESULTS OF IN-SITU HYDRAULIC CONDUCTIVITY TEST

COMMENTS: BAIL TEST

TIME (seconds)	Ho	ht	DRAWDOWN (feet)	LOG drawdown
0	71.1	45.5	2.95	0.47044577
6	71.1	50.9	2.33	0.36755718
12	71.1	54.3	1.94	0.28751509
18	71.1	57.2	1.60	0.20522061
24	71.1	59.0	1.40	0.14499118
36	71.1	60.8	1.19	0.07504303
48	71.1	62.0	1.05	0.02124720
60	71.1	63.2	0.91	-0.04016710
84	71.1	65.0	0.70	-0.15246436
102	71.1	66.0	0.59	-0.23022402

COORDINATES OF BEST FIT LINE (Y=A+BX)

Regression Output		X COORD	Y COORD
Constant	0.251660122	0	0.25166012
Std Err of Y Est	0.006135022	6	0.22299004
R Squared	0.998486474	12	0.19431996
No. of Observations	6	18	0.16564988
Degrees of Freedom	4	24	0.13697980
		36	0.07963964
X Coefficient(s)	-0.004778	48	0.02229947
Std Err of Coef.	0.0000930	60	-0.03504069
		84	-0.14972101
		102	-0.23573126

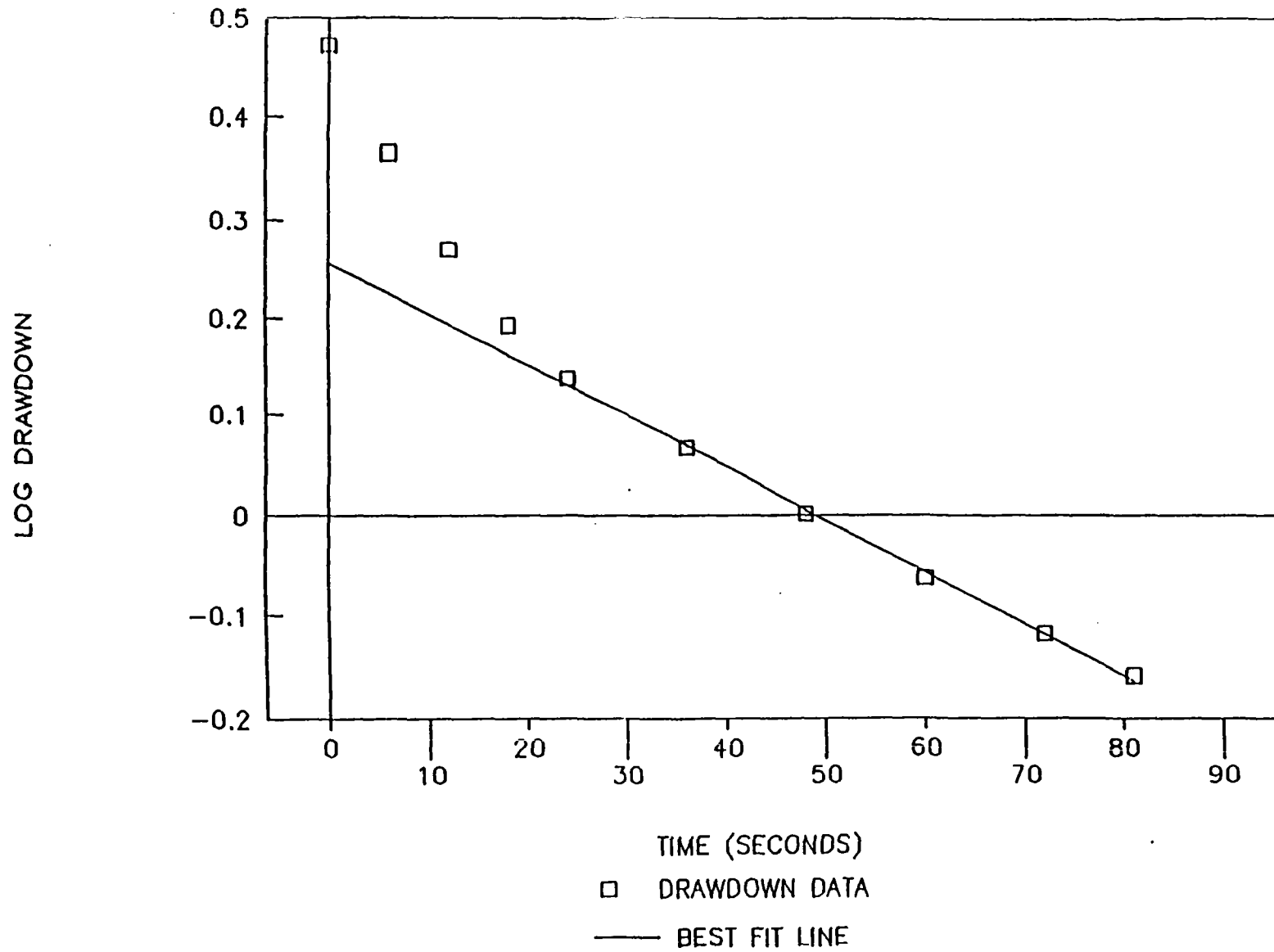
SCREEN LENGTH (L) = 99.24 INCHES
 CASING RADIUS (r) = 1.38 INCH
 BOREHOLE RAD. (R) = 2.00 INCHES
 H1 = 1.37 FEET
 T1 = 24.00 SECONDS
 H2 = 1.20 FEET
 T2 = 36.00 SECONDS

$$\text{HYDRAULIC CONDUCTIVITY} = \frac{(r^2) \ln(L/R) \ln(H1/H2) * 2.54}{2L(T2-T1)} \text{---[CEDERGREN, 1977]}$$

HYDRAULIC CONDUCTIVITY = 1.0E-03 CM/SEC

TIME VS. LOG DRAWDOWN

UA-05 TEST 2



WELL NO: UA-05
 TEST NO: 2
 TEST DATE: 6-29-93

JOB NO: 6802-02
 JOB NAME: CONTINENTAL STEEL
 DATE: 1-18-94

RESULTS OF IN-SITU HYDRAULIC CONDUCTIVITY TEST

COMMENTS: BAIL TEST

TIME (seconds)	Ho	ht	DRAWDOWN (feet)	LOG drawdown
0	71.1	45.4	2.97	0.47213893
6	71.1	51.0	2.32	0.36540187
12	71.1	55.0	1.86	0.26903168
18	71.1	57.6	1.56	0.19253958
24	71.1	59.2	1.37	0.13775277
36	71.1	61.0	1.17	0.06652718
48	71.1	62.4	1.00	0.00172506
60	71.1	63.6	0.87	-0.06273293
72	71.1	64.5	0.76	-0.11825026
81	71.1	65.1	0.69	-0.15964294

COORDINATES OF BEST FIT LINE (Y=A+BX)

Regression Output:		X COORD	Y COORD
Constant	0.256127675	0	0.25612768
Std Err of Y Est	0.006036340	6	0.22488679
R Squared	0.997715115	12	0.19364591
No. of Observations	6	18	0.16240503
Degrees of Freedom	4	24	0.13116415
		36	0.06868239
X Coefficient(s)	-0.005206	48	0.00620062
Std Err of Coef.	0.0001245	60	-0.05628114
		72	-0.11876290
		81	-0.16562423

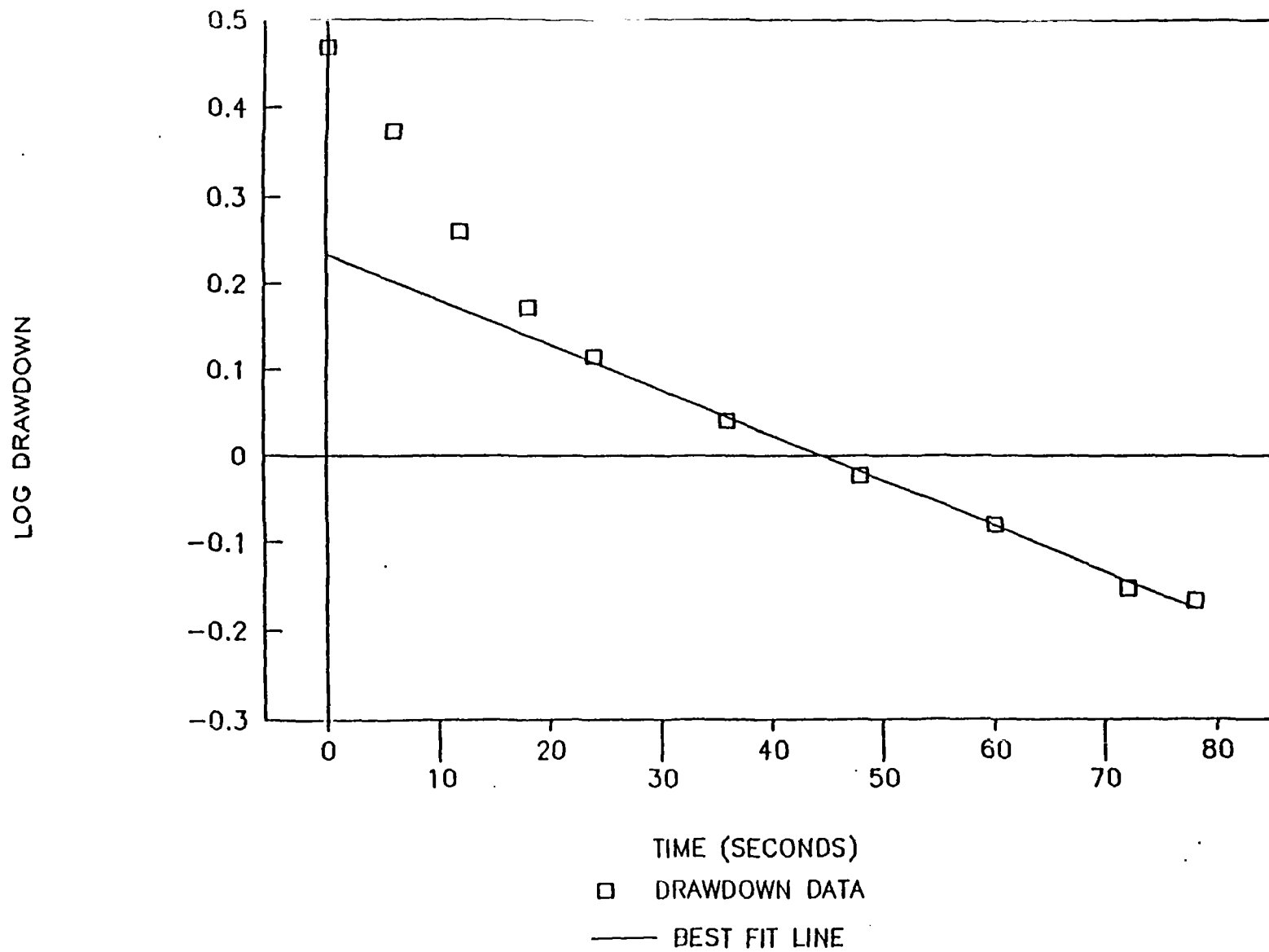
SCREEN LENGTH (L) = 99.24 INCHES
 CASING RADIUS (r) = 1.38 INCH
 BOREHOLE RAD. (R) = 2.00 INCHES
 H1 = 1.35 FEET
 T1 = 24.00 SECONDS
 H2 = 1.17 FEET
 T2 = 36.00 SECONDS

$$\text{HYDRAULIC CONDUCTIVITY} = \frac{(r^2) \ln(L/R) \ln(H1/H2) * 2.54}{2L(T2-T1)} \text{---[CEDERGREN, 1977]}$$

HYDRAULIC CONDUCTIVITY = 1.1E-03 CM/SEC

TIME VS. LOG DRAWDOWN

UA-05 TEST 3



WELL NO: UA-05
 TEST NO: 3
 TEST DATE: 6-29-93

JOB NO: 6802-02
 JOB NAME: CONTINENTAL STEEL
 DATE: 1-19-94

RESULTS OF IN-SITU HYDRAULIC CONDUCTIVITY TEST

COMMENTS: BAIL TEST

TIME (seconds)	Ho	ht	DRAWDOWN (feet)	LOG drawdown
0	71.1	45.6	2.94	0.46874599
6	71.1	50.7	2.35	0.37183598
12	71.1	55.3	1.82	0.26086290
18	71.1	58.2	1.49	0.17279552
24	71.1	59.8	1.30	0.11528425
36	71.1	61.6	1.10	0.03992941
48	71.1	62.9	0.95	-0.02398034
60	71.1	63.9	0.83	-0.08046169
72	71.1	65.0	0.70	-0.15246436
78	71.1	65.2	0.68	-0.16694218

COORDINATES OF BEST FIT LINE (Y=A+BX)

Regression Output:		X COORD	Y COORD
Constant	0.23440322	0	0.23440322
Std Err of Y Est	0.008021860	6	0.20279842
R Squared	0.995781803	12	0.17119363
No. of Observations	6	18	0.13958883
Degrees of Freedom	4	24	0.10798403
		36	0.04477444
X Coefficient(s)	-0.005267	48	-0.01843515
Std Err of Coef.	0.0001714	60	-0.08164475
		72	-0.14485434
		78	-0.17645914

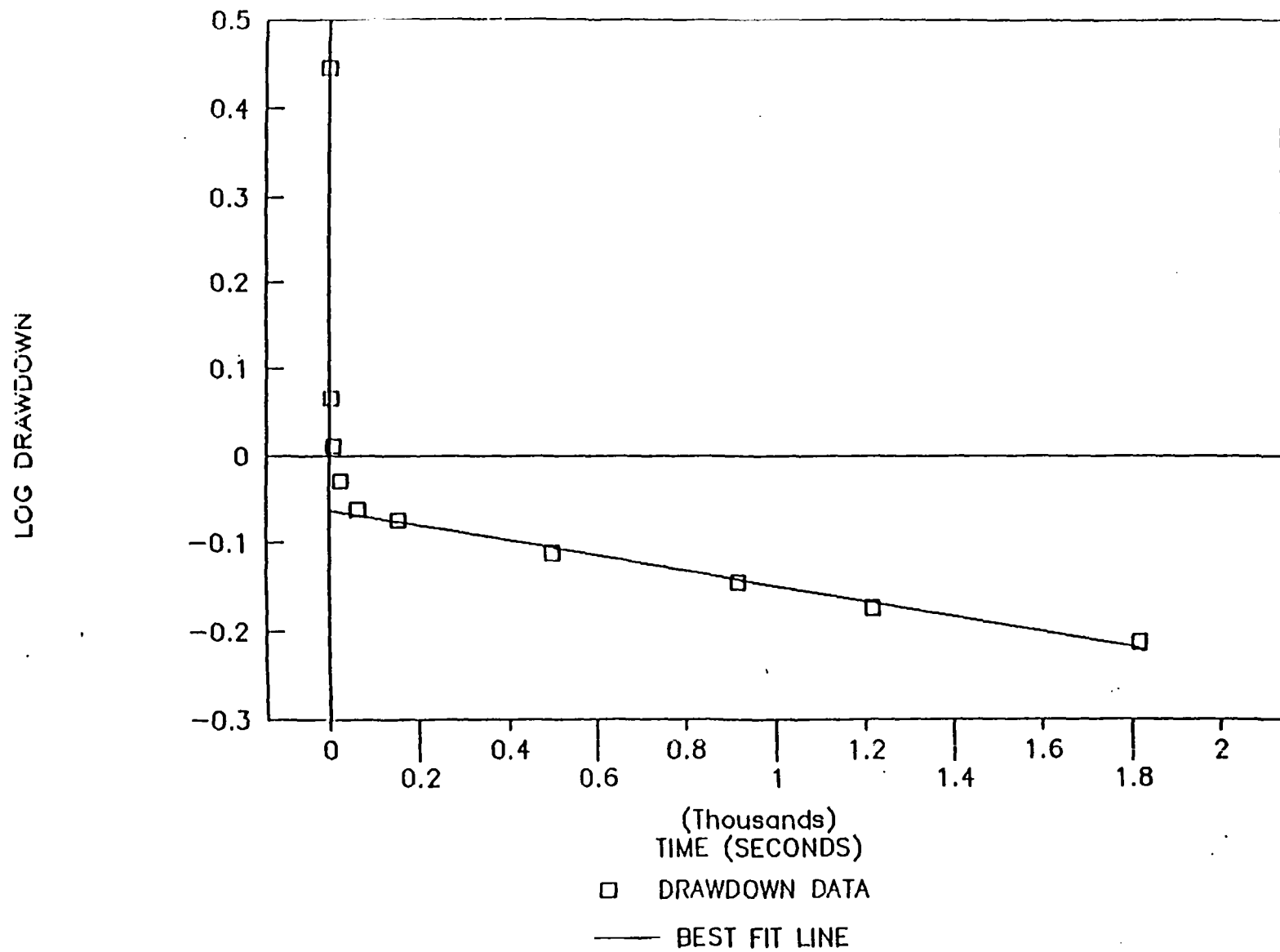
SCREEN LENGTH (L) = 99.24 INCHES
 CASING RADIUS (r) = 1.38 INCH
 BOREHOLE RAD. (R) = 2.00 INCHES
 H1 = 1.28 FEET
 T1 = 24.00 SECONDS
 H2 = 1.11 FEET
 T2 = 36.00 SECONDS

$$\text{HYDRAULIC CONDUCTIVITY} = \frac{(r^2) \ln(L/R) \ln(H1/H2) * 2.54}{2L(T2 - T1)} \text{---[CEDERGREN, 1977]}$$

HYDRAULIC CONDUCTIVITY = 1.2E-03 CM/SEC

TIME VS. LOG DRAWDOWN

UA-7 TEST 1



WELL NO: UA-7
 TEST NO: 1
 TEST DATE: 6-29-93

JOB NO: 6802-02
 JOB NAME: CONTINENTAL STEEL
 DATE: 1-18-94

RESULTS OF IN-SITU HYDRAULIC CONDUCTIVITY TEST

COMMENTS: BAIL TEST

TIME (seconds)	Ho	ht	DRAWDOWN (feet)	LOG drawdown
0	53.2	29.0	2.79	0.44602117
4	53.2	43.1	1.17	0.06652718
8	53.2	44.3	1.03	0.01159582
24	53.2	45.1	0.93	-0.02930917
63	53.2	45.7	0.87	-0.06273293
153	53.2	45.9	0.84	-0.07447133
495	53.2	46.5	0.77	-0.11171939
915	53.2	47.0	0.72	-0.14540250
1215	53.2	47.4	0.67	-0.17436620
1815	53.2	47.9	0.61	-0.21351832

COORDINATES OF BEST FIT LINE (Y=A+BX)

Regression Output		X COORD	Y COORD
Constant	-0.06324838	0	-0.06324839
Std Err of Y Est	0.006366573	4	-0.06359437
R Squared	0.990531031	8	-0.06394035
No. of Observations	6	24	-0.06532427
Degrees of Freedom	4	63	-0.06869757
		153	-0.07648211
X Coefficient(s)	-0.000086	495	-0.10606337
Std Err of Coef.	0.0000042	915	-0.14239124
		1215	-0.16833971
		1815	-0.22023666

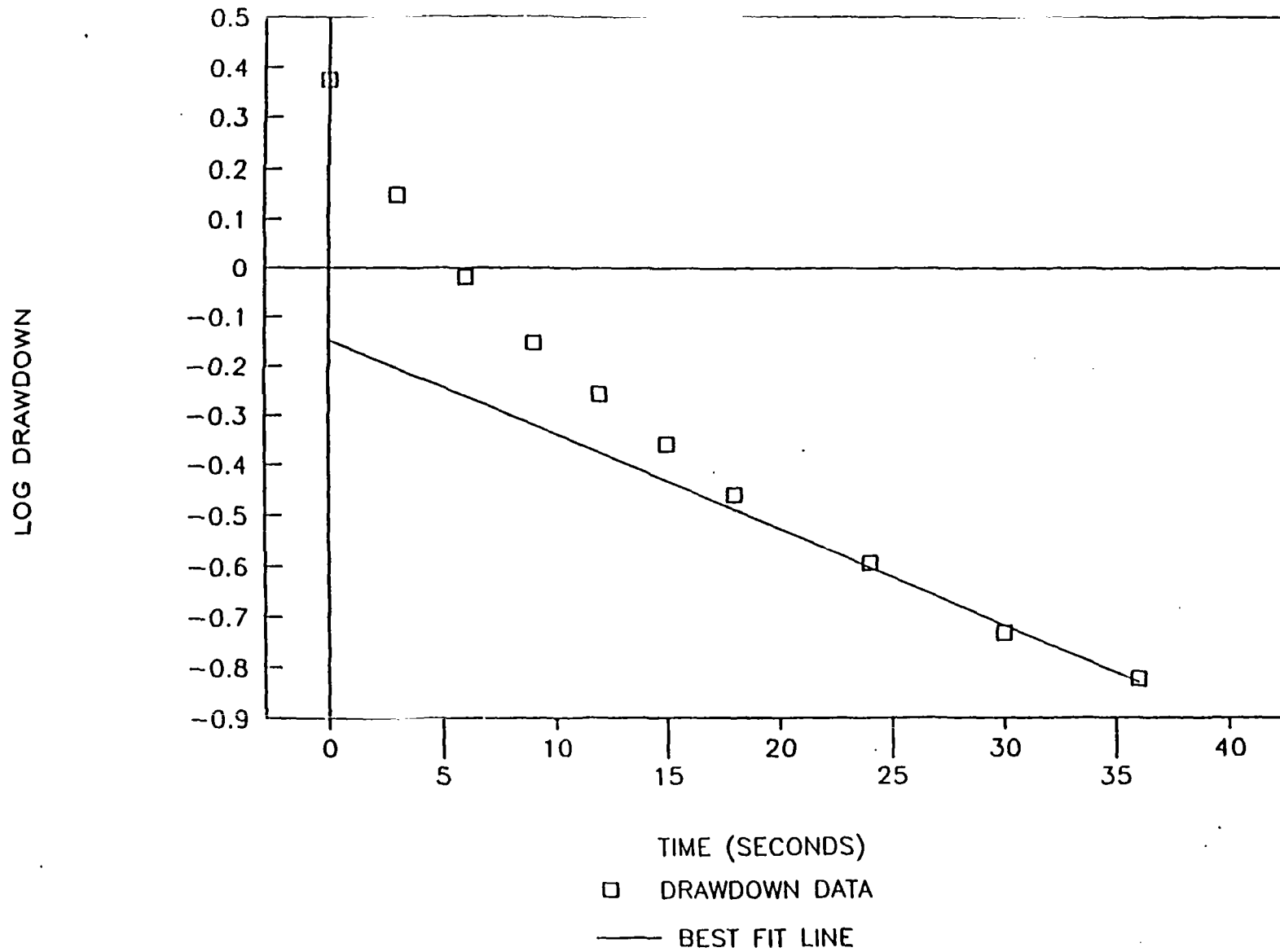
SCREEN LENGTH (L) = 48.12 INCHES
 CASING RADIUS (r) = 1.17 INCH
 BOREHOLE RAD. (R) = 1.50 INCHES
 H1 = 0.85 FEET
 T1 = 63.00 SECONDS
 H2 = 0.84 FEET
 T2 = 153.00 SECONDS

$$\text{HYDRAULIC CONDUCTIVITY} = \frac{(r^2) \ln(L/R) \ln(H1/H2) * 2.54}{2L(T2-T1)} \text{---[CEDERGREN, 1977]}$$

HYDRAULIC CONDUCTIVITY = 2.5E-05 CM/SEC

TIME VS. LOG DRAWDOWN

UA-12 TEST 1



WELL NO: UA-12
 TEST NO: 1
 TEST DATE: 6-29-93

JOB NO: 6802-02
 JOB NAME: CONTINENTAL STEEL
 DATE: 1-18-94

RESULTS OF IN-SITU HYDRAULIC CONDUCTIVITY TEST

COMMENTS: BAIL TEST

TIME (seconds)	Ho	ht	DRAWDOWN (feet)	LOG drawdown
0	74.0	53.5	2.37	0.37395967
3	74.0	61.8	1.41	0.14856564
6	74.0	65.7	0.96	-0.01871610
9	74.0	67.9	0.70	-0.15246436
12	74.0	69.2	0.55	-0.25655295
15	74.0	70.2	0.44	-0.35801059
18	74.0	71.0	0.35	-0.46067294
24	74.0	71.8	0.25	-0.59537151
30	74.0	72.4	0.18	-0.73367421
36	74.0	72.7	0.15	-0.82385084

COORDINATES OF BEST FIT LINE (Y=A+BX)

Regression Output		X COORD	Y COORD
Constant	-0.14643386	0	-0.14643386
Std Err of Y Est	0.019647384	3	-0.20355370
R Squared	0.9854263	6	-0.26067353
No. of Observations	3	9	-0.31779336
Degrees of Freedom	1	12	-0.37491319
		15	-0.43203303
X Coefficient(s)	-0.019039	18	-0.48915286
Std Err of Coef.	0.0023154	24	-0.60339252
		30	-0.71763219
		36	-0.83187185

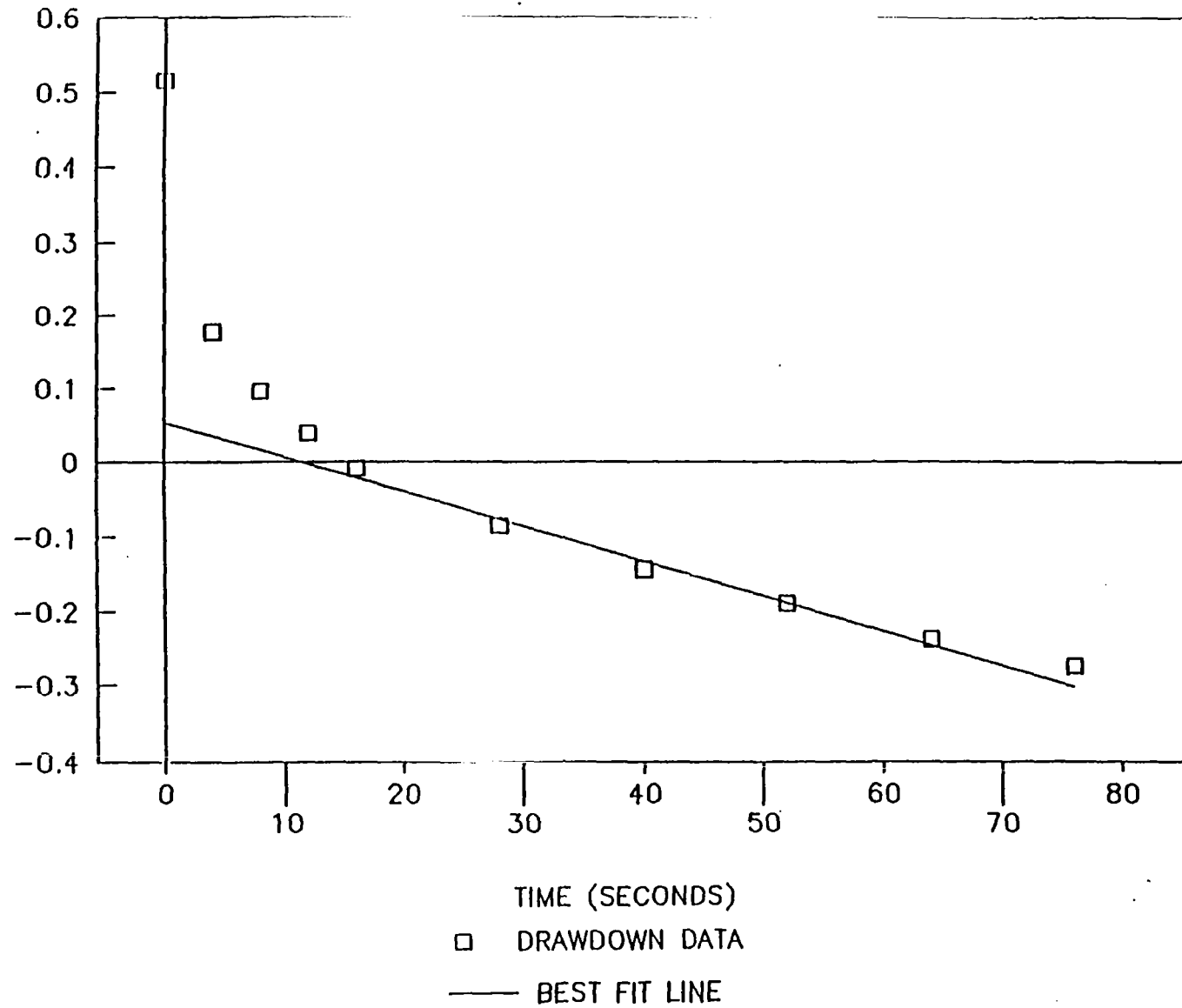
SCREEN LENGTH (L) = 120.00 INCHES
 CASING RADIUS (r) = 1.00 INCH
 BOREHOLE RAD. (R) = 1.50 INCHES
 H1 = 0.42 FEET
 T1 = 12.00 SECONDS
 H2 = 0.37 FEET
 T2 = 15.00 SECONDS

$$\text{HYDRAULIC CONDUCTIVITY} = \frac{(r^2) \ln(L/R) \ln(H1/H2) * 2.54}{2L(T2-T1)} \text{---[CEDERGREN, 1977]}$$

HYDRAULIC CONDUCTIVITY = 2.0E-03 CM/SEC

TIME VS. LOG DRAWDOWN

UA-14 TEST 1



WELL NO: UA-14
 TEST NO: 1
 TEST DATE: 6-29-93

JOB NO: 6802-02
 JOB NAME: CONTINENTAL STEEL
 DATE: 1-18-94

RESULTS OF IN-SITU HYDRAULIC CONDUCTIVITY TEST

COMMENTS: BAIL TEST

TIME (seconds)	Ho	ht	DRAWDOWN (feet)	LOG drawdown
0	74.5	46.1	3.28	0.51552415
4	74.5	61.5	1.50	0.17614916
8	74.5	63.7	1.25	0.09562956
12	74.5	65.0	1.10	0.03992941
16	74.5	66.0	0.98	-0.00837527
28	74.5	67.4	0.82	-0.08653584
40	74.5	68.3	0.72	-0.14540250
52	74.5	68.9	0.65	-0.18960616
64	74.5	69.5	0.58	-0.23882419
76	74.5	69.9	0.53	-0.27503636

COORDINATES OF BEST FIT LINE (Y=A+BX)

Regression Output:		X COORD	Y COORD
Constant	0.054240596	0	0.05424060
Std Err of Y Est	0.012086746	4	0.03544166
R Squared	0.986407873	8	0.01664272
No. of Observations	5	12	-0.00215622
Degrees of Freedom	3	16	-0.02095516
		28	-0.07735198
X Coefficient(s)	-0.004699	40	-0.13374879
Std Err of Coef.	0.0003185	52	-0.19014561
		64	-0.24654243
		76	-0.30293924

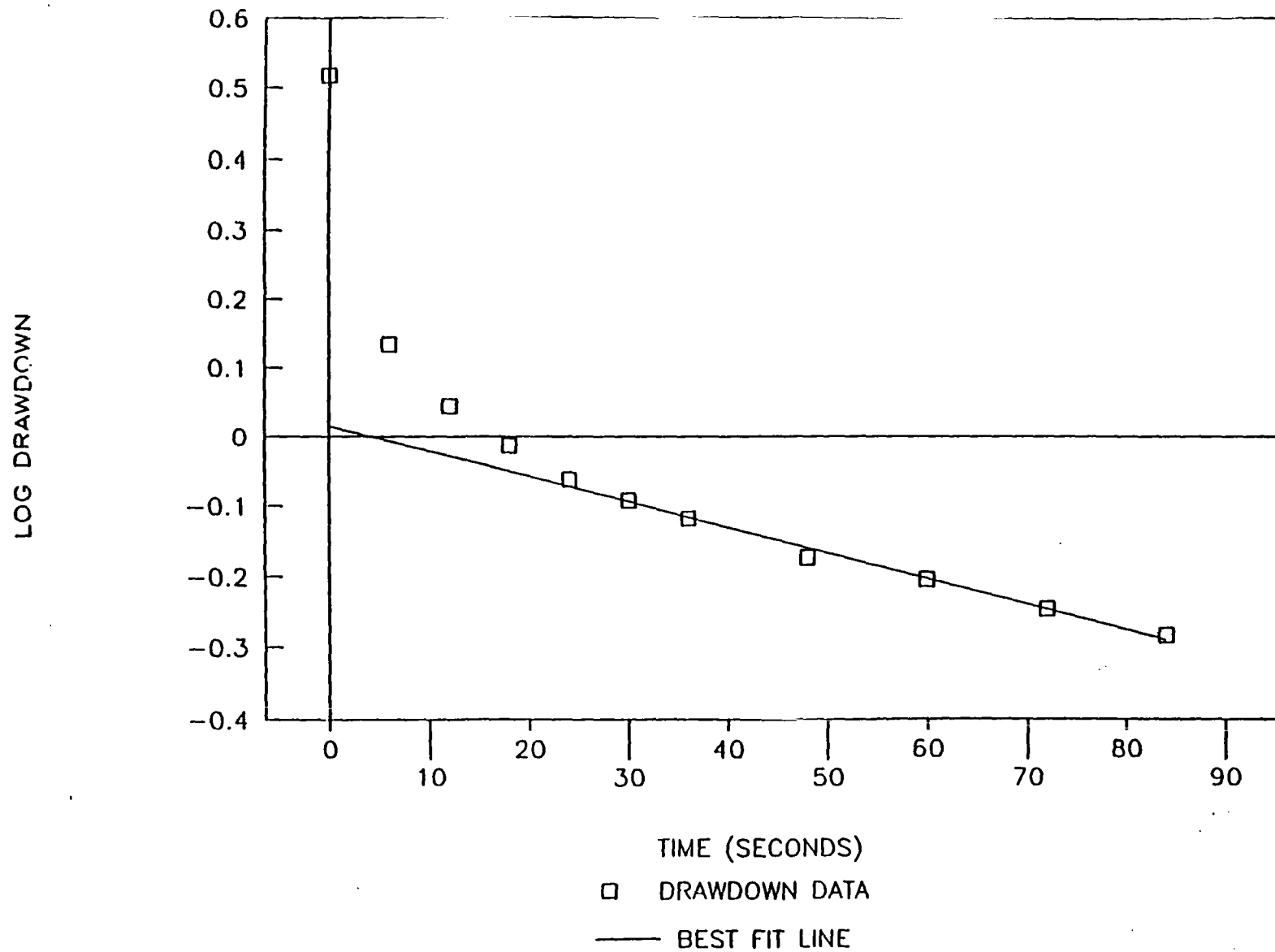
SCREEN LENGTH (L) = 120.00 INCHES
 CASING RADIUS (r) = 1.00 INCH
 BOREHOLE RAD. (R) = 3.00 INCHES
 H1 = 0.95 FEET
 T1 = 16.00 SECONDS
 H2 = 0.84 FEET
 T2 = 28.00 SECONDS

$$\text{HYDRAULIC CONDUCTIVITY} = \frac{(r^2) \ln(L/R) \ln(H1/H2) * 2.54}{2L(T2 - T1)} \text{---[CEDERGREN, 1977]}$$

HYDRAULIC CONDUCTIVITY = 4.2E-04 CM/SEC

TIME VS. LOG DRAWDOWN

UA-14 TEST 2



WELL NO: UA-14
 TEST NO: 2
 TEST DATE: 6-29-93

JOB NO: 6802-02
 JOB NAME: CONTINENTAL STEEL
 DATE: 1-18-94

RESULTS OF IN-SITU HYDRAULIC CONDUCTIVITY TEST

COMMENTS: BAIL TEST

TIME (seconds)	Ho	ht	DRAWDOWN (feet)	LOG drawdown
0	74.5	46.0	3.29	0.51705067
6	74.5	62.7	1.36	0.13408782
12	74.5	64.9	1.11	0.04447704
18	74.5	66.1	0.97	-0.01351491
24	74.5	67.0	0.87	-0.06273293
30	74.5	67.5	0.81	-0.09269615
36	74.5	67.9	0.76	-0.11825026
48	74.5	68.7	0.67	-0.17436620
60	74.5	69.1	0.62	-0.20540043
72	74.5	69.6	0.57	-0.24759811
84	74.5	70.0	0.52	-0.28458168

COORDINATES OF BEST FIT LINE (Y=A+BX)

Regression Output:		X COORD	Y COORD
Constant	0.015381215	0	0.01538122
Std Err of Y Est	0.008433642	6	-0.00653903
R Squared	0.991236303	12	-0.02845927
No. of Observations	7	18	-0.05037951
Degrees of Freedom	5	24	-0.07229975
		30	-0.09421999
X Coefficient(s)	-0.003653	36	-0.11614023
Std Err of Coef.	0.0001536	48	-0.15998072
		60	-0.20382120
		72	-0.24766168
		84	-0.29150217

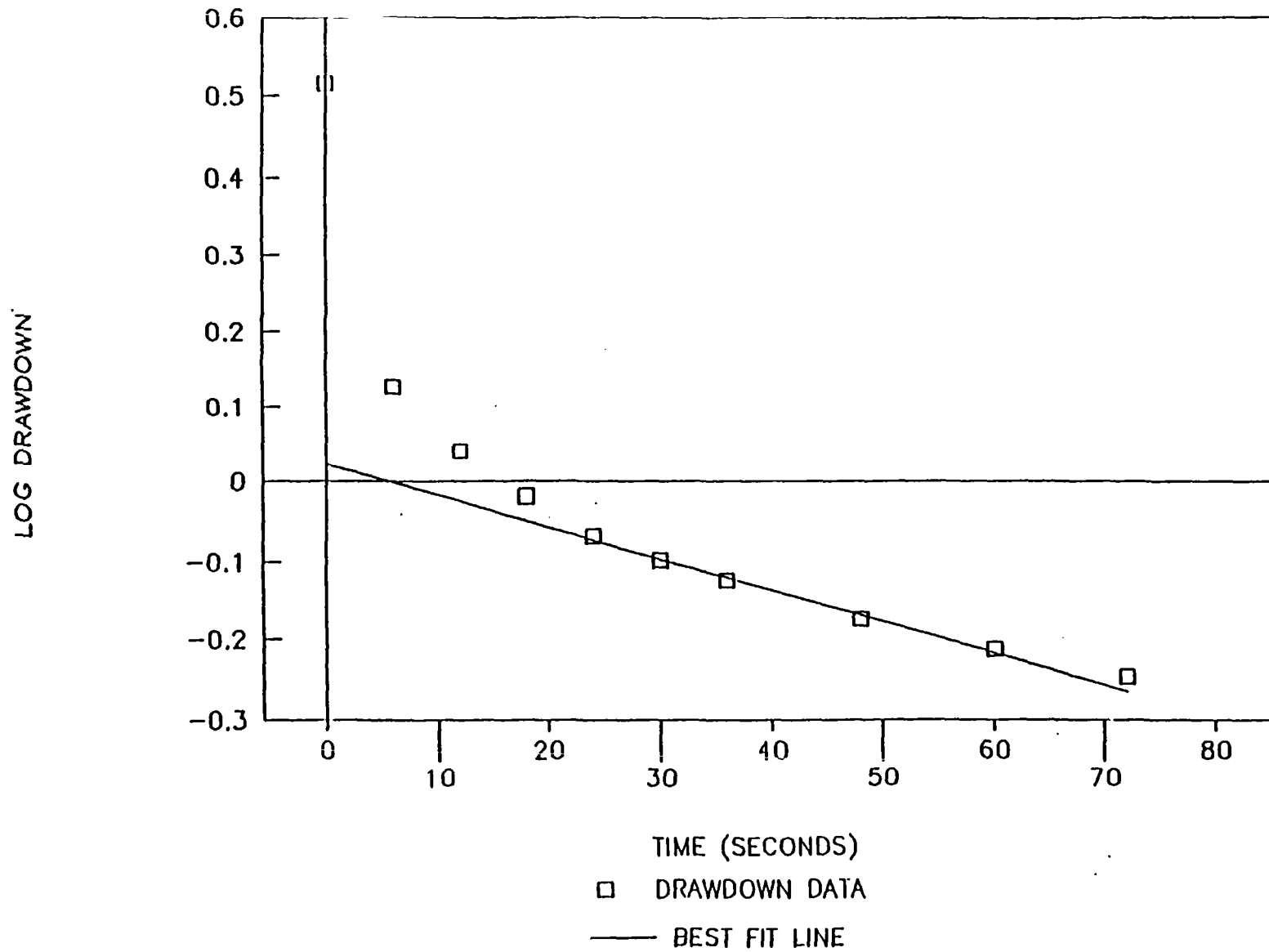
SCREEN LENGTH (L) = 120.00 INCHES
 CASING RADIUS (r) = 1.00 INCH
 BOREHOLE RAD. (R) = 3.00 INCHES
 H1 = 0.85 FEET
 T1 = 24.00 SECONDS
 H2 = 0.80 FEET
 T2 = 30.00 SECONDS

$$\text{HYDRAULIC CONDUCTIVITY} = \frac{(r^2) \ln(L/R) \ln(H1/H2) * 2.54}{2L(T2-T1)} \text{---[CEDERGREN, 1977]}$$

HYDRAULIC CONDUCTIVITY = 3.3E-04 CM/SEC

TIME VS. LOG DRAWDOWN

UA-14 TEST 3



WELL NO: UA-14
 TEST NO: 3
 TEST DATE: 6-29-93

JOB NO: 6802-02
 JOB NAME: CONTINENTAL STEEL
 DATE: 1-19-94

RESULTS OF IN-SITU HYDRAULIC CONDUCTIVITY TEST

COMMENTS: BAIL TEST

TIME (seconds)	Ho	ht	DRAWDOWN (feet)	LOG drawdown
0	74.5	46.1	3.28	0.51552415
6	74.5	62.9	1.34	0.12666380
12	74.5	65.0	1.10	0.03992941
18	74.5	66.2	0.96	-0.01871610
24	74.5	67.1	0.85	-0.06856247
30	74.5	67.6	0.80	-0.09894510
36	74.5	68.0	0.75	-0.12488083
48	74.5	68.7	0.67	-0.17436620
60	74.5	69.2	0.61	-0.21351832
72	74.5	69.6	0.57	-0.24759811

COORDINATES OF BEST FIT LINE (Y=A+BX)

Regression Output		X COORD	Y COORD
Constant	0.022849485	0	0.02284948
Std Err of Y Est	0.005072027	6	-0.00122689
R Squared	0.994294035	12	-0.02530326
No. of Observations	5	18	-0.04937964
Degrees of Freedom	3	24	-0.07345601
		30	-0.09753239
X Coefficient(s)	-0.004012	36	-0.12160876
Std Err of Coef.	0.0001755	48	-0.16976151
		60	-0.21791426
		72	-0.26606701

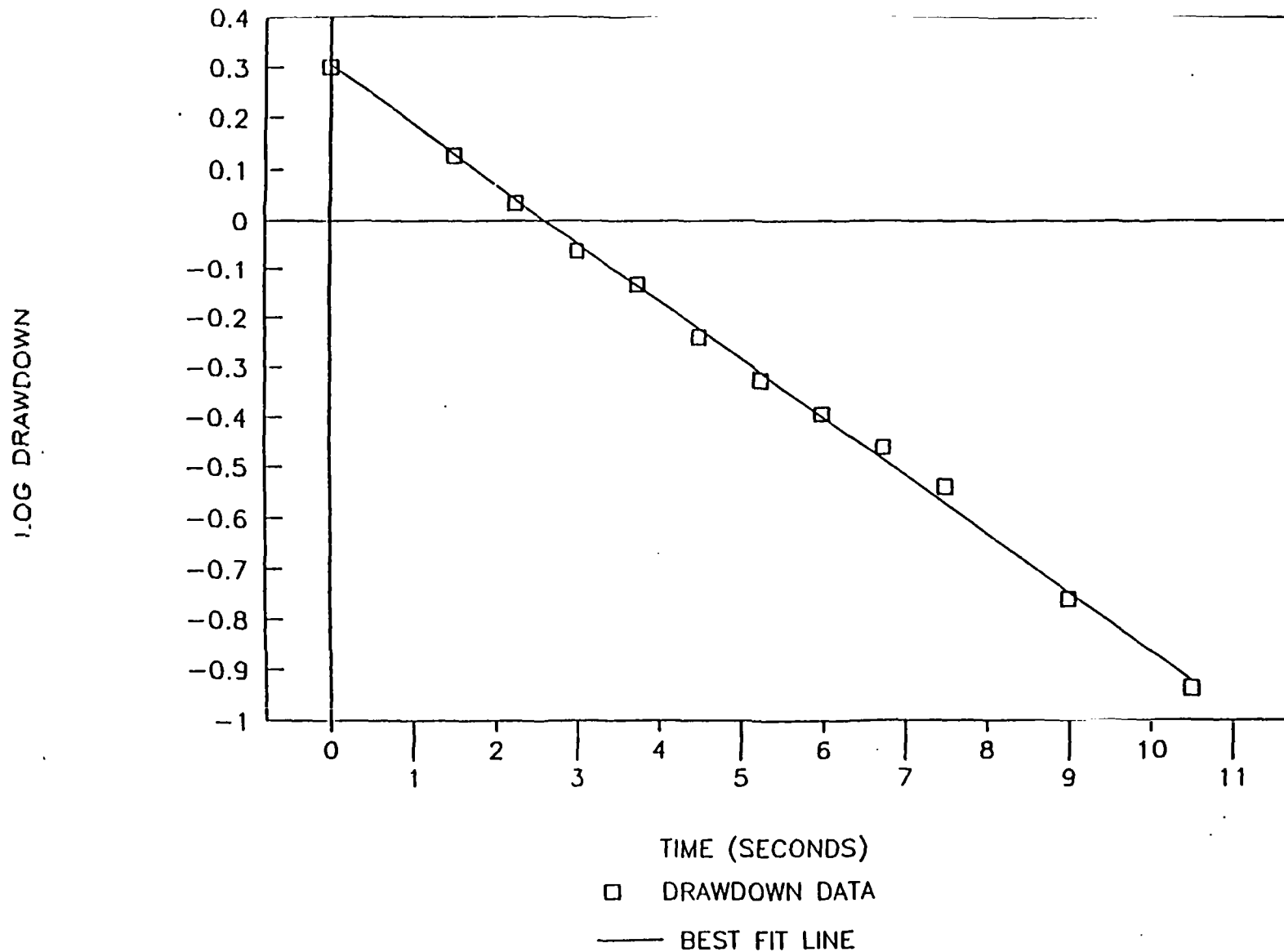
SCREEN LENGTH (L) = 120.00 INCHES
 CASING RADIUS (r) = 1.00 INCH
 BOREHOLE RAD. (R) = 3.00 INCHES
 H1 = 0.84 FEET
 T1 = 24.00 SECONDS
 H2 = 0.80 FEET
 T2 = 30.00 SECONDS

HYDRAULIC CONDUCTIVITY =
$$\frac{(r^2) \cdot \ln(L/R) \ln(H1/H2) \cdot 2.54}{2L(T2-T1)}$$
 [CEDERGREN, 1977]

HYDRAULIC CONDUCTIVITY = 3.6E-04 CM/SEC

TIME VS. LOG DRAWDOWN

UA-16 TEST 1



WELL NO: UA-16
 TEST NO: 1
 TEST DATE: 6-29-93

JOB NO: 6802-02
 JOB NAME: CONTINENTAL STEEL
 DATE: 1-18-94

RESULTS OF IN-SITU HYDRAULIC CONDUCTIVITY TEST

COMMENTS: BAIL TEST

TIME (seconds)	Ho	ht	DRAWDOWN (feet)	LOG drawdown
0	75.1	57.8	2.00	0.30025191
1.5	75.1	63.5	1.34	0.12666380
2.25	75.1	65.7	1.08	0.03533366
3	75.1	67.6	0.87	-0.06273293
3.75	75.1	68.7	0.74	-0.13161422
4.5	75.1	70.1	0.58	-0.23882419
5.25	75.1	71.0	0.47	-0.32501033
6	75.1	71.6	0.40	-0.39372615
6.75	75.1	72.1	0.35	-0.46067294
7.5	75.1	72.6	0.29	-0.53985418
9	75.1	73.6	0.17	-0.76170293
10.5	75.1	74.1	0.12	-0.93779419

COORDINATES OF BEST FIT LINE (Y=A+BX)

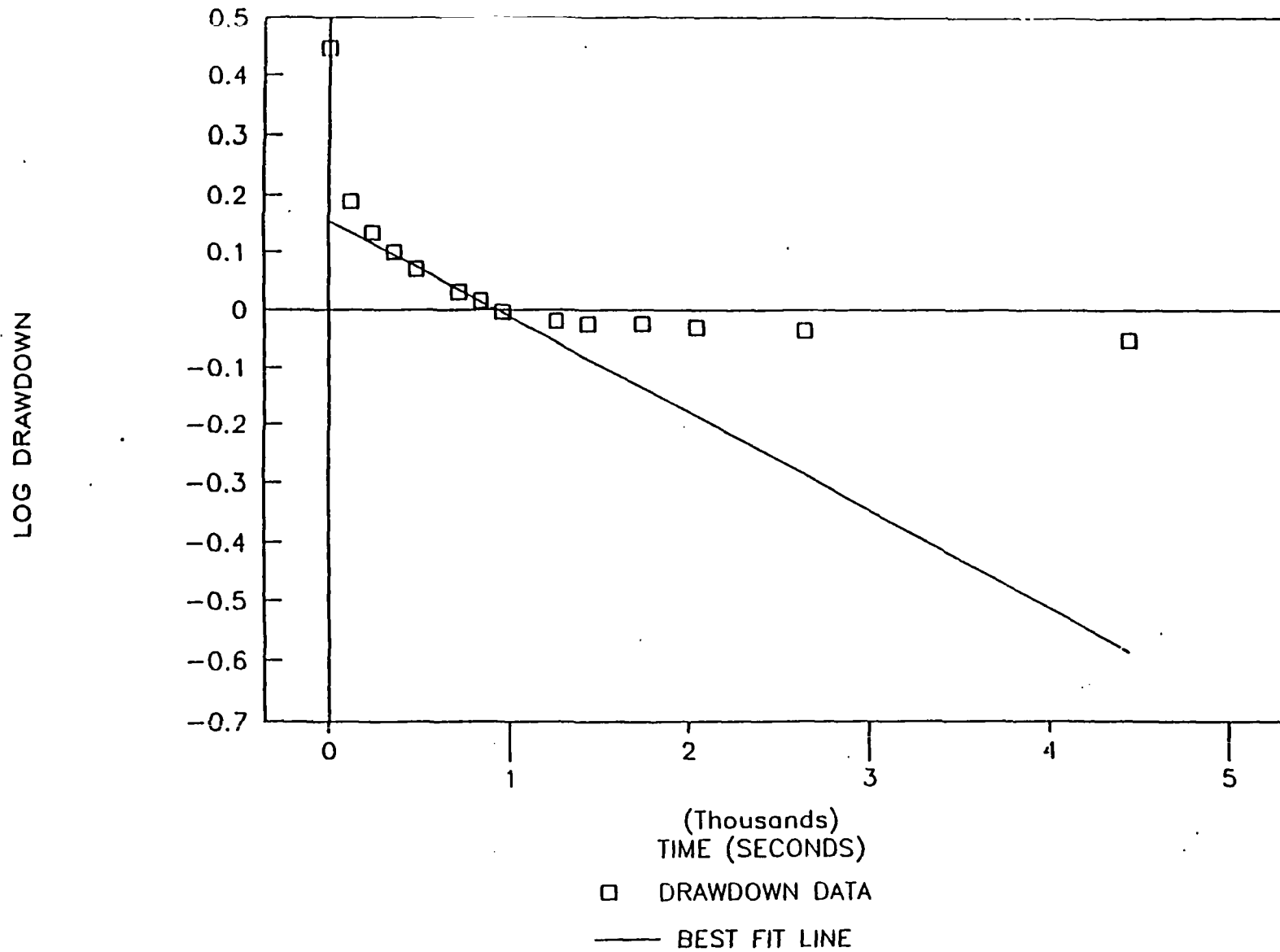
Regression Output:		X COORD	Y COORD
Constant	0.304696729	0	0.30469673
Std Err of Y Est	0.022788604	1.5	0.12922818
F. Squared	0.992979649	2.25	0.04149391
No. of Observations	7	3	-0.04624036
Degrees of Freedom	5	3.75	-0.13397464
		4.5	-0.22170891
X Coefficient(s)	-0.116979	5.25	-0.30944318
Std Err of Coef.	0.0043987	6	-0.39717745
		6.75	-0.48491173
		7.5	-0.57264600
		9	-0.74811455
		10.5	-0.92358309
SCREEN LENGTH (L) =	120.00 INCHES		
CASING RADIUS (r) =	1.17 INCH		
BOREHOLE RAD. (R) =	1.50 INCHES		
H1 =	0.49 FEET		
T1 =	5.25 SECONDS		
H2 =	0.40 FEET		
T2 =	6.00 SECONDS		

$$\text{HYDRAULIC CONDUCTIVITY} = \frac{(r^2) \ln(L/R) \ln(H1/H2) * 2.54}{2L(T2-T1)} \text{---[CEDERGREN, 1977]}$$

HYDRAULIC CONDUCTIVITY = 1.7E-02 CM/SEC

TIME VS. LOG DRAWDOWN

UA-18 TEST 1



WELL NO: UA-18
 TEST NO: 1
 TEST DATE: 6-29-93

JOB NO: 6802-02
 JOB NAME: CONTINENTAL STEEL
 DATE: 1-31-94

RESULTS OF IN-SITU HYDRAULIC CONDUCTIVITY TEST

COMMENTS: BAIL TEST

TIME (seconds)	Ho	ht	DRAWDOWN (feet)	LOG drawdown
0	72.2	48.0	2.79	0.44602117
120	72.2	58.8	1.55	0.18931061
240	72.2	60.4	1.36	0.13408782
360	72.2	61.3	1.26	0.09963231
480	72.2	62.0	1.18	0.07080598
720	72.2	62.9	1.07	0.03068876
840	72.2	63.2	1.04	0.01644832
960	72.2	63.6	0.99	-0.00329574
1260	72.2	63.9	0.96	-0.01871610
1440	72.2	64.0	0.95	-0.02398034
1740	72.2	64.0	0.95	-0.02398034
2040	72.2	64.1	0.93	-0.02930917
2640	72.2	64.2	0.92	-0.03470420
4440	72.2	64.5	0.89	-0.05130347

COORDINATES OF BEST FIT LINE (Y=A+BX)

Regression Output:		X COORD	Y COORD
Constant	0.155162034	0	0.15516203
Std Err of Y Est	0.004563690	120	0.13510737
R Squared	0.991048630	240	0.11505271
No. of Observations	5	360	0.09499805
Degrees of Freedom	3	480	0.07494338
		720	0.03483406
X Coefficient(s)	-0.000167	840	0.01477940
Std Err of Coef.	0.0000091	960	-0.00527527
		1260	-0.05541192
		1440	-0.08549391
		1740	-0.13563057
SCREEN LENGTH (L) =	202.80 INCHES	2040	-0.18576723
CASING RADIUS (r) =	1.38 INCH	2640	-0.28604054
BOREHOLE RAD. (R) =	2.00 INCHES	4440	-0.58686048
H1 =	1.24 FEET		
T1 =	360.00 SECONDS		
H2 =	0.88 FEET		
T2 =	1260.00 SECONDS		

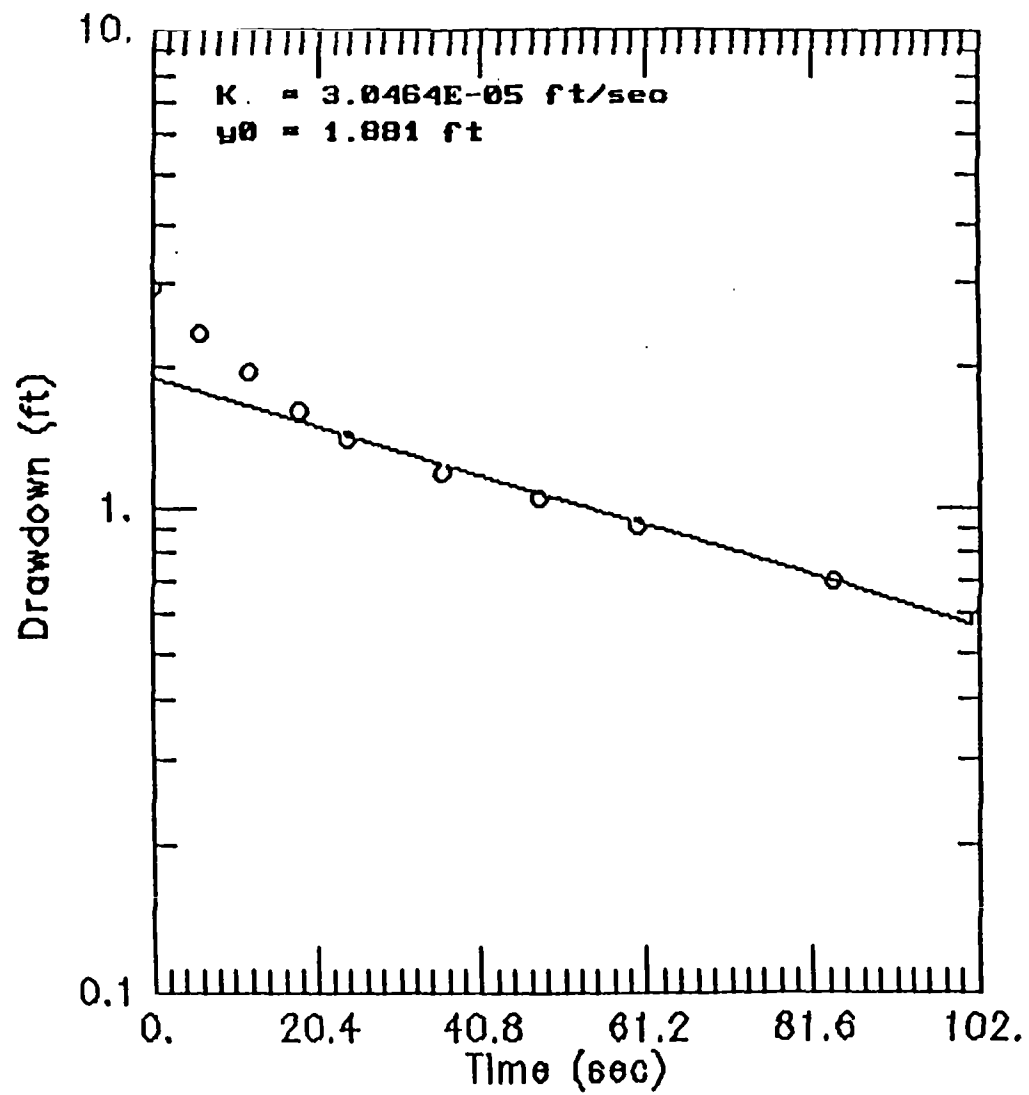
$$\text{HYDRAULIC CONDUCTIVITY} = \frac{(r^2) \cdot \ln(L/R) \ln(H1/H2) \cdot 2.54}{2L(T2-T1)} \text{---[CEDERGREN, 1977]}$$

$$\text{HYDRAULIC CONDUCTIVITY} = 2.1\text{E}-05 \text{ CM/SEC}$$

ATTACHMENT B
EXISTING AND SHALLOW MONITORING WELLS
BOUWER AND RICE RESULTS

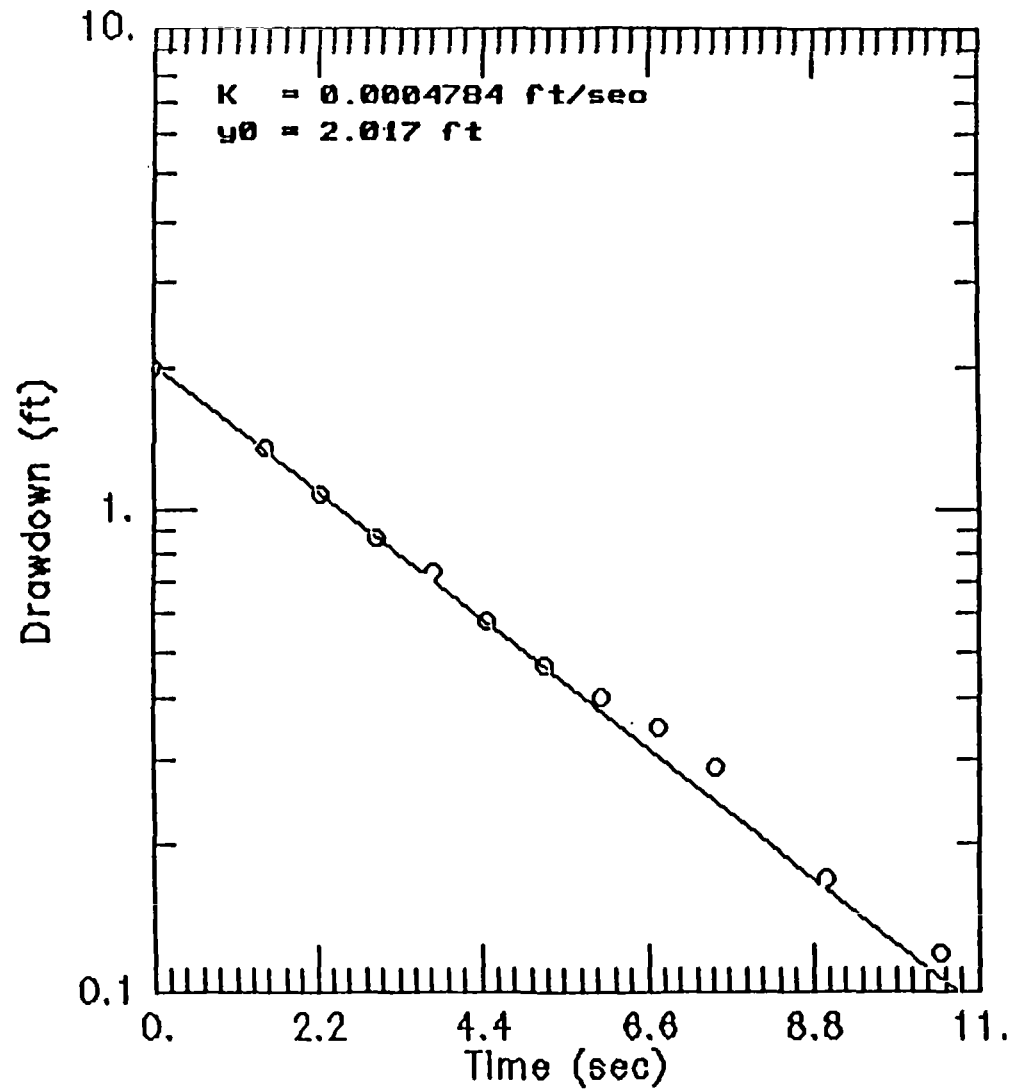
LOG DRAWDOWN VS. TIME

UA-05



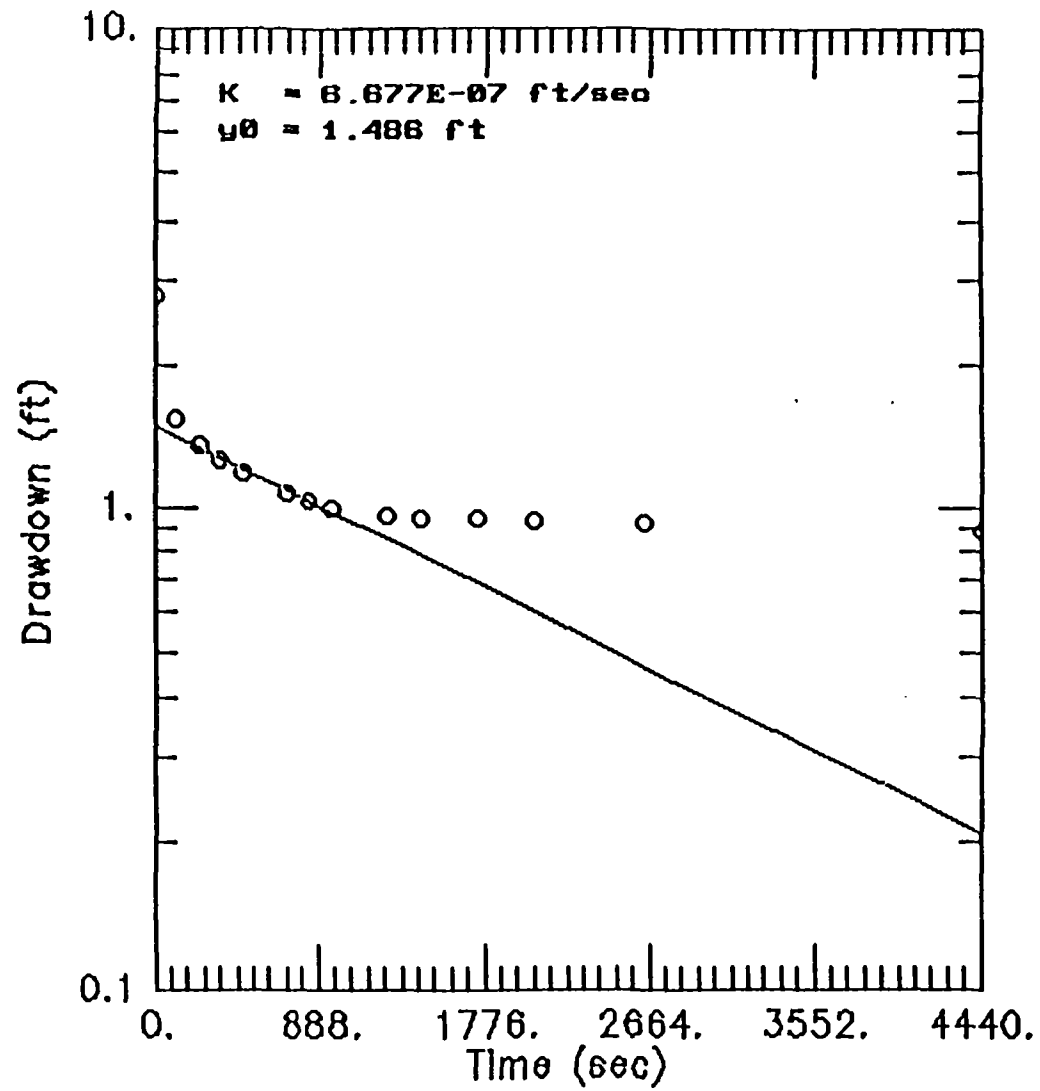
LOG DRAWDOWN VS. TIME

UA-16



LOG DRAWDOWN VS. TIME

UA-18



ATTACHMENT C
MLMS ZONES
COOPER RESULTS

CALCULATION OF HYDRAULIC CONDUCTIVITY
FOR MLMS ZONES

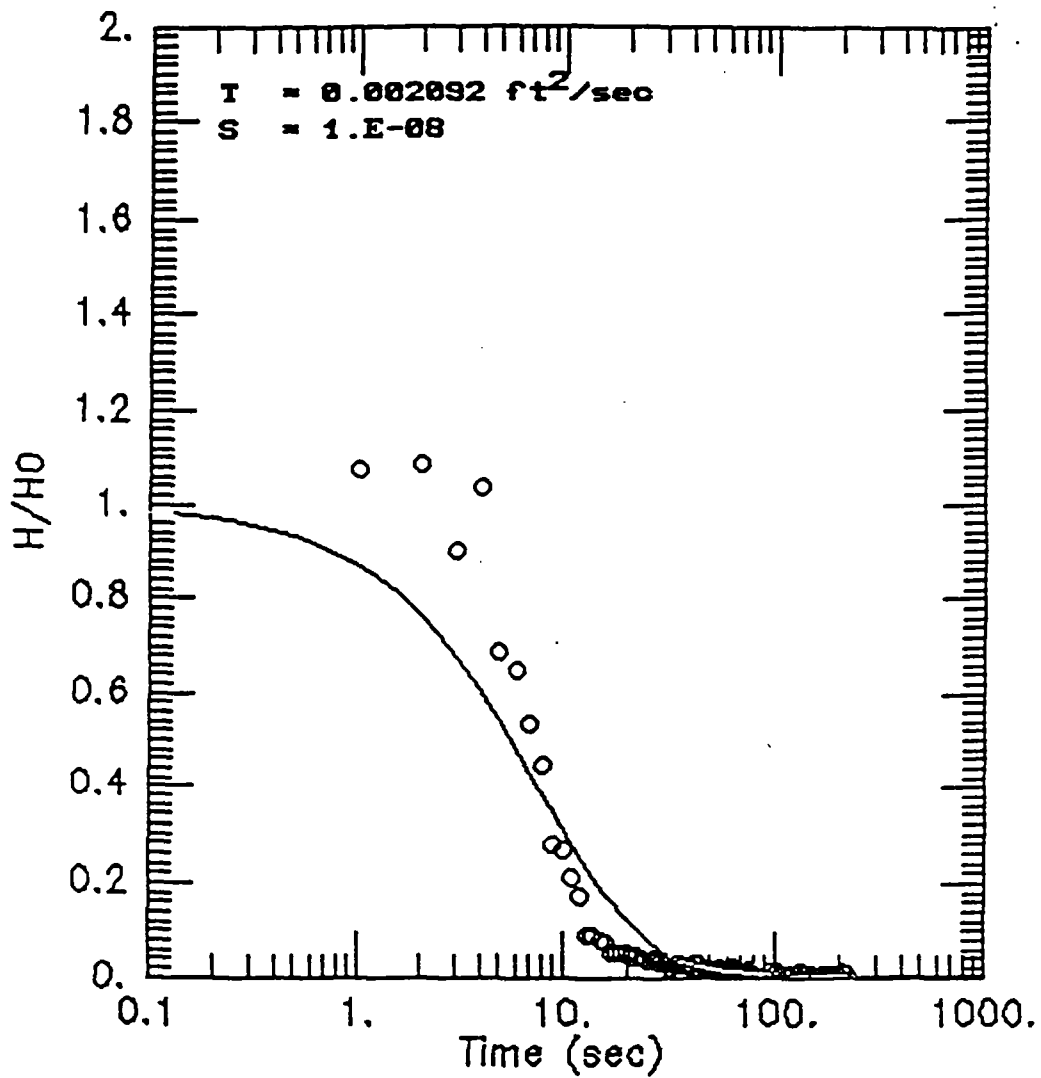
LOCATION	ZONE DEPTH (FEET)	TRANSMISSIVITY ¹ (FEET ² /SECOND)	SATURATED THICKNESS (FEET)	HYDRAULIC CONDUCTIVITY (CENTIMETERS/ SECOND)
LA-02	45-57	2.1X10 ⁻³ 2.1X10⁻³	116	5.5X10 ⁻⁴
LA-02	60-72	1.7X10 ⁻⁴ 1.7X10⁻⁴	116	4.4X10 ⁻⁵
LA-02	112-132	1.8X10 ⁻³ 1.8X10⁻³	109	5.2X10 ⁻⁴
LA-03	27-39	6.8X10 ⁻³	99	2.1X10 ⁻³
LA-03	42-54	3.6X10 ⁻³	98	1.1X10 ⁻³

Note:

¹ Results obtained by Cooper et al. method applied through the computer code AQTESOLV™.

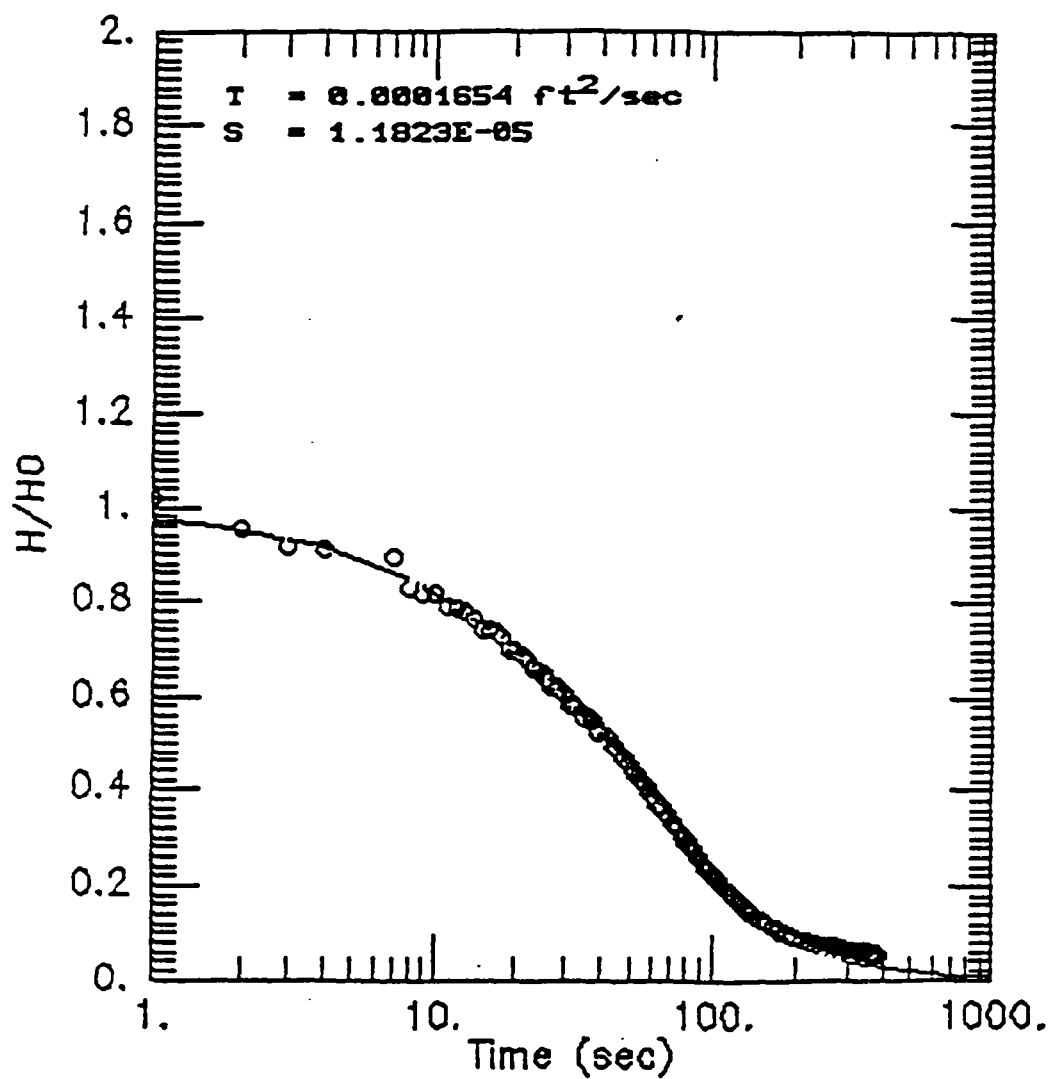
DISPLACEMENT VS. LOG TIME

LA-02 45-57 FEET - FALLING-HEAD TEST



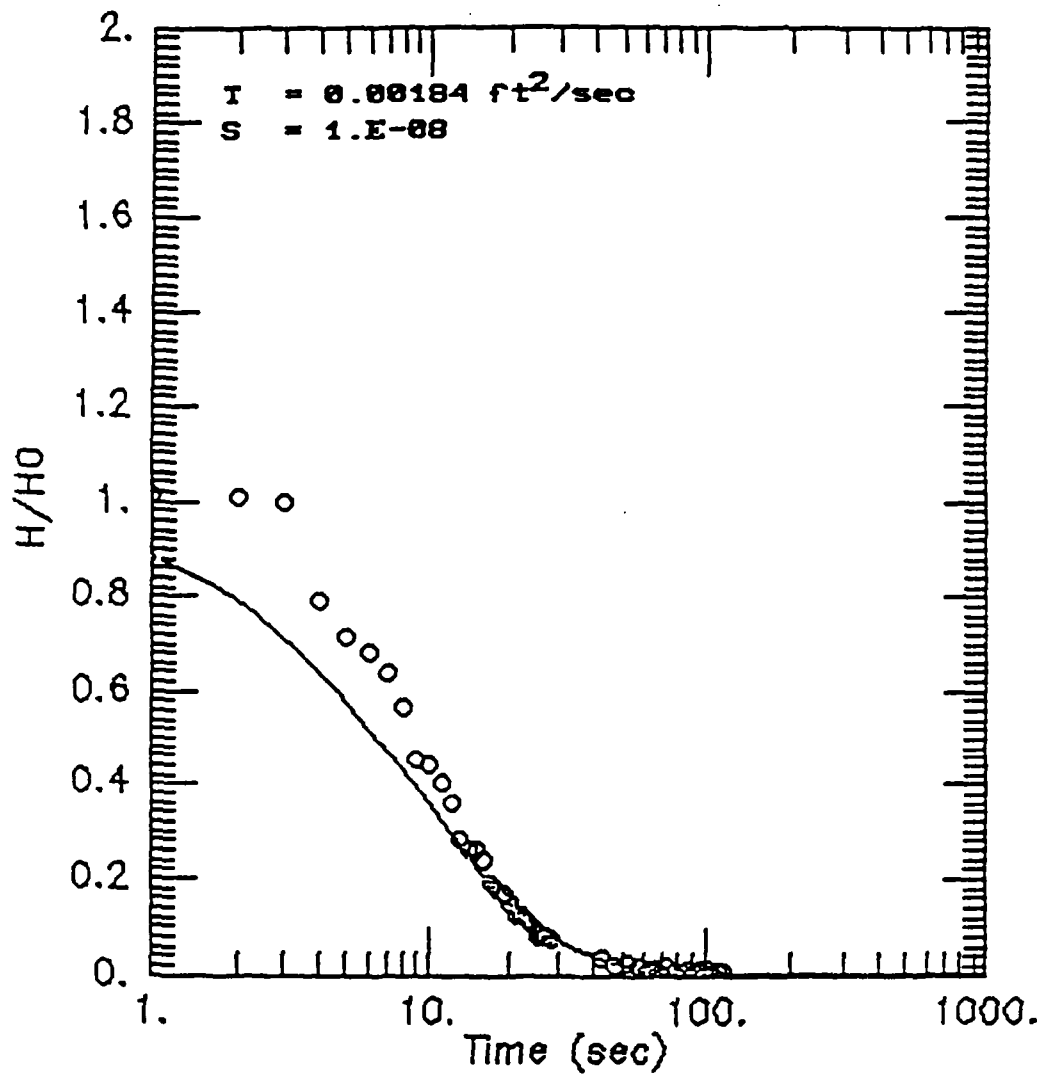
DISPLACEMENT VS. LOG TIME

LA-02 60-72 FEET - RISING-HEAD TEST



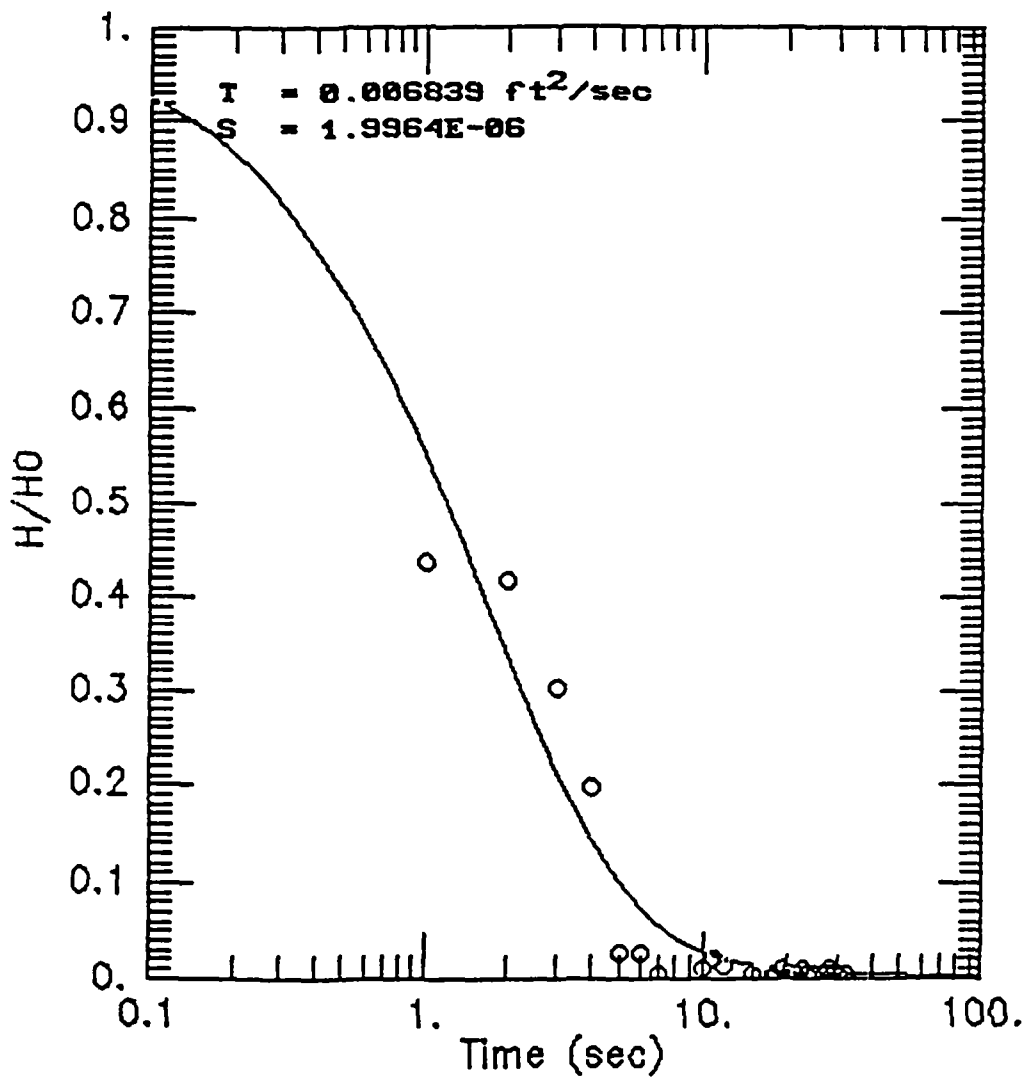
DISPLACEMENT VS. LOG TIME

LA-02 112-132 FEET - FALLING-HEAD TEST



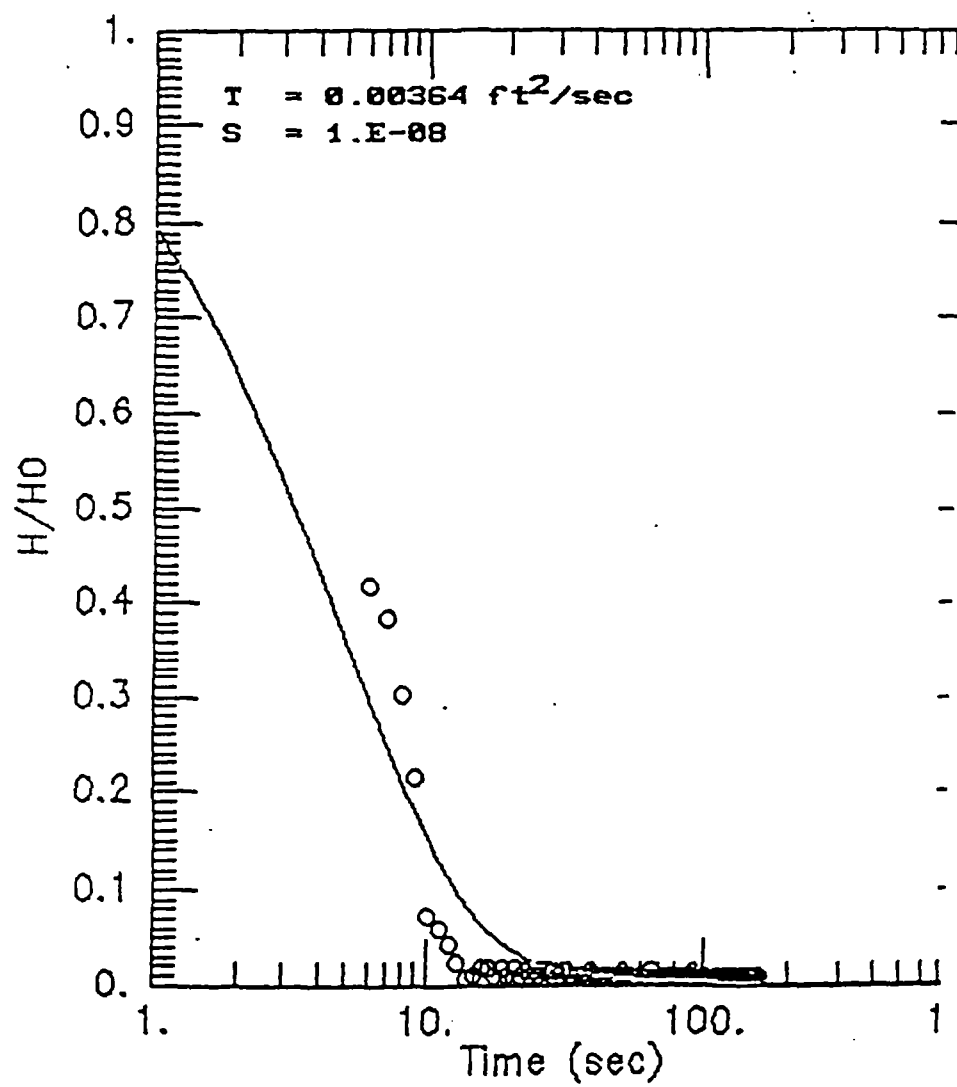
DISPLACEMENT VS. LOG TIME

LA-03 27-39 FEET - FALLING-HEAD TEST



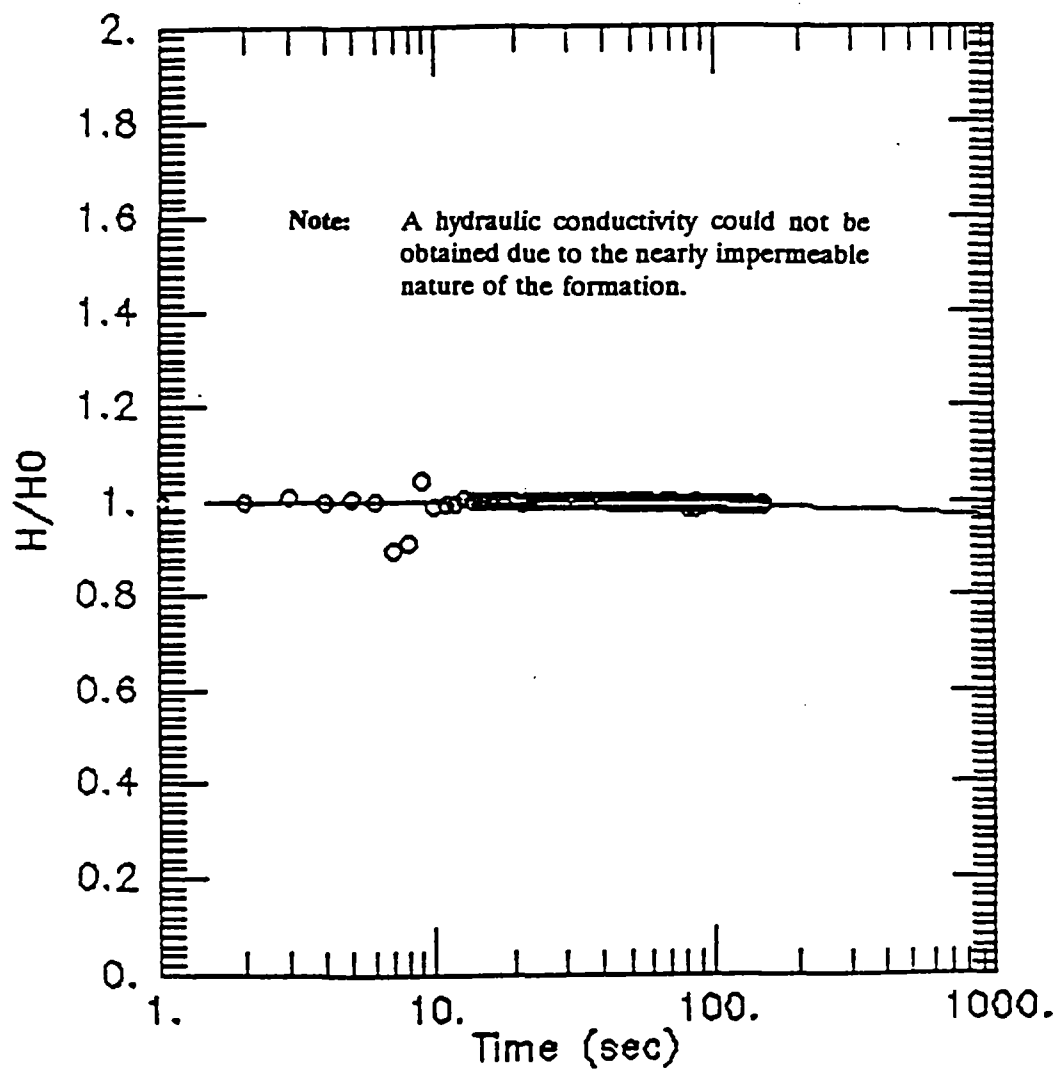
DISPLACEMENT VS. LOG TIME

LA-03 42-54 FEET - FALLING-HEAD TEST



DISPLACEMENT VS. LOG TIME

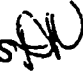
LA-05 110-131 FEET - RISING-HEAD TEST





MEMORANDUM

TO: Art Garceau and Bill Davis, IDEM

FROM: Donald A. Walsh, ABB-ES 

DATE: June 8, 1994

SUBJECT: Stepped-Discharge Aquifer Pumping Test Results
Continental Steel, Kokomo, Indiana
(Revised Memorandum)

On September 21, 1993, a stepped-discharge aquifer pumping test was conducted at PW-01. A condensed summary of the findings and recommendations is provided below.

TEST OBJECTIVES

A stepped-discharge aquifer pumping test was conducted at PW-01 to estimate the optimal pumping rate for the constant-discharge test and to provide data to assist in the selection of observations wells for the constant-discharge test.

METHODOLOGY

The stepped-discharge test was conducted following the procedures outlined in Attachment A-15 of the Sampling and Analysis Plan. The test involved measuring the water level in well PW-01 while incrementally increasing (stepping) the discharge rate from 0.56, to 0.74, to 1.26 gallons per minute (gpm). The discharge rate was measured volumetrically using a container of known volume and a stop watch. The duration of each step was 120 minutes. Field personnel were fairly successful in maintaining a constant discharge rate throughout each test. Extracted groundwater and decontamination fluids were contained in steel drums for disposal at a later time.

ANALYSIS

Time-drawdown data from each step was plotted on a semi-logarithmic graph and a best-fit line was drawn through each set of data. This graph is provided as Figure 1. Each line was extended to estimate drawdown in the well after three days of pumping. By evaluating the estimated drawdown, a discharge rate of 1 gpm was selected for the constant-rate test. At a rate of 1 gpm, it was estimated that drawdown in the pumping well would be 4 feet.

To estimate aquifer transmissivity, the data were analyzed using the Cooper-Jacob straight-line method (Cooper and Jacob, 1946) and the Birsoy and Summers (1980) method. The equations and assumptions of these methods are provided in Attachment A.

SEMI-LOGARITHMIC GRAPH OF DRAWDOWN VERSUS TIME AT PW-01
STEPPED-DISCHARGE TEST AT PW-01

CONTINENTAL STEEL, KOKOMO, INDIANA

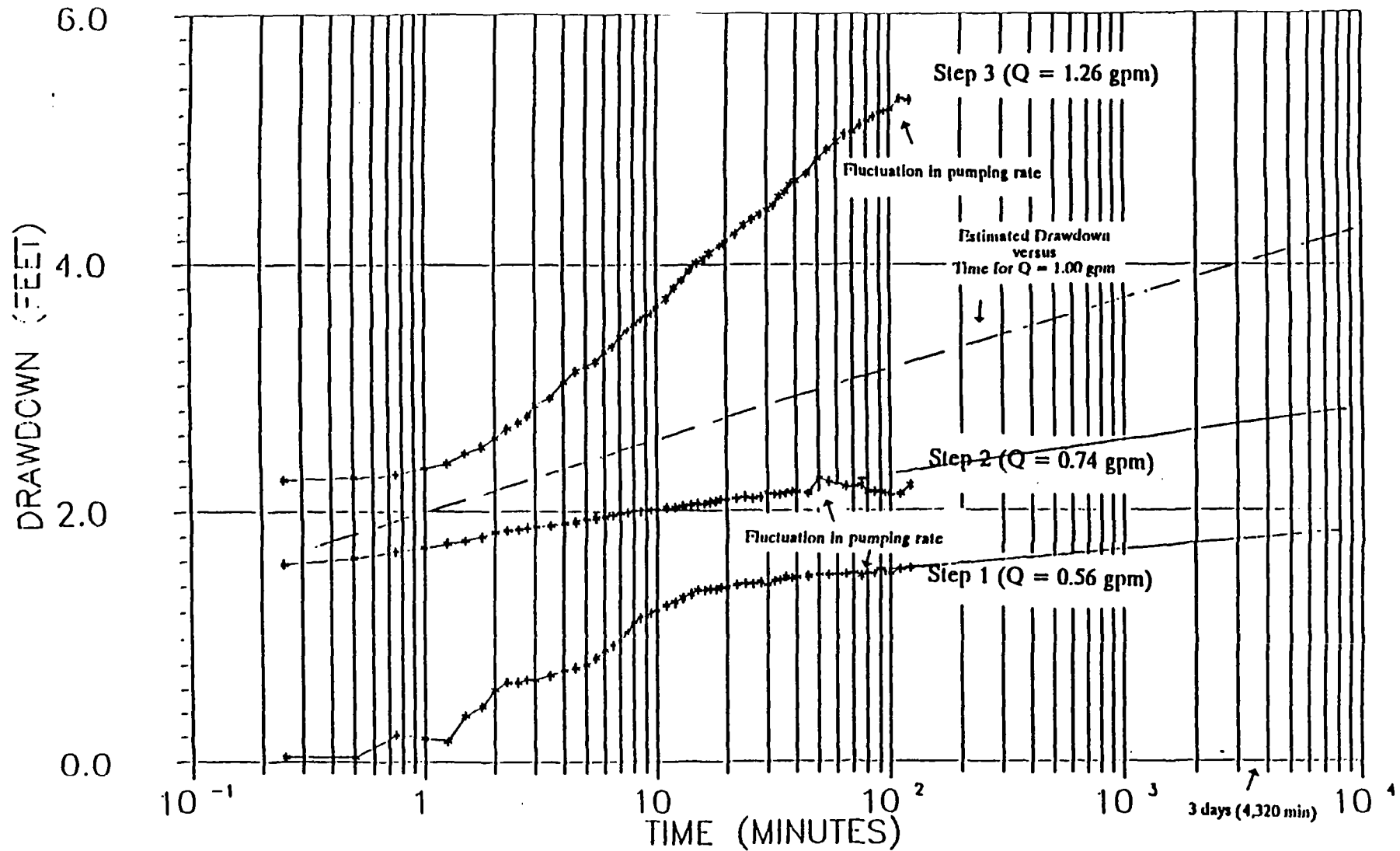


FIGURE 1

Both of these analyses assume that the aquifer is confined. The conditions in the area of the pumping well are believed to be unconfined; however, confined aquifer models can be used reliably as long as the drawdown is small compared to the saturated thickness of the aquifer. If the saturated thickness decreases by more than 20 percent, then a correction factor should be applied. Since the saturated thickness decreased by more than 20 percent, drawdown data was corrected using the procedure presented in Appendix 9.C of F.G. Driscoll's Groundwater and Wells, Johnson Division, 1986 prior to use in the Cooper-Jacob straight-line and the Birsoy and Summers methods.

TEST RESULTS

The transmissivity values obtained from the time-drawdown analyses are listed below.

METHOD	TRANSMISSIVITY (ft ² /day)	HYDRAULIC CONDUCTIVITY (ft/day)	HYDRAULIC CONDUCTIVITY (cm/sec)
Cooper-Jacob	139	11	4 x 10 ⁻³
Birsoy-Summers (step 1)	141	11	4 x 10 ⁻³
Birsoy-Summers (step 2)	176	14	5 x 10 ⁻³
Birsoy-Summers (steps 1&2)	<u>95</u>	<u>7</u>	<u>2 x 10⁻³</u>
Average	138	11	4 x 10 ⁻³

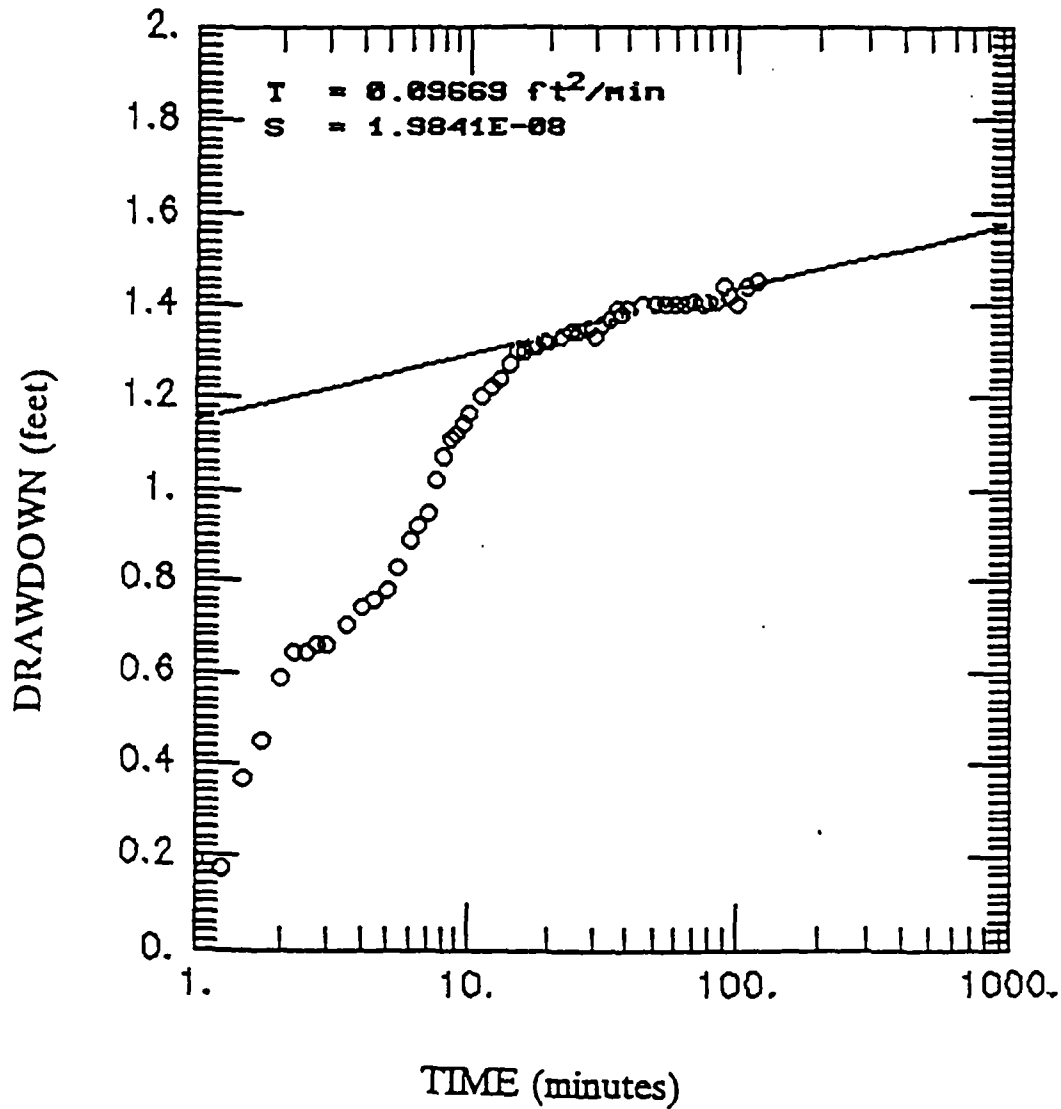
The Cooper-Jacob straight-line method is based on the assumption that the pumping rate is constant; therefore, this method could only be applied to the data obtained during the first step. A transmissivity of 139 feet squared per day (ft²/day) was calculated from the straight line portion of the first step (see Figure 2) using the Cooper-Jacob straight-line method. The influence from casing storage effects on the data was limited to the first 30 minutes of the first step. After 30 minutes, the ratio of the casing volume to the total volume of water removed was small (0.15); therefore, the data after 30 minutes was used in the Cooper-Jacob's calculation.

Figure 3 is a Birsoy and Summers semi-logarithmic plot of specific drawdown versus adjusted time for the three steps at PW-01. "Adjusted time" is the term given to the product of an equation used to adjust time for all steps after the first step to account for the drawdown in the previous step (see Attachment A). The data for the first two steps plot as almost parallel lines instead of falling on one ideally straight line (as is theorized in the equation). This indicates that well efficiency decreases with each increase in the pumping rate. The data for the third step plot along a line with a significantly greater slope than the first two steps, and there is also a change in slope at approximately 130 minutes. This could indicate that boundary conditions exist within hydraulic reach of the third step.

A transmissivity of 141 ft²/day was calculated using the straight line (latter) portion of the first step. Using the straight line (latter) portion of the second step, a similar value of transmissivity, 176 ft²/day, was calculated. A line fitted to the latter parts of the first and second steps yields a transmissivity value of 95 ft²/day. The third step was not selected for analysis due to possible boundary conditions. These results were similar to the transmissivity calculated using the Cooper-Jacobs' method.

SEMI-LOGARITHMIC GRAPH OF DRAWDOWN VERSUS TIME AT PW-01
STEPPED-DISCHARGE TEST AT PW-01

CONTINENTAL STEEL, KOKOMO, INDIANA



Pumping Rate = $0.075 \text{ ft}^3/\text{min.} = 0.56 \text{ gpm}$

$r = 0.29 \text{ ft}$ = radial distance from
pumping well to observation well

FIGURE 2

SEMI-LOGARITHMIC GRAPH OF SPECIFIC DRAWDOWN VERSUS ADJUSTED TIME
STEPPED-DISCHARGE TEST AT PW-01

CONTINENTAL STEEL, KOKOMO, INDIANA

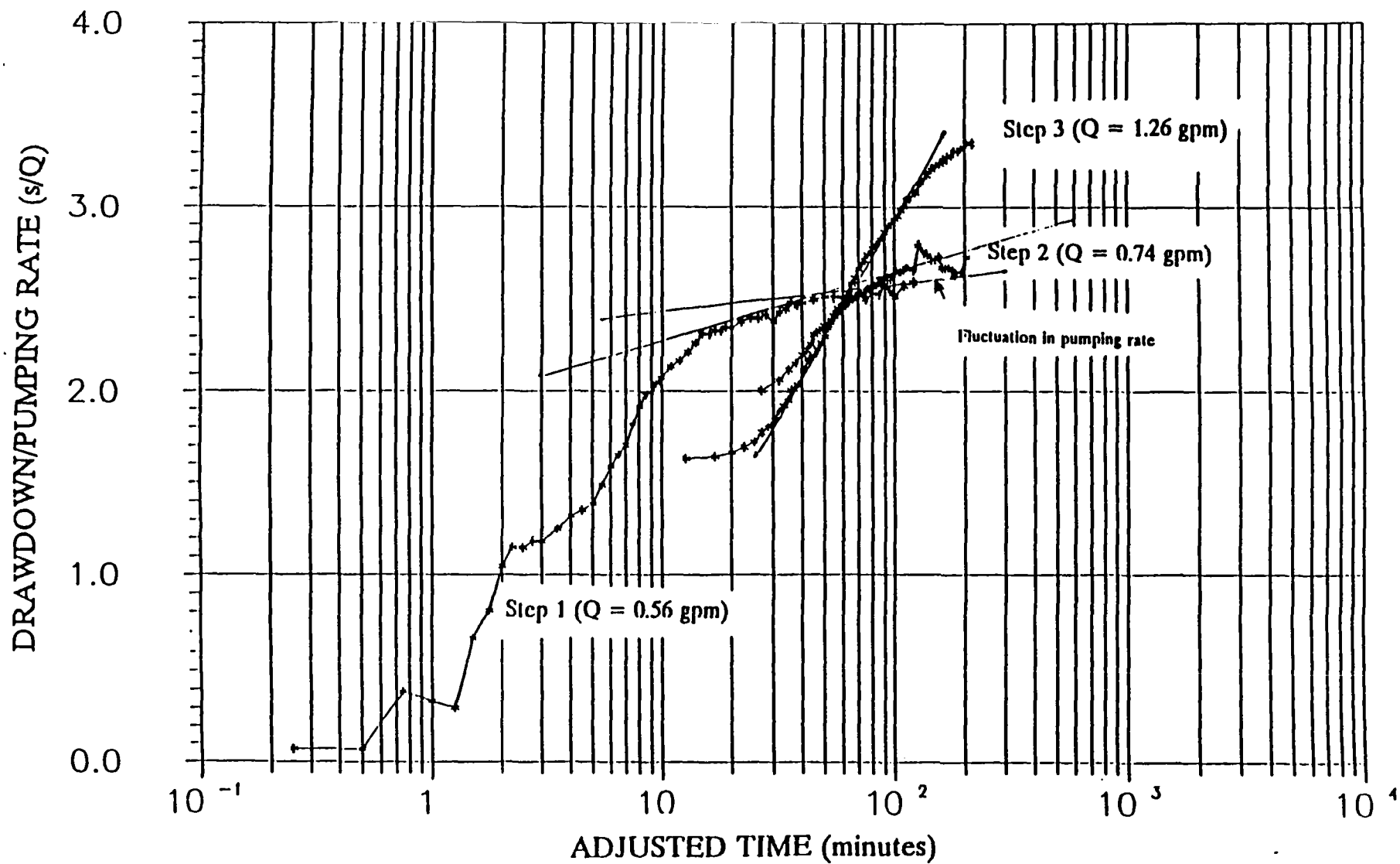


FIGURE 3

A hydraulic conductivity of 11 feet per day (ft/day) or 4×10^{-3} centimeters per second (cm/sec) was calculated from an average transmissivity value of 138 ft²/day and using an aquifer thickness of 13 feet. This is consistent with hydraulic conductivity values obtained from slug tests performed on surrounding wells.

PROJECTIONS FOR MULTI-DAY CONSTANT RATE TEST

Aquifer parameters were input into the Theis equation using the PT1 program, a pumping test design model from William C. Walton's Ground Water Pumping Tests-Design and Analysis, Lewis Publishers, 1987. The model was used to provide a preliminary estimate of the area of influence obtained by pumping well PW-01 at a constant rate of 1 gpm for three days, using the average hydraulic conductivity (11 ft/day). For unsteady-state conditions, the area of influence from pumping is significantly affected by the storage parameter. Because the specific yield, S_y , cannot be reliably calculated from a stepped-discharge test, S_y values ranging from 0.1 to 1×10^{-4} were used to assess the area of influence. A typical value for the storage parameter in moderately fractured bedrock is 1×10^{-3} . A summary of the simulation results is provided below.

S_y	DRAWDOWN (feet)				
	$r = 0.29$	$r = 73$	$r = 183$	$r = 460$	$r = 1,155$
1×10^{-1}	1.26	0.04	0.00	0.00	0.00
1×10^{-2}	1.54	0.24	0.07	0.00	0.00
1×10^{-3}	1.83	0.49	0.29	0.11	0.01
1×10^{-4}	2.13	0.76	0.55	0.34	0.15

r = radial distance from pumping well

The radius of influence, as defined by 0.1 feet of drawdown, ranged between 46 and 1,155 feet.

CONCLUSIONS AND RECOMMENDATIONS

The transmissivities estimated from slug test results and the stepped-discharge test represent the aquifer transmissivities for localized areas around the tested wells. A primary purpose of the constant-discharge pumping test at PW-01 will be to provide a more reliable estimate of the transmissivity over a large area of the aquifer. Also, the constant-discharge test will be used to determine the specific yield of the aquifer.

A pumping rate of 1.0 gpm is recommended for the three-day constant-rate test. A higher pumping rate may result in excessive drawdown at the pumping well, precluding a three-day test duration.

Computer simulations indicate that 0.1 feet of drawdown should be measurable at approximately 500 feet from PW-01 during the constant-rate test (assuming a 1.0 gpm pumping rate). It is difficult to accurately predict the radius of influence because the predicted drawdown depends significantly on the value of specific yield used in the simulation. At this time, the specific yield is unknown.



The prediction of long-term drawdown in a fractured bedrock well, based on a six-hour stepped-discharge test, inherently has some uncertainty; however, given the available information, wells OW-01, UA-05, UA-06, UA-07, UA-28, and UA-29 were selected for observation during the constant-discharge test.

Well UA-01 is selected for monitoring background water levels. This well is beyond the 500 feet radius of influence predicted by the computer simulations.

ATTACHMENT A
METHODOLOGY ASSUMPTIONS

UNSTEADY FLOW TO A WELL IN A CONFINED AQUIFER MODIFIED METHOD

REFERENCE: Cooper, H. H. and C. E. Jacob, 1946. A generalized graphical method for evaluating formation constants and summarizing well field history, Am. Geophys. Union Trans., vol. 27, pp. 526-534.

ASSUMPTIONS: aquifer has infinite areal extent
aquifer is homogeneous, isotropic, and of uniform thickness
aquifer potentiometric surface is initially horizontal
pumping rate is constant
pumping well is fully penetrating
flow to pumping well is horizontal
aquifer is confined
flow is unsteady
water is released instantaneously from storage with decline of hydraulic head
diameter of pumping well is very small so that storage in the well can be neglected
values of u are small (i.e., r is small and t is large)

SOLUTION:

The Cooper-Jacob method is a modification of the Theis (1935) method for confined aquifers.

$$s = Q / (4 \pi T) w(u)$$

where:

$$u = r^2 S / (4 T t)$$

The Theis well function, $w(u)$, can be evaluated by the following infinite series:

$$w(u) = -0.5772 - \ln u + u - \frac{u^2}{2 \cdot 2!} + \frac{u^3}{3 \cdot 3!} \dots$$

UNSTEADY FLOW TO A WELL
IN A CONFINED AQUIFER,
MODIFIED METHOD
(continued)

For small values of u ($u < 0.01$), the terms of this series can be neglected after the first two terms. Thus, drawdown is approximated by the following linear expression:

$$s = Q / (4 \pi T) \left[-0.5772 - \ln \frac{r^2 S}{4 T t} \right]$$

DRAWDOWN RESPONSE IN A CONFINED AQUIFER PUMPED STEP-WISE OR INTERMITTENTLY

REFERENCE: Birsoy & Summers, 1980, Birsoy, Y.K., and W.K. Summers, 1980. "Determination of Aquifer Parameters from Step Tests and Intermittent Pumping Data"; Ground Water; Vol. 18, No. 2; pp. 137-145; March-April 1980.

- ASSUMPTIONS:
- 1) The aquifer is confined;
 - 2) The aquifer has a seemingly infinite areal extent;
 - 3) The aquifer is homogeneous, isotropic, and of uniform thickness over the area influenced by the test;
 - 4) Prior to pumping, the piezometric surface is horizontal (or nearly so) over the area that will be influenced by the test;
 - 5) The aquifer is pumped step-wise or intermittently at a variable discharge rate or is intermittently pumped at a constant discharge rate;
 - 6) The well penetrates the entire thickness of the aquifer and thus receives water by horizontal flow;
 - 7) The flow to the well is in an unsteady state; and
 - 8) $\frac{r^2 S}{4KD} \times \frac{1}{\beta_{i(n)}(t-t_n)} < 0.01$

SOLUTION: Applying the principle of superposition to Cooper-Jacob's approximation of the Theis equation, the following expressions for the drawdown in the aquifer at time t during the n th pumping period of intermittent pumping is obtained

$$S_n = \frac{230Q_n}{4(3.14)KD} \log \left\{ \left(\frac{2.25KD}{r^2 S} \right) \right\} \beta_{i(n)}(t-t_n)$$

where

- $t-t_i$ = time since the i -th pumping period started
 t'_i = time at which the i -th pumping period ended
 $t-t'_i$ = time since the i -th pumping period ended
 Q_i = constant well discharge during the i -th pumping period

For step-wise or uninterrupted pumping, $t'_{(i-1)} = t_i$, and the 'adjusted time' $\{\beta_{i(n)}(t-t_n)\}$ becomes

$$\beta_{i(n)}(t-t_n) = \prod_{i=1}^n (t-t_i)^{\Delta Q_i/Q_n}$$

or

$$\beta_{i(n)}(t-t_n) = (t-t_1)^{\Delta Q_1/Q_n} \times (t-t_2)^{\Delta Q_2/Q_n} \times \dots \times (t-t_n)^{\Delta Q_n/Q_n}$$

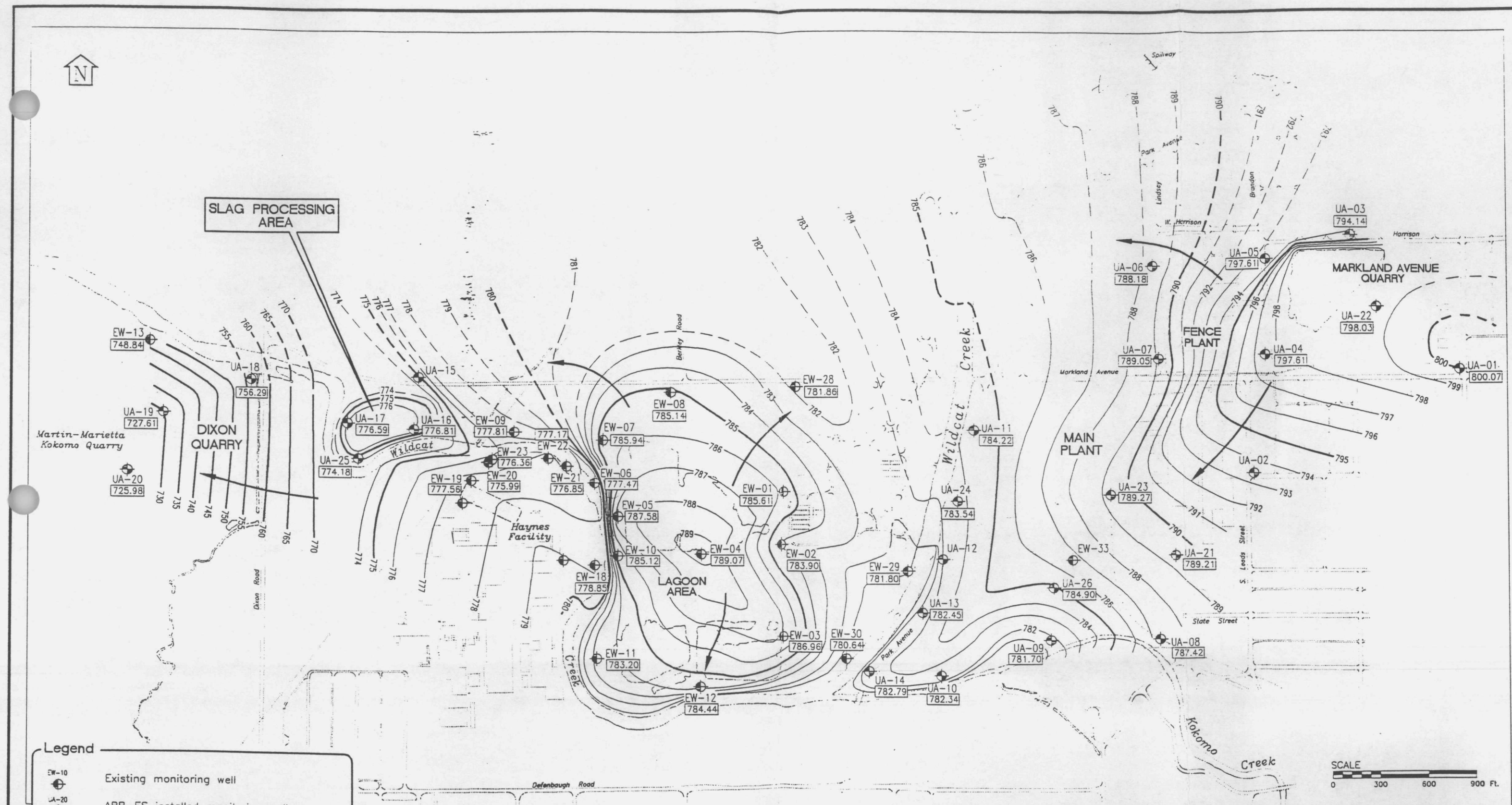


FIGURE 3-11
GROUNDWATER TABLE - MAY 1993
CONTINENTAL STEEL RI
KOKOMO, INDIANA

ABB Environmental Services, Inc.

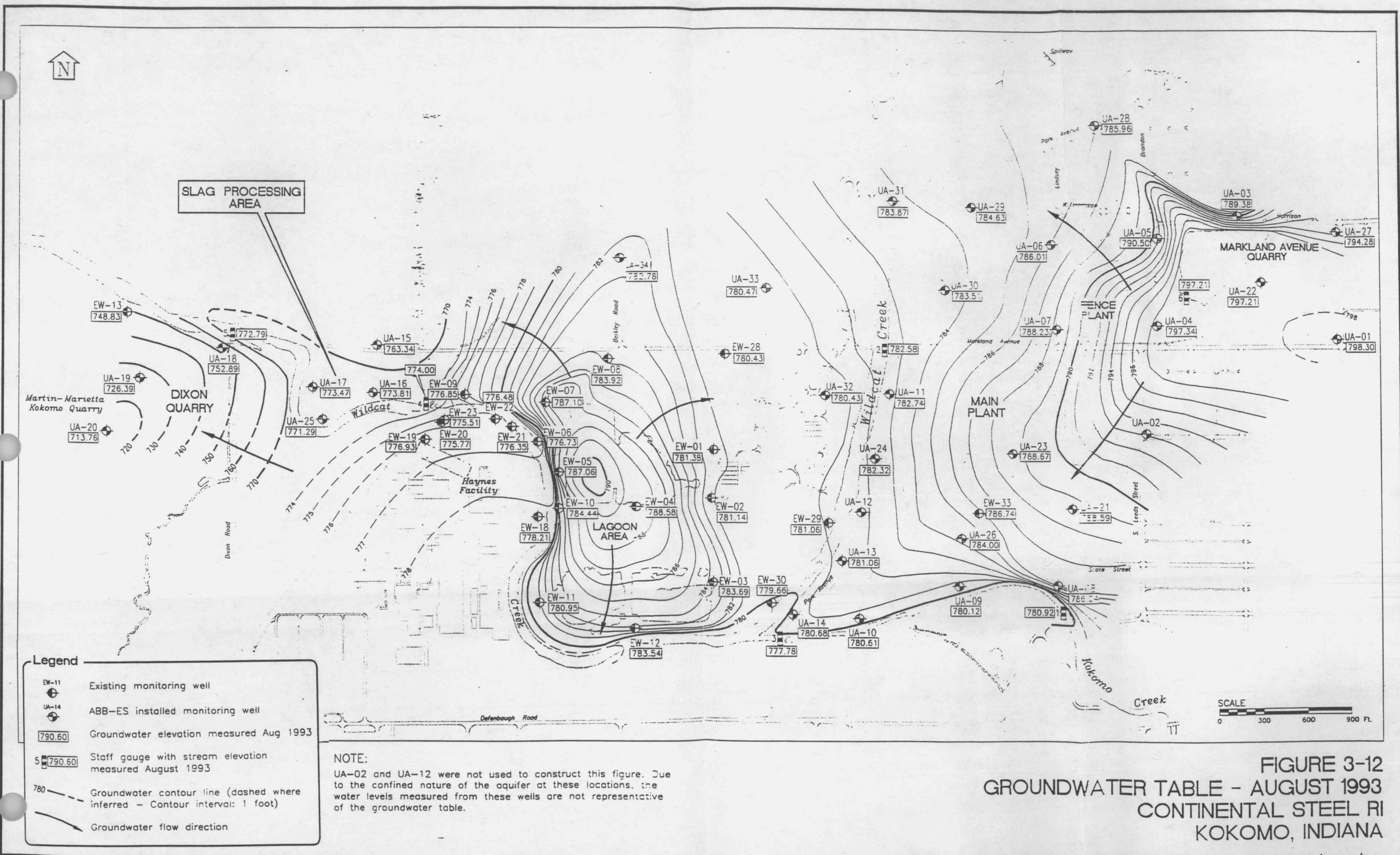


FIGURE 3-12
GROUNDWATER TABLE - AUGUST 1993
CONTINENTAL STEEL RI
KOKOMO, INDIANA

ABB Environmental Services, Inc.

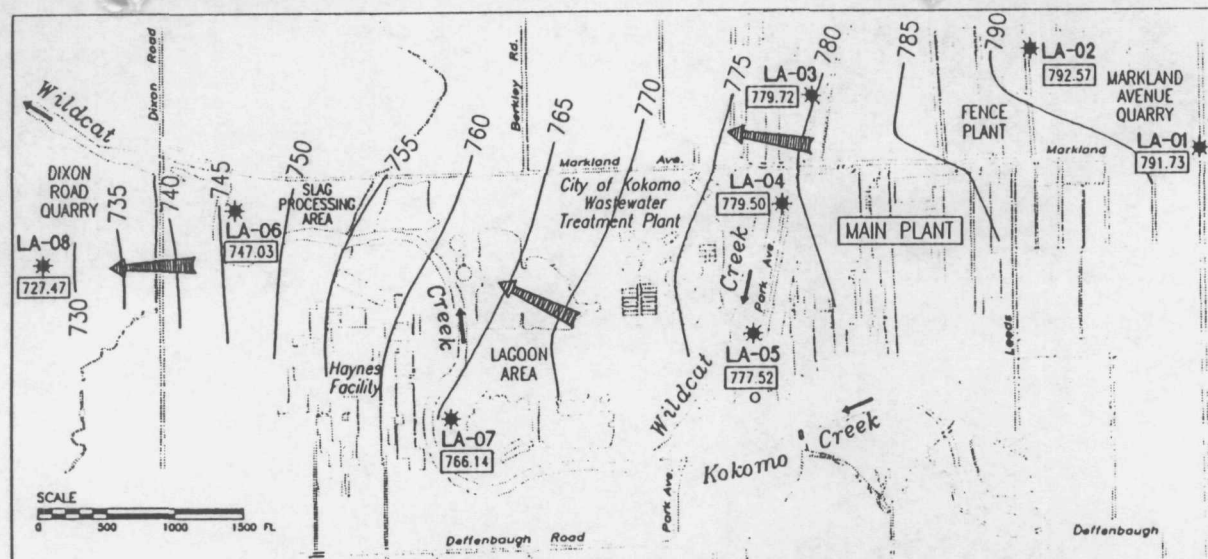


FIGURE 3-14a

Liston Creek, Unit A

Lower Aquifer Zone Designation	Zone Depth (feet bgs)	Zone Elevation (feet msl)
1	69-81	724-736
2	60-72	728-740
3	42-54	737-749
4	52-64	730-742
5	50-62	731-743
6	53-65	721-733
7	63-75	717-729
8	42-54	720-732
8	57-69	705-717

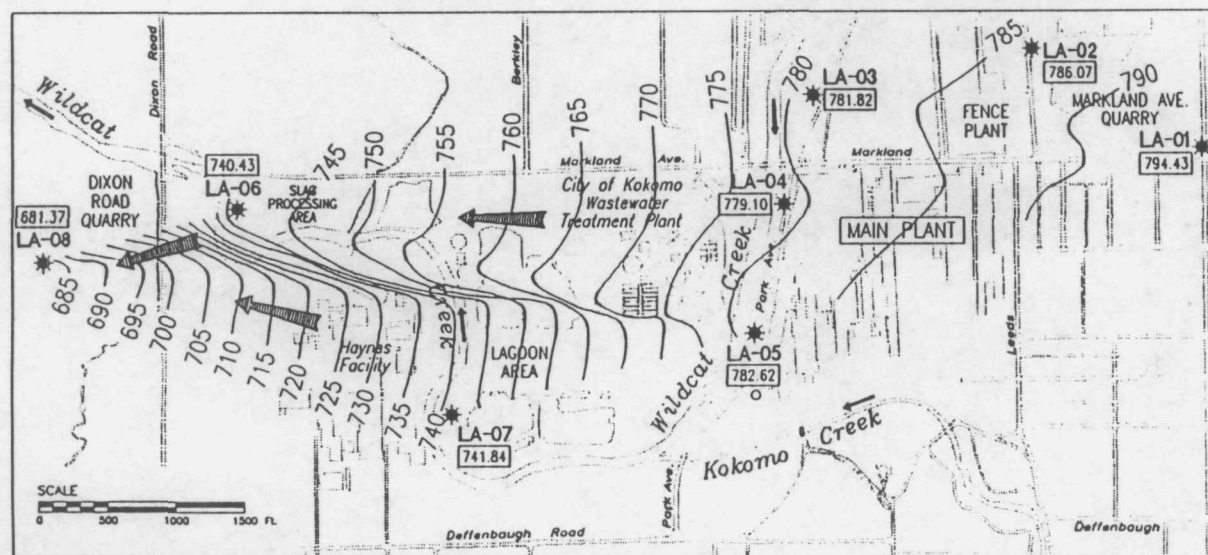


FIGURE 3-14b

Liston Creek, Unit B Mississenewa Shale

Lower Aquifer Zone Designation	Zone Depth (feet bgs)	Zone Elevation (feet msl)
1	116-136	668-689
2	112-132	668-688
3	107-130	661-684
4	109-129	664-685
5	110-131	662-683
6	98-118	668-688
7	100-121	671-692
8	92-107	667-681

Legend

- Groundwater flow direction
- Lower aquifer monitoring well
- Groundwater elevation measured August 1993
- Line of equal hydraulic potential (feet msl)
- River flow direction
- bgs - Below ground surface msl - Mean sea level

FIGURE 3-14
HORIZONTAL GROUNDWATER FLOW DIRECTIONS
IN THE DEEP FLOW SYSTEM
CONTINENTAL STEEL RI
KOKOMO, INDIANA

ABB Environmental Services, Inc.



November 3, 1993

Ms. Gabriele Hauer
IDEM-OER, Superfund Section
105 S. Meridian Street
P.O. Box 6015
Indianapolis, IN 46206-6015

Subject: OU1/Task 3C, Fracture Trace Analysis
Continental Steel RI, Kokomo, IN
6802-08-TKK

Dear Ms. Hauer:

Enclosed are two figures. The first figure illustrates interpreted fracture trace lineaments around the site based upon the fracture trace analysis. The second figure is a rose histogram of fracture orientations measured in outcrops and quarries adjacent to the site. These figures serve as the deliverable for OU1/Task 3C, Fracture Trace Analysis.

It is ABB-ES' understanding that IDEM has declined to approve the invoice for this task because the technical adequacy of the work could not be evaluated based upon the previously submitted deliverable. As agreed in our October 13 meeting, these figures provide the information needed by IDEM.

Please call me if you have any questions regarding this matter.

Respectfully,

ABB ENVIRONMENTAL SERVICES, INC.

A handwritten signature in dark ink, appearing to read 'Don Walsh', is written over the company name.

Don Walsh
Site Manager

enclosure

cc: Kim Kesler-Arnold, Program Manager

ABB Environmental Services, Inc.

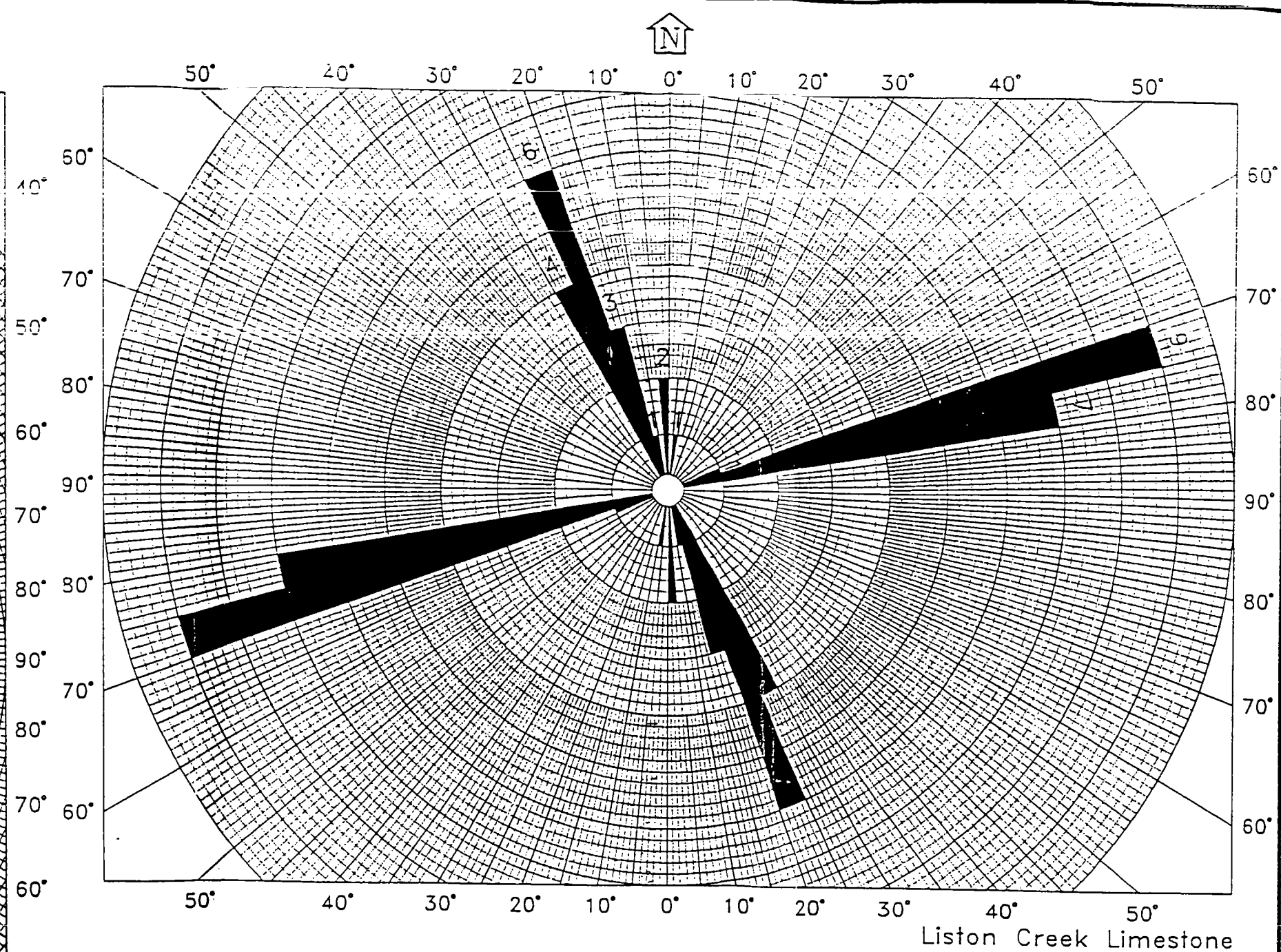
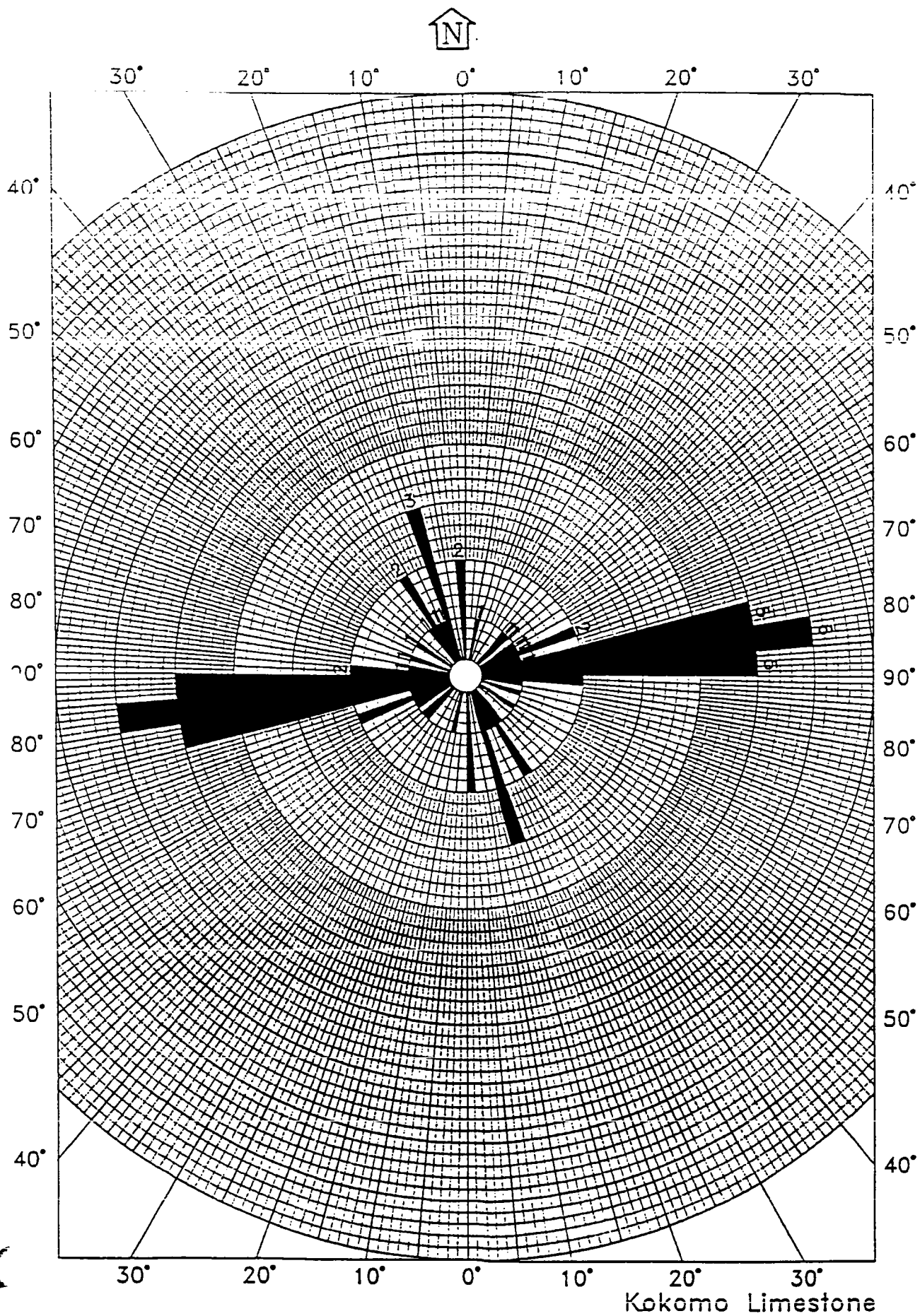


FIGURE 3-8
ROSE HISTOGRAM OF FRACTURE ORIENTATIONS
CONTINENTAL STEEL RI
KOKOMO, INDIANA

